ELECTROCHEMICAL AND ISOTHERMAL TITRATION CALORIMETRY STUDIES ASSOCIATED WITH POLYMER-MICELLE COMPLEXES AND SURFACTANT/CYCLODEXTRIN INCLUSION COMPLEXES

By

HEZRON KAPAGA OZANNE MWAKIBETE

Dip. (Ed.)(Sc.) (Mkwawa)
B.Sc. (Ed.)(Hons.) (Dar es Salaam)
M.Sc. (Salford)

A THESIS SUBMITTED TO THE UNIVERSITY OF SALFORD IN CANDIDATURE FOR THE DEGREE OF DOCTOR OF PHILOSOPHY

SCIENCE RESEARCH INSTITUTE, CHEMICAL SCIENCES DIVISION,
UNIVERSITY OF SALFORD

NOVEMBER, 1994

DECLARATION

The work contained in this thesis is my own original work and was carried out by myself in the Physical Chemistry Laboratories of the Chemical Sciences Division, Science Research Institute, University of Salford between 1991 and 1994 under supervision of Professor Evan Wyn-Jones. The Omega ITC work was carried out at the Fritz-Haber-Institut der Max-Planck-Gesellschaft, Berlin, Germany in May, 1994 under guidance of Professor Dr. Josef F. Holzwarth.

This work to the best of my knowledge has not been submitted and is not currently being submitted for any other degree in any other University.

Candidate: _____

HEZRON KAPAGA OZANNE MWAKIBETE

Supervisor: _____

Professor EVAN WYN-JONES

DEDICATION

I dedicate this thesis to my mother ARUSI IGOMOLE ISWASU and to my daughters BUPE BERTHA and KISA NAOMI.

Walk in wisdom toward them that are without,
redeeming the time. **[Col. 4:5]**

For I am now ready to be offered,
and the time of my departure is at hand.
I have fought a good fight,
I have finished my course,
I have kept my faith. **[2 Tim. 4:6-7]**

For this cause
I bow my knees unto the Father
of our Lord Jesus Christ. **[Ephes. 3:14]**

Make a joyful noise unto the LORD,
all ye lands.
Serve the LORD with gladness;
come before his presence with singing.
Know ye that the LORD he is God;
it is he that hath made us,
and not we ourselves;
we are his people,
and the sheep of his pasture.
Enter into his gates with thanks-giving,
and into his courts with praise;
be thankful unto him,
and bless his name.
For the LORD is good;
his mercy is everlasting;
and his truth endureth to all generations. **[Psalm 100]**

IN THE NAME OF JESUS CHRIST, OUR LORD. AMEN.

TABLE OF CONTENTS

Table of Contents v

Acknowledgement xi

Abstract xii

CHAPTER ONE: SURFACTANTS, MICELLES AND POLYMER-MICELLE COMPLEXES IN AQUEOUS SOLUTIONS

1.1 INTRODUCTION 1

1.2 CLASSIFICATION AND APPLICATIONS OF SURFACTANTS 3

1.3 THE CRITICAL MICELLE CONCENTRATION (cmc) 5

1.4 EFFECT OF COUNTERIONS AND SUPPORTING ELECTROLYTES ON MICELLIZATION 7

1.4.1 Counterions 7

1.4.2 Supporting Electrolytes 8

1.5 THE STRUCTURE, SIZE AND SHAPE OF THE MICELLE 9

1.6 POLYMER-MICELLE COMPLEXES 14

1.6.1 Interactions between neutral water-soluble polymers and cationic surfactants 16

1.6.1.1 Poly(propylene Oxide) (PPO) (M_w=1000) 17

1.6.1.2 Poly(vinylmethylether) (PVME) (M_w=27000) 18

1.6.1.3 Ethyl(hydroxyethyl)cellulose (EHEC) (M_w=120000) 18

1.7 THE MASS BALANCE EQUATION AND CRITICAL POINTS IN POLYMER-SURFACTANT SYSTEMS 20

1.7.1 The Mass Balance Equation 20

1.7.2 The Critical Concentrations 22

1.8 REFERENCES 24

CHAPTER TWO: INTRODUCTION TO SURFACTANT SELECTIVE ELECTRODES AND EMF MEASUREMENT IN IONIC SURFACTANT SYSTEMS

2.1 INTRODUCTION 28

2.2 BASIC CONCEPTS FOR ION SELECTIVE ELECTRODES(ISE) 29

2.2.1 The Membrane Potential 29

2.2.2 The Cell Potential, E_{cell} 30

2.2.3 Asymmetry Potential of the Membrane 32

2.2.3.1 Factors Causing Asymmetry in the Membrane 33

2.2.3.2 Basic Theory of Asymmetry Potential 33

2.3 HISTORICAL DEVELOPMENT OF ION SELECTIVE ELECTRODES 36

2.4 EXPERIMENTAL PROCEDURES 43

2.4.1 Preparation of cetyltrimethylammonium bromide PVC membrane 43

2.4.1.1 Purification of CTAB and conditioning of PVC 43

2.4.1.2 Casting of the membrane and making the CTAB selective membrane electrode 44

2.4.2 Calibration of the CTAB selective membrane electrode 45

2.4.2.1 Preparation of Solutions 45

2.4.2.2 The Calibration Experiment 47

2.5 REFERENCES 49

CHAPTER THREE: THERMODYNAMICS OF MICELLE FORMATION

3.1 INTRODUCTION 53

3.2 THERMODYNAMICS OF MICELLE FORMATION TREATED BY A PSEUDO-PHASE SEPARATION MODEL 54

3.3 THERMODYNAMICS OF MICELLE FORMATION TREATED BY A MASS-ACTION MODEL 57

3.3.1 Nonionic Surfactant systems 57

3.3.2 Ionic Surfactant systems 58

3.4 TREATMENT BY MASS-ACTION MODEL INVOLVING THE MEAN ACTIVITY COEFFICIENT $\gamma_{\pm}$ 59

3.5 CONTRIBUTING FORCES TO THE FREE ENERGY CHANGE OF SURFACTANT MICELLIZATION 60

3.6 AN ADDITIVE CONTRIBUTION APPROACH FOR THERMODYNAMIC PARAMETERS OF MICELLE FORMATION BASED ON ION BINDING MODEL 63

3.6.1 The Gibbs Free Energy Change of Micelle Formation 63

3.6.2 Enthalpy and Entropy Changes of Micelle Formation by La Mesa's Reduced Variables Approach 68

3.7 REFERENCES 75

CHAPTER FOUR: INTERACTIONS BETWEEN CETYLTRIMETHYLAMMONIUM BROMIDE AND UNCHARGED WATER-SOLUBLE POLYMERS IN AQUEOUS SOLUTIONS

4.1 INTRODUCTION 77

4.2 MICELLIZATION IN CTAB SYSTEMS IN THE ABSENCE OF POLYMERS 78

4.2.1 EMF measurements Procedures 78

4.2.2 The critical micelle concentration (cmc) 80

4.2.3 Measurement of monomeric surfactant concentration m_1 86

4.2.4 Determination of free Counterions concentration m_2 88

4.2.5 Effective degree of Micellar dissociation α 90

4.2.6 Thermodynamic parameters of micellization based on α and cmc from electrode data 94

4.2.7 Discussion 100

4.3 POLYMER-MICELLE COMPLEXES 103

4.3.1 Preparation of uncharged water-soluble polymer solutions 103

4.3.2 EMF measurement in CTAB-0.5%polymer systems 105

4.3.3 Effective degree of Micellar dissociation, α 105

4.3.4 Binding Isotherms and Critical points T_1 and T_2 109

4.3.5 Discussion 126

4.4 REFERENCES 131

CHAPTER FIVE: INTRODUCTION TO CYCLODEXTRINS AND INCLUSION COMPLEXES:

5.1 PREAMBLE 134

5.2 CYCLODEXTRINS 135

5.2.1 Characteristics of α-, ß- and γ-CDs 138

5.3 CYCLODEXTRIN INCLUSION PROCESSES 140

5.3.1 Review of Surfactant/Cyclodextrin work 141

5.3.1 General Guest-Host Inclusion forces 146

5.3.2 Geometrical Consideration for Surfactant-Cyclodextrin Inclusion Complexes 150

5.4 REFERENCES 155

CHAPTER SIX: EQUILIBRIUM STUDIES ASSOCIATED WITH INCLUSION COMPLEXES OF CATIONIC SURFACTANTS TO α- AND ß-CYCLODEXTRINS USING SURFACTANT SELECTIVE ELECTRODES:

6.1 INTRODUCTION 158

6.2 EXPERIMENTAL PROCEDURES 159

6.2.1 Synthesis of alkylpyridinium bromides 159

6.2.2 Preparation of alkylpyridinium ions PVC Membranes 161

6.2.3 EMF measurements in Cyclodextrin/Surfactant systems 162

6.3 TREATMENT OF ELECTRODE DATA 178

6.4 RESULTS 191

6.4.1 Decylpyridinium bromide (C_{10}PyBr) 203

6.4.2 Dodecylpyridinium bromide (C_{12}PyBr) 203

6.4.3 Tetradecylpyridinium bromide (C_{14}PyBr) 204

6.4.4 Cetylpyridinium bromide (C_{16}PyBr) 204

6.4.5 Tetratrimethylammonium bromide (C_{14}TAB) 205

6.5 REFERENCES 207

CHAPTER SEVEN: THE OMEGA ISOTHERMAL TITRATION CALORIMETRY (ITC) STUDIES ASSOCIATED WITH CYCLODEXTRIN/ SURFACTANT INCLUSION COMPLEXES:

7.1 INTRODUCTION 209

7.2 WORKING THEORY OF THE OMEGA ITC 210

7.2.1 General Principles of Calorimeters 211

7.2.2 An ITC Operational Theory 215

7.2.3 Improved Response Times and Experimental Signal Interpretation 217

7.3 OMEGA ITC EXPERIMENTAL PROCEDURES 219

7.3.1 Preparation of Solutions for an ITC Experiment 219

7.3.2 Setting $\Delta T \approx 0$ (The Control Module) 222

7.3.3 Setting an Omega ITC Reaction Cell for Experiment 223

7.3.4 Setting the Injection Matrix for an Omega ITC Experiment 226

7.4 OMEGA ITC DATA ANALYSIS 228

7.4.1 Single Binding Site Systems 229

7.4.2 Two-Consecutive Binding Sites Systems 232

7.5 OMEGA ITC RESULTS 234

7.5.1 1:1 α- and ß-CD/Surfactant Inclusion Complexes 237

7.5.1 1:1 and 2:1 CD/Surfactant Inclusion Complexes 238

7.6 REFERENCES 244

CHAPTER EIGHT: DISCUSSION ON ELECTROCHEMICAL AND OMEGA ITC RESULTS ON CYCLODEXTRIN/SURFACTANT INCLUSION COMPLEXES

8.1 INTRODUCTION 246

8.2 THE FIRST BINDING CONSTANT K_1 249

8.2.1 ß-CD/Surfactant Systems 249

8.2.2 α-CD/Surfactant Systems 253

8.3 THE SECOND BINDING CONSTANT K_2 254

8.4 INCLUSION COMPLEXES OF TETRAETHYLENE GLYCOL MONO N-OCTYL ETHER WITH α-, ß- AND γ-CDs 256

8.5 THERMODYNAMIC PARAMETERS FOR INCLUSION COMPLEX FORMATION 258

8.5.1 1:1 Inclusional Complexes 258

8.5.2 1:1 and 2:1 Inclusional Complexes 261

8.6 ALKYL CHAIN DEPENDENCE OF INCLUSION COMPLEX FORMATION 263

8.7 REFERENCES 268

APPENDICES

Appendix 4: Electrochemical data for CTAB/SALT and POLYMER/CTAB/SALT system 270

Appendix 6: Electrochemical data for CYCLODEXTRIN/SURFACTANT Inclusion complexes systems 274

Appendix 7: Omega ITC Computer fit plots for CYCLODEXTRIN/SURFACTANT Inclusion Complexes systems 286

ACKNOWLEDGEMENT

I wish to thank The Norwegian Agency for Development and Co-operation (NORAD) for the scholarship offer and THE BRITISH COUNCIL for administration. I would like to extend a hand of appreciation to my employer, THE UNIVERSITY OF DAR ES SALAAM, for a study leave offer and THE UNIVERSITY OF SALFORD for allowing me the opportunity to use their facilities.

I wish to express my deepest appreciation and gratitude to my supervisor Professor Evan Wyn-Jones for his guidance, supervision and undiminished interest in my work. Special thanks to Dr. Derek M. Bloor for using his computer programs, proof-reading this thesis and day-to-day advise on experimental work when needed. I also wish to thank Professor Dr. Josef F. Holzwarth of the Fritz-Haber-Institut (FHI) der Max-Planck-Gesellschaft, Berlin, Germany for allowing me to use the Isothermal Titration Calorimetry (ITC) facilities.

I acknowledge my colleagues in the laboratories G11, G12 and G13: Stuart, Andrew, Donna, Jason, Yan, Greg and Fred for creating a friendly working environment. I wish also to acknowledge Mr. Charles Maina Migwi and Mumly Musi for being available to help when in need.

And finally, I wish to express special appreciation and gratitude to my mother ARUSI IGOMOLE ISWASU for taking care of her granddaughters BUPE BERTHA and KISA NAOMI in my absence; and to MARTHA for hope.

ABSTRACT

The effective degree of micellar dissociation of cetyltrimethylammonium bromide (CTAB) micelles has been determined from electrochemical (EMF) measurements using a CTAB selective electrode. Thermodynamic parameters have been determined using the 'Ion binding model' and show dominance of hydrophobic interactions in free CTAB micellization. The enthalpy contribution is insignificant.

The binding of the surfactant CTAB onto the neutral water-soluble hydrophobic polymers: poly(propylene oxide) (PPO), poly(vinylmethylether) (PVME) and ethyl(hydroxyethyl) cellulose (EHEC) has also been investigated by the EMF technique. In all cases it has been shown that the surfactant binds to the polymer and the bound surfactant exists in the form of small aggregates. The EMF data has been used to investigate the characterization of the binding process.

The formation of inclusion complexes between alkyl-pyridinium bromide (C_nPyBr) and alkyltrimethylammonium bromide (C_nTAB) with α- and ß-cyclodextrins (CDs) have also been investigated by the EMF technique. In addition the thermodynamics of the inclusion on α- and ß-CDs by the surfactants: C_nTAB, C_nPyBr, alkylsulfates (C_nOSO_3Na), and alkanesulfonates (C_nSO_3Na) have been carried out using an Omega isothermal titration calorimeter (ITC). Whereas ß-CD systems form predominantly 1:1 complexes, α-CD form 1:1 and

a 2:1 complexes with surfactants having long hydrophobic tails. For both α- and ß-CD the complexation constants increase as the chain length of the surfactant increases, showing that the driving force dominating the formation of these complexes is the hydrophobic effect. The 1:1 ß-CD/surfactant complexation is accompanied by large increase in entropy. The 1:1 α-CD/surfactant complexation and all 2:1 complexation are accompanied by a large increase in enthalpy.

CHAPTER ONE: SURFACTANTS, MICELLES AND POLYMER-MICELLE COMPLEXES IN AQUEOUS SOLUTIONS

1.1 INTRODUCTION

The word *surfactant* is a technical term, derived from the phrase *surf*ace *act*ive a*gent*. Therefore, surfactant is a functional term, because in itself it describes the behaviour of these substances[1]. Surfactants are amphiphilic compounds (Greek: amphi = 'on both sides'; phileein = 'to love'). They have two distinct moieties; one with high affinity for water, 'hydrophilic' and one with a low affinity 'hydrophobic'. Hartley[2] named these compounds 'amphiphatic' because they contain one part that has 'sympathy' and another that has 'antipathy' for water. This phenomenon of surfactants explains the cleansing power in soaps and detergents as well as aggregation behaviour of aqueous solutions of surfactants, because of the dislike of water for the hydrophobic moiety.

Surfactants as natural or synthetic products have been in use since ancient times and so surfactant history is as old as human civilization itself. Moreover, the technology and architecture of surfactants has been developing to suit demands arising from human social and economic development (i.e. civilization). In the early days surfactants in the form of simple soaps were widely used in all parts of human civilization. The use of these simple soaps can be traced as early as Roman times (B.C.). The alkali metal soaps were used by the Phoenicians as early as 600 B.C., that is, at

least 2500 years ago[3]. The soap industry grew from making soap for home use to commercial manufacturing to cope up with high demand by woolen industry in the 13th Century. Synthetic detergents came very late in the 1940s and 1950s due to high demand in quality and quantity of the growing domestic and industrial cleansing. There is a saying that, 'life as we know today, would not be possible without surfactants' and therefore surfactants makes an important part of modern civilization.

Sometimes surfactants needed to be mixed with some other substances to attain certain features, such as high viscosities. The early useful mixtures contained proteins and the formation and existence of lipo-protein aggregates in biological fluids were recognized in the early part of this century[4].

On the basis of this widened demand on both quality and quantity of surfactants, research involving improvement on surfactant architecture and on useful surfactant mixtures has increased as evidenced by number of publications produced[1]. The interest among researchers, industrialists, consumers and the environment is to have surfactants of high functional efficiency, economical (low production cost and cheap to the consumer), easy and safer storage and environmentally friendly (e.g. should be biodegradable). Notwithstanding early pioneering work by Saito[5] on the interactions between polyethoxylated nonionic surfactants

and polycarboxylic acid, a substantial amount of work on association involved in the protein/surfactant systems by Putman, Lundgren, Neurath, Tanford, and many others[1] laid the foundation to current studies.

1.2 CLASSIFICATION AND APPLICATIONS OF SURFACTANTS

Different authors classify surfactants differently according to their background and intended audience or readers. However, the most notable classifications, acceptable in research and academia, are:

(a) by chemical nature of the hydrophobic group:

(i) hydrocarbons (C_nH_{2n+1}-K), (ii) fluorocarbons (HC_nF_{2n}-K), (iii) siloxane {K-[-OSi(CH3)2]n-O-K}, etc where K is the head group.

(b) by chemical nature of the hydrophilic group:

(i) anionic: hydrophilic group bears a negative charge; e.g. alkylsulfates ($ROSO_3^-M^+$), alkanesulfonates ($RSO_3^-M^+$), alkylcarboxylates ($RCOO^-M^+$), etc where R and M^+ are the alkyl group and metallic ion respectively.

(ii) cationic: hydrophilic group bears a positive charge; e.g.alkyltrimethylammonium halides, $RN^+(CH_3)_3X^-$, alkylpyridinium halides, $RN^+C_5H_5X^-$, alkylammonium halides, $RNH_3^+X^-$, etc where R and X^- are the alkyl group and halide ion respectively.

(iii) nonionic: the hydrophilic group bears no charge but it is highly polar. Polyoxethylenes ($-OCH_2CH_2O-$) are more popular in this category.

(iv) zwitterionic (and amphoteric): the surfactant

molecule contain both negative and positive charges. Sulfobetaines $\{RN^{+}(CH_3)_2CH_2CH_2SO_3^{-}\}$ is a good example in this group of surfactants.

(c) by applications:

(i) soap and detergents, (ii) emulsifiers, (iii) lubricants, (iv) adsorbants, (v) pharmaceuticals, etc.

The use of surfactants cover a wide spectrum of domestic, clinical and industrial applications. Apart from the most common and historical application as detergents, surfactants due to their distinctive features: (i) moderate maximum concentration of molecularly dispersed species, (ii) they cause depression of interfacial tension in very dilute solution by the adsorption and orientation of molecules at the interface, (iii) micelle formation above a certain concentration resulting in a decrease of the free energy of the system, and (iv) solubilization of water-insoluble substances by micelles. For example, surfactants with low critical micelle concentration (cmc), good salt properties, pH stability, good foaming properties and biodegradability are used as soaps and detergents irrespective of their chemical structure. On the other hand, surfactants with proper hydrophile-lipophile balance (HLB), environmental and biological safer, are used as emulsifiers. Others as lubricants, food additives, pharmaceuticals, used in tertiary oil recovery and mineral flotation, etc.

1.3 THE CRITICAL MICELLE CONCENTRATION (cmc)

The existence of a discontinuity in physical properties of dilute surfactant solutions is attributed to the formation, at a certain total surfactant concentration, of aggregates of surfactant molecules called *micelles*, whose contribution to physical properties of the system is different from that of individual surfactant molecules. The total surfactant concentration, at which this occurs, is called *the critical micelle concentration* (*cmc*)[6]. Apart from this general definition, the idea of the cmc is not well conceived. However, the cmc value is essential to a better understanding of the thermodynamics of micellization and other surfactant characteristics. Mukerjee[7] and Tanford[8] define the cmc as 'a narrow concentration range below which the surfactant exists only in monomeric form and above which all added surfactant form micelles of sufficiently large aggregation numbers by a cooperative mechanism'. On the other hand Myers[9] defines cmc as 'a solubility limit of monomeric surfactant and that any increase in surfactant concentration will be directed almost completely to the formation of more micelles'. Finally Shinoda[10] sees the cmc as a 'saturation concentration of monomeric surfactant'. The Mukerjee, Tanford, Myers and Shinoda definitions are based on the law of phase separation and so they emphasize cmc as boundary phenomenon between two separate phases.

Experimentally measured cmc values depends on many factors. The cmc is a parameter derived from a plot of a solution

physical property measured (electromotive force, surface tension, conductivity, etc) as a function of total surfactant concentration and will depend on[11]: (i) the way data are plotted and lines extrapolated, (ii) the characteristics of the measurements, (iii) the specific technique used to measure the physical property, (iv) the accuracy of experimental method, and (v) the judgement of individual investigators. From different techniques used, physical properties measured, and judgement of individual investigators; the critical micelle concentration (cmc) will inevitably differ with some magnitude of error, and it seems the results in literature influence the definition of cmc from different authors[8-12], e.g. it justifies cmc as a narrow range and not a specific point.

For a specific physical property, the technique used and judgement of the individual investigator will dictate how correct the cmc value will be, and it largely depends on how sharp[1] the discontinuity in the physical property appears. If the aggregation number n is high enough many physical properties give perfect discontinuity[13,14]. The cmc's obtained in cases like this are less erroneous.

The critical micelle concentration of surfactants vary with: (i) the hydrophobic chain length, (ii) the head groups, (iii) the counterions, (iv) additives to surfactant solutions; electrolytes, polymers, polyelectrolytes, monomeric organics, etc, and (v) the temperature at which

the measurements are carried out. More discusion on factors affecting cmc is included in Chapter 3 dealing with thermodynamics of micellization.

1.4 EFFECT OF COUNTERIONS AND SUPPORTING ELECTROLYTES ON MICELLIZATION

1.4.1 Counterions

Reduction of the cmc in the presence of a supporting electrolyte is caused by a reduction in the inter-head-group electrostatic repulsion. This directly reduces the contribution to the free energy term opposing micellization ($\Delta G^{\circ}_{mic}(-W)$) and accordingly the free energy term favouring micellization ($\Delta G^{\circ}_{mic}(hc)$) becomes dominant leading to much lower free energy of micellization (ΔG°_{mic}) and thus forming stable micelles at a lower cmc.

The impact of counterions is significant for both cationic and anionic surfactants. Factors which contribute to the differences between the effect of one counterion to another are: (i) radius of ionic hydration, and (ii) the effective degree of micellar dissociation. It has been found that the cmc of surfactants in aqueous solutions decreases as the effective degree of micellar dissociation decreases (when more counterions are bound to the micelle they induce micellization by screening effect). For a given hydrophobic tail and anionic head group the cmc increases in the order $Li^+ > Na^+ > K^+ > Cs^+ > N(CH_3)_4^+ > N(CH_2CH_3)_4^+ > Ca^{2+} \approx Mg^{2+}$ as observed in metal dodecylsulphates[15,16] ($C_{12}H_{25}OSO_3M$, $M = Li^+$,

Na^+, K^+, Cs^+) has cmc's 10.5, 8.9, 7.8 and 6.9 mmol dm^{-3} respectively at 40°C. On the other hand, for a given cationic head group and hydrophobic tail, the cmc decreases[7] in the order F^- > Cl^- > Br^- > I^- as demonstrated by the dodecylpyridinium halides[17] ($C_{12}H_{25}PyX$, X = Cl^-, Br^-, I^-) which have cmc's 17.0, 11.0 and 5.3 mmol dm^{-3} respectively at 25°C. Although the size of the hydrated counterion for a given valency has some significant effect, larger effects are observed when there are changes in the valency of the counterion. The cmc decreases rapidly when the counterion valency is changed from monovalent to divalent or trivalent.

1.4.2 Supporting Electrolytes

Salts, with surfactant counterion as one of their ionic species used as additives to a surfactant solution affects the cmc in three ways: (i) the effect resulting from the concentration C_s (the amount of added salt in solution), (ii) the effect resulting from the charge number on the counter ions (e.g. Na^+, Mg^{2+} and Al^{3+}), and (iii) the radius of ionic hydration of the coion (e.g. Na^+ against K^+). A number of publications have reported a linear dependence of log(cmc) on log(C_s) as summarized in the Corrin Equation[18]

$$\log(\text{cmc}) = -a\log(C_s) + b \qquad (1\text{-}1)$$

where "a" and "b" are experimental constants for a given ionic head group at a particular temperature[17] with values of "a" ranging between 0.4 to 0.6 and C_s is the total

concentration of monovalent counterions in moles per litre. The value "a" is dependent on the number of ionic head groups in the surfactant; for surfactants with two head groups equation (1-1)[10] becomes $\log(cmc) = -2a\log(C_s) + b$.

The impact of added electrolyte is less pronounced for nonionic and zwitterionic, and so the free energy contributed from the repulsion forces of head groups ΔG^{o}_{mic} (-W) is negligible and equation (1-1) does not apply for these types of surfactants. Instead, the effect is given better by Shinoda's equation[19]

$$\log(cmc) = -KC_s + \text{constant}; \quad C_s < 1 \text{ mol dm}^3 \qquad (1\text{-}2)$$

which shows linear dependence of the logarithm of cmc on added salt concentration. Tori[20] and Ray[21] extended work using equation (1-2) proposed by Shinoda. The value of K increases with an increase in the hydrophobic chain length and with the counterion charge number[20]. The change in the cmc of nonionics and zwitterionics on the addition of neutral salts has been attributed[20,21] mainly to the "salting out" and "salting in" of the hydrophobic groups in the aqueous solvent by the salt, rather than effect on the hydrophilic groups of the surfactant as in ionic surfactants.

1.6 THE STRUCTURE, SIZE AND SHAPE OF THE MICELLE

The micelle size, structure and shape depends largely on the balance between the two main contributing forces to the

micelle formation. Whereas the hydrophobic part of the surfactant dictates the lower limit to the micelle size, hydrophilic part determines the optimum size and shape. There is a limit to the number of surfactant molecules aggregating with each other before an effective elimination of the hydrocarbon core-water interface can be achieved. A stable micelle can not be formed by two, three or four surfactant molecules and therefore there should be a cooperative mechanism of association until a stable micelle is obtained ($S_1 + S_{n-1} = S_n$, where n = 2, 3, 4,..; S is the monomeric surfactant, S_{n-1} and S_n are successive aggregates).

The optimum shape and size (aggregation number n) of the micelles are determined by the hydrophilic part of the free energy, $\Delta G^{\circ}_{mic}(-W)$. The geometrical considerations of the micelle suggest that: (i) the head groups must approach closer to each other as the micelle size (n) increases, (ii) the head group repulsion forces must increase continuously with micelle size (n). So there is repulsion and work opposing repulsion to reach a resultant force, $\Delta G^{\circ}_{mic}(-W)$; therefore, to reach optimum size and shape: (i) the head group repulsion must increase to certain level and not continuously, (ii) the head groups can approach each other close enough but not a touching closeness due to the nature of the charge on the head group. At this point a micelle of optimum size and shape is obtained. The hydrophilic part of the free energy of micelle formation, $\Delta G^{\circ}_{mic}(-W)$, is dependent on the structure (bulkiness) and

charge on the head group.

In most recent publications, the surfactant critical packing parameter[22], $V_H/(l_{max}.a_o)$, has been used to approximate the shape and size of the micelle. The variables[8,23,24]; $V_H = 27.4 + 26.9(n_c-1)$ and $l_{max} = 1.500 + 1.265(n_c-1)$ are the volume occupied by hydrophobic group in cubic nanometres and the maximum extension length of the hydrophobic group in nanometres in the micellar core respectively, n_c is the hydrophobic chain length and a_o is the cross-sectional area occupied by the hydrophilic head group at the micelle-solution interface.

The total volume of the hydrophobic core can either be calculated using the maximum extension length of the hydrophobic group l_{max} as radius[22], $(4/3)\pi(l_{max})^3$, or as sum of individual volumes of hydrophobic groups in the micellar core, $N \times V_H$, yielding

$$\text{Volume} = N \times V_H = (4/3)\pi(l_{max})^3 \qquad (1\text{-}3)$$

and the surface area of the micelle is either calculated as a sum of surface areas of individual head groups, $N \times a_o$, or calculated using the radius of the micelle as

$$\text{Surface area} = N \times a_o = 4\pi(l_{max}+\Delta)^2 \qquad (1\text{-}4)$$

where Δ is the added length of the radius of the sphere due to hydrophilic group[25].

Brackman and coworkers[26] used surface area-to-volume ratios to estimate shapes of micelles. Using surface area and volume as given in equations (1-3) and (1-4) we obtain

$$\frac{\text{Surface area}}{\text{Volume}} = \left(\frac{a_o}{V_H}\right) = \left[\frac{3(l_{max}+\Delta)^2}{(l_{max})^3}\right] \qquad (1\text{-}5)$$

Equation (1-5) can be converted into an equation involving surfactant critical packing parameter by rearranging the reciprocal of this equation

$$\frac{V_H}{l_{max}.a_o} = \left[\frac{(l_{max})^2}{3(l_{max}+\Delta)^2}\right] \qquad (1\text{-}6)$$

which is the relationship between the surfactant critical packing parameter and a third of the ratio between the squares of the radii of the hydrophobic micellar core (l_{max}) and the micelle ($l_{max}+\Delta$). For simple, single chain surfactants and relatively small to medium head groups, $l_{max} >> \Delta$. So $l_{max}+\Delta \approx l_{max}$ and the ratio $l_{max}/(l_{max}+\Delta) \approx 1$ and so $V_H/(l_{max}.a_o) < ⅓$. Under this conditions the surfactant micelle will either be spherical or ellipsoidal in shape. Other considerations are as shown in table 1.1. $V_H/(l_{max}.a_o) > 0.5$ for surfactants with two chains and $V_H/(l_{max}.a_o) > 1$ for reversed micelles in non-aqueous solvents are not considered in this discussion.

From equation (1-4) l_{max} increases (i.e. carbon chain length) with aggregation number (n) for a given head group (a_o is constant). For example, the alkyltrimethylammonium bromides

homologous series[27] $C_nH_{2n+1}N(CH_3)_3^+Br^-$ (n = 10, 12, 14, 16) have aggregation numbers 39, 55, 70 and 86 respectively at 20°C. Also for a given hydrophobic chain (l_{max} is constant), as a_o increases aggregation number (n) decreases. This is demonstrated in the tetradecyltrialkylammonium bromides homologous series[27,28] $C_{14}H_{29}N(C_nH_{2n+1})_3^+Br^-$ (n = 1, 2 and 3) have aggregation numbers 70, 55 and 35 respectively.

Table 1.1: Approximation of micelle shapes using surfactant critical packing parameter

$V_H/(l_{max}.a_o)$	Surfactant	Geometrical shape
< 0.33	Simple Surfactant, single chain, relatively large head group.	Spherical or Ellipsoidal
0.33-0.50	Simple Surfactant, small head groups or ionics presence of large amounts of electrolyte.	Cylindrical or rod-like

Evidence from various sources show that initially micelles, formed at the cmc and immediately after, have relatively small aggregation numbers (50-100) and roughly spherical in shape. At higher concentrations and under appropriate conditions spherical micelles transform into other forms: disc-like, cylindrical, ellipsoidal, or laminar shapes. Although, it is well known that the shapes of the micelles depend on surfactant molecular structure (head group and hydrophobic chain), their shapes also vary with surfactant concentration. An increase in surfactant concentration above the cmc, can be accommodated either by increasing the

number of micelles of a given size or by modifying the micellar structure to allow a larger number of molecules to be incorporated into each micelle. This is achieved by transforming the shape of the micelle to disc-like or cylindrical shapes in which repulsion between head groups is decreased. This phenomenon is referred to as micellar growth.

1.6 POLYMER-MICELLE COMPLEXES

The mutual modification of the physicochemical properties of micelles and polymer in polymer-micelle complexes were recognized very early in the development of this research area. For example, the solubilization power[1,5,29] of surfactants becomes much greater on the addition of polymers[30,31] and occurs at concentrations lower than the cmc. In addition, viscosities of the surfactant/polymer mixtures are higher than those of individual surfactant and polymer solutions[31]. The mechanism of solubilization is described as a result of polymer-micelle complex formation (adsorption of surfactant molecules on the polymer)[32,33]. Furthermore, association between ionic surfactants and polymers usually leads to a stabilization of the micelles, which is evidenced in the reduced values of the cmc's[1,34]. Commercial interest and a wide range of industrial and domestic applications, such as: formulations of paints and coatings, cosmetics products, laundry detergents, tertiary oil recovery and many others, have attracted academics and industrialists to invest in surfactant-polymer research.

This field of research in polymer/surfactant solutions has strong roots in biochemistry although later it was developed in a much wider chemical perspective. Importance of the lipo-protein aggregates in biological fluids were recognized early and this led to the study of mixed-polymer surfactant systems. A large amount of work on protein/ionic surfactant systems was carried out in the 1940's and 1950's and led to a better understanding of the importance of electrical forces of attraction. The interactions were referred to as 'binding' of the ionic surfactant by the polymer. During the course of these studies, conformational changes in the protein were also recognized.

These studies developed from proteins to involve a much wider range of uncharged water-soluble synthetic polymers interacting with ionic surfactants[35]. In addition, charged pairs, that is, polyelectrolytes (anionic or cationic) and ionic surfactants have also been studied[35]. In the early studies it was found that cationic surfactants interact weakly or not at all with neutral polymers. Recent studies however have shown that this is not so. It is also interesting to note, there are some studies which indicate that nonionic surfactants interact with polymers[31,35].

Although surfactant-polymer systems have been investigated for almost half a century now, the morphology of micelles and the nature of interactions involved have as yet, not been well established[36-38].

Different investigative methods are utilized to measure either macroscopic behaviour or changes in molecular properties. Some of the investigative methods that have been used in this area of research are: electrochemical (potentiometry using surfactant selective electrodes), conductometry, ultrasonic relaxation, light scattering, small angle neutron scattering, surface tension, viscometry, gel filtration, and many more.

1.6.1 Interactions between neutral water-soluble polymers and cationic surfactants

Complexes formed between micelles and uncharged water-soluble polymers have received a lot of attention in recent years[1,31]. However, most of this attention was centred on anionic surfactants, especially sodium dodecylsulfate ($C_{12}OSO_3Na$), because until recently interactions between cationic surfactants and polymers were thought to be very weak or completely absent[5,26,35]. Most recent studies on cationic surfactants, especially cetyltrimethylammonium bromide (CTAB) and other alkyltrimethylammonium bromides homologous series, have shown that provided the polymers used are sufficiently hydrophobic these interactions do exist[31,39-42].

The purpose of this work is to investigate these interactions using cetyltrimethylammonium bromide as the surfactant and three "hydrophobic" polymers, namely poly(propylene oxide) (PPO), poly(vinylmethylether) (PVME) and ethyl(hydroxyethyl)cellulose (EHEC).

1.6.1.1 Poly(propylene oxide) (PPO) (M_w=1000)

Poly(propylene oxide) (PPO) (M_w=1000 and M_o=58) is a nonionic hydrophobic PPO-oligomer with cloud point at 32°C[43,44]. Solubility of PPO is thought to result from hydrogen bonding between water and the polymers' etheric linkage oxygen atoms and a terminal hydroxyl groups by overcoming the hydrophobic interactions between polymer segments[45]. This solubility falls off markedly with increasing molecular weights[44]. For PPOs of higher molecular weights (M_w ≥ 1200)[1,46] solubility is practically impossible in pure water but they do dissolve in surfactant solutions due to interactions with micelles. In higher PPOs hydrogen bonding is insignificant compared to hydrophobic interactions between $[-OCH(CH_3)CH_2-]_nOH$ with OH groups separated by many segments as compared to only 17 segments for PPO (1000). The limiting molecular weight for water solubility for PPO is M_w=1200[1,43,46].

In order to have any effective interactions between cationic surfactants and neutral polymers the polymers must be sufficiently hydrophobic. There is recent evidence available from aggregation numbers of CTAB in PPO that a significant interaction occurs. Due to its low molecular weight, PPO (1000), a number of PPO chains are adsorbed on a single micelle[34].

1.6.1.2 Poly(vinylmethylether) (PVME) (M_w=27000)

Poly(vinylmethylether) (PVME) is a nonionic water-soluble polymer[26,34,47]. Poly(vinylmethylether) (M_w=27000) has cloud point at 34°C and its monomer segments $[-CH_2CH(OCH_3)-]_n$ (M_o=58) are isomeric to those of PPO $[-CH(CH_3)CH_2-O-]_n$. PVME and PEO (poly(ethylene oxide)) share the distinction of being the only two members of this group of polymers whose high molecular weights forms are water soluble at ambient temperatures[48]. On the other hand, the main differences between PPO and PVME are: (a) the position of etheric linkage oxygen atoms (main chain etheric oxygen atom for PPO and side chain for PVME), and (b) the molecular weights of their giant molecules.

Studies of the aggregation numbers of CTAB[32,34] and n-dodecyldimethylamine oxide (DDAO)[26] in PVME show interaction of the same magnitudes as PPO.

1.6.1.3 Ethyl(hydroxyethyl)cellulose (EHEC) (Mw=120000)

Ethyl(hydroxyethyl)cellulose (EHEC)[35,49-52] is a nonionic hydrophobic cellulose ether available in versions soluble in water or organic solvents[52]. Solubility behaviour of EHEC is determined by relative ratios of hydroxyethyl to ethyl substitution. Highly ethoxylated EHEC with low amounts of hydroxyethyl substitution is soluble in organic solvents and a water-soluble EHEC is highly hydroxyethyl-substituted. Solubility of EHEC is affected by inorganic

salts due to the so-called salting-in and salting-out effect[35]. Interactions of EHEC with ionic surfactants show dramatic changes in physical properties such as solubility, cloud points (CP), Krafft points, viscosities and many others. The nontrivial dependence of these properties on temperature and added salt concentration[35,50] are explained as an effect of conformational changes of the substituents and the backbone of EHEC. According to Zana *et al*[49], this temperature-induced conformational transition is attributed to an increase in the hydrophobicity of the EHEC molecule with increasing temperature. Carlsson *et al*[50] on the other hand, sees the charge on the polymer-micelle complexes as the main cause of inter- and intramolecular electrostatic repulsions which in turn causes an increase in CP and viscosities. Few studies carried out using SDS selective electrodes produced binding isotherms which show binding of surfactant to a polymer to be strongly cooperative[49,50,53].

EHEC is highly applicable in different fields of surface and colloidal chemistry. It acts as[52]: a thickener in latex paints, emulsifier in foodstuffs, tablet binder in pharmaceuticals and as green-strength binding in ceramics. Its use, however, is mostly dependent on the presence of surface active agents. Moreover, the interactions of EHEC to those molecules leads, in most cases, to unwanted effects. EHEC interacts very strongly with anionic surfactants[35,51,53] in the presence of small added salt and this results in a dramatic change in solubility of the formed

polymer-micelle complexes.

1.7 THE MASS BALANCE EQUATION AND CRITICAL POINTS IN POLYMER-SURFACTANT SYSTEMS

In polymer/surfactant systems two kinds of micelles are considered: (i) the free micelles, and (ii) the polymer-micelle complexes. The main question here is preference, competitiveness and factors guiding formation of these species. With the help of the mass balance equation, the critical concentrations (T_1 and T_2), the aggregation numbers (N_b and N_f) and the equilibrium constant (K_b and K_f), preference factors are considered in the following two sections.

1.7.1 The Mass Balance Equation

The aggregate mole fraction containing i molecules (χ_i) is related to the mole fraction of monomeric surfactant molecules (χ_1) by the expression[8,54-56]

$$\chi_i = (\chi_1)^i \exp[-i(\mu^\circ_i - \mu^\circ_1)/kT] \qquad (1\text{-}7)$$

This expression is referred to as the 'size distribution equation' for the micelles. The terms μ°_i and μ°_1 are the standard chemical potentials per surfactant molecule in the micelles and monomeric surfactant molecules. i is the aggregation number. The equilibrium constant of micellization $(K_f)^i = \exp(-i(\mu^\circ_i - \mu^\circ_1)/kT = \chi_i/(\chi_1)^i$ and $\chi_i = (K_f\chi_1)^i$. k and T take their usual meaning.

The maximum aggregation number N_f is obtained in the neighbourhood of the cmc for monodisperse micelles. Around this point it is expected the size distribution term has a high contribution. The aggregation number N_f can be evaluated from the condition of the maximum of χ_i[54]

$$\ln\chi_1 - (\mu^\circ_i-\mu^\circ_1)/kT + N_f[d((\mu^\circ_i-\mu^\circ_1)/kT)di]_{i=Nf} = 0 \qquad (1\text{-}8)$$

The critical molar fraction χ_{cmc} is approximated by the expression[56,57] $kT\ln\chi_{cmc} \approx \mu^\circ_{Nf}-\mu^\circ_1$ but at the cmc, χ_1 is equal to χ_{cmc}, equation (1-8) reduces to

$$\frac{d(\mu^\circ_i-\mu^\circ_1)}{di} \approx 0 \text{ for } i = N_f \qquad (1\text{-}9)$$

Applying this information on free surfactant micelles to polymer-micelle complexes, let us denote the aggregation number by N_b which can be evaluated in equation similar to (1-9)

$$\frac{d(\mu^\circ_{ib}-\mu^\circ_1)}{di} \approx 0 \text{ for } i_b = N_b \qquad (1\text{-}10)$$

If we denote the number of polymer binding sites as n, the number of aggregates per polymer molecule which contain surfactant molecules (if we assume that interactions between aggregates are negligible) is obtained from the adsorption equation[1,58] $\Gamma = n[(K_b\chi_1)^{Nb}/(1+(K_b\chi_1)^{Nb}]$ in which $K_b = \exp[-(\mu^\circ_i-\mu^\circ_1)/kT]$ and Γ is the degree of binding. Finally, the mass balance equation ($\chi_t = \chi_1 + N_f\chi_f + N_b\chi_b$) is written in such a way that it relates the total concentration (χ_t) to

that of monomeric surfactant molecules (χ_1) [1,54]

$$\chi_t = \chi_1 + N_f(K_f\chi_1)^{Nf} + N_b\left[\frac{n\chi_p K_b\chi_1)^{Nb}}{1+(K_b\chi_1)^{Nb}}\right] \qquad (1\text{-}11)$$

where $(K_f\chi_1)^{Nf} = \chi_f = [\text{micelle}]_f$ and $n\chi_p[(K_b\chi_1)^{Nb}/(1+(K_b\chi_1)^{Nb}] = \chi_b = [\text{micelle}]_b$ and equation (1-11) becomes

$$\chi_t = \chi_1 + N_f\chi_f + N_b\chi_b$$

$$= [\text{monomer}] + N_f[\text{micelle}]_f + N_b[\text{micelle}]_b \qquad (1\text{-}12)$$

At $\chi_t \leq T_1$, $[\text{micelle}]_f = [\text{micelle}]_b = 0$ and so $\chi_t = \chi_1$. In this region the Nernstian plot ($\text{Log}(\chi_t)$ vs emf) is linear. Within the region T_1 to T_2 there are two possibilities: EITHER we have $\chi_t = \chi_1 + [\text{micelle}]_b$ if T_2 is a true saturation point of a polymer and that below T_2 there is no formation of free micelles OR $\chi_t = \chi_1 + [\text{micelle}]_b + [\text{micelle}]_f$. However, we are certain above T_2 we have $\chi_t = \chi_1 + [\text{micelle}]_b + [\text{micelle}]_f$. Factors leading to this kind of circumstance are discussed in section 1.7.2.

1.7.2 The Critical concentrations

The competitive nature of polymer-micelle complex formation and surfactant self-aggregation (micelle formation) is illustrated better by using the parameters K_f, K_b, N_f and N_b. Differences in aggregation numbers, N_f and N_b, play a crucial role in determining chemical process boundaries and preferences. So apart from the usual role of equilibrium constant K_f and K_b, there is some dependence on aggregation

numbers (size of micelles or polymer-micelle complexes).

First, if $K_f > K_b$ and $N_f \approx N_b$ the formation of free micelles occurs in preference to polymer surfactant complexation. Under these circumstances, the only possiblility of complexation is the polymer to interact with free micelles and not a usual build-up of polymer-micelle complexes between T_1 and T_2. Therefore, we can conclude non-existence of acclaimed cooperative nature of interactions and probably we can say there is no polymer surfactant interactions.

Second, if $K_f < K_b$ and $N_f \approx N_b$ complexation occurs in preference to the formation of free micelles. In this case the region $T_1 <$ cmc $< T_2$ is well defined, complexation starts at T_1 and a build-up of polymer-micelle complexes continues until T_2 at which the polymer binding sites are saturated. It is also very clear free micelles start to form and there will be no competition at all.

Finally, $K_f < K_b$ and $N_f > N_b$ formation of free micelles may start before T_2 and leaving a certain part of the region T_1 < cmc < T_2 (very likely between cmc and T_2) in real competitive chemical equilibrium in existence.

1.8 REFERENCES

1. GODDARD, E.D., *Colloid surf.*, 19 (1986) 255.

2. HARTLEY, G.S. "*Aqueous Solutions of Paraffin-Chain Salts*", Hermann & Cie., Paris (1936).

3. SISLEY, J.P., *Am. Dyestuff Reporter*, 43 (1954) 741.

4. D.G. DERVICHIAN in Lipo-proteins, Discuss. Faraday Soc. 6 (1949).

5. SAITO, S., *Kolloid.-Z.*, 154 (1957) 19.

6. EVERETT, D.H., "*Basic Principles of Colloid Science*", Royal Society of Chemistry, London (1988).

7. MUKERJEE, P. *Adv. Colloid Interface Sci.* 1 (1967) 241.

8. TANFORD, C. "*The Hydrophobic effect: Formation of Micelles and Biological Membranes*", 2nd ed, Wiley-Interscience, New York (1980).

9. MYERS, D. "*Surfaces, Interfaces and Colloids: Principles and Applications*", VCH Publishers, New York (1991)

10. SHINODA, K.; NAKAGAWA, T.; TAMAMUSHI, B. and ISEMURA, T. "*Colloidal Surfactants*", Academic Press, New York (1963).

11. MYERS, D. "*Surfactant Science and Technology*", VCH Publishers, New York (1988)

12. ROSEN, M.J. "*Surfactants and Interfacial Phenomena*", 2nd Ed, John Wiley & Sons, New York (1989).

13. SHAW, D.J. "*Introduction to Colloid and Surface Chemistry*", Butterworth & Co., London (1970).

14. MAEDA, T. and Satake, I., *Bull. Chem. Soc. Jpn*, 57 (1984) 2396.

15. KLEVENS, H.B., *J. Chem. Phys.*, 14 (1940) 742.

16. MEGURO, K.; KONDO, T.; YODA, O.; INO, T. and OODA, N., *J. Chem. Soc. Japan*, 77 (1956) 1236.

17. ROSEN, M.J.; DAHANAYAKE, M. and COHEN, A.W. *Colloid Surf.* 5 (1982) 159.

18. CORRIN, M.L. and HARKINS, W.D. *J. Am. Chem. Soc.* 69 (1947) 684.

19. SHINODA, K.; YAMAGUCHI, T. and HORI, R. *Bull. Chem.*

Soc. Japan, 34 (1961) 237.

20. TORI, K. and NAGAKAWA, T. *Kolloid-Z. Z. Polym.* 189 (1963) 50.

21. RAY, A. and NEMETHY, G. *J. Am. Chem. Soc.* 93 (1971) 6787.

22. ISRAELACHVILI, J.N.; MITCHELL, D.J. and NINHAM, B.W. *J. Chem. Soc. Faraday Trans. 2*, 72 (1976) 1925.

23. TARTAR, H.V., *J. Phys. Chem.*, 59 (1985) 1195.

24. TANFORD, C., *J. Phys. Chem.*, 76 (1977) 3020.

25. HSIAO, L.; DUNNING, H.N. and LORENZ, P.B. *J. Phys. Chem.*, 69 (1956) 657.

26. BRACKMAN, J.C. and ENGBERTS, J.B.F.N. *Langmuir*, 8 (1992) 424.

27. LIANOS, P. and ZANA, R., *J. Colloid Interface Sci.* 88 (1981) 594.

28. LIANOS, P. and ZANA, R., *J. Colloid Interface Sci.* 84 (1981) 100.

29. BREUER, M.M. and ROBB, I.D. *Chem. Ind. (London)*, 13 (1972) 530.

30. TOKIWA, F. and TSUJII, K. *Bull. Chem. Soc. Jpn.*, 46 (1973) 2684.

31. BRACKMAN, J.C. and ENGBERTS, J.B.F.N. *Chem. Soc. Reviews*, 22(2) (1993) 85.

32. SATA, N. and SAITO, S. *Kolloid.-Z.*, 128 (1952) 154.

33. (a) ISEMURA, T. and KIMURA, Y. *J. Polymer Sci.*, 16 (1955) 92; (b) ISEMURA, T. and IMANISHI, A. *J. Polymer Sci.*, 33 (1958) 337.

34. BRACKMAN, J.C. and ENGBERTS, J.B.F.N. *Langmuir*, 7 (1991) 2097.

35. CARLSSON, A.; KARLSTRÖM, G. and LINDMAN, B. *Langmuir*, 2 (1986) 536.

36. WITTE, F.M. *Colloid and Polymer Sci.*, 265 (1987) 42.

37. BLOOR, D.M.; WYN-JONES, E. *J. Chem. Soc. Faraday Trans. 2*, 78 (1982) 657.

38. GODDARD, E.D. and HANNAN, R.B. *J. Am. Oil Chem. Soc.*, 54 (1977) 561.

39. ZANA, R.; LANG, J. and LIANOS, P. *J. Phys. Chem.*, 89 (1985) 41.

40. PERRON, G.; FRANCOEUR, J.; DESNOYERS, J. and KWAK, J. *Can. J. Chem.*, 65 (1987) 990.

41. WINNIK, F.; WINNIK, M. and TAZUKE, S. *J. Phys. Chem.*, 91 (1987) 594.

42. WINNIK, F.; RINGSDORF, H. and VENZMER, J. *Langmuir*, 7 (1991) 905.

43. MOLYNEUX, P. "*Water-soluble Synthetic Polymers: Properties and Behaviour*", Volume 1, CRC Press, Florida (1983).

44. VALENTINE, L. *J. Polymer Sci.*, 27 (1958) 313.

45. SCHWUGER, M.J. *J. Colloid Interface Sci.*, 43 (1973) 491.

46. PLETNEV, M. YU. and TRAPEZNIKOV, A.A. *Kolloidn. Zh.*, 40 (1978) 948.

47. BRANDRUP, J. and IMMERGUT, E.H. *Polymer Handbook*, 2nd Ed., Wiley, New York (1975).

48. KLOTZ, I.M. "The Role of Water Structure in Macromolecules" *Fed. Proc., Fed. Am. Soc. Exp. Biol.*, 24(Suppl. 15) S-24 (1965).

49. ZANA, R.; BINANA-LIMBELĒ, W.; KAMENKA, N. and LINDMAN, B. *J. Phys. Chem.*, 96 (1992) 5461.

50. CARLSSON, A.; LINDMAN, B.; WATANABE, T. and SHIRAHAMA, K. *Langmuir*, 5 (1989) 1250.

51. HOLMBERG, C.; NILSSON, S.; SINGH, S.K. and SUNDELÖF, L.-O. *J. Phys. Chem.*, 96 (1992) 871.

52. JUST, E.K. and MAJEWICZ, T.G. *Encycl. of Polymer Sci.& Eng.*, 2nd Ed. Wiley, New York, Volume 3, pp257-260 (1985).

53. WAN-BADHI, W.A. *PhD Thesis*, University of Salford (1993)

54. RUCKENSTEIN, E.; HUBER, G. and HOFFMANN, H. *Langmuir*, 3 (1984) 382.

55. RUCKENSTEIN, E. and NAGARAJAN, R. *J. Phys. Chem.*, 79 (1975) 2622.

56. NAGARAJAN, R. and RUCKENSTEIN, E. *J. Colloid Interface. Sci.*, 91 (1983) 500.

57. EVANS, D.F. and NINHAM, B.W. *J. Phys. Chem.*, 87 (1983) 5025.

58. NAGARAJAN, R. *Colloid Surf.*, 13 (1985) 1.

CHAPTER TWO: INTRODUCTION TO SURFACTANT SELECTIVE ELECTRODES AND EMF MEASUREMENTS IN IONIC SURFACTANT SYSTEMS

2.1 INTRODUCTION

Numerous studies on ionic surfactant systems over half a century have centred mainly on the chemical equilibrium existing between the monomeric surfactant ions, their partially monodisperse micelles and their counterions. Despite the enormous success of the majority of these studies there were certain unresolved issues, for example: (a) the availability of an analytical technique to monitor monomer surfactant concentration in the presence of micelles and/or additives, (b) the inability of most techniques (mainly macroscopic techniques) to derive accurate and reliable effective degree of micellar dissociation (α) in their analysis, and (c) unnecessary approximation of the mean activity coefficients to extremes (unity and zero) or their complete neglect.

As a result of the development of reliable and thermodynamically reversible surfactant selective electrodes in the 1980s and 90s there has been considerable progress in the derivation of monomer surfactant concentration, the mean activity coefficient $\gamma_{\pm}$ also the effective degree of micellar dissociation (α) in surfactant systems.

2.2 BASIC CONCEPTS FOR ION SELECTIVE ELECTRODES (ISE)

2.2.1 The Membrane Potential

An isothermal electrochemical system of two surfactant solutions of different concentration with activities a_1 and a_2 separated by an electrochemical membrane is presented as

Solution (1)|membrane|Solution (2)
x=p x=q

and the potential difference between solutions (1) and (2) at zero current is known as "Membrane Potential" (sometimes it is referred to as the 'Nernst Potential'). The notation x=p and x=q are distance coordinates at the two surfaces of membrane facing solution (1) and (2) respectively.

The surfactant ion is the component of interest in the system found on both phases (1) and (2) and is characterized by electrochemical potential $\mu_s(1)$ and $\mu_s(2)$ defined as

$$\mu_s(1) = \mu^\circ_s(1) + RT\ln(a_1) + zF\phi(1) \qquad (2\text{-}1)$$

$$\mu_s(2) = \mu^\circ_s(2) + RT\ln(a_2) + zF\phi(2) \qquad (2\text{-}2)$$

where $\mu^\circ_s(1)$ and $\mu^\circ_s(2)$ are standard chemical potentials, $\phi(1)$ and $\phi(2)$ are electric potentials for phases (1) and (2) respectively, and z is the charge number of the surfactant ion. Utilizing the phase-equilibrium condition for the two phases in contact (1) and (2), the equality of surfactant ion electrochemical potentials $\mu_s(1) = \mu_s(2)$, the membrane potential is defined as

$$\Delta\phi_m = \phi(2) - \phi(1)$$

$$= - \left[\frac{\mu^\circ_s(2) - \mu^\circ_s(1)}{zF}\right] + \left(\frac{RT}{zF}\right) \ln\left(\frac{a_1}{a_2}\right) \qquad (2\text{-}3)$$

for surfactant ions selective to the membrane in both phases. And since the same solvent was used in both phases (1) and (2), $\mu^\circ_s(2) = \mu^\circ_s(1)$ and so the term $(\mu^\circ_s(2) - \mu^\circ_s(1))/zF$ vanishes to zero reducing equation (2-3) to[1-3]

$$\Delta\phi_m = \pm\left(\frac{RT}{zF}\right) \ln\left(\frac{a_1}{a_2}\right) \qquad (2\text{-}4)$$

where a_1 and a_2 represent activities of the surfactant ions in the two aqueous phases separated by the membrane. R is the gas constant in J mol^{-1} K^{-1}, T is temperature in K, F is the Faraday constant (F = 96500 C mol^{-1} or C$(equiv)^{-1}$), z is the charge number (z = 1 in univalent surfactants studied in this work). For most electrochemical surfactant systems the activity a_2 is kept constant and that reduces equation (2-4) to

$$\Delta\phi_m = \pm\left(\frac{RT}{zF}\right) \ln(a_1) + K \qquad (2\text{-}5)$$

where the term $K = - (RT/zF) \ln(a_2)$.

2.2.2 The Cell Potential, E_{cell}

If two reference electrodes are dipped in solutions (1) and (2) in a cell shown in section 2.3.1 then a cell presented below is formed

RE|Solution (1)|membrane|Solution (2)|IRE

where RE and IRE are the reference electrode and inner reference electrode respectively. From the cell shown above we define the "ion selective electrode" as

membrane|Solution (2)|IRE

where "membrane" is selective to a specific ion of interest and "solution (2)" is termed as the inner reference solution with a constant activity (a_2). "Solution (1)" is the test solution and the activity a_1 is the activity of the ion of interest to be measured. The cell potential is the potential measured corresponding to activity a_1 in a cell and is given as

$$E_{cell} = E^{o}_{IRE} + \Delta\phi_m - E^{o}_{RE} \qquad (2\text{-}6)$$

$\Delta\phi_m$ is known from section 2.3.1 and the combination of equations (2-4) and (2-6) gives the cell potential in the form

$$E_{cell} = E^{o}_{IRE} \pm \left(\frac{RT}{zF}\right) \ln\left(\frac{a_1}{a_2}\right) - E^{o}_{RE} \qquad (2\text{-}7)$$

which can also be written as

$$E_{cell} = E^{o}_{IRE} - E^{o}_{RE} - \left(\frac{RT}{zF}\right) \ln(a_2) \pm \left(\frac{RT}{zF}\right) \ln(a_1) \qquad (2\text{-}8)$$

where the reference electrode potentials E_{RE} and E_{IRE} are constant at constant temperature and pressure as well as

the activity term $-(RT/zF)\ln(a_2)$. If we define $E_{IRE} - E_{RE} - (RT/zF)\ln(a_2) = E^{\circ}_{cell}$ then we end up with the Nernst equation of the system given in the cell above

$$E_{cell} = E^{\circ}_{cell} + \left(\frac{RT}{zF}\right)\ln(a_1) \qquad (2\text{-}9)$$

which applies for cationic species (i.e. cationic surfactants, drugs, dyes, etc) and

$$E_{cell} = E^{\circ}_{cell} - \left(\frac{RT}{zF}\right)\ln(a_1) \qquad (2\text{-}10)$$

for systems with anionic species (i.e. anionic surfactants, etc). E_{cell} from both equations (2-9) and (2-10) are commonly termed as 'cell potentials'.

2.2.3 Asymmetry Potential of the Membrane

Asymmetry potential of the membrane have been extensively studied as a problem to glass membranes[2-5] as well as an embodied membrane parameter[6,7] of ion selective membrane electrodes[6-12]. The effect is caused by mechanical and chemical properties of the membrane polymeric matrix which is mainly dependent on composition[9] and geometric properties of the membrane[10]. In this respect, flat membranes give more stable and reproducible results than those based on spherical geometry. It is predicted that an excess of free energy and polarization in the membrane are most probable reasons for occurance of the asymmetry potential[11]. It is argued that, existence of a zero asymmetry potential is a

consequence of theory, which is applied to the determination of the thermodynamic properties of solutions in contact with the membrane[12].

2.2.3.1 Factors Causing Asymmetry in the Membrane

The ion-exchange reaction in the membrane is not uniform or effective in the whole membrane due to very likely varying concentration of complexed ion-exchange sites (very low at the core of the membrane and high at interfaces x = p and x = q). Another explanation is the likeliness of two chemical processes occurring simultaneously in the membrane: (i) the ion-exchange reaction at the interfaces and (ii) ion-conduction or diffusion at the core of the membrane. These lead to asymmetry in the membrane and the potential contributed in this way is called "asymmetry potential" (E_a)[13-15] sometimes it is called "diffusion potential"[13,16]. The causes of this asymmetry potential undoubtly include such factors as:

(1) differences in strains[14,15,17] which lead to differences in ion-exchange capacities established within the two surfaces during the manufacture of the membrane[15,17,18],

(2) mechanical and chemical attack of the surfaces of the membrane[17], and

(3) contamination (poisoning) of the outer surface (facing the sample solution of the cell) during use[17].

2.2.3.2 Basic Theory of asymmetry potential

An electrochemical system of two bulk phases, (1) and (2),

of homogeneous solutions separated by a solid electrochemical membrane is used as a model for the understanding of asymmetry potential. The cell in section 2.3.2 will be used. The cell potential given in equation (2-6) is correct, if and only if, the membrane is symmetrical, that is, the interface contributions are equal and opposite. The real membrane potential should be:

$$\Delta\phi_m = \frac{[\mu^*(1) - \mu^\circ(1) - \mu^*(2) + \mu^\circ(2)]}{F} + \left(\frac{RT}{F}\right) \ln\left[\frac{C_1}{C_2}\right] \qquad (2\text{-}11)$$

Utilization of the most important phase-equilibrium condition for phase interactions, that is, the equality of electrochemical potentials for a common component in both phases[16], $\mu^*(1) = \mu^*(2)$, reduces equation (2-11) to

$$\Delta\phi_m = -\frac{[\mu^\circ(1) - \mu^\circ(2)]}{F} + \left(\frac{RT}{F}\right) \ln\left[\frac{C_1}{C_2}\right] \qquad (2\text{-}12)$$

The constant term $-[\mu^\circ(1) - \mu^\circ(2)]/F$ takes into account the chemistry of the dependence of membrane potential on composition, structure and physical properties of the membrane.

If the membrane behaves ideally and the same solvent is used in both phases (1) and (2), $\mu^\circ(1) = \mu^\circ(2)$ and the term $-[\mu^\circ(1) - \mu^\circ(2)]/F$ is zero[19]. The concentration-dependent membrane potential is sometimes termed as 'Nernst potential'[16]. Although in most cases if the same solvent is used the term $-[\mu^\circ(1) - \mu^\circ(2)]/F$ is rarely found to be zero.

If we define a site m in the core of the membrane, the distance magnitudes from m to interfaces x = p and x = q, |m-p| and |q-m| are not necessarily equal. The term $-[\mu^\circ(1)-\mu^\circ(2)]/F$ can be improved in order to satify the equality of chemical potentials $\mu^\circ(1) = \mu^\circ(2)$ for the same solvent condition as:

$$\Delta\phi_m = -\frac{[\mu^\circ(1)-\mu^\circ(p,m)-\mu^\circ(2)+\mu^\circ(m,q)]}{F} + \left(\frac{RT}{F}\right)\ln\left[\frac{C_1}{C_2}\right] \quad (2\text{-}13)$$

and now the equality of the terms $\mu^\circ(1)$ and $\mu^\circ(2)$ eliminates them from equation (2-13) reducing the term $-[\mu^\circ(1)-\mu^\circ(p,m)-\mu^\circ(2)+\mu^\circ(m,q)]/F$ to $[\mu^\circ(p,m)-\mu^\circ(m,q)]/F$. The terms $\mu^\circ(p,m)$ and $\mu^\circ(m,q)$ will be equal if and only if (i) the distance magnitudes |m-p| and |q-m| are equal which means site m is a symmetrical centre, and (ii) there is homogeneity in the distribution of ionic sites on both sides of the membrane. In many cases m is not a symmetrical centre, the term $[\mu^\circ(p,m)-\mu^\circ(m,q)]/F$ is not equal to zero and is termed the asymmetry potential of the membrane (E_a) and equation (2-13) becomes

$$\Delta\phi_m = E_a + \left(\frac{RT}{F}\right)\ln\left[\frac{C_1}{C_2}\right] \quad (2\text{-}14)$$

When $\Delta\phi_m$ in equation (2-14) is combined into equation (2-6) above we obtain

$$E_{cell} = E^\circ_{IRE} + E_a - E^\circ_{RE} + \left(\frac{RT}{F}\right)\ln\left[\frac{C_1}{C_2}\right] \quad (2\text{-}15)$$

A plot of E_{cell} against $\log[C_1/C_2]$ gives 2.303RT/F as slope and $E^\circ_{IRE}+E_a-E^\circ_{RE}$ as intercept. In order to evaluate asymmetry

potential of a membrane reference electrodes IRE and RE have to be chosen and should have stable and known standard electrode potentials. In the author's[20] drug selective membrane electrodes work, standard calomel electrode (SCE) and silver-silver chloride were used as RE and IRE respectively. The asymmetry potential derived contributed almost more than half of the constant term of the plot according to equation (2-15).

2.3 HISTORICAL DEVELOPMENT OF ION SELECTIVE ELECTRODES

Wilhem Ostwald in 1890; following the pioneering electrochemical works by Galvan (1791), Gibbs (1875), Arrhenius (1887), Nernst (1888-9) and Planck (1890); carried out studies on the properties of semi-permeable membranes. Electrochemical concepts such as diffusion and electric potential were already well defined from the studies by Nernst[21,22] and Planck[23,24] on transport processes in electrolytes, Ostwald added concepts such as potential difference and ion mobility. The electrochemistry of membranes as we know today evolved from these early works.

Intensive search for suitable models for membrane systems dominated electrochemical as well as biochemical research at the beginning of the 20th Century. Cremer[25] in 1906 developed a glass membrane electrode selective to hydrogen ions and Haber[26] did systematic investigation on this electrode a few years later. Glass membrane electrodes selective to other univalent cations were developed by

Eisenman[27] by varying the glass composition. During this period the concept and theory of selectivity was adopted and selectivity was intensively investigated. Liquid membranes containing dissolved ion-exchangers were developed by Sollner and Shean[28,29]. Although these liquid membrane electrodes showed perm-selectivity, they added another dimension to ion selective electrodes and proved useful and capable of development.

Other developments on invention and construction of non-glass ion-selective electrodes were carried out by Tandeloo[30], Kolthoff and Sanders[31], Pungor and Hallós-Rokosinyi[32], and many others. Among many electrodes constructed during this period, only Pungor and Hallós-Rokosinyi managed to produce a working electrode of high selectivity and good Nerstian response.

Amphiphilic ion selective electrodes (surfactants, drugs, dyes, etc) originated from the liquid membrane electrode selective to calcium ion developed by Ross[33]. Gavach[34,35] attempted to develop a liquid membrane electrode reversible to surfactant ions using a water-insoluble cation-anion complex dissolved in nitrobenzene. Birch and Clarke[36] followed up this development by employing the Orion Calcium electrode as their surfactant electrode body with a solution of cetyltrimethylammonium-dodecyl sulphate complex (CTA-DS complex) in nitrobenzene supported by a millipore filter disc as ion-exchange liquid. However, this electrode

failed, it gave a lower cmc due to solubilization of nitrobenzene from liquid membrane by the surfactant. Birch and Clarke[37] attempting to solve this problem decided to use a water-immiscible liquid o-dichlorobenzene. The improved electrode gave good cmc but at temperatures below 32°C the electrode failed to function correctly due to solubility of the ion association complex in this solvent. Addition of hexachlorobenzene and bromoacetoanilide solved the problem. Although there were many improvements, this liquid membrane electrode failed to work in the micellar region. To solve problems arising from the liquid membrane electrode, attempts were made by Fogg and coworkers[38] to make a heterogeneous solid-state surfactant membrane.

The electrode developed by Fogg was good but depreciated rapidly after several days. Improvement to this electrode was carried out by Cutler[39,40] who used a plasticised polymeric membrane. Cutler's investigation on a wide range of polymer-plasticiser combinations laid down the basis for the surfactant selective electrode used in this work. Although Cutler's membrane (made from the polymer polyvinylchloride and tricresyl phosphate plasticiser) showed good performance compared to liquid membranes, it had two major defects: (i) the ion-exchange complex solubilized after few hours, and (ii) it responded to both cationic and anionic surfactants due to its cation-anion surfactant ion exchange complex. The problems of Cutler's first electrode were solved by (i) having membranes with

fixed ionic sites covalently bonded to the polymer to protect them from being lost by solubilization, and (ii) the ionic sites in the polymer were of opposite charge to the surfactant they are selective to.

This electrode, however, had a limited life span, continuous use for more than six hours gave inaccurate readings and the electrode had to be washed and dried properly to be used again. It had been noted also that progressive loss of liquid plasticiser changed the composition of the membrane and made the electrode insensitive after continuous use. The problem was finally solved by Davidson[41] who used a polymeric plasticiser miscible with polyvinylchloride. Among many commercially available plasticisers, Elvaloy 742 and Elvaloy 741 from Du Pont, have worked efficiently. The Davidson's electrode was used successfully on a number of surfactants and drugs despite mechanical problems with the membrane which shortened its life span.

Bromley[42] developed a method of sticking the membrane to an electrode tip using tetrahydrofuran. Bromley's technique almost completely reduced the mechanical problem observed from the Davidson's work. A simple electrode body made from a modified EDT Calcium ion electrode was used rather than the one designed by Davidson.

In this laboratory the Davidson/Bromley form of the

surfactant selective electrode (shown in Figure 2-1) has worked successfully on surfactant systems of different complexities: (i) micellization in aqueous and non-aqueous surfactants systems[43,44,45], (ii) pre-micellar aggregation[46], (iii) cyclodextrin-drug interactions[47,48,49] (iv) surfactant-cyclodextrin interactions[50-53], (v) drug-DNA interactions[54], and (vi) neutral water-soluble hydrophobic polymer-surfactant interactions[55,56,57].

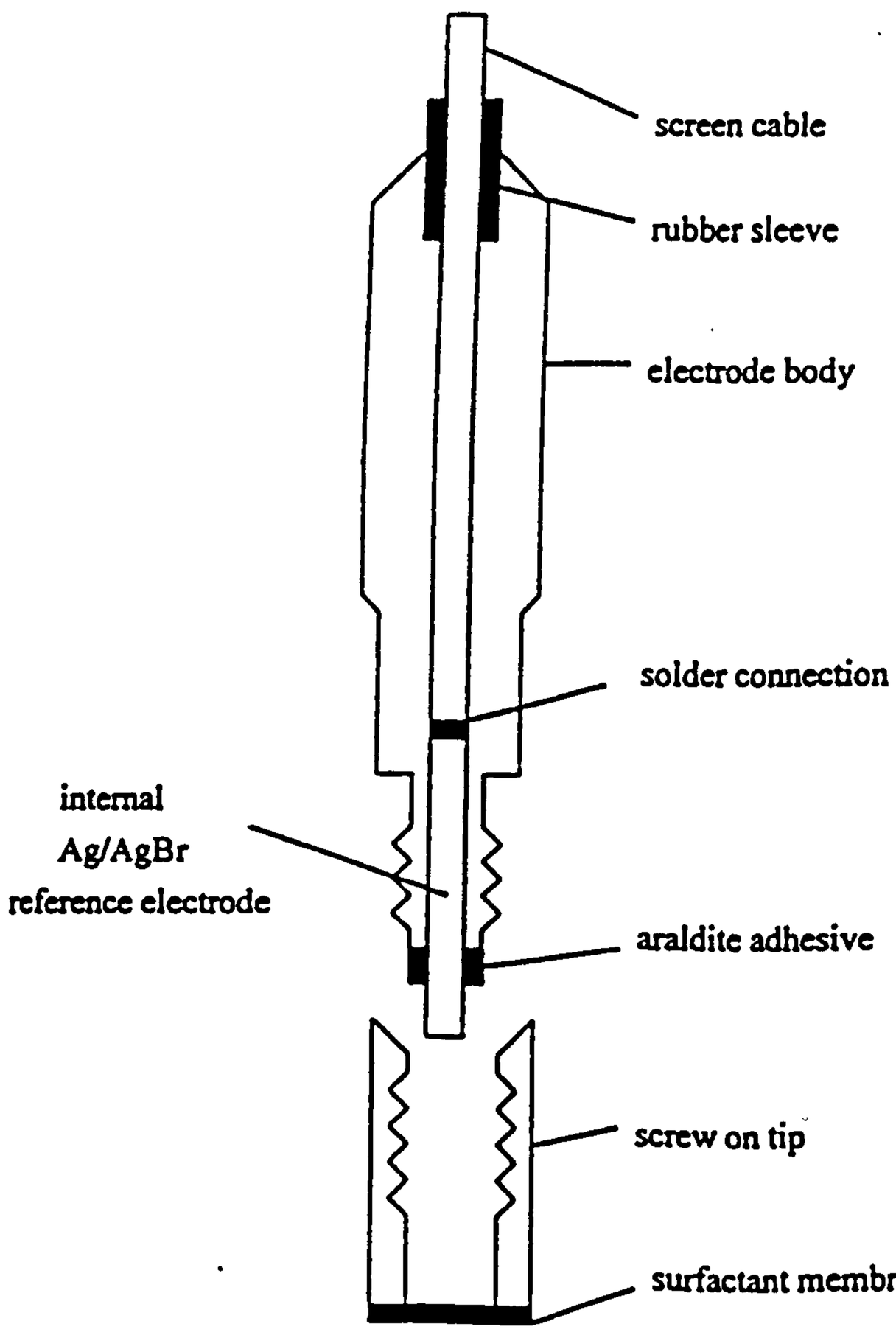

Figure 2-1: Schematic presentation of a surfactant selective electrode

Figure 2-2: Surface Tension data (mNm^{-1}) as a function of total CTAB concentration

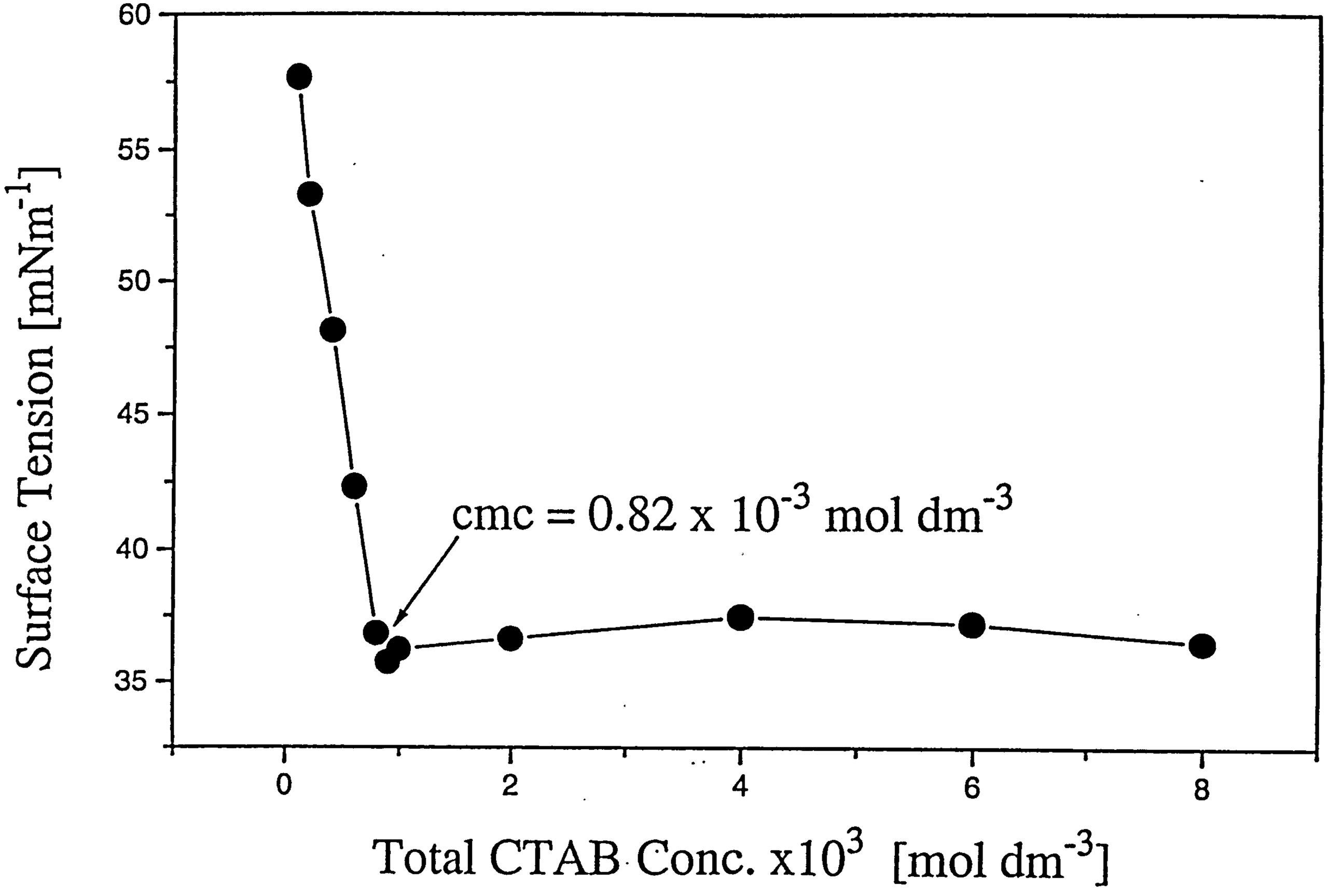

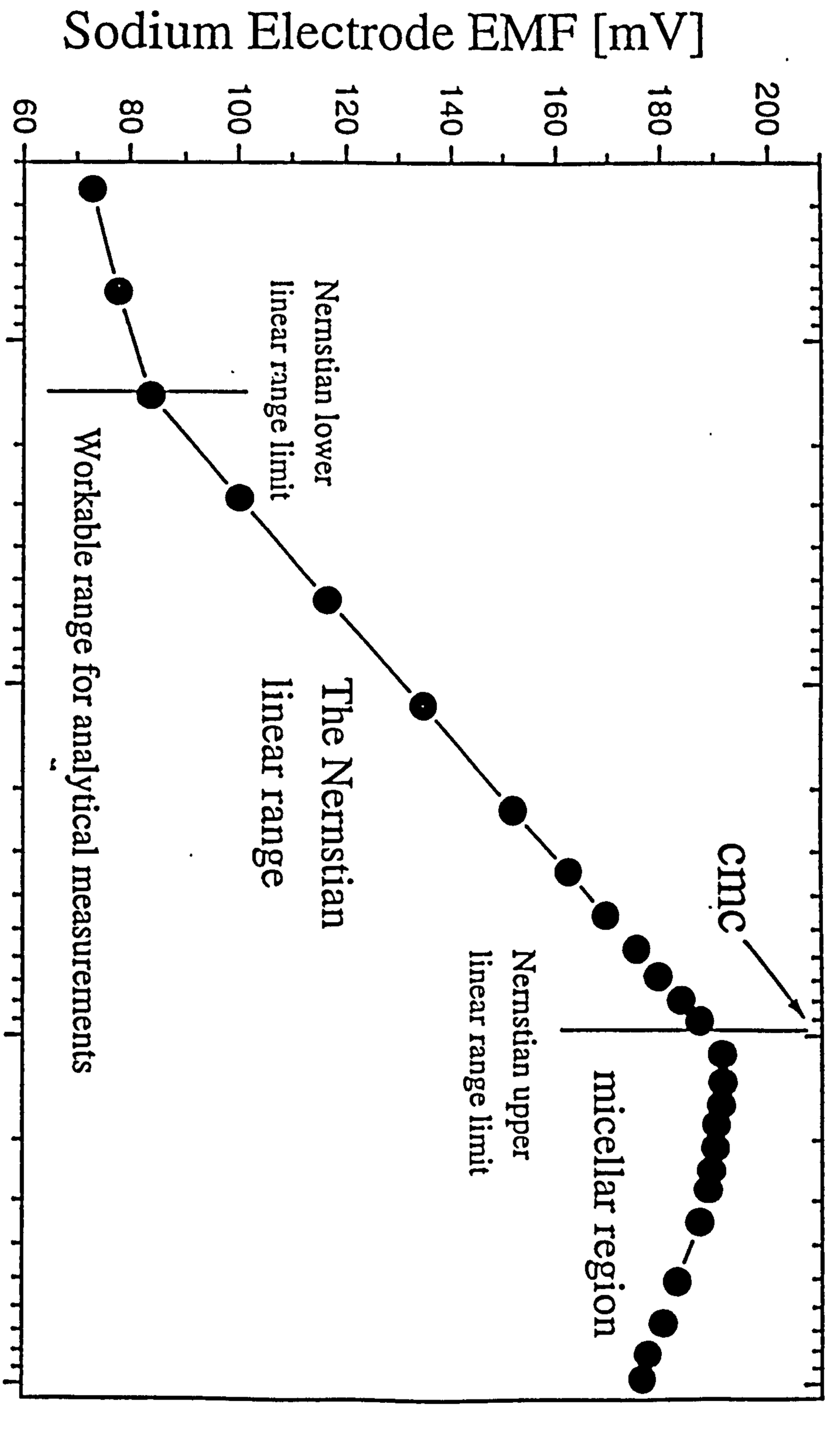

Figure 2-3: Pure CTAB EMF versus $\log(C_1)$ calibration plot

2.4 EXPERIMENTAL PROCEDURES

In the work described in Chapter 4 a cetyltrimethylammonium bromide selective electrode is used and the procedure for constructing the electrode is described below:

2.4.1 Preparation of cetyltrimethylammonium bromide PVC membrane

Although procedures of formulating surfactant cation-selective membrane are generally the same, they differ to some extent in detailed specific steps. In this sub-section the experimental procedures used to prepare cetyltrimethylammonium cation-selective membrane will be describe in detail.

2.4.1.1 Purification of CTAB and conditioning of PVC

10.0 g of cetyltrimethylammonium bromide (CTAB or $CH_3(CH_2)_{15}N^+(CH_3)_3Br^-$) was recrystallized three times from ethanol (AnalaR)[9]. The CTAB crystals formed in cold ethanol were washed using cold ethanol first and finally with double distilled deionized water in a buchner sinitered filter. The sample was then put into a vacuum dessicator to dry overnight at room temperature. The purity of CTAB was checked using surface tension measurements (Figure 2-2) and the cmc's compared well with literature values.

500 mg of purified poly(vinylchloride) (PVC) with 0.1% carboxylic ionic end groups (0.1%-COO^-H^+) was dissolved into 30 ml stirred doubly distilled tetrahydrofuran (THF). This

2.4 EXPERIMENTAL PROCEDURES

In the work described in Chapter 4 a cetyltrimethylammonium bromide selective electrode is used and the procedure for constructing the electrode is described below:

2.4.1 Preparation of cetyltrimethylammonium bromide PVC membrane

Although procedures of formulating surfactant cation-selective membrane are generally the same, they differ to some extent in detailed specific steps. In this sub-section the experimental procedures used to prepare cetyltrimethylammonium cation-selective membrane will be describe in detail.

2.4.1.1 Purification of CTAB and conditioning of PVC

10.0 g of cetyltrimethylammonium bromide (CTAB or $CH_3(CH_2)_{15}N^+(CH_3)_3Br^-$) was recrystallized three times from ethanol (AnalaR)[9]. The CTAB crystals formed in cold ethanol were washed using cold ethanol first and finally with double distilled deionized water in a buchner sinitered filter. The sample was then put into a vacuum dessicator to dry overnight at room temperature. The purity of CTAB was checked using surface tension measurements (Figure 2-2) and the cmc's compared well with literature values.

500 mg of purified poly(vinylchloride) (PVC) with 0.1% carboxylic ionic end groups (0.1%-COO^-H^+) was dissolved into 30 ml stirred doubly distilled tetrahydrofuran (THF). This

was followed by dissolving 72.9 mg of purified CTAB in 200 ml triple distilled water (2.11 mmol dm^{-3} CTAB is roughly twice the cmc of CTAB ≈ 1.0 mmol dm^{-3}) was contained in a 500 ml beaker. The 150 ml of specially dried methanol (GPR) was added to the CTAB solution. Then the solution of PVC in THF was added drop by drop and a clean fibre-precipitate of CTAB-PVC complex precipitated out while the solution was kept stirred throughout. After complete addition of the PVC/THF solution, the solution was left to stir for 48 hours to complete thorough precipitation and conditioning. After this process the CTAB-PVC complex was filtered, washed thoroughly using doubly distilled deionized water and left to dry overnight in a vacuum dessicator at room temperature.

2.4.1.2 Casting of the membrane and making of the CTAB selective membrane electrode

180 mg of polymeric plasticiser, Elvaloy 742 (Du Pont) (60%), was dissolved in 30 ml of double distilled THF and stirred until total dissolution. To this plasticiser-THF solution 120 mg of CTAB-PVC complex (40%) was added gradually and then left to stir until there was no gel left in the solution (approx. 2 to 3 hours). The solution was filtered into a flat bottomed beaker (55 mm diameter) using a Type LC 10 μm filter (Millipore SA, Molsheim, France). The beaker containing the filtrate was sealed by two or three normal filter papers and then covered by an appropriate beaker. This keeps the filtrate dust-free as gradual THF evaporation occurs. The beaker was placed on a

levelled flat position in order to get a membrane of uniform thickness. Evaporation took 2 to 4 days depending on the surrounding conditions.

The electrode body of the surfactant ion selective electrode is a modified calcium ion E.D.T. research electrode (ISE 310) shown in Figure 2.1. The calcium membrane on the electrode tip was removed to be replaced by a PVC membrane. The internal silver coil was used without changing although in many cases it is replaced by silver rod[51,58-60]. The solid CTAB-PVC membrane was peeled off from the beaker using a scalpel blade supported by doubly distilled deionized water. A circular membrane piece was then cut using cork borer size 6 or 7 to fit the electrode tip. It was attached to an electrode tip using freshly doubly distilled THF. The seal to the tip was tested to make sure no leakage occurs.

2.4.2 Calibration of CTAB selective membrane electrode

2.4.2.1 Preparation of solutions

Three types of solutions are prepared for a calibration experiment: (i) the inner reference solution, (ii) the initial sample solution, and (iii) a concentrated sample solution. To prepare these solutions; purified CTAB (section 2.4.1.1), sodium bromide of AnalaR grade and doubly distilled deionized water were used.

The inner reference solution consists of 1×10^{-5} mol dm^{-3}

CTAB in 1 x 10^{-4} mol dm^{3} sodium bromide. This solution is filled into the screw on tip (Figure 2-1) which in turn is screwed to the electrode body to cover the inner reference electrode (in this case Ag/AgBr reference electrode) to complete the CTAB selective membrane electrode.

The initial sample solution consists of 1 x 10^{-4} mol dm^{3} sodium bromide only. The initial sample volume required depends on the concentration requirement of the experiment. However, a minimum volume required should be capable of immersing the electrode tip. In this work a minimum of 20 ml is required and most experiments were carried out using initial volumes 25 and 30 ml.

The aim here is to keep the concentration of sodium bromide constant and equal on both sides of the membrane. Due to the permselectivity nature of surfactant electrodes, sodium ions are competitors and can interfere with measurement of the surfactant ion activity. This problem is completely eradicated by eliminating the 'concentration gradient' between the two sides of the membrane for sodium ions.

The concentrated CTAB solution is made in 1 x 10^{-4} mol dm^{3} sodium bromide. The concentration of CTAB used depends on the concentration requirement of the experiment. Unfortunately, CTAB due its low cmc poses limitations to the concentration that can be handled at room temperature. In addition, CTAB concentrations as low as 5 x 10^{-2} mol dm^{3}

solidify around 20°C to 25°C. It was possible to make 1 x 10^{-1} mol dm^{-3} but the solution was kept in a warm water bath at around 40°C to 50°C. This allowed the experiment to be carried out to CTAB concentration as high as 2.5 x 10^{-2} mol dm^{-3}. Addition of concentrated CTAB solution into a test solution was carried out using 0.2 ml and 2.0 ml microliter syringes GS-1100 and GS-1200 (GILMONT) respectively.

2.4.2.2 The Calibration Experiment

The cell is set up consisting of a surfactant selective membrane electrode as a working electrode and a sodium ion electrode (Kent, EIL) as a reference electrode,

CTAB-ISE | Sample Solution | Sodium ion Electrode

In order to make observation easier on EMF changes corresponding to CTAB concentration changes, a standard addition technique is used. In this addition technique, additions are made in such a way that concentration changes double, either in a single addition or in a number of additions (Table 2.1). Let changes of concentration $C_1(i)$ to $C_1(f)$ be such that $C_1(f) = 2C_1(i)$ with Nernst equations

$$E_{cell}(i) = E^{\circ}_{cell} + (2.303RT/F).\log(C_1(i))$$

and

$$E_{cell}(f) = E^{\circ}_{cell} + (2.303RT/F).\log(C_1(f))$$

respectively. The difference $E_{cell}(r) - E_{cell}(i)$ gives

$$E_{cell}(f) - E_{cell}(i) = (2.303RT/F).\log(2) = 17.8091 \text{ mV}$$

and for a 10-fold concentration change $C_1(f) = 10C_1(i)$ and the difference

$$E_{cell}(f) - E_{cell}(i) = (2.303RT/F).\log(10) = 59.16057 \text{ mV}$$

The values 17.8091 mV and 59.16057 mV at 298.15K gives, on the spot, evaluation of the electrode and the experiment in general. Practically values ranging from 16-18.5 mV and 55-60 mV for a two-fold change and ten-fold change respectively are experimentally acceptable. Table 2.1 and Figure 2-3 shows raw experimental data.

Table 2.1: EMF data for CTAB electrode in 10^{-4} mol dm^{-3} sodium bromide

C_1	E_{cell}	ΔE	C_1	E_{cell}	ΔE
0.0036	72.6	-	1.1300	191.6	-
0.0072	77.6	-	1.3600	191.7	-
0.0144	83.6	-	1.5800	191.4	-
0.0287	100.1	16.5	1.8000	190.5	-
0.0574	116.5	16.4	2.1000	190.3	-
0.1150	134.7	18.2	2.4500	189.6	-
0.2290	151.9	17.2	2.7800	189.0	-
0.3430	162.5	-	3.4500	187.4	-
0.4570	169.7	16.8	5.0800	183.2	-
0.5710	175.6	-	6.6500	180.6	-
0.6840	179.7	-	8.1600	177.7	-
0.7970	184.0	-	9.6190	176.6	-
0.9100	187.4	17.7			

Nernstian parameters: Slope = 58.002, Intercept = 363.300
Correlation Coefficient = 0.999718

2.5 REFERENCES

1. BARD, A.J. and FAULKNER, L.R. "*Electrochemical Methods: Fundamentals and Applications*", New York (1980).

2. BATES, R.G. and ALFENAAR, M. in "*Ion-Selective Electrodes*": Proceedings of a Symposium held at Gaithersburg, Maryland Jan 30-31 (1969) Edited by R.A. DURST.

3. KORYTA, J. Ions, *Electrodes and Membranes*, John Wiley and Sons, New York (1982).

4. HUGHES, W.S. *J. Am. Chem. Soc.*, 44 (1922) 2860.

5. KERRIDGE, P.T. *Biochem. J.*, 19 (1925) 611.

6. ELDER, Jr., L.W. *J. Am. Chem. Soc.*, 51 (1929) 3266.

7. KAHLER, H.; De EDS, F.; ROSENTHAL, S.M. and VOEGTLIN, C. *Am. J. Phys.*, 91 (1930) 225.

8. BAUMANN, E.W. *J. Electroanal. Chem.*, 34 (1972) 238.

9. CATON, Jr., D.C. and WOLFE, C.R. *Anal. Chem.*, 43 (1971) 660.

10. DURSELEN, L.F.J.; WEGMANN, D.; MAY, K.; OESCH, U. and SIMON, W. *Anal. Chem.*, 60 (1988) 1455.

11. FEDOTOV, N.A.; KHITOV, L.M.; ZARINSKII, V.A.; KOTOTYRKINA, I. YA. and LAZARAV, V.G. *Zh. Anal. Khim.*, 37 (1982) 80.

12. WHITFIELD, W. *Electrochim. Acta*, 15 (1970) 83.

13. FISHER, A.R. *Zh. Anal. Khim.*, 40 (1985) 935.

14. LESOURD, J.B.; PENELOUX, A. and DOUCET, Y. *J. Phys. - Chim. Biol.*, 72 (1975) 153.

15. COVINGTON, A.K. in "*Ion-Selective Electrodes*", DURST, R.A. Editor, Proceedings of a Symposium held at the National Bureau of Standards Gauthensburg, Maryland, Jan. 30-31, 1969, Chapter 4.

16. FØRLAND, K.S.; FØRLAND, T. and RATKJE, S.K. "*Irreversible Thermodynamics: Theory and Applications*", John Wiley & Sons Ltd., Chichester, (1988).

17. CROW, D.R. "*Principles and Applications of Electrochemistry*", 2nd Edition, Chapman and Hall, London, (1979).

18. KORYTA, J. and STULIK, K. "*Ion Selective Electrodes*", Cambridge University Press, Cambridge, U.K.(1975).

19. SKOOG, D.A. and WEST, D.M. "*Fundamentals of Analytical Chemistry*", 4th Edition, Holt-Saunders Japan, Tokyo (1982).

20. MWAKIBETE, H., Unpublished results.

21. NERNST, W. *Z. Physik. Chem.*, 2 (1988) 613.

22. NERNST, W. *Z. Physik. Chem.*, 4 (1988) 129.

23. PLANCK, M. *Ann. Phys. Chem. N.F.*, 39 (1890) 196.

24. PLANCK, M. *Ann. Phys. Chem.* N.F., 40 (1890) 561.

25. CREMER, M. *Z. Biol.*, 47 (1906) 562.

26. HABER, F. and KLEMENSIEWICZ, Z. *Z. Physik. Chem.*, 67 (1909) 385.

27. EISENMAN, G.; RUDIN, D.O. and CASBY, J.V. *SCIENCE N.Y.*, 126 (1957) 871.

28. SOLLNER, K. and SHEAN, G.M. *J. Am. Chem. Soc.*, 86 (1964) 1901.

29. SOLLNER, K. and SHEAN, G.M. *Protoplasma*, 63 (1964) 174.

30. TANDELOO, H.J.C. *J. Biol. Chem.*, 113 (1936) 333.

31. KOLTHOFF, I.M. and SANDERS, H.L. *J. Am. Chem. Soc.*, 59 (1937) 416.

32. PUNGOR, E. and HALLOS-ROKOSINYI, E. *Acta Chim. Acad. Sci. Hung.*, 27 (1961) 63.

33. ROSS, J.W. *Science N.Y.*, 156 (1967) 3780.

34. GAVACH, C. *J. Chim. Phys.*, 64 (1967) 799.

35. GAVACH, C. and SETA, P. *Anal. Chim. Acta*, 50 (1970) 407.

36. BIRCH, B.J. and CLARKE, D.E. *Anal. Chim. Acta*, 61 (1972) 159.

37. BIRCH, B.J. and CLARKE, D.E. *Anal. Chim. Acta*, 67 (1973) 387.

38. FOGG, A.G.; PATHAN, A.S. and BURNS, D.J. *Anal. Chim. Acta*, 69 (1974) 238.

39. CUTLER, S.G.; HALL, D.G. and MEARES, P. *J.*

Electroanal. Chem., 85 (1977) 145.

40. CUTLER, S.G.; HALL, D.G. and MEARES, P. *J. Chem. Soc. Faraday Trans. 1*, 74 (1978) 1758.

41. DAVIDSON, C. J. *PhD Thesis*, University of Aberdeen (1983).

42. BROMLEY, N.C.: *Unilever Internal Report* (1985)

43. GHARIBI, H.; TAKISAWA, N.; BROWN, P.; THOMASON, M.A.; PAINTER, D.M.; BLOOR, D.M.; HALL, D.G. and WYN-JONES, E. *J. Chem. Soc. Faraday Trans. 1*, 87 (1991) 707.

44. GHARIBI, H.; PALEPU, R.; TIDDY, G.J.T.; HALL, D.G. and WYN-JONES, E. *J. Chem. Soc. Chem. Comm.*, 115 (1990).

45. GHARIBI, H.; PALEPU, R.; BLOOR, D.M. and WYN-JONES, E. *Langmuir*, 8 (1992) 782.

46. WAN-BADHI, W.A.; MWAKIBETE, H.; BLOOR, D.M.; PALEPU, R.; and WYN-JONES, E. *J. Phys. Chem.*, 96 (1992) 918.

47. TAKISAWA, N.; BROWN, P.; BLOOR, D.M.; HALL, D.G. and WYN-JONES, E. *J. Chem. Soc. Faraday Trans. 1*, 85 (1989) 2099.

48. THOMASON, M.A.; MWAKIBETE, H. and WYN-JONES, E. *J. Chem. Soc. Faraday Trans.*, 86 (1990) 1511.

49. MWAKIBETE, H.; BLOOR, D.M. and WYN-JONES, E. *J. Incl. Phenomena*, 10 (1991) 497.

50. WAN-YUNUS, W.M.Z.; TAYLOR, J.; BLOOR, D.M.; HALL, D.G. and WYN-JONES, E. *J. Phys. Chem.*, 96 (1992) 8979.

51. LUKAS, T. *PhD Thesis*, University of Salford, UK (1990).

52. TAYLOR, J. Unpublished results.

53. MWAKIBETE, H.; BLOOR, D.M. and WYN-JONES, E. *Langmuir* in press (1994).

54. DALY, C.L. *MSc. Thesis*, University of Salford (1987).

55. WAN-BADHI, W.A. *PhD Thesis*, University of Salford, UK (1993).

56. WAN-BADHI, W.A.; PALEPU, R.; BLOOR, D.M.; HALL, D.G.; and WYN-JONES, E. *J. Phys. Chem.*, 95 (1991) 6642.

57. WAN-BADHI, W.A.; WAN-YUNUS, W.M.Z.; BLOOR, D.M.; HALL, D.G.; and WYN-JONES, E. *J. Chem. Soc. Faraday Trans.*, 89 (1993) 2737.

58. GHARIBI, H., *PhD Thesis*, University of Salford, 1990.

59. TAKISAWA, N.; HALL, D.G.; WYN-JONES, E. and BROWN, P. *J. Chem. Soc., Faraday Trans. 1*, 84 (1988) 3054.

60. MWAKIBETE, H., *MSc Thesis*, University of Salford, 1989.

CHAPTER THREE: THERMODYNAMICS OF MICELLE FORMATION

3.1 INTRODUCTION

Classical literature on thermodynamics of micelle formation (micellization) have predominantly used two models[1-4]; the pseudo-phase separation model and the mass-action model, to explain surfactant aggregation phenomenon in aqueous as well as non-aqueous solutions.

In the pseudo-phase separation model the micelle is assumed to be a separate phase. With this model, the concentration of monomeric surfactant is expected to be constant at cmc and above[4]. The aggregation numbers of most surfactant micelles range from 30 to 2000 and are not quite large enough to treat the micelle as a separate phase, though it seems adequate to call it a pseudo-phase[3,5]. The critical micelle concentration (cmc) in this model is considered as a solubility limit[4] or saturation concentration[3] of the monomeric species, which, when exceeded leads to the production of a new phase (the micellar phase). Due to this phenomenon the cmc is a narrow transition (critical) concentration range between the two assumed pseudo-phases. The pseudo-phase separation model, therefore, treats monomeric surfactant species below cmc as a pseudo-phase and a micelle pseudo-phase at and above cmc.

The mass-action model treats micelles and monomeric surfactant species to be in a chemical equilibrium. This

treatment makes the mass-action model unaffected by how large or small are the aggregation numbers of the micelles. However, in most recent work the two models have been used simultaneously depending on the nature of results required.

Highly advanced surfactant micellization models by Tanford[1], Israelachvili[6], Hall[7,8], Aamodt[9], Nagarajan[10-13] and Ruckenstein[14,15] have been developed in recent years. These models attempt, in general, to recognize the importance of other thermodynamic factors. Tanford[1] and Israelachvili[6] emphasize more on the importance of molecular geometry in defining the characteristics of an aggregating system. However, these approaches are mathematically intensive and need the highest level of mathematical knowledge and will not be treated here; rather an overview of micellization will be given.

3.2 THERMODYNAMICS OF MICELLE FORMATION TREATED BY A PSEUDO-PHASE SEPARATION MODEL

To use this model, two standard states in the two assumed pseudo-phases are defined. In the monomeric surfactant species in water the standard state is defined as a solvated surfactant monomer at unit mole fraction (χ_s=1). On the other hand in the micellar pseudo-phase the micelle is treated as the standard state.

If we define chemical potential μ_s and μ_c for monomeric surfactant and counterion species in water, μ_M for the

micelle pseudo-phase respectively, then utilizing the equality of chemical potentials in the two pseudo-phases at equilibrium[3], $\mu_s + \mu_c = \mu_M$, and the activity/chemical potential definition for the monomeric surfactant phase,

$$\mu_{s/c} = \mu^{\circ}_{s/c} + RT\ln(a_s) + RT\ln(a_c) \qquad (3\text{-}1)$$

where $\mu_{s/c} = \mu_s + \mu_c$ and $\mu^{\circ}_{s/c} = \mu^{\circ}_s + \mu^{\circ}_c$. In the micellar phase, the chemical potential is given as

$$\mu_M = \mu^{\circ}_M + RT\ln(a_M) \qquad (3\text{-}2)$$

if the micellar pseudo-phase is assumed to resemble a solid phase, $a_M \sim 1$ and $RT\ln(a_M) \sim 0$. These considerations reduces equation (3-2) to

$$\mu_M = \mu^{\circ}_M \qquad (3\text{-}3)$$

If experiments are carried out at low surfactant concentration ($C_s < 0.1$ mol dm^{-3}, Debye-Hückel limiting law), which is the case for most electrochemical measurements, then activities a_s and a_c can be approximated to concentrations C_s and C_c respectively. It is also known that a certain fraction, α, of surfactant molecules involved in micellization dissociate leaving free counterions and so the micelles become charged to a certain degree. Utilizing this fact, the concentration C_s and C_c are not equal but relate as $C_c = (1-\alpha)C_s$ and equation (3-1) becomes

$$\mu_{s/c} = \mu^{\circ}_{s/c} + (2-\alpha)RT\ln(C_s) \qquad (3\text{-}4)$$

where $\mu^{\circ}_{s/c}$ and C_s are the chemical potential in the standard

state and concentration of the monomeric surfactant species respectively and α is the effective degree of dissociation of surfactant molecules in the micelles. For fully ionized ionic surfactants $\alpha = 1$ and so $2-\alpha=1$ which removes the coefficient $2-\alpha$ in equation (3-4) to give nonionic like chemical potential equation, $\mu_s = \mu^\circ_s + RT\ln(C_s)$.

Free monomeric surfactant concentration C_s can be approximated as a mole fraction χ_s $\{\chi_s = n_s/(n_s+n_w)$; where n_s and n_w are the number of moles of free monomeric surfactant and water in one litre of solution respectively at low concentration. Accordingly the standard free energy change of micellization is[16]

$$\Delta G^\circ_{mic} = (2-\alpha)RT\ln(\chi_{cmc}). \qquad (3\text{-}5)$$

Equation (3-5) may be converted into molar concentration units as[4]; $\Delta G^\circ_{mic} = (2-\alpha)RT(\ln(cmc) - \ln(w))$ where w is the molar concentration of water (w = 55.3 moles per litre at 25°C).

Standard enthalpy and entropy changes of micellization, ΔH°_{mic} and ΔS°_{mic} respectively, follow accordingly from the known standard free energy change of micellization, ΔG°_{mic}, using a classical thermodynamic relationship[17]; $\Delta G^\circ_{mic}=\Delta H^\circ_{mic}-T\Delta S^\circ_{mic}$, in which $\Delta H^\circ_{mic}=T^2\partial(\Delta G^\circ_{mic}/T)/\partial T$ and $\Delta S^\circ_{mic} = \partial(\Delta G^\circ_{mic})/\partial T$ if ΔH°_{mic} and ΔS°_{mic} are constant over the temperature range studied respectively. In this treatment data are at varied temperature. When equation (3-5) is written in terms of

$\log(\chi_{cmc})$ then[17]

$$\log(\chi_{cmc}) = \frac{\Delta G^{\circ}_{mic}}{2.3(2-\alpha)RT} \qquad (3-6)$$

and when the degree of counterion binding β (α=1-β) is introduced into equation (3-6): ΔG°_{mic}=2.3(1+β)RT$\log(\chi_{cmc})$[18].

For nonionic surfactants undissociated molecules aggregate and so the idea of counterion binding is invalid. From this criterion we can assume the value of α to be zero and ß is meaningless reducing equation (3-5) to just $\Delta G^{\circ}_{mic} = RT\ln(\chi_{cmc})$ or $\Delta G^{\circ}_{mic} = 2.3RT\log(\chi_{cmc})$.

3.3 THERMODYNAMICS OF MICELLE FORMATION TREATED BY A MASS-ACTION MODEL

3.3.1 Nonionic surfactant systems

The mass-action model treats micelles and monomeric surfactant species to be in a chemical equilibrium with equilibrium constant[2,4,19,20]

$$K_m = [S_n]/[S]^n \qquad (3-7)$$

where S and S_n are the monomeric surfactant species and micelles respectively. If C_m and m_1 denote surfactant in micellar form and monomeric form then equation (3-7) becomes

$$K_m = C_m/(m_1)^n \qquad (3-8)$$

At certain stages around the equilibrium total surfactant concentration C_{eq}, micellar and free monomeric concentration

are equal, that is, $m_1 = C_m = 0.5C_{cq}$. It is well known that total surfactant concentration (C_t) is the sum of micellar (C_m) and free monomeric concentration (m_1), that is, $C_t = m_1 + C_m$ which leads to the relation[2] $C_m/C_{cq} = 2^{n-1}m_1/C_{cq}$. Standard free energy change of micellization derived from mass-action model is given by

$$\Delta G^{o}_{mic} = - RT\ln[S_n] + nRT\ln[S] \qquad (3\text{-}9)$$

At the critical micelle concentration (cmc) or on its neighbourhood, $[S_n] \approx [S] \approx$ cmc. After this consideration the standard free energy change of micellization per mole micelle is derived from equation (3-9) as

$$\Delta G^{o}_{mic} = (n-1)RT\ln(\chi_{cmc}) \approx nRT\ln(\chi_{cmc}) \qquad (3\text{-}10)$$

and per mole surfactant[21]

$$\Delta G^{o}_{mic}/n = RT\ln(\chi_{cmc}) \qquad (3\text{-}11)$$

3.3.2 Ionic surfactant systems

For ionic surfactants, the degree of surfactant molecules dissociation per micelle (α) plays an important role. The chemical equilibrium in this case involves ionic species S^+ (surfactant cation) and C^- (the counterion) and micelles M as follows

$$nS^+ + (n-p)C^- = M \qquad (3\text{-}12)$$

with equilibrium constant

$$K_M = C_M/C_s^n.C_c^{n-p} \qquad (3\text{-}13)$$

where n and n-p are the surfactant and counterion stoichiometric numbers respectively and C_M is the concentration of aggregated surfactant. When equation (3-9) is extended to this system the free energy of micellization per mole surfactant molecules for this system is given by

$$\Delta G^{\circ}_{mic} = RT[\ln(C_s) + (1-p/n)\ln(C_c) - (1/n)\ln(C_M)] \qquad (3\text{-}14)$$

At cmc $C_s = C_c$ = cmc for a fully ionized surfactant. For higher aggregation numbers (n > 30), which is true for most surfactant systems[3], a term $-(1/n)\ln(C_M)$ in equation (3-14) is negligible and can be neglected. If we take $\alpha = p/n$ then equation (3-14) can be rewritten as[16]

$$\Delta G^{\circ}_{mic} = (2-\alpha)RT\ln(\chi_{cmc}) \qquad (3\text{-}15)$$

which when rearranged gives equation (3-6) derived by the pseudo-phase separation model in section 3.2.

3.4 TREATMENT BY MASS-ACTION MODEL INVOLVING THE MEAN ACTIVITY COEFFICIENT $\gamma_{\pm}$

If we denote C_3 as the concentration of added salt in the system then concentrations of surfactant ions C_s and C_c are given as C_s = cmc and C_c = cmc + C_3. Using these definitions, the mean activity coefficient $\gamma_{\pm}$ and equations (3-13) and (3-14) we obtain

$$\Delta G^{\circ}_{mic}/2.3RT = \log[(cmc).\gamma_{\pm}] + (1-\alpha)\log[(cmc+C_3).\gamma_{\pm}] - (1/n)\log(C_M) \qquad (3\text{-}16)$$

again for larger aggregation numbers the term $-(1/n)\log(C_M)$

in equation (3-16) may be ignored, giving the expression[22]

$$\log[(cmc)\gamma_{\pm}] = \Delta G^{\circ}_{mic}/2.3RT - (1-\alpha)\log[(cmc+C_3).\gamma_{\pm}] \quad (3-17)$$

which can be used to determine the effective degree of micelle dissociation (α) as well as the standard free energy of micellization, ΔG°_{mic}, by just doing measurements at different added salt concentration. A plot of $\log[(cmc).\gamma_{\pm}]$ against $\log[(cmc+C_3).\gamma_{\pm}]$ is linear with $-(1-\alpha)$ and $\Delta G^{\circ}_{mic}/2.3RT$ as slope and intercept respectively. So what is needed in this exercise is the cmc values at different added salt, the concentrations of added salt (C_3) and the mean activity coefficient ($\gamma_{\pm}$). These type of data are provided directly from electrochemical measurements of surfactant ions and counterions.

3.5 CONTRIBUTING FORCES TO THE FREE ENERGY CHANGE OF SURFACTANT MICELLIZATION

Micellization represents a balance of forces tending to favour aggregation and those opposing aggregation. There are hydrophobic forces which provide the driving force for the system to aggregate and the repulsive forces between head groups limits the size and shape that a micelle can attain. The standard free energy of transfer in favour of aggregation is caused by hydrophobic effect[1] from both $-CH_2-$ and terminal $-CH_3$ groups, that is, $\Delta G^{\circ}_{mic}(-CH_2-)$ and $\Delta G^{\circ}_{mic}(-CH_3)$ respectively. On the other hand the work required to overcome inter-head-group repulsion to a certain level and bring the hydrophilic head groups into close proximity at

the micelle phase, $\Delta G^{\circ}_{mic}(-W)$, is of paramount importance in micellization processes. However, both factors must vary with the micelle size. For example, if the standard free energy gained in micellization by virtue of the hydrophobic effect were independent of size, there would be no lower limit to the micelle size and no way to account for the observed cooperativity of micelle formation. With this conception, the standard free energy change of micellization, ΔG°_{mic}, can be summarized as a sum of these major contributing forces

$$\Delta G^{\circ}_{mic} = \Delta G^{\circ}_{mic}(-W) + (n_c-1).(\Delta G^{\circ}_{mic}(-CH_2-)) + \Delta G^{\circ}_{mic}(-CH_3) \qquad (3-18)$$

where $\Delta G^{\circ}_{mic}(-CH_2-)$ is a constant contribution from each $-CH_2-$ group and n_c is the surfactant hydrophobic chain length. The standard free energy change contribution from the terminal CH_3- group is equal to $\Delta G^{\circ}_{mic}(-CH_2-)$ + G and so differs by a constant G from the free energy change contributed by each $-CH_2-$ groups in the chain. Different contributing factors are summarized in equation (3-19)

$$\Delta G^{\circ}_{mic} = \Delta G^{\circ}_{mic}(-W) + n_c.(\Delta G^{\circ}_{mic}(-CH_2-)) + G \qquad (3-19)$$

$\Delta G^{\circ}_{mic}(-W)$ is independent of the chain-length (n_c). So after this consideration equation (3-19) and χ_{cmc} = cmc/w is substituted into equation (3-6) to yield[16]

$$\log(cmc) = \frac{\Delta G^{\circ}_{mic}(-W)+G}{2.3(2-\alpha)RT} + n_c.\left\{\frac{\Delta G^{\circ}_{mic}(-CH_2-)}{2.3(2-\alpha)RT}\right\} + \log(w) \qquad (3-20)$$

where w is the number of moles of water per litre of

solution (w = 55.3 at 25°C) and the parameter G originates from the extra contribution from the terminal CH_3- group. The magnitude of free energies $\Delta G^{\circ}_{mic}(-CH_2-)$ and $\Delta G^{\circ}_{mic}(-CH_3)$ are available in literature[1,6,23] determined by the laws of mass action and phase separation ($\Delta G^{\circ}_{mic}(-CH_2-) = -3449$ J mol^{-1} and $\Delta G^{\circ}_{mic}(-CH_3) = -8778$ J mol^{-1}). From these values the value of a constant G can be estimated as $G = \Delta G^{\circ}_{mic}(-CH_3) - \Delta G^{\circ}_{mic}(-CH_2-) = -5329$ J mol^{-1}.

The logarithm of critical micelle concentration (cmc in moles per litre) is linearly dependent on the chain length and so fits well in the Klevens[24] equation

$$\log(cmc) = A - Bn_c \qquad (3\text{-}21)$$

where A and B are constants specific to a homologous series of surfactants under constant conditions (temperature, pressure, etc) and n_c is the chain length (number of carbon atoms in the hydrophobic chain). The value A is approximately constant for a particular ionic head group. B is a constant, approximately equal to log2 for all paraffin (Alkyl) chain of ionic surfactants with single ionic head group. When this equation is matched to equation (3-20) the Klevens values A and B are given by

$$A = \frac{\Delta G^{\circ}_{mic}(-W)+G}{2.3(2-\alpha)RT} + \log(w) \qquad (3\text{-}22a)$$

and

$$B = - \frac{\Delta G^{\circ}_{mic}(-CH_2-)}{2.3(2-\alpha)RT} \qquad (3\text{-}22b)$$

Equation (3-20) does not apply for nonionic and zwitterionic surfactants, however, equivalent parameters to constants A and B, A^* and B^* respectively are derived from empirical relationship between cmc and the number of oxyethylene $(OE)_y$ group present[1,25], $\log(cmc) = A^* + B^*y$. A^* and B^* are constants related to a given hydrophobic group. The term $\Delta G^{\circ}_{mic}(-W)/2.3(2-\alpha)RT$ in equation (3-20) and (3-22a) becomes insignificant and so it is neglected.

The critical micelle concentration (cmc) and the effective degree of micellar dissociation (α) are easily derived from electrode data. Using these values together with tabulated values of A and B, the approximate estimate values of $\Delta G^{\circ}_{mic}(-W)$ and $\Delta G^{\circ}_{mic}(-CH_2-)$ can be estimated for any surfactant system without added salt. For surfactant systems with added salt $\Delta G^{\circ}_{mic}(-W)$ is estimated as

$$\Delta G^{\circ}_{mic}(-W) = \Delta G^{\circ}_{mic} - n_c.\Delta G^{\circ}_{mic}(-CH_2-) - G \qquad (3.22c)$$

where G = 5329 J mol^{-1}.

3.6 AN ADDITIVE CONTRIBUTION APPROACH FOR THERMODYNAMIC PARAMETERS OF MICELLE FORMATION BASED ON THE ION BINDING MODEL

3.6.1 The Gibbs free energy change of micelle formation

The system to be considered here is limited to concentrations in the neighbourhood of the cmc and assumed,

apart from solvent, to consist of micelles, monomers, counterions, and coions only. The micelles formed in this system will be assumed to be monodisperse, independent of surfactant concentration (but not coion concentration) and micelles remain spherical in shape even though N may change with added salt. Polydispersity is unnecessary and an unimportant complication which in this treatment will be avoided[23]. And finally the solute species shall be considered to be non-interacting except via the diffusion potential and the very strong, very short-range interactions which cause micelles to form.

For these kind of micelles thermodynamic properties for micelle formation are well characterized by a thermodynamic equilibrium between monomers, counterions and micelles given in an equation of the form[23,26-28]

$$KC_m = C_1^N C_2^Q \qquad (3\text{-}23)$$

where C_m is the concentration of micelles, C_1 is the concentration of monomeric surfactant, C_2 is the total concentration of counterions (C_3+C_1), K is the equilibrium constant, N and Q are the number of aggregated surfactant molecules and number of bound counterions per micelle respectively.

In order to avoid proliferating algebra; monomeric surfactant ions, counterions and coions will be assumed to be univalent. With this assumption and the requirement of

charge neutrality in the system brings the following equation

$$C = C_1 + NC_m = C_2 + QC_m - C_3 \qquad (3\text{-}24)$$

where C is the total surfactant concentration, and C_3 is the concentration of coions.

Equations (3-23) and (3-24) determines C_1, C_2 and C_m as functions of C and C_3. If we define C_o by the relation[23,26,28]

$$K = NC_o^{N-1}(C_3 + C_o)^Q \qquad (3\text{-}25)$$

then it can be shown that the system exhibits a critical micelle concentration (cmc) for large N given by cmc ≈ C_o. Equation (3-25) can be used to determine equilibrium constant (K) in terms of the experimentally known cmc. The concentration of micelles at C_o is zero and for large N as surfactant concentration increases, the concentration of micelles exhibits a step-function jump from an initial value of zero. The ratio C_m/C remains nearly constant with a slight decline until what is called second cmc[23,26] is exhibited at high surfactant concentration. On the other hand, with smaller N this behaviour becomes a much more gradual phenomenon.

If we define ß = Q/N as "the degree of counterion binding to micelles" and α (= 1-ß) as "the effective degree of micellar dissociation" then the cmc in mole fraction units is defined in terms of[23,29]

$$RT\ln(\chi_{cmc}) = \Delta G^{\circ}_{hc} - \beta RT\ln(\chi_{cmc} + \chi_3) \qquad (3\text{-}26)$$

where χ_{cmc} is the surfactant concentration in mole fraction units at cmc, χ_3 is the concentration of coions in mole fraction units, and ΔG°_{hc} is the constant hydrophobic free energy of transfer of hydrocarbon tails from water to the hydrophobic core[23,29,30] (an oil-like region which forms the micellar interior).

The equilibrium constant between monomer surfactant species and micelles is defined using the law of mass-action as[6,23]

$$\chi_N = N\chi_1^N \exp[N(\mu_1^{\circ} - \mu_N^{\circ})/RT] \qquad (3\text{-}27)$$

where χ_N/N is the concentration of micelles in mole fraction units, χ_1 is the concentration of monomeric surfactant in mole fraction units, μ_N° is the chemical potential of micelles of aggregation number N, and μ_1° is the chemical potential of monomeric surfactant species.

Upon rearrangement, equation (3-27) yields an equation relating concentration and chemical potential

$$RT\ln(\chi_1) - (RT/N)\ln(\chi_N/N) = \mu_N^{\circ} - \mu_1^{\circ} \qquad (3\text{-}28)$$

but the term $(RT/N)\ln(\chi_N/N) << RT\ln(\chi_1)$, for large N; $\chi_1 = \chi_{cmc}$ at cmc, and therefore from equation (3-28) the following equation is obtained

$$RT\ln(\chi_{cmc}) \approx \mu_N^{\circ} - \mu_1^{\circ} = \Delta G^{\circ}_{hc} + \Delta G^{\circ}_{s} \qquad (3\text{-}29)$$

where ΔG°_{s} is the free energy change contribution from headgroup, counterion and surface interaction[26] (also known as electrostatic interactions contribution)[29,31].

Equations (3-26) and (3-29) are equivalent and so by matching terms we obtain a clear expression of free energy contribution from headgroup, counterion and surface interaction (the electrostatic interactions)

$$\Delta G^{\circ}_{s} = - \beta RT \ln(\chi_{cmc} + \chi_3) \qquad (3\text{-}30)$$

and the hydrophobic/water interaction contribution to free energy change is obtained by combining equations (3-26) and (3-30)

$$\Delta G^{\circ}_{hc} = - \Delta G^{\circ}_{s} + RT \ln(\chi_{cmc}) \qquad (3\text{-}31)$$

and finally equations (3-30) and (3-31) sum up to give the total free energy change, ΔG°_{m}, as

$$\Delta G^{\circ}_{m} = \Delta G^{\circ}_{hc} + \Delta G^{\circ}_{s} = RT \ln(\chi_{cmc}) \qquad (3\text{-}32)$$

Equations (3-30), (3-31) and (3-32) applies for systems with added salt. In systems without added salt ($C_3 = 0$ implying that $\chi_3 = 0$) the terms $\ln(\chi_{cmc} + \chi_3)$ in these equations are reduced to $\ln(\chi_{cmc})$ which simplifies them as cmc dependent equations[27]: $\Delta G^{\circ}_{m} = RT \ln(\chi_{cmc})$, $\Delta G^{\circ}_{s} = - \beta RT \ln(\chi_{cmc})$ and $\Delta G^{\circ}_{hc} = (1 + \beta) RT \ln(\chi_{cmc})$.

3.6.2 Enthalpy and entropy changes of micelle formation by La Mesa's reduced variables approach

The vant Hoff's isotherm in which a plot of log(K) against 1/T, where K is the equilibrium constant in mole fraction units, is usually used to derive enthalpy and entropy changes (as slope $-(\Delta H/2.3R)$ and intercept $(\Delta S/2.3R)$ respectively) of different systems fails in this case due to dependence of enthalpy change on temperature. An alternative approach to derive these parameters was introduced and used first by Lamesa[32]. The technique termed as 'reduced variables analysis' is summarized in the following empirical equation[30,32]

$$(cmc-cmc^*)/cmc^* = ABS((T-T^*)/T^*)^{\gamma} \qquad (3\text{-}33)$$

where an exponent γ has numerical value of 1.74 ± 0.03. The value of γ has no significant physical meaning and is independent of the system. This technique utilizes the dependence of cmc on intensive variables (temperature (T) and pressure (p)). In the treatment of these data special attention is focussed on temperature dependence of cmc which will lead to approximation and discussion on heat capacities, enthalpy and entropy changes of micelle formation.

For shorter temperature ranges the heat capacity (ΔC_p) can be assumed to be approximately constant and accordingly enthalpy and entropy changes of micelle formation, ΔH°_m and ΔS°_m respectively, are given as

$$\Delta H^{\circ}_{m} = \Delta H^{\circ}_{m^*} + \Delta C_p.(T-T^*) \qquad (3\text{-}34a)$$

$$\Delta S^{\circ}_{m} = \Delta S^{\circ}_{m^*} + \Delta C_p.\ln(T/T^*) \qquad (3\text{-}34b)$$

where ΔC_p is the heat capacity of micelle formation, $\Delta H^{\circ}_{m^*}$ and $\Delta S^{\circ}_{m^*}$ are enthalpy and entropy changes respectively at T^* and so they relate to cmc^* (the minimal cmc at T^*). If we apply the classical Gibbs-Duhem equation for the enthalpy change of micellization[16,17,30,31]: $\Delta H^{\circ}_{m} = [\partial(\Delta G^{\circ}_{m}/T)/\partial(1/T)]_p = -[(RT^2\partial(\ln(\chi_{cmc}))/\partial T]_p$, which is valid under conditions of constant pressure, then $\Delta H^{\circ}_{m^*}$ vanishes at T^* reducing equation (3-34a)

$$\Delta H^{\circ}_{m} = \Delta C_p.(T-T^*) \qquad (3\text{-}35)$$

$\Delta S^{\circ}_{m^*}$, the entropy change of micellization at T^*, relate to Gibbs free energy change of micellization as: $\Delta S^{\circ}_{m^*}=-\Delta G^{\circ}_{m^*}/T^*$. Using this relationship, a classical thermodynamic relation $\Delta G^{\circ}_{m}=\Delta H^{\circ}_{m}-T\Delta S^{\circ}_{m}$, equations (3-34b) and (3-35) we derive an equation in ΔG°_{m}

$$\Delta G^{\circ}_{m} = \Delta C_p.[T - T^* - T\ln(T/T^*)] - T\Delta S^{\circ}_{m^*} \qquad (3\text{-}36a)$$

and equivalently it can be written in the form

$$\Delta G^{\circ}_{m} = \Delta G^{\circ}_{m^*} + \Delta C_p.[T - T^* - T\ln(T/T^*)] \qquad (3\text{-}36b)$$

which is a synonym form of equations (3-34a) and (3-34b) for Gibbs free energy change.

The total Gibbs free energy change of micellization for the surfactant systems is confusing in the sense that it is

completely independent of added electrolyte as given in equation (3-32) [$\Delta G^{\circ}_{m} = RT\ln(\chi_{cmc})$] but the cmc varies with added salt concentration and that makes ΔG°_{m} vary as well. Combination of equations (3-32) and (3-36a) gives

$$\ln(\chi_{cmc}) = [\Delta C_p/R][1-T^*/T + \ln(T^*/T)] - \Delta S^{\circ}_{m*}/R \qquad (3\text{-}37)$$

Under conditions where $T = T^*$ which also implies that $\Delta S^{\circ}_{m} = \Delta S^{\circ}_{m*}$ and cmc = cmc*, equation (3-37) is simply reduced to

$$\ln(\chi^*_{cmc}) = - \Delta S^{\circ}_{m*}/R \qquad (3\text{-}38)$$

where ΔS°_{m*} is an approximate entropy change of micelle formation at T (=T*)

$$\Delta S^{\circ}_{m}{}^{*} = -R\ln(\chi^*_{cmc}) = -\Delta G^{\circ}_{m*}/T^* \qquad (3\text{-}39)$$

Combination of equations (3-37) and (3-38) by replacing $-\Delta S^{\circ}_{m*}/R$ by $\ln(\chi^*_{cmc})$ and putting $F(T,T^*) = 1 - T^*/T + \ln(T^*/T)$ in equation (3-37) leads to another important physical parameter of micelle formation (the heat capacity):

$$\ln(\chi_{cmc}/\chi^*_{cmc}) = (\Delta C_p/R).F(T,T^*) \qquad (3\text{-}40)$$

and so the heat capacity of micelle formation (ΔC_p) can be estimated from equation

$$\Delta C_p = \frac{R\ln(\chi_{cmc}/\chi^*_{cmc})}{F(T,T^*)} \qquad (3\text{-}41)$$

Entropy changes contributed from hydrophobic-water interactions (ΔS°_{hc}) and surface-headgroup-counterion interactions ($\Delta S^{\circ}_{,}$) at $T = T^*$ can be estimated from ΔG°_{hc*} (eq.

(3-31)) and ΔG°_{s*} (eq. (3-30)) using the relation $\Delta S = -\Delta G/T$

$$\Delta S^{\circ}_{s*} = \beta R \ln(\chi^{*}_{cmc}+\chi_3) \qquad (3\text{-}42a)$$

$$\Delta S^{\circ}_{hc*} = -\beta R \ln(\chi^{*}_{cmc}+\chi_3) - R \ln(\chi^{*}_{cmc}) \qquad (3\text{-}42b)$$

Under these conditions ($T = T^{*}$) the total enthalpy change of micelle formation is zero and so due to additive nature of contribution from hydrophobic-water interactions and surface-headgroup-counterion interactions, the enthalpies ΔH°_{hc*} and ΔH°_{s*} are equal in magnitude but opposite in sign, such that: $\Delta H^{\circ}_{hc*}+\Delta H^{\circ}_{s*}=\Delta H^{\circ}_{m*}=0$ that is $\Delta H^{\circ}_{hc*}=2\beta RT^{*}\ln(\chi^{*}_{cmc}+\chi_3)$ and $\Delta H^{\circ}_{s*}=-2\beta RT^{*}\ln(\chi^{*}_{cmc}+\chi_3)$.

However, under conditions where $T > T^{*}$ or $T < T^{*}$, ΔH°_{m} is not equal to zero, it is either negative or positive depending on the system itself. Entropy changes can be estimated from equations (3-34a,b), (3-36b) and (3-42a,b)

$$\Delta S^{\circ}_{m} = -R \ln(\chi^{*}_{cmc}) + \Delta C_p.F(T,T^{*}) \qquad (3\text{-}43a)$$

$$\Delta S^{\circ}_{hc} = -\beta R \ln(\chi^{*}_{cmc}+\chi_3) - R \ln(\chi^{*}_{cmc}) + \Delta C_p.F(T,T^{*}) \qquad (3\text{-}43b)$$

$$\Delta S^{\circ}_{s} = \beta R \ln(\chi^{*}_{cmc}+\chi_3) \qquad (3\text{-}43c)$$

On the other hand, enthalpy changes of micelle formation ΔH°_{hc} and ΔH°_{s} can accordingly be derived from the corresponding calculated free energy and entropy changes using the classical thermodynamic equation $\Delta H^{\circ} = \Delta G^{\circ}+T\Delta S^{\circ}$.

Parameters derived from this model, for systems without added electrolyte, can be easily tested using the ratio $\Delta G^{\circ}_{hc}/\Delta G^{\circ}_{s} = [(1+\beta)RT\ln(\chi_{cmc})]/-\beta R\ln(\chi_{cmc}) = -(1+\beta)/\beta$ which has

an approximate constant value of -2.27±0.15[23,30] for most surfactant systems. It is expected as well to have both ratios $\Delta H^{\circ}_{hc}/\Delta H^{\circ}_{s}$ and $\Delta S^{\circ}_{hc}/\Delta S^{\circ}_{s}$ equal to $-(1+\beta)/\beta$ as theory predicts although in reality slight deviations may occur. Moreover, although it is well known that ß values vary with temperature, changes are so small ($\partial\alpha/\partial T \sim 0$) to affect the aforementioned expected ratio. Furthermore, the ratio $\Delta S^{\circ}_{m}/\Delta C_{p}$ has been found to be approximately equal to -0.26 irrespective of surfactant systems and this gives another dimension of testing parameters derived using this technique. However, many authors differ on this aspect of the theory which leads them to question whether the theoretical basis is correct. On the other hand, some systems have shown good agreement with this theory. The model looks much simpler on additive contributions than the Klevens based proportionated contributions shown in the previous section.

Moreover, in order to avoid conflicting views, Muller[30] proposes a compromising free energy change of micelle formation as $\Delta G^{\circ}_{m} \approx \Delta G^{\circ}_{hc} = (1+\beta)RT\ln(\chi_{cmc})$ which agrees well with the existing approach[1-4,17] for ΔG°_{m} but when he assumes $\Delta G^{\circ}_{s} \sim 0$ he differs with the phase separation, mass action and the Evans and Ninham approaches. It is well known ΔG°_{s} is very important in determining optimum shape and size of the micelle and so if it is agreed universally to be equal to zero we have to find a way of explaining the optimum shape and size of the micelle. Furthermore, Muller's

explanation is not convincing enough to justify ΔG°_{s} to be universally zero because this makes micelle formation process look as if is completely dominated by hydrophobic forces. It is acceptable to be zero in some isolated systems but it can't be taken as a universal statement. Bearing in mind that present surfactant theory differentiates nonionic and ionic surfactants by their head group interactions, it will be very difficult to argue in the same way. He argues about opposing forces, attractive and repulsive interactions which in actual fact will give $\Delta G^{\circ}_{s} \sim 0$ only when they are approximately equal in magnitude.

On the other hand, Emerson and Holtzer[29,32] agree with Evans and Ninham[23,26] that: (i) $\Delta G^{\circ}_{m} = RT\ln(\chi_{cmc})$ and (ii) $\Delta G^{\circ}_{m} = \Delta G^{\circ}_{hc} + \Delta G^{\circ}_{s}$. However, they differ in technique and mathematical formulation in the way they estimate ΔG°_{hc} and ΔG°_{s}. In their model ΔG°_{s} is given as $N_o \xi \psi_{b,\tilde{N}}$ where N_o is the Avogadro number, ξ is the magnitude of the protonic or electronic charge, and $\psi_{b,\tilde{N}}$ is the magnitude of the electrostatic potential at the micellar surface. The value $\psi_{b,\tilde{N}}$, which depends on electric charge on the micelle and the ionic surroundings, is estimated by solving a nonlinearized form of the Poisson-Boltzmann equation. The solution, however, involves intensive numerical solutions by electronic computation.

In Table 3.1 below differences and similarities of mathamatical formulations for free energy changes are shown from different authors and models.

Table 3.1: Differences in ΔG°_{m}, ΔG°_{hc} and ΔG°_{s} according to views of authors and models

Model	ΔG°_{m}	ΔG°_{hc}	ΔG°_{s}
M-A/P-S models	$(1+\beta)RT\ln(\chi_{cmc})$	$2.3n_c\beta(1+\beta)RT+G$	$2.3(1+\beta)RT(A-4.56)-G$
I.B. model	$RT\ln(\chi_{cmc})$	$(1+\beta)RT\ln(\chi_{cmc})$	$-\beta RT\ln(\chi_{cmc})$
Muller's I.B.	$(1+\beta)RT\ln(\chi_{cmc})$	$(1+\beta)RT\ln(\chi_{cmc})$	0
E.P. model	$RT\ln(\chi_{cmc})$	$RT\ln(\chi_{cmc})-N_o\xi\psi_{b,\hat{N}}$	$N_o\xi\psi_{b,\hat{N}}$

where: M-A/P-S based on the laws of mass-action and phase-separation, I.B. model is a model based on ion binding by Evans, D.F. and Ninham B.W.[23,26], Muller's I.B. is the contribution by Muller, N. to I.B. model[30], E.P. model is a model based on electrostatic potential at the micellar surface by Emerson and Holtzer[29,31], A and B are Klevens parameters from equation $\ln(cmc) = A - B.n_c$, and n_c is the chain length (number of carbon atoms in the alkyl chain).

3.8 REFERENCES

1. TANFORD, C. "*The Hydrophobic effect: Formation of Micelles and Biological Membranes*", 2nd ed, Wiley-Interscience, New York (1980).

2. MYERS, D. "*Surfaces, Interfaces and Colloids: Principles and Applications*", VCH Publishers, New York (1991)

3. SHINODA, K.; NAKAGAWA, T.; TAMAMUSHI, B. and ISEMURA, T. "*Colloidal Surfactants*", Academic Press, New York (1963).

4. MYERS, D. "*Surfactant Science and Technology*", VCH Publishers, New York (1988)

5. HUTCHINSON, E. *Z. Physik. Chem. (Frankfurt)*, 5 (1955) 344.

6. ISRAELACHVILI, J.N.; MITCHELL, D.J. and NINHAM, B.W. *J. Chem. Soc. Faraday Trans. 2*, 72 (1976) 1925.

7. HALL, D.G. *Trans. Faraday Soc.*, 66 (1972) 1351, 1359.

8. HALL, D.G. *Kolloid-Z*, 250 (1972) 895.

9. AAMODT, M.; LANDGRAN, M. and JONSSON, B. *J. Phys. Chem.*, 96 (1992) 945, 950.

10. NAGARAJAN, R. *Adv. Colloid Interface Sci.*, 26 (1986) 205.

11. NAGARAJAN, R.; CHAIKO, M.A. and RUCKENSTEIN, E. *J. Phys. Chem.*, 88 (1984) 2916.

12. NAGARAJAN, R. *Colloid Surf.*, 13 (1985) 1.

13. NAGARAJAN, R. and RUCKENSTEIN, E. *J. Colloid Interface Sci.*, 91 (1983) 500.

14. RUCKENSTEIN, E.; HUBER, G. and HOFFMANN, H. *Langmuir*, 3 (1984) 382.

15. RUCKENSTEIN, E. and NAGARAJAN, R. *J. Phys. Chem.*, 87 (1984) 382.

16. GHARIBI, H.; PALEPU, R.; BLOOR, D.M. and WYN-JONES, E. *Langmuir*, 8 (1992) 782.

17. ROSEN, M.J. "*Surfactants and Interfacial Phenomena*", 2nd Ed, John Wiley & Sons, New York (1989).

18. NUSSELDER, J.J.H. and ENGBERTS, J.B.F.N. *Langmuir*, 7 (1991) 2089.

19. EVERETT, D.H., "*Basic Principles of Colloid Science*", Royal Society of Chemistry, London (1988).

20. TANFORD, C. *J. Phys. Chem.* 78 (1974) 2469.

21. DEBYE, P. *Am. N.Y. Acad. Sci.*, 51 (1949) 5751.

22. WAN-BADHI, W.; MWAKIBETE, H.; BLOOR, D.M.; PALEPU, R.; and WYN-JONES, E. *J. Phys. Chem.*, 96 (1992) 918.

23. EVANS, D.F. and NINHAM, B.W. *J. Phys. Chem.*, 87 (1983) 5025.

24. KLEVENS, H.B., *J. Am. Oil Chem. Soc.*, 30 (1953) 74.

25. HSIAO, L.; DUNNING, H.N. and LORENZ, P.B. *J. Phys. Chem.*, 69 (1956) 657.

26. EVANS, D.F.; MUKHERJEE, S.; MITCHELL, D.J. and NINHAM, B.W. *J. Colloid Interface Sci.*, 93 (1983) 184.

27. MUKERJEE, P. *J. Phys. Chem.*, 66 (1962) 1375.

28. BRADY, J.E.; EVANS, D.F.; WARR, G.G.; GRIESER, F. and NINHAM, B.W. *J. Phys. Chem.*, 90 (1986) 1853.

29. EMERSON, M.F. and HOLTZER, A. *J. Phys. Chem.*, 71 (1967) 1898.

30. MULLER, N. *Langmuir*, 9 (1993) 96.

31. EMERSON, M.F. and HOLTZER, A. *J. Phys. Chem.*, 69 (1965) 3718.

32. LA MESA, C. *J. Phys. Chem.*, 94 (1990) 323.

CHAPTER FOUR: INTERACTIONS BETWEEN CETYLTRIMETHYLAMMONIUM BROMIDE AND UNCHARGED HYDROPHOBIC WATER-SOLUBLE POLYMERS IN AQUEOUS SOLUTIONS

4.1 INTRODUCTION

Due to the diversity of the properties of aqueous and non-aqueous surfactant solutions a number of investigative methods have been used to derive important information on micellization in these systems. For example some experimental methods are[1]: electromotive force, surface tension, viscosity, electrical conductivity, electrophoresis, ultracentrifugation, and gel filtration. In each case measurements are carried out as functions of total surfactant concentration (C_t). Each separate technique has weaknesses in certain areas so may fail to show some important behaviour. In such circumstances other complementary investigative methods are used to supply the missing information or confirm accuracy of the information derived by the first set of measurements. Sometimes two or more experimental methods are used in micellization studies.

A study associated with the interactions between the cetyltrimethylammonium halide surfactant family (CTAX; X = F, Cl, Br, I)) and uncharged hydrophobic water-soluble polymers has attracted attention from many researchers due the wide applications of these systems[1-5]. In recent studies some interesting effects have been observed, provided sufficiently hydrophobic polymers are used[5-9]. Due to low solubility at room temperature and low cmc, the studies on

polymer/CTAB interactions using the surfactant selective electrode has received very little attention despite the fact that binding isotherm can be readily obtained from the EMF data. In this work a study on CTAB micelles and polymer/CTAB interaction is described using a CTAB surfactant selective electrode.

4.2 MICELLIZATION IN CTAB SYSTEMS IN THE ABSENCE OF POLYMER

4.2.1 EMF Measurement Procedures

The electromotive force (EMF) of the cetyltrimethylammonium ion (CTA^+) electrode was measured relative to two ionic species, bromide ion and sodium ion, in two combined cells. In order to attain these measurements a CTA^+ selective membrane electrode constructed as described in section 2.4 was used together with reference electrodes reversible to sodium and bromide ions to make cell assemblies of type I and II[10-12].

CTAB-ISE	Sample solution Surf(C); NaBr(x)	Electrode reversible (I) to sodium ions

and

CTAB-ISE	Sample solution Surf(C); NaBr(x)	Electrode reversible (II) to counterions

EMF corresponding to free monomer surfactant concentration was measured relative to a standard sodium ion electrode (Kent, EIL) (cell (I)) and simultaneously bromide-ion-selective electrode (Corning solid state ISE 30-35-00) was used to measure EMF corresponding to $C_1C_2.\gamma_\pm^2$ (cell (II))[10]. The set up of the cell is shown in Figure 4-1.

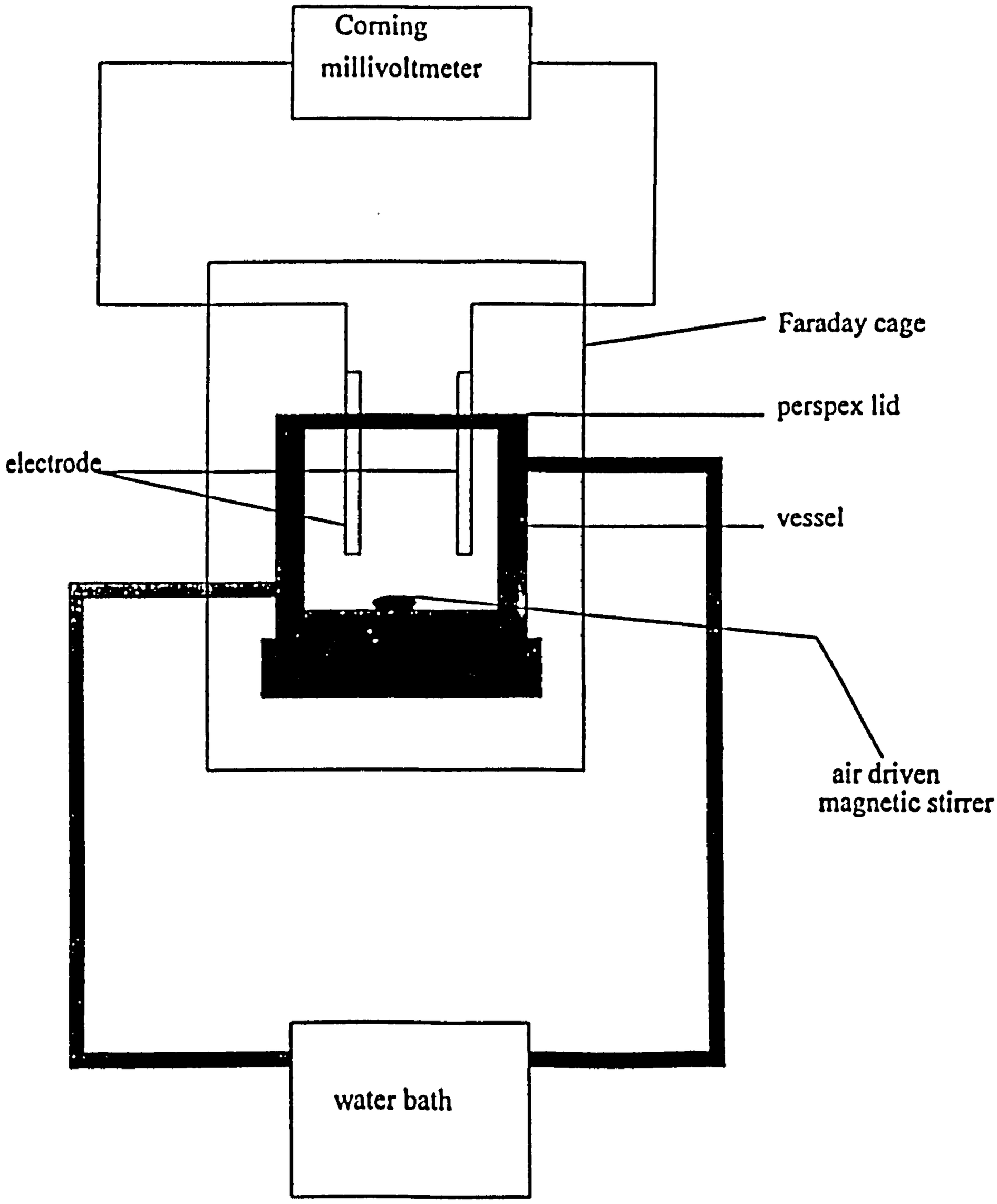

Figure 4-1: The diagramatic cell set-up

All solutions studied in this work were made up in a constant amount of sodium bromide (AnalaR) to keep the sodium ion concentration constant. The concentrated CTAB solution was added into a sample solution using a 200 μl and 2000 μl microliter syringe GS-1100 and GS-1200

(GILMONT) respectively. The EMF was measured to within ±0.1 mV from a pH/millivoltmeter (Corning ion analyzer 250) at equilibrium after each addition. The temperature was controlled within ±0.1°C by passing thermostatted water through a double walled all-glass cell.

Table 4.1: Electrode parameters of the CTAB selective electrode doped with NaBr

Conc. of NaBr/ mmol dm^{-3}	Sodium Electrode		Bromide Electrode	
	S_1 mV dec^{-1}	E_o, mV	S_2 mV dec^{-1}	E_o, mV
0.01	55.2	346.9	110.7	489.4
0.10	57.1	562.1	110.6	557.4
0.50	58.5	470.7	112.6	498.4
1.00	56.5	375.3	113.9	432.8

The EMF measurements carried out in cells of type I and II are intended to be used to evaluate: (a) the cmc, (b) the monomer concentration of CTAB in the micellar range, and (c) the effective degree of micellar dissociation, α, in the presence of different added salt concentrations. The Nernstian characteristics for CTAB selective electrode at different added salt concentration are summarized in Table 4.1.

4.2.2 The critical micelle concentration (cmc)

A break point in the plot $E_{cell,I}$ against $\log(C_1)$ according to equation (2-9) (Figures 4-2 to 4-5) correspond to the critical micelle concentration (cmc). The data are summarized in Table 4.2. The EMF plots are Nernstian up to

Figure 4-2 : EMF vs log(C_1) plot for CTAB electrode in 10^{-5} mol dm^{-3} sodium bromide

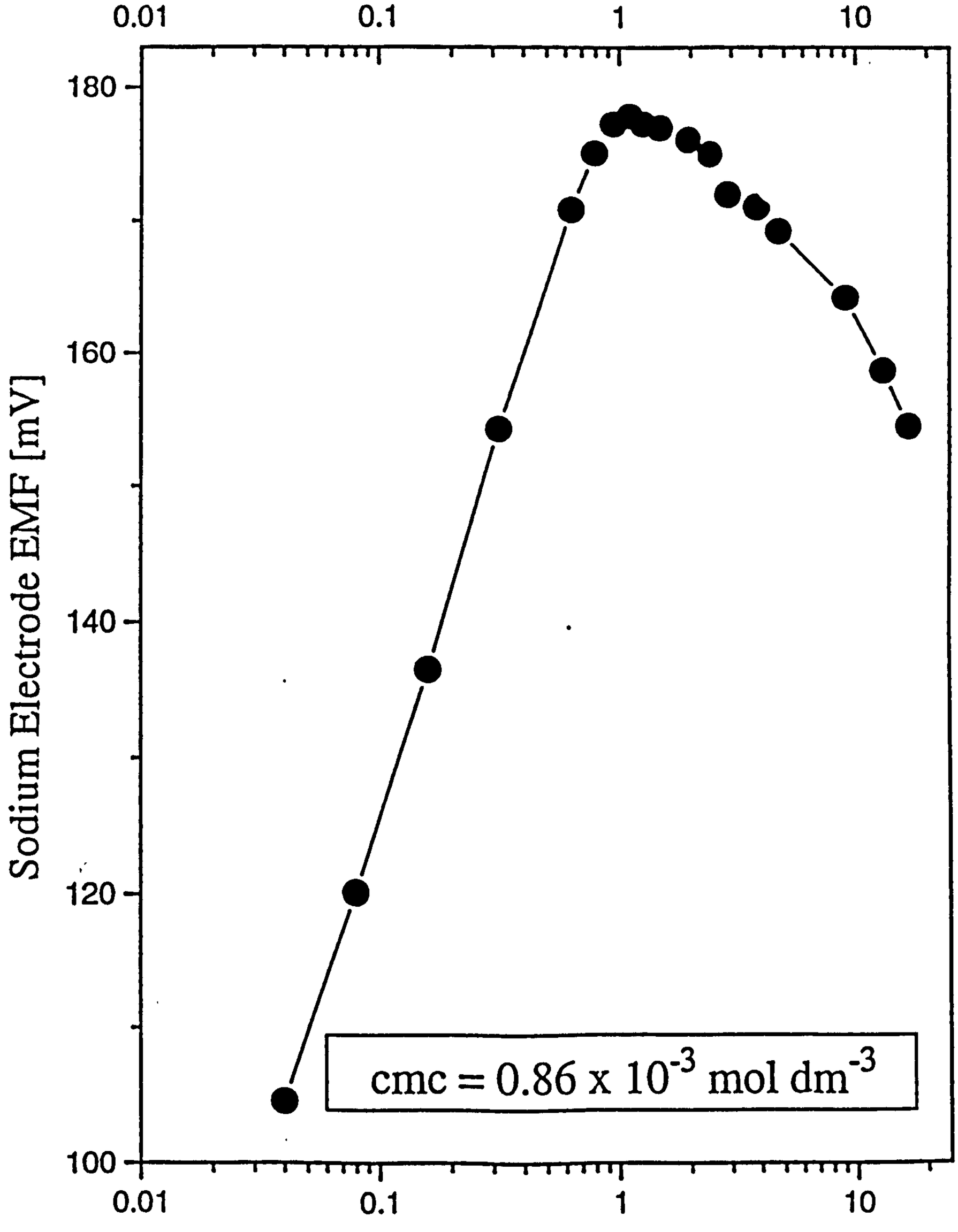

Figure 4-3: EMF vs log (C_1) for CTAB electrode in 10^{-4} mol dm^{-3} sodium bromide

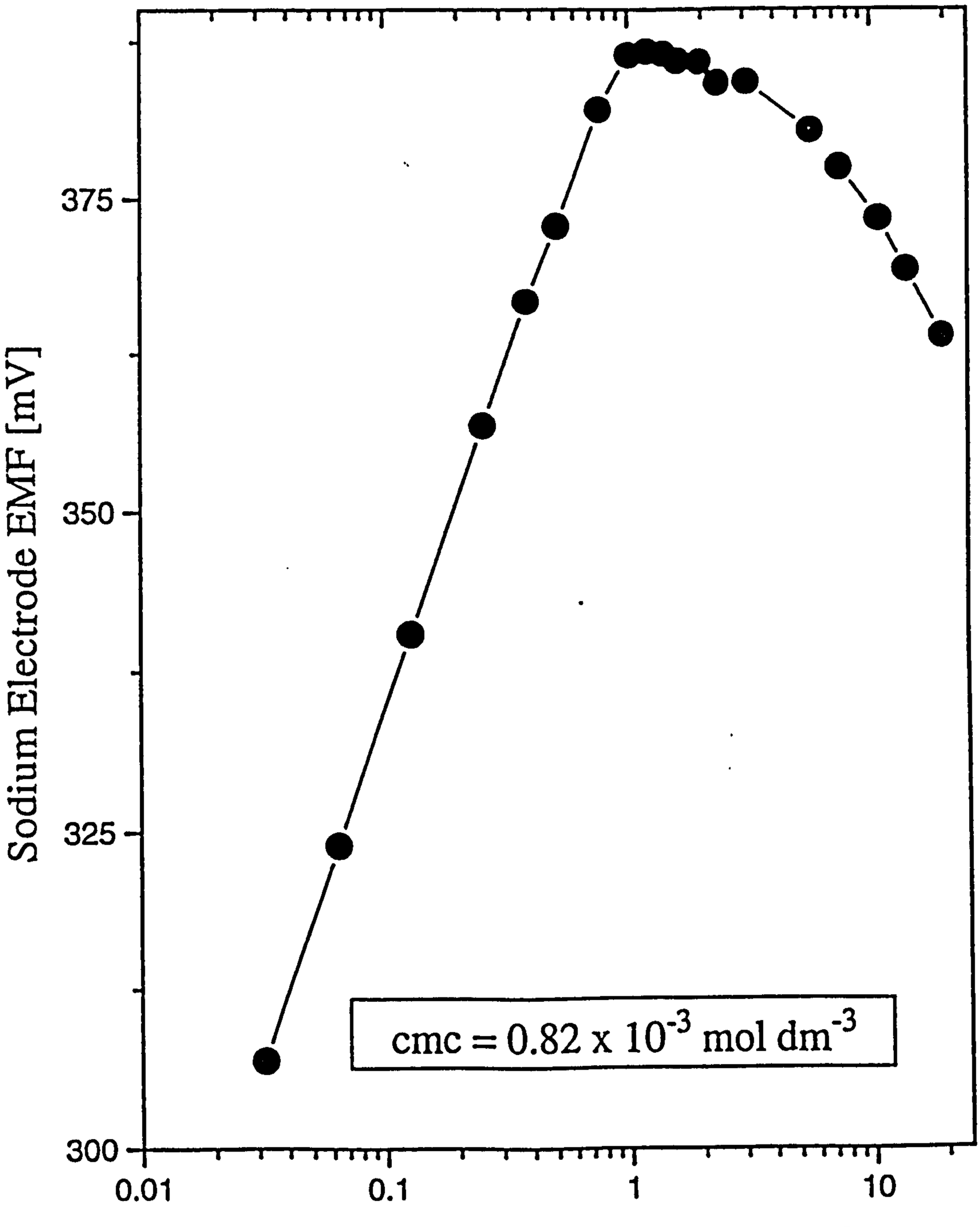

Figure 4-4: EMF vs log(C_1) plot for CTAB electrode in
5×10^{-4} mol dm^{-3} sodium bromide

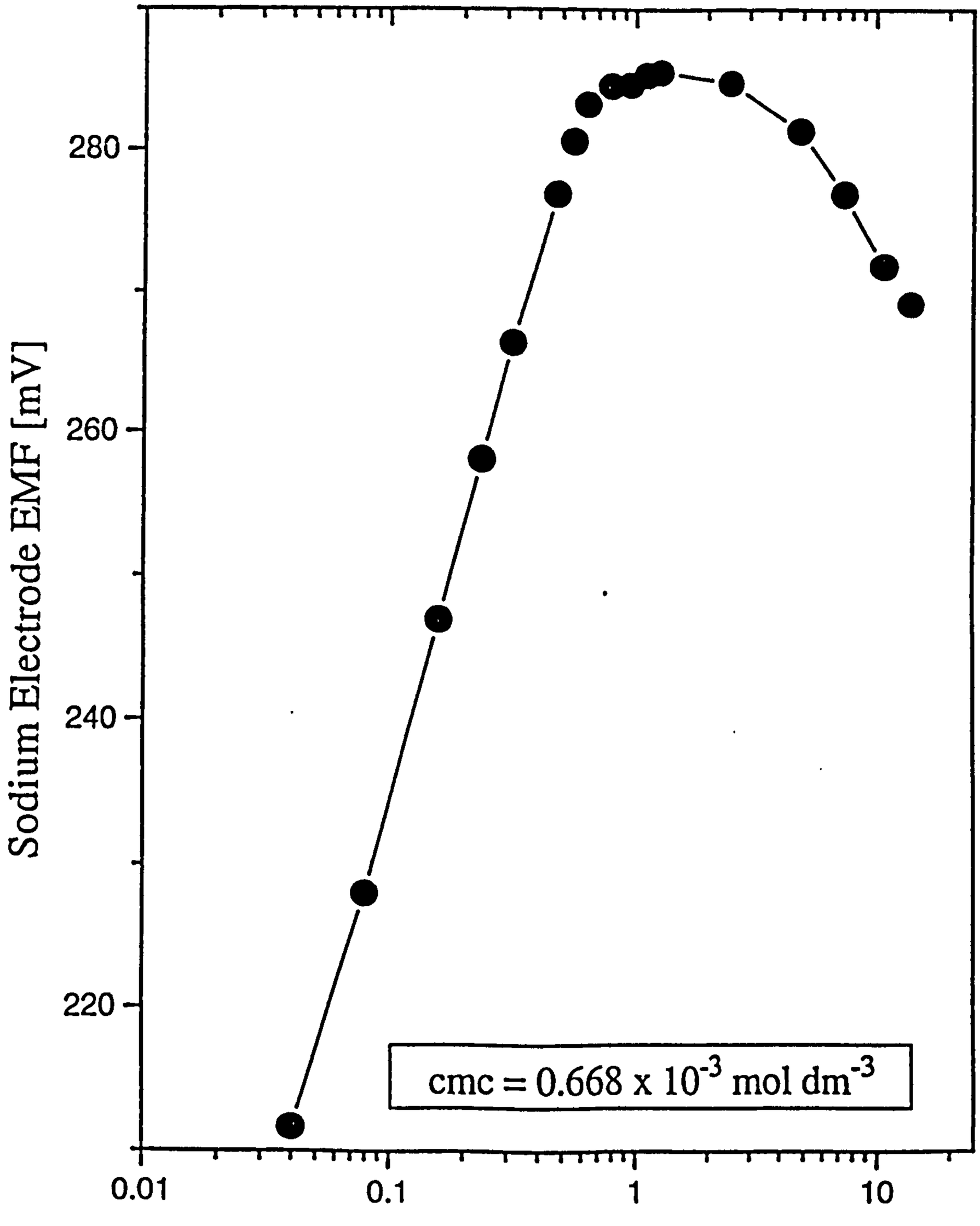

Figure 4-5: EMF vs log(C_1) plot for CTAB electrode in 10^{-3} mol dm^{-3} sodium bromide

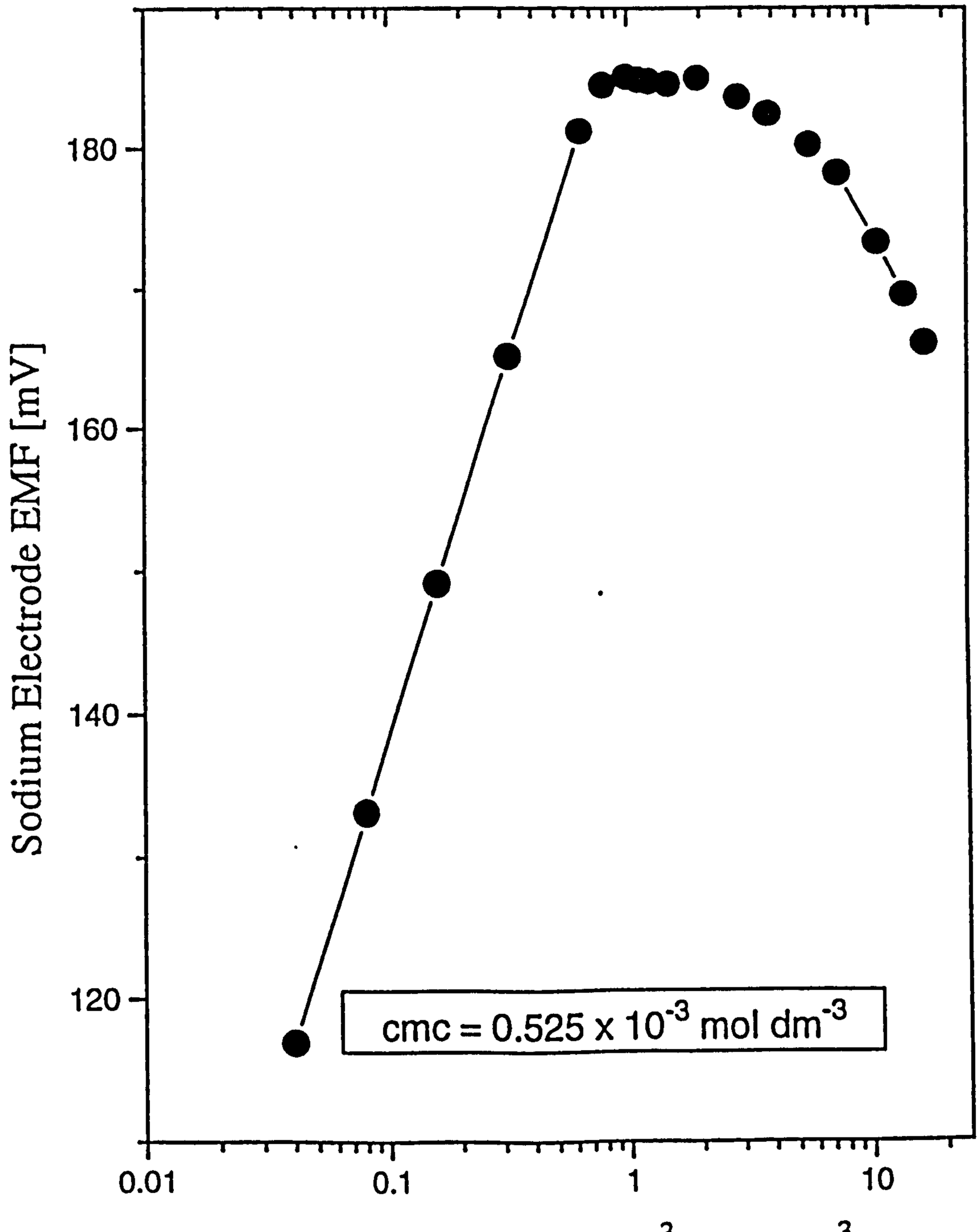

the start of micellization, where at this point there is a significant change of slope. At the cmc or just below the Nernstian linear range ends and the free monomer surfactant concentration measured by the electrode cell (m_1) is less than total surfactant concentration C_1. In this region m_1 either remains constant or decreases[13,14] as in the case for cetyltrimethylammonium bromide system.

Table 4.2: Micellar properties of CTAB doped with NaBr

Medium mmol dm^{-3}	Nernstian linear range, mmol dm^{-3}	cmc mmol dm^{-3}	cmc[a] mmol dm^{-3}
0.00	not applicable	1.000[b] (0.950)[c]	-
0.01	0.01 - 0.861	0.861	0.871
0.10	0.01 - 0.822	0.822	0.795
0.50	0.01 - 0.708	0.668	-
1.00	0.01 - 0.525	0.525	-

[a] cmc (surface tension technique) [b] cmc (at $C_3 = 0$)[15].

[c] cmc (at $C_3 = 0$ by conductivity measurements)[16]

The error in the cmc value obtained from $E_{cell,I}$ vs $\log(C_1)$ plot depends on the sharpness of the cmc turning point. If the break point is sharp there is very minimal error in the cmc value obtained. On the other hand if the break point is not sharp errors in the cmc values are inevitable. In the present work the cmc values are estimated from fairly sharp turning points in the EMF curves.

4.2.3 Measurement of monomeric surfactant concentration $\underline{m}_1$

The surfactant ion selective electrodes are capable of monitoring both the monomeric surfactant ions and the free counterions. A cell of type I[10-12] made up of a surfactant ion selective electrode and a reference electrode reversible to a coion (sodium ions in this case) monitors accurately the surfactant ion activity (a_1).

The Nernstian cell potential equation for cells of type I is given below:

$$E_{cell,I} = E^{\circ}_{I} + \left(\frac{RT}{F}\right) \ln\left(\frac{a_1 . a_{Na}}{a_2 . a'_{Na}}\right) \qquad (4\text{-}1)$$

where a_1 and a_2 are surfactant concentrations in the sample solution and inner reference solution respectively. a_{Na} and a'_{Na} are sodium bromide concentrations in the sample solution and inner reference solution respectively. Since sodium bromide concentration was kept constant and equal in the two sides of the membrane then $a_{Na} = a'_{Na}$. The use of the Debye-Hückel activity-concentration relationships $a_1 = \gamma_{\pm} . C_1$ and $a_2 = \gamma_{\pm} . C_2$ into equation (4-1) yields

$$E_{cell,I} = E^{\circ}_{I} + \left(\frac{RT}{F}\right) \ln\left(\frac{\gamma_{\pm} . C_1}{\gamma_{\pm} . C_2}\right) \qquad (4\text{-}2)$$

It is well known that the activity coefficients of monovalent ions of the same charge are approximately equal. Application of this consideration into equation (4-2)

yields

$$E_{cell,I} = E^{\circ}_{I} + \left(\frac{RT}{F}\right) \ln\left(\frac{C_1}{C_2}\right) \qquad (4\text{-}3)$$

The inner reference solution surfactant concentration C_2 is kept constant and the term $(RT/F)\ln(C_1/C_2)$ in equation (4-3) can be split as follows

$$E_{cell,I} = E^{\circ}_{I} + \left(\frac{RT}{F}\right) \ln(C_1) - \left(\frac{RT}{F}\right) \ln(C_2) \qquad (4\text{-}4)$$

If we define $E^{\circ}_{cell,I} = E^{\circ}_{I} - (RT/F)\ln(C_2)$ then equation (4-4) becomes

$$E_{cell,I} = E^{\circ}_{cell,I} + \left(\frac{RT}{F}\right) \ln(C_1) \qquad (4\text{-}5)$$

or in logarithm base 10 as

$$E_{cell,I} = E^{\circ}_{cell,I} + 2.3\left(\frac{RT}{F}\right) \log(C_1) \qquad (4\text{-}6)$$

In the Nernstian linear region a plot of $E_{cell,I}$ against $\log(C_1)$ gives a slope of $2.3(RT/F)$. In this region we assume there is total dissociation and so $C_1 = m_1$. In actual fact the cell measures free monomer surfactant concentration m_1 and equation (4-6) can simply be written as

$$E_{cell,I} = E^{\circ}_{cell,I} + 2.3\left(\frac{RT}{F}\right) \log(m_1) \qquad (4\text{-}7)$$

This cell is capable of determining m_1 in surfactant systems containing a variety of additives.

4.2.4 Determination of free counterion concentration, m_2

Determination of m_2 requires combined measurements from the cell assemblies of type I and II. The emf for cell of type II monitors the product $a_1.a_2$ and so does not provide directly the free counterion activity, a_2. The Nernstian equation for this cell is given as

$$E_{cell,II} = E^{o}_{cell,II} + \left(\frac{RT}{F}\right) \ln(a_1.a_2) \qquad (4\text{-}8)$$

Again the Debye-Hückel theory is applied to involve concentrations instead of activities, $a_1.a_2 = (\gamma_{\pm}.C_1).(\gamma_{\pm}.C_2) = \gamma_{\pm}^2.(C_1.C_2)$ where C_1 and C_2 are the total concentration of surfactant ions and counterions respectively; $C_2 = C_1 + C_3$ where C_3 is the concentration of added salt. Substitution of $\gamma_{\pm}^2.(C_1.C_2)$ into equation (4-8) gives the Nernstian equation in concentration terms of cells of type II below cmc

$$E_{cell,II} = E^{o}_{cell,II} + 2\left(\frac{RT}{F}\right) \ln(\gamma_{\pm}.(C_1.C_2)^{1/2}) \qquad (4\text{-}9)$$

or involving m_1 and m_2 in the micellar range (above cmc)

$$E_{cell,II} = E^{o}_{cell,II} + 2\left(\frac{RT}{F}\right) \ln(\gamma_{\pm}.(m_1.m_2)^{1/2}) \qquad (4\text{-}10)$$

In order to obtain m_2 both m_1 and $\gamma_{\pm}$ are required. m_1 is obtained from equation (4-7) as $m_1 = 10\exp[(E_{cell,I} - E^{o}_{cell,I})/\text{slope}]$. In this exercise the mean activity coefficient $\gamma_{\pm}$ is also unknown and cannot be approximated to unity.

These unknown variables m_2 and $\gamma_\pm$ are estimated by an iterative numerical procedure in the micellar region involving an expanded form of equation (4-10)[10-12].

$$\left(\frac{RT}{zF}\right)\ln(m_2) = E_{cell,II} - E^{\circ}_{cell,II} - 2\left(\frac{RT}{zF}\right)\ln(\gamma_\pm) - \left(\frac{RT}{zF}\right)\ln(m_1) \qquad (4\text{-}11)$$

and the Debye-Hückel equation:

$$\log(\gamma_\pm) = -A\sqrt{I}/(1 + \sqrt{I}) \qquad (4\text{-}12)$$

where I is the effective solution ionic strength defined as

$$I = \tfrac{1}{2}(m_1 + C_3 + m_2) \qquad (4\text{-}13)$$

and A is the Debye-Hückel constant for a given temperature and solvent composition (A = 0.509 $mol^{-1/2}dm^{3/2}$ under conditions used in this work).

<u>Iterative Procedure for calculating m_2 and $\gamma_\pm$</u>

In the micellar range the quantity $\gamma_\pm^2 m_1 m_2$ is obtained from equation (4-10). Initial estimates of m_2 are obtained by assuming $\gamma_\pm = 1$ and substituting the m_1 values obtained from equation (4-7). Once an estimate of m_2 is obtained, the $\gamma_\pm$ value can then be evaluated from equations (4-11) and (4-12). The new $\gamma_\pm$ values are inserted into equation (4-9) together with m_1 from equation (4-7) giving a new value of m_2, which in turn leads to a new estimate of $\gamma_\pm$ using equations (4-11) and (4-12). This iterative procedure is repeated until both m_2 and $\gamma_\pm$ converge to constant values. This procedure is carried out using a computer program

designed by Dr. D. M. Bloor.

The values of m_1, m_2 and $\gamma_\pm$ are tabulated in Tables 4.A1, 4.A2, 4.A3 and 4.A4 as functions of C_1 respectively in 10^{-5}, 10^{-4}, 5 x 10^{-4} and 10^{-3} mol dm^{-3} sodium bromide salt.

4.2.5 The effective degree of micellar dissociation, α

A surfactant system consisting of surfactant ions (denoted 1), counterions (2), coions (3), and micelles (r) is considered here. According to Hall[12,18,19] the behaviour of the critical micelle concentration (cmc) can be described using the following equation[12,18]

$$\left(\frac{H/\bar{N}-h_1^\circ+\frac{1}{2}\alpha(h_3+h_3^\circ)}{kT^2}\right)dT - \left(\frac{V/\bar{N}-v_1^\circ+\frac{1}{2}\alpha(v_3+v_3^\circ)}{kT}\right)dp$$

$$+ d\ln(m_1.\gamma_\pm) + (1-\alpha).d\ln(m_2.\gamma_\pm) \approx 0 \qquad (4\text{-}14)$$

where H, V and $\bar{N}$ are partial molar enthalpy, partial molar volume and the mean aggregation number;

$h_1^\circ = Tv_1^\circ(dp/dT) - T^2(d\mu_1^\circ/T)dT$ (is the standard partial molecular enthalpy for surfactant and its counterion);

$h_3^\circ = Tv_3^\circ(dp/dT) - T^2(d\mu_3^\circ/T)dT$ (is the standard partial molecular enthalpy for a coion);

$h_3 = -T^2[(\partial\mu_3/T)/\partial T]_{p,mr,m1,m3}$ (is the partial molecular enthalpy for a coion);

$v_1^\circ = T(d\mu_1^\circ/T)dp + (h_1^\circ/T)dT/dp$ (is the standard molecular volume for a surfactant and its counterion);

$v_3^\circ = T(d\mu_3^\circ/T)dp + (h_3^\circ/T)dT/dp$ (is the standard molecular

volume for a coion);

$v_3 = (\partial\mu_3/\partial p)_{T,mr,m1,m3}$ (is the partial molecular volume for a coion);

α is as defined by Hall[12,18,19] and Mijnlieff[20] as the effective degree of micellar dissociation.

Table 4.3: The effective degree of micellar dissociation α for CTAB systems in varied added salt concentrations.

		Derived α from equation:			
[salt] mM	cmc mM	Eq.(4-16)	Eq.(4-20)	Eq.(4-22)	Eq.(4-25)
0.00	1.000	n.a.			
0.01	0.861	0.10			
0.10	0.822	0.13	0.11	0.11	0.12
0.50	0.668	0.14			
1.00	0.525	0.10			

Recent theoretical considerations of the thermodynamics of micellization in ionic surfactant systems suggest that if micelles are present with larger $\bar{N}$ at constant temperature and pressure, then $dT = dp = 0$ and as a result the enthalpy and volume terms of equation (4-14) are reduced to zero. Equation (4-14) with some arithmetical rearrangement becomes

$$\left[\frac{\partial \ln(m_1 . \gamma_\pm)}{\partial \ln(m_2 . \gamma_\pm)}\right]_{T,p,cmc} = -(1-\alpha) \qquad (4\text{-}15)$$

which defines $-(1-\alpha)$ as slope of the plot $\ln(m_1.\gamma_\pm)$ versus $\ln(m_2.\gamma_\pm)$. Integration of equation (4-15) yields[10,12,16,19,21]

$$\log(m_1.\gamma_\pm) = M - (1-\alpha).\log(m_2.\gamma_\pm) \qquad (4\text{-}16)$$

where M is a constant. A plot of $\log(m_1.\gamma_\pm)$ against $\log(m_2.\gamma_\pm)$ should be linear with $-(1-\alpha)$ and M as slope and intercept respectively (Figure 4-6). Emf data measured using cells of type I and II lead to values of m_1, m_2 and $\gamma_\pm$ (Tables 4.A1, 4.A2, 4.A3 and 4.A4) which are needed in order to evaluate α graphically using equation (4-15). The average value of α obtained is 0.12 ± 0.02, α at different salt concentrations are summarized in Table 4.3.

Equation (4-16) at the cmc can be used to evaluate α at different salt concentrations using the cmc values derived from electrode data. It is well known, in the micellar range that the total surfactant concentration (C_1) relates to monomeric and micelle concentrations (m_1 and m_2 respectively) as follows

$$C_1 = m_1 + Nm_2 \qquad (4\text{-}17)$$

At the cmc very few micelles are present in the system and therefore $m_2 \sim 0$. This consideration leads to the approximation

$$C_1 \approx m_1 \approx \text{cmc} \qquad (4\text{-}18)$$

Again, at the cmc a very small number of micelles are present and there is not much counterion binding thus $m_3 \sim C_3$ and

$$m_2 \approx m_1 + m_3 \approx m_1 + C_3 \approx \text{cmc} + C_3 \qquad (4\text{-}19)$$

Substitution of m_1 and m_2 from equations (4-18) and (4-19) respectively into equation (4-16) yields

$$\log(cmc.\gamma_{\pm}) = M - (1-\alpha).\log[(cmc+C_3).\gamma_{\pm}] \qquad (4\text{-}20)$$

and if we denote cmc and $\gamma_{\pm}$ at $C_3 = 0$ as cmc° and $\gamma_{\pm}^{\circ}$ then equation (4-20) reduces to

$$\log(cmc^{\circ}.\gamma_{\pm}^{\circ}) = M - (1-\alpha).\log[(cmc^{\circ}.\gamma_{\pm}^{\circ}] \qquad (4\text{-}21)$$

Combination of equations (4-20) and (4-21) by subtraction removes the constant M leaving the following equation[10,11,19,22]

$$\log\left(\frac{cmc}{cmc^{\circ}}\right).\left(\frac{\gamma_{\pm}}{\gamma_{\pm}^{\circ}}\right) = -(1-\alpha)\log\left(\frac{cmc+C_3}{cmc^{\circ}}\right).\left(\frac{\gamma_{\pm}}{\gamma_{\pm}^{\circ}}\right) \qquad (4\text{-}22)$$

and rearrangement of equation (4-21) provides a definition for M based on initial or boundary condition as[23,24]

$$M = (2-\alpha)\log(cmc^{\circ}.\gamma_{\pm}^{\circ}) = \Delta G^{\circ}_m/2.303RT \qquad (4\text{-}23)$$

or simply

$$\Delta G^{\circ}_m = 2.303RTM = 2.303RT(2-\alpha)\log(cmc^{\circ}.\gamma_{\pm}^{\circ}) \qquad (4\text{-}24)$$

A plot of $\log[(cmc/cmc^{\circ}).(\gamma_{\pm}/\gamma_{\pm}^{\circ})]$ against $\log[((cmc+C_3)/cmc^{\circ}).(\gamma_{\pm}/\gamma_{\pm}^{\circ})]$ is a straight line giving $-(1-\alpha)$ as slope. Equations (4-20) and (4-22) also give the same $\alpha = 0.11$ and the plots are shown in Figures 4-7 and 4-7a respectively. Equation (4-24) gives the free energy of micellization ΔG°_m = -33.523 kJ mol^{-1} (M = -5.872). With some simple algebra a term in activity coefficient is separated from the cmc

terms as follows[17,19]

$$\log\left(\frac{cmc}{cmc^{\circ}}\right) = -(2-\alpha)\log.\left(\frac{\gamma_{\pm}}{\gamma_{\pm}^{\circ}}\right) - (1-\alpha)\log\left(\frac{cmc+C_3}{cmc^{\circ}}\right) \qquad (4\text{-}25)$$

which means that cmc values at different added salt concentrations can be used to derive α. A plot $\log[cmc/cmc^{\circ}]$ against $\log[(cmc+C_3)/cmc^{\circ}]$ gives $-(1-\alpha)$ as slope and $-(2-\alpha)\log(\gamma_{\pm}/\gamma_{\pm}^{\circ})$ as intercept. Equation (4-25) gave an α value of 0.12 (see Figure 4-7b).

4.2.6 Thermodynamic Parameters of Micellization based on α and cmc from electrode data

The phase-separation and mass-action models give a similar free energy of micellization (equations (3-5) and (3-15) respectively for ionic surfactants). Evans and Ninham's 'ion binding model' give free energy of micellization in equation (3-32). Free energies of micellization in different salt concentrations from different models are summarized in Table 4.4.

Table 4.4: Free energies of micellization (in kJ mol^{-1}) based on α and cmc from different models

[salt]	Eq.(3-15)	Eq.(3-32)	Eq.(4-24)
0.00	-51.11	-27.07	-32.311
0.01	-51.67	-27.37	-32.987
0.10	-52.05	-27.56	-32.978
0.50	-53.02	-28.07	-32.973
1.00	-54.14	-28.67	-32.985

Figure 4-6: Derivation of α from a plot $\ln(m_{1\pm})$ versus $\ln(m_2.\gamma_\pm)$ in CTAB systems doped with salt

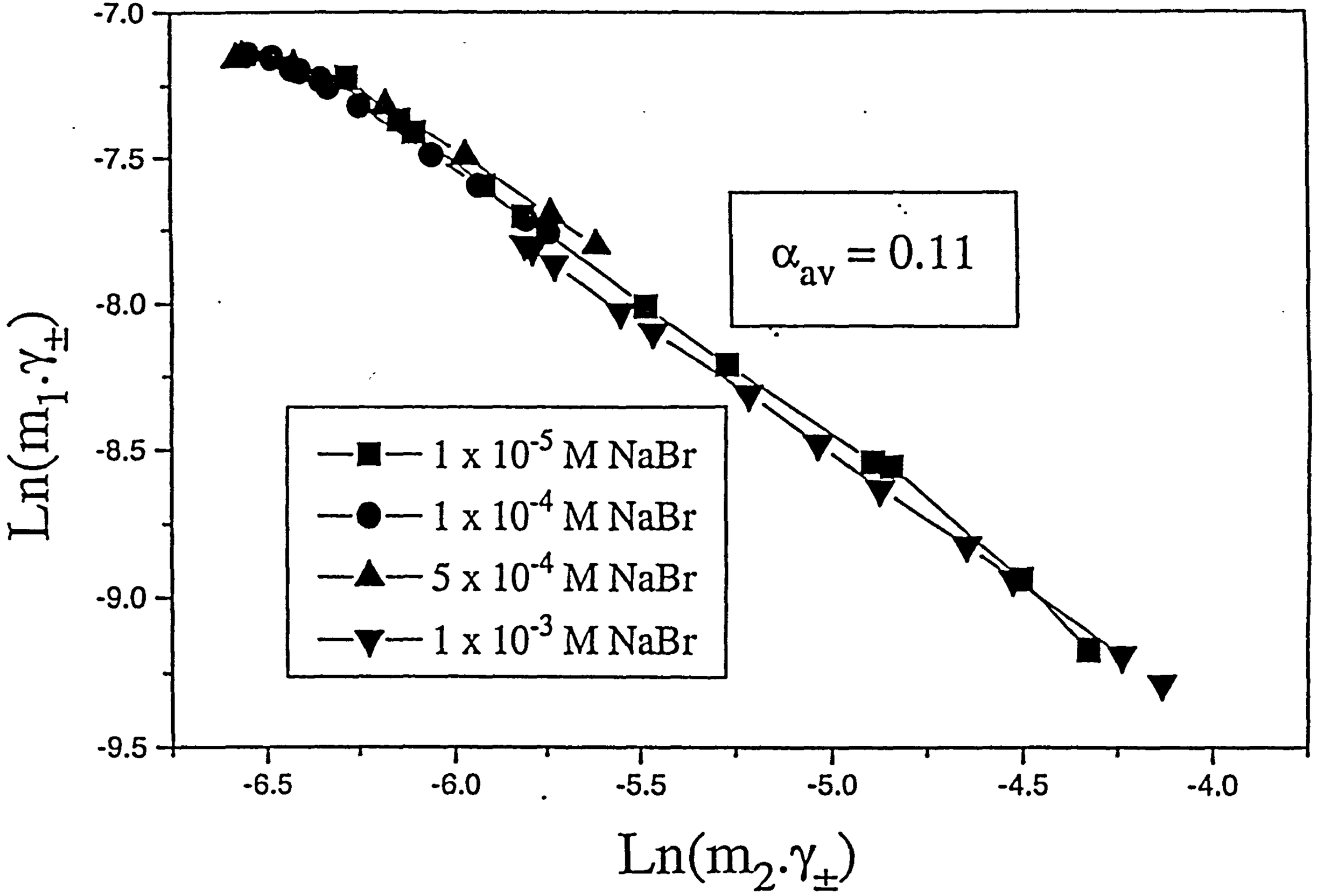

Figure 4-7: Derivation of α from cmc, cmc^o, $\gamma_\pm$ and $\gamma_\pm^o$ in CTAB systems

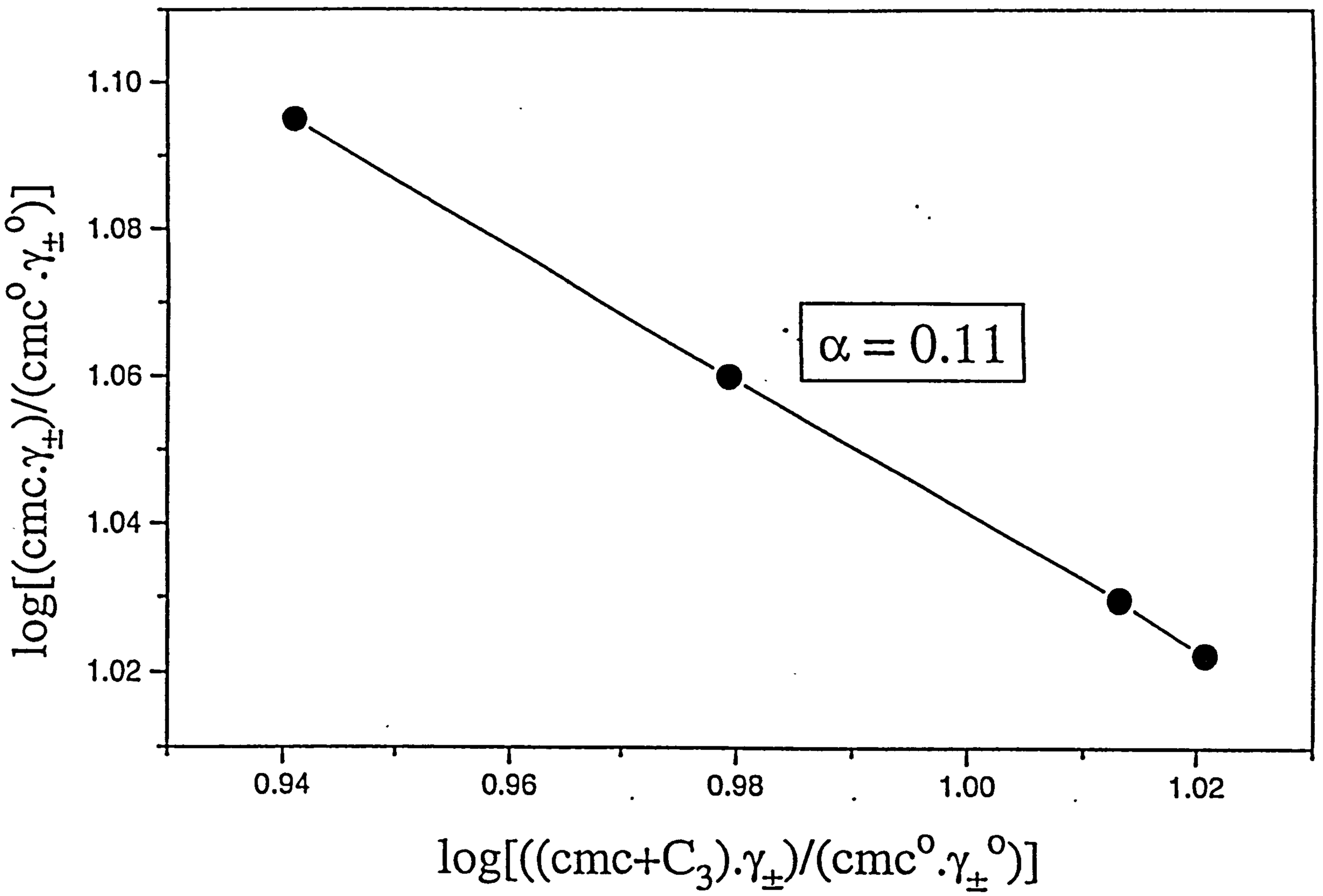

Figure 4-7a: Derivation of α from cmc and $\gamma_{\pm}$ without involving cmc^{o} and $\gamma_{\pm}{}^{o}$ in CTAB systems

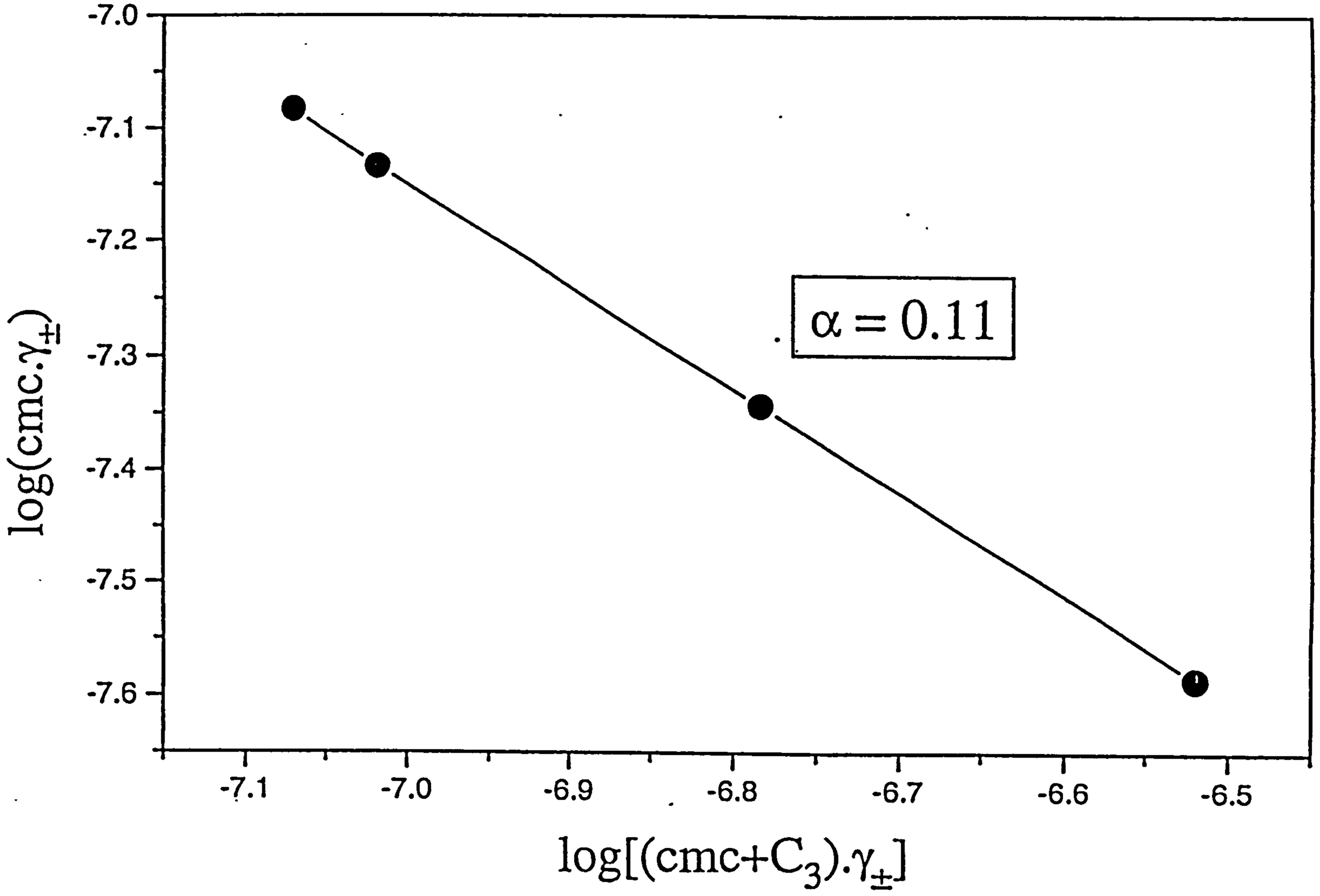

Figure 4-7b: Derivation of α from cmc and cmc^o in CTAB systems

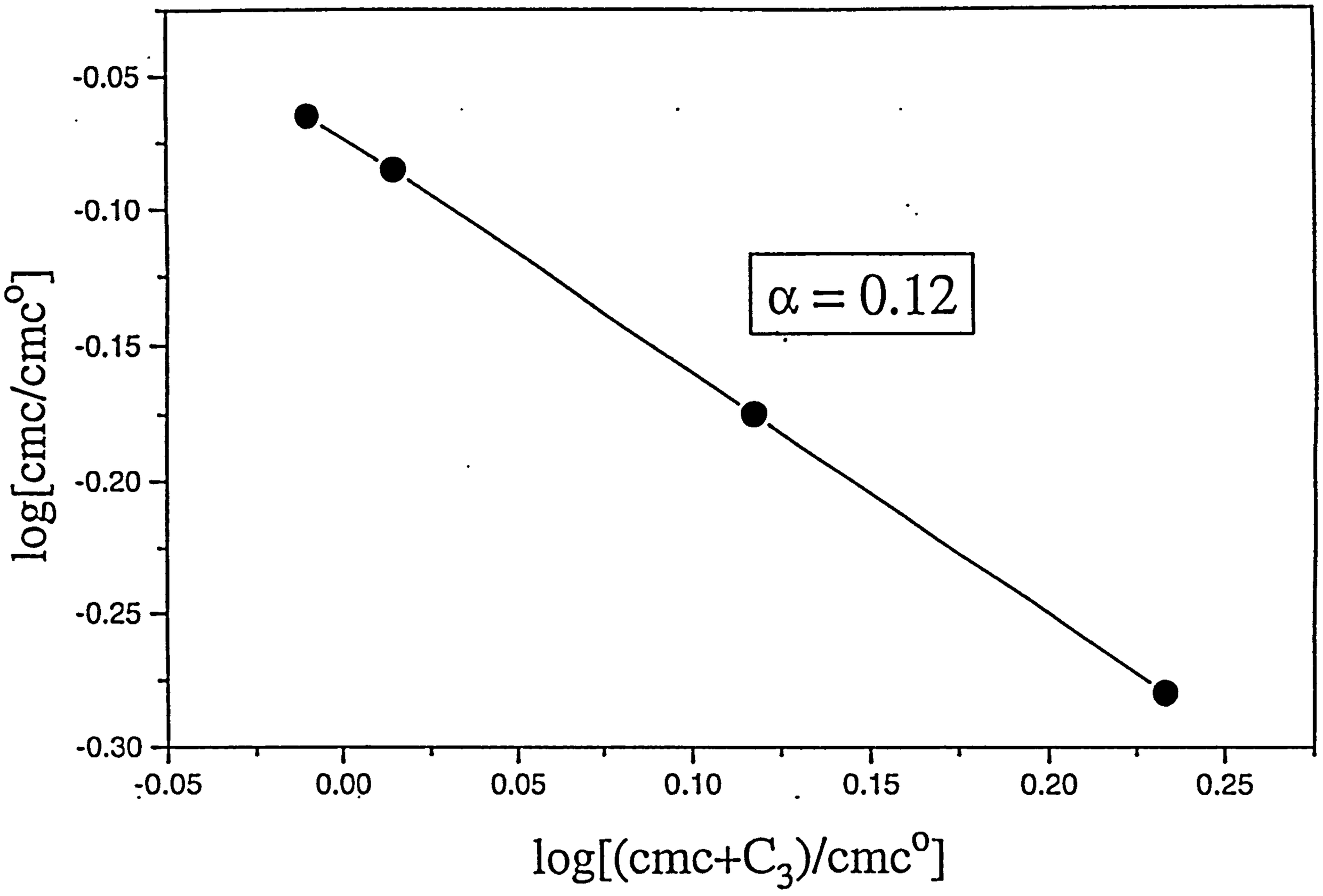

Mathematical models discussed in Chapter 3 also offer a way of calculating hydrophobic and hydrophilic free energy contributions. The Klevens contribution is given in equations (3-22a) and (3-22b). The value of G in equation (3-22a) is known from literature[25,26] (G = -5329 J mol^{-1} and w = 55.3 at 25°C). Results for hydrophobic and hydrophilic contributions are tabulated in Table 4.5.

Table 4.5: Comparison of hydrophobic and hydrophilic free energy contribution (in kJ mol^{-1}) from 'ion binding model' and the 'Klevens based models'

	Klevens based Models			Ion binding model		
[salt]	ΔG°_{mic}	ΔG°_{mic}(hc)	ΔG°_{mic}(-W)	ΔG°_m	ΔG°_{hc}	ΔG°_s
0.00	-51.19	-57.05	+5.94	-27.08	-51.18	+24.10
0.01	-51.89	-57.05	+5.38	-27.45	-51.86	+24.41
0.10	-52.11	-57.05	+5.00	-27.57	-51.85	+24.28
0.50	-53.08	-57.05	+4.03	-28.08	-51.84	+23.76
1.00	-54.21	-57.05	+2.91	-28.68	-51.85	+23.17

Table 4.6: Hydrophobic and hydrophilic contributive enthalpy (kJ mol^{-1}) and entropy (J mol^{-1} K^{-1}) of micellization from La Mesa's 'reduced variables techniques' and 'ion binding model'

[salt]	ΔS°_m	ΔS°_{hc}	ΔS°_s	ΔH°_m	ΔH°_{hc}	ΔH°_s
0.00	+91.96	+173.72	-81.76	+0.36	+0.63	-0.27
0.01	+91.96	+173.63	-81.67	+0.04	+0.06	-0.02
0.10	+91.96	+172.92	-80.96	-0.14	-0.28	+0.14
0.50	+91.96	+170.39	-78.43	-0.66	-1.04	+0.38
1.00	+91.96	+169.10	-76.14	-1.26	-1.73	+0.47

The 'ion binding model' applying La Mesa's 'reduced variables technique' offers a way of deriving the contributions of enthalpy and entropy of micellization. Equations (3-43a), (3-43b) and (3-43c) gives total, hydrophobic and hydrophilic entrcpy of micellization respectively. With the known free energies and entropies, the enthalpies of micellization can be calculated from the classical thermodynamic equation: $\Delta H^\circ = \Delta G^\circ + T\Delta S^\circ$. The results are tabulated in Table 4.6.

4.2.7 DISCUSSION

From equation[25] $\Delta G^\circ_m = RT\ln(\chi_{cmc}) = \Delta H^\circ_m - T\Delta S^\circ_m$ is easily reduced to $\Delta G^\circ_m = RT\ln(\chi_{cmc}) \sim -T\Delta S^\circ_m$ if $T \sim T^*$ because $\Delta H^\circ_{m^*} \sim 0$ and $\Delta H^\circ_m \sim \Delta H^\circ_{m^*} + \Delta C_p.(T-T^*) \sim \Delta C_p.(T-T^*) \sim 0$ at and close to T^*. In this work, studies were carried out at $T = 298.15K$ which is very close to T^* ($= 302.1K$) and ΔH°_m is expected to be very small in magnitude as evidenced in the results of this work in Table 4.6 ($-1.255 \leq \Delta H^\circ_m \leq +0.353$ kJ mol^{-1}). Added salt variation has effect on ΔH°_m, as C_3 increase ΔH°_m decrease as shown in Table 4.6. ΔH°_m calculated using the classical thermodynamic equation $\Delta H^\circ_m = \Delta G^\circ_m + T\Delta S^\circ_m$ gives the same magnitudes as $\Delta H^\circ_m = \Delta H^\circ_{hc} + \Delta H^\circ_s$ showing validity, reliability and reproducibilty of the additive approach.

As predicted by Muller[26] at temperatures close to T^*, ΔG°_{hc} and ΔG°_s are of entropic origin. This phenomenon is much more clear for ΔG°_{hc} in which the transfer of hydrocarbon tail from bulky water to the micellar is more or less entropic.

On the other hand, ΔG°_{s} involves head group-counterions-surface interactions (electrostatic interactions) which in one way or another disturbs layered (ordered) water around surfactant charged group to less ordered in the bulky water. The results of Bežan *et al*[24] from the homologous alkylpyridinium bromides show predominantly entropic contribution ($\Delta H^{\circ}_{m} <<< T\Delta S^{\circ}_{m}$). As an explanation, Lindman *et al*[27] briefly indicated that the electrostatic contribution to ΔG°_{m} is predominantly entropic.

Muller's approximation[26] that $\Delta G^{\circ}_{hc} \approx \Delta G^{\circ}_{m} = RT\ln(\chi_{cmc})$ does not agree with theory nor experimental results. The ΔG°_{s} obtained in this work (Table 4.5) are very significant to the micellization process. The magnitudes of ΔG°_{s} are significant enough not to be neglected. Emerson *et al*[28] describes the electrostatic repulsion of the ionic head groups as a factor which limits the micelle number and Evans *et al*[29] on the other hand describes repulsions between cationic head groups as inhibitors of micelle growth (i.e. determines size and shape of the micelle). Again, we find that, the magnitudes of ΔG°_{s} are high enough to fit in with this explanation.

Apart from being marginally low in magnitude the enthalpy changes ΔH°_{hc} and ΔH°_{s} to some extent obey Muller's ratio rule $\Delta H^{\circ}_{hc}/\Delta H^{\circ}_{s} = -(1+ß)/ß$ as shown in Table 4.7. The values for $\Delta H^{\circ}_{hc}/\Delta H^{\circ}_{s}$ (-2.90±0.70) and $-(1+ß)/ß$ (-2.13±0.02) are in some degree of agreement, although, as shown in Table 4.7, are

not consistent. Other ratios $\Delta G^\circ_{hc}/\Delta G^\circ_s$ and $\Delta S^\circ_{hc}/\Delta S^\circ_s$ give more agreeable values -2.16±0.05 and -2.15±0.03 respectively as compared to $-(1+\beta)/\beta$ = -2.13±0.02 and a theoretical value of -2.27±0.15[26].

Table 4.7: The ratio $-(1+\beta)/\beta$ as related to free energy, entropy and enthalpy ratios.

C_3/mM	$\Delta G^\circ_{hc}/\Delta G^\circ_s$	$\Delta S^\circ_{hc}/\Delta S^\circ_s$	$\Delta H^\circ_{hc}/\Delta H^\circ_s$	$-(1+\beta)/\beta$
0.00	-2.12	-2.12	-2.29	-2.12
0.01	-2.13	-2.13	-3.69	-2.11
0.10	-2.14	-2.14	-2.04	-2.15
0.50	-2.18	-2.17	-2.73	-2.16
1.00	-2.24	-2.21	-3.73	-2.11
mean±σ	-2.16±0.05	-2.15±0.03	-2.90±0.70	-2.13±0.02

The effective degree of micellar dissociation α from Wan-Badhi's[30] electrochemical work on sodium dodecylsulfate (SDS) as well as those derived in this work (Table 4.3) does not vary with added salt concentration (i.e $d\alpha/dC_3 \approx 0$). This observation reduces the doubts indicated by Muller[26] on systems with added salts, these systems can now be accomodated in this theory. The ratios $\Delta G^\circ_{hc}/\Delta G^\circ_s$, $\Delta S^\circ_{hc}/\Delta S^\circ_s$ and $\Delta H^\circ_{hc}/\Delta H^\circ_s$ in 0.01, 0.10, 0.50 and 1.00 mmol dm^{-3} are listed in Table 4.7 and show consistency as evidenced by σ_{n-1} of ±0.05, ±0.03 and ±0.70 respectively. The values compares well with $-(1+\beta)/\beta$ (-2.13+0.02).

4.3 POLYMER-MICELLE COMPLEXES

4.3.1 Preparation of uncharged hydrophobic water-soluble polymer solutions

Poly(propylene oxide) (PPO) {weight-average molecular weight (M_w=1000), Aldrich} was used as received. Poly(propylene oxide) has monomer units of $H[-OCH(CH_3)CH_2-]_nOH$ with unit molecular weight 58 gram per PPO monomer.

Poly(vinylmethylether) (PVME) (50% (w/w) solution in water, Aldrich) was freeze-dried[15]. The yellow residue was dissolved in ethanol and heated with activated carbon. It was then filtered to eliminate carbon and the solvent was evaporated and the final residue was dissolved in water, dialyzed (Dialysis Tubing-Visking size 5-24/32" Dialysis membrane, BDH) for four days in doubly distilled deionized water (water was changed every 24 hours), and finally freeze-dried. The polymer was stored as 4% (w/w) stock solution in water. The viscosity-average molecular weight (M_w) of PVME (determined by viscosity measurement in butanone[16]) is 27000 g mol^{-1}. Poly(vinylmethylether) has monomer units of $[-CH_2CH(OCH_3)-]_n$ with unit molecular weight 58 gram per PVME monomer.

Ethyl(hydroxyethyl)cellulose (EHEC), Bermocoll CST-103, M_w=120000 (estimated by Wan-Badhi[30] using viscosity-average molecular weight techniques), Berol Nobel (Sweden); was dissolved in doubly distilled deionized water. The solution was heated for 2 hours at 80°C, left to stir for

solution was heated for 2 hours at 80°C, left to stir for more than 2 hours and then shaken on a warm water bath (70°C) for half an hour. It was then left to stir at room temperature for another two hours. After that, the solution was cooled to 8°C and then poured into 1000 ml flask which was filled to mark to make a 5 g dm^{-3} (0.5 g dL^{-1}) solution. The solution was placed on an ice-bath and kept stirred for a further 4 hours. The EHEC stock solution was freed from remaining salt by dialysis (Dialysis Tubing-Visking size 5-24/34" Dialysis membrane, BDH) for 4 days in doubly distilled deionized water[31]. The dialysed EHEC solutions were collected together and the concentration of the sample was determined by drying a 10 ml sample to constant weight. Finally the concentration of the EHEC solution was adjusted to 0.5 g/dL. Ethyl(hydroxyethyl)cellulose has monomer units of molecular mass 234 gram per EHEC monomer and its structure is given in Figure 4-8.

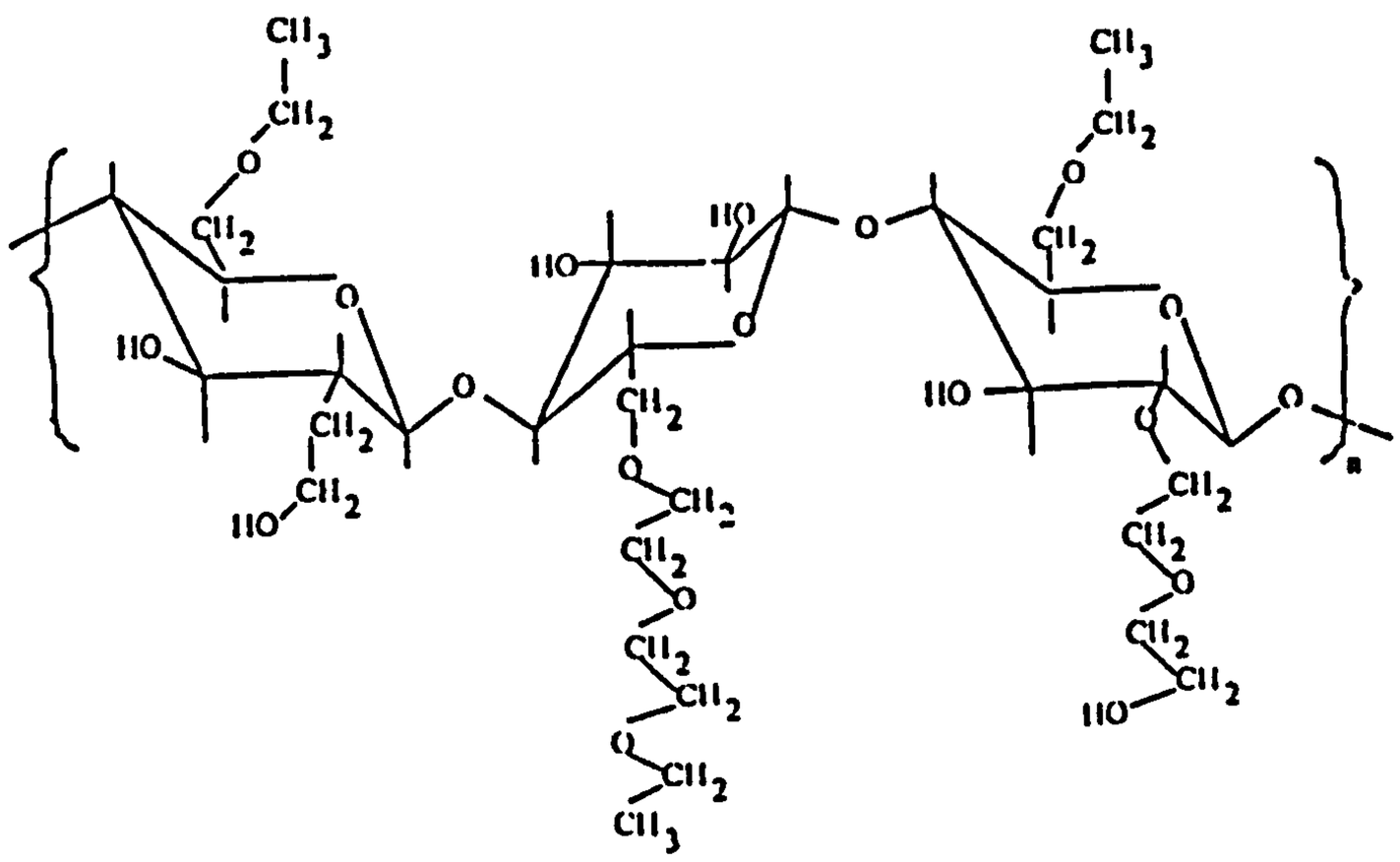

Figure 4-8: The structure of EHEC (ethyl(hydroxyethyl)-cellulose) monomer (234 g (monomole EHEC)$^{-1}$)

4.3.2 EMF Measurements in CTAB-0.5%Polymer Systems

The emf measurements procedures in polymer/CTAB systems are similar to those of CTAB/added salt systems in section 4.2.1. The same cell assemblies of type I and II are used to derive m_1 and $C_1C_2.\gamma_{\pm}^2$ and the iterative procedure used in section 4.2 was used to determine m_2 and $\gamma_{\pm}$. A summary of the Nernstian characteristics of the CTAB selective electrode in these systems is given in Table 4.8 and typical log(C_1) versus EMF plots for PPO/CTAB, PVME/CTAB and EHEC/CTAB systems are shown in Figure 4-9. The values m_1, m_2 and $\gamma_{\pm}$ are summarized in Tables 4.A5, 4.A6 and 4.A7 respectively for PPO/CTAB, PVME/CTAB and EHEC/CTAB.

Table 4.8: Electrode parameters of the CTAB selective electrode in polymer/CTAB systems doped with 0.1 mM NaBr

CTAB-NaBr-0.5%polymer system	Sodium Electrode		Bromide Electrode	
	S_1 mV dec^{-1}	E_o,mV	S_2 mV dec^{-1}	E_o,mV
PPO	56.14	565.89	114.01	572.75
PVME	56.85	396.56	112.97	559.84
EHEC	56.81	345.72	115.48	519.75

4.3.3 The effective degree of micellar dissocation α in polymer/CTAB systems

Under ideal conditions the effective degree of micellar dissociation for polymer/surfactant systems can be derived from equations (4-15), (4-20), (4-22) and (4-25). This is not possible for the present polymer/surfactant mixtures because of limitations with the polymer solubility and

precipitation problem when more than 10^{-4} mol dm^{-3} of salt is added. For all polymers studied only data in 10^{-4} mol dm^{-3} NaBr are available. The alternative way to obtain α was to use the mass balance equation.

The Mass balance equations for different species in an ionic surfactant system are

$$C_1 = m_1 + \Sigma_r \bar{N}_r C_r \qquad (4\text{-}26a)$$

$$m_2 = \Sigma_i z_i m_i + z_3 C_3 + \Sigma_r \beta_r C_r \qquad (4\text{-}26b)$$

$$m_3 = \Sigma_i z_i m_i / z_3 + C_3 \qquad (4\text{-}26c)$$

for the surfactant ions, counterions and coions respectively. If we assume the following conditions for the system (i) $z_3=1$ (1:1 added salt), (ii) monodisperse micelles ($\Sigma_r \beta_r C_r = \beta_m C_m$ and $\Sigma_r \bar{N}_r C_r = N_m C_m$), and (iii) 1:1 surfactant ($i=1$, $z_i=1$, $m_i=m_1$) the equations (4-26a) and (4-26b) become

$$C_1 = m_1 + N_m C_m \qquad (4\text{-}27a)$$

$$m_2 = m_1 + C_3 + \beta_m C_m \qquad (4\text{-}27b)$$

where N_m and C_m are the aggregation number and concentration for monodisperse micelles respectively. The parameter β_m, according to Hall[19], is a function of T only and is the number of counterions required per micelle to neutralize its effective charge. It should not be confused with the degree of counterion binding ß. Equation (4-27a) give C_m as

$$C_m = (C_1 - m_1)/N_m \qquad (4\text{-}28)$$

which when substituted into equation (4-27b) yields

$$m_2 = m_1 + C_3 + \beta_m(C_1-m_1)/N_m \qquad (4\text{-}29)$$

Since the value of the fraction β_m/N_m is α, the final form of equation (4-29) becomes

$$m_2 = m_1 + C_3 + \alpha.(C_1-m_1) \qquad (4\text{-}30)$$

which is a very useful mass balance equation for the counterions.

With known C_1, m_1, m_2 and C_3, the value of α can be calculated at different surfactant concentrations. Thus

$$\alpha = \left(\frac{m_2-m_1-C_3}{C_1-m_1}\right) \qquad (4\text{-}31)$$

Plots α against C_1 are shown in Figures 4-10, 4-11 and 4-12 for PPO/CTAB, PVME/CTAB and EHEC/CTAB systems respectively. These plots show that once binding of CTAB to the polymers occurs then counterion binding takes place which is a good indication that the bound surfactant exists in the form of aggregates. In addition, α decreases as the surfactant concentration increases in the binding region. These plots also indicate that the value of α levels-off at higher surfactant concentrations. The most important conclusion from this value is that the degree of counterion binding to the bound aggregates increases as the aggregates grow in the binding region.

Figure 4-9: EMF versus log(C_1) plots for pure CTAB, PPO/CTAB, PVME/CTAB and EHEC/CTAB systems

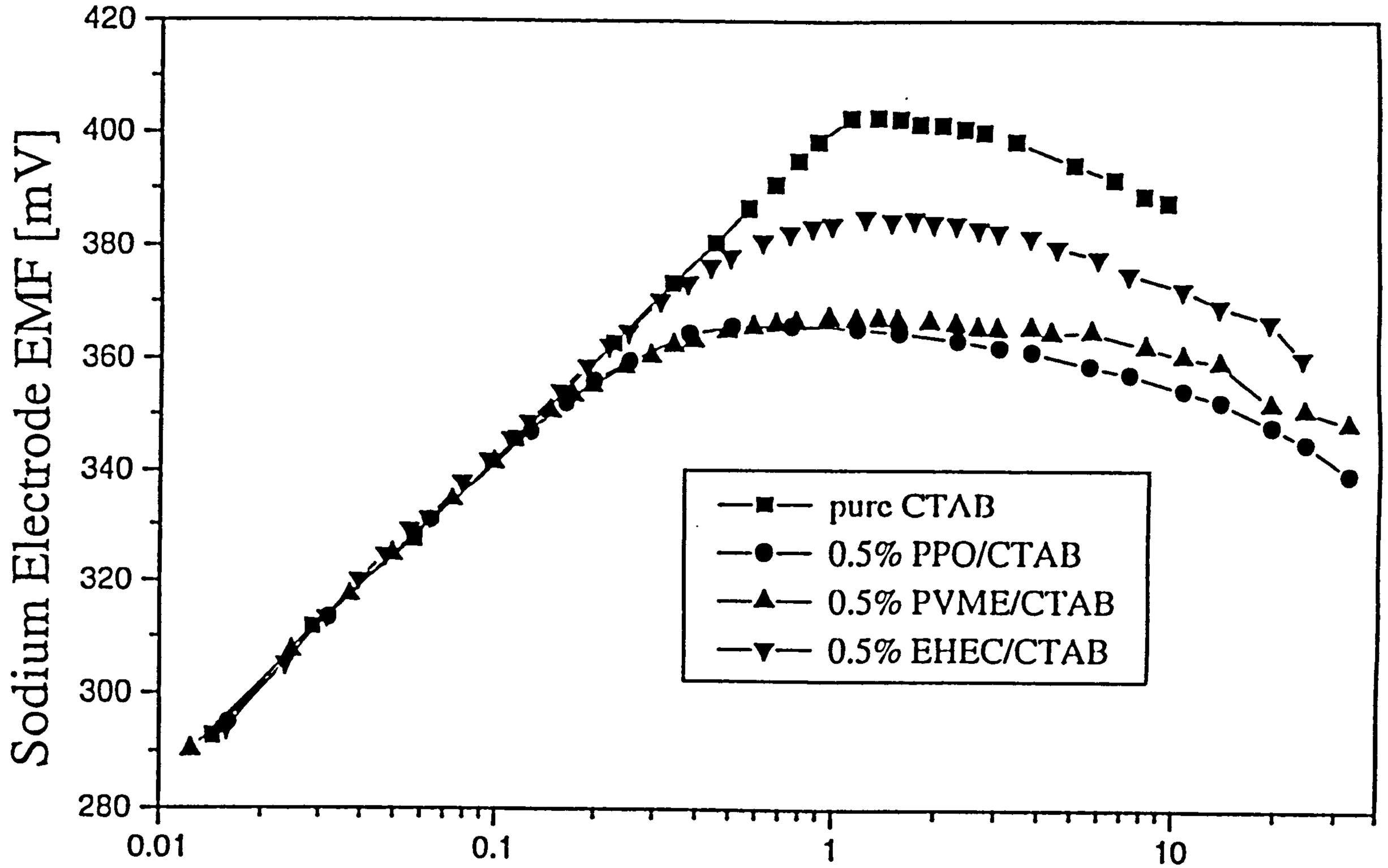

Figure 4-10: Derivation of α as a convergent value in a plot α versus C_1 in CTAB/0.5%PPO system

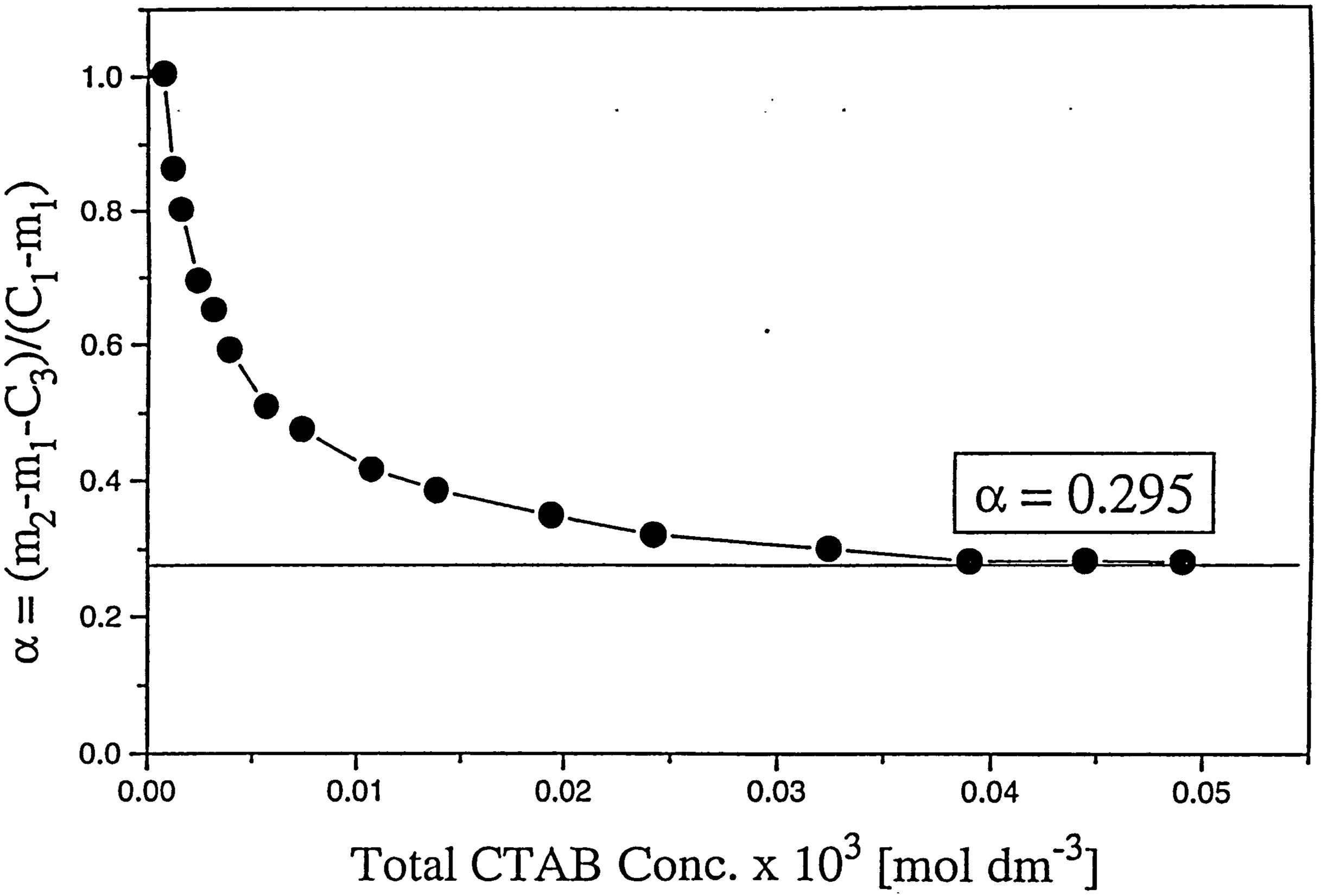

Figure 4-11: Derivation of α as a convergent value in a plot α versus C_1 in CTAB/0.5%PVME system

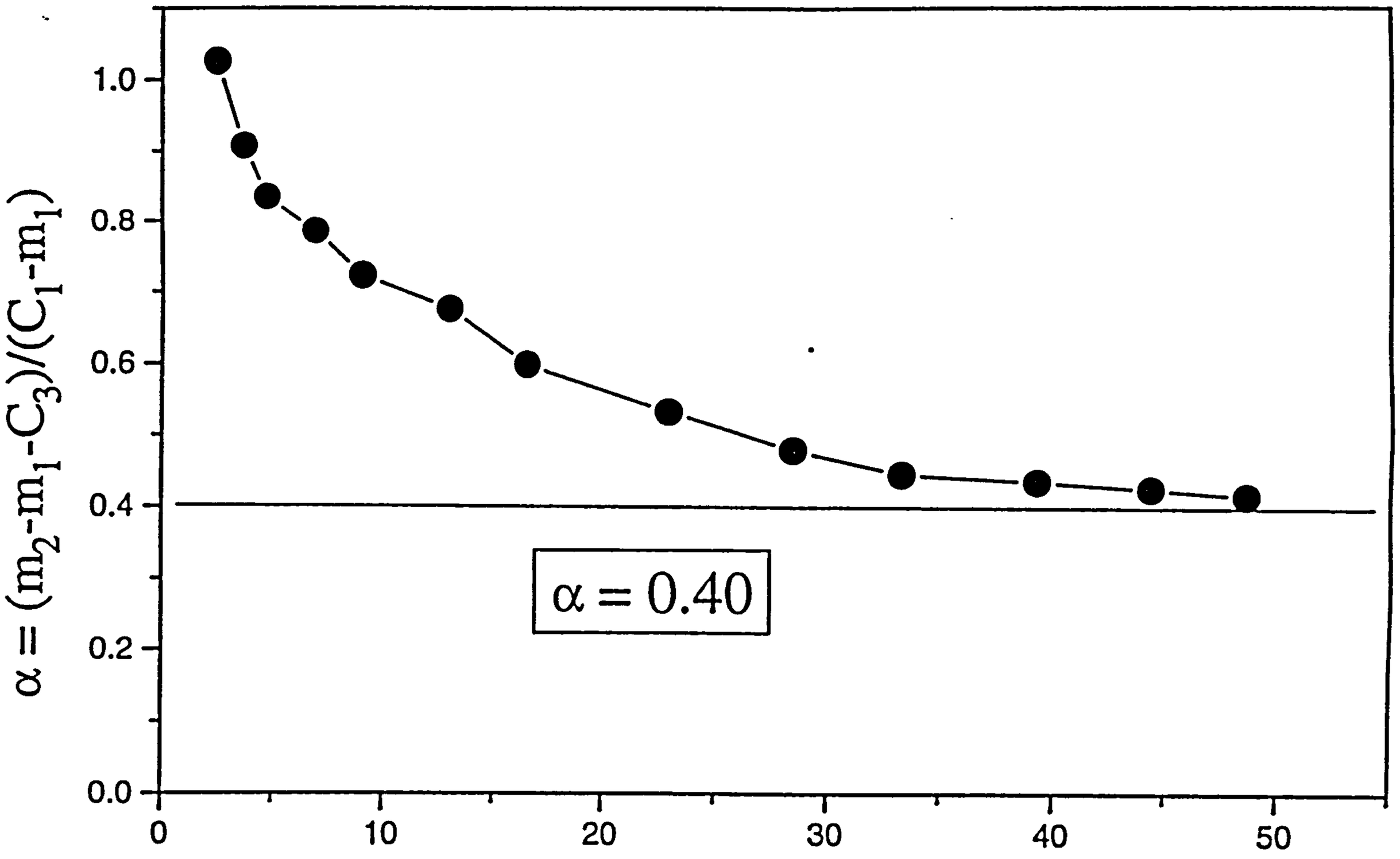

Figure 4-12: Derivation of α as a convergent value in a plot α versus C_1 in CTAB/0.5%EHEC system

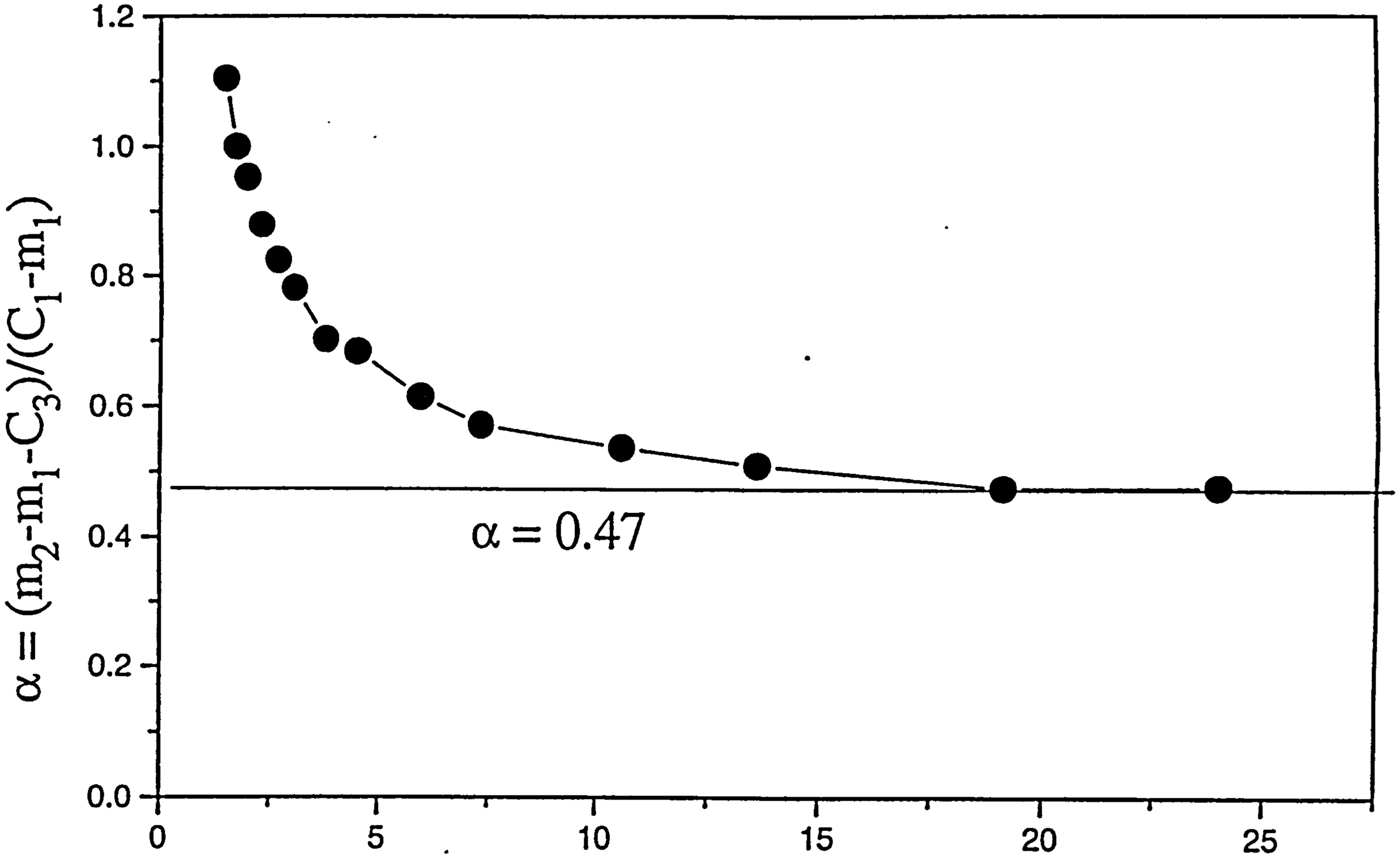

4.3.4 Binding Isotherms and Critical Points T_1 and T_2

In this work the measurements were carried out using a fixed polymer concentration (C_p) and constant added salt concentration (C_3 = 10^{-4} mol dm^{-3}). In these systems the total CTAB concentration C_1 is expressed as

$$C_1 = m_1 + \Gamma C_p \qquad (4\text{-}32)$$

where C_p is the polymer concentration expressed in mole of polymer monomer dm^{-3}, m_1 is the CTAB monomeric concentration derived from electrode data and Γ is the amount of CTAB bound per mole of polymer monomer (commonly known as a 'binding ratio'). Γ is given by the expression

$$\Gamma = \left(\frac{C_1 - m_1}{C_p}\right) \qquad (4\text{-}33)$$

The m_1 values at each C_1 are known from electrode data, C_p is known and the Γ values corresponding to each C_1 are calculated using equation (4-33). A plot Γ against m_1 form the basis of the binding isotherms between CTAB and the polymers (PPO, PVME and EHEC) and are shown in Figures 4-13, 4-14 and 4-15 respectively.

We now consider the critical concentrations associated with the binding of CTAB to the polymers. These concentrations are denoted by T_1 and T_2 as described in Chapter 1 section 1.7.

The critical concentration T_1 has its usual meaning as the onset of polymer-surfactant interactions. T_1 is estimated from EMF/surfactant plots shown in Figure 4-9 and corresponds to the total surfactant concentration at which the EMF starts deviating from Nernstian behaviour. The T_1 values for PPO/CTAB, PVME/CTAB and EHEC/CTAB (shown in Table 4.9) are approximately equal. It is generally regarded that T_1 is affected by all factors affecting the cmc, such as: temperature[32], added salt[30,33], and surfactant chain length[1,34,35]. It is also interesting to note that at T_1 the EMF of the surfactant electrode measured against the commercial bromide electrode starts deviating from Nernstian behaviour indicating that counterion binding take place. This is regarded as strong evidence that the bound surfactant exists in the form of small micellar type aggregates.

Table 4.9: T_1, ΔG_1 and ΔG_1-ΔG values in polymer/CTAB systems doped with 10^{-4} mol dm^{-3} NaBr

System	PPO/CTAB	PVME/CTAB	EHEC/CTAB
$T_1 \times 10^{-3}$ mol dm^{-3}	0.125	0.134	0.125
ΔG_1 kJ mol^{-1}	-22.283	-22.110	-22.283
ΔG_1-ΔG kJ mol^{-1}	-4.670	-4.497	-4.670

where ΔG = -17.613 kJ mol^{-1} for CTAB/10^{-4} mol dm^{-3} NaBr system.

The Gibbs free energies of stabilization of the micelle by polymer complexation[35,36] (ΔG_1-ΔG = 2.303RTlog(T_1/cmc)) listed in Table 4.9 are approximately equal and negative for all polymer/CTAB systems. This is a clear evidence that: (i)

there is stabilization of the micellar aggregates in presence of polymers, and (ii) the onset affinity for polymer micelle formation is independent of the nature of polymers. This observation is supported by Hoffmann and Huber[7] who gets almost the same T_1 values for PVAA/CTAB (PVAA is the neutral copolymer poly(vinyl alcohol-co-vinyl acetate) as T_1 for PPO/CTAB, PVME/CTAB and EHEC/CTAB.

In the earlier work[33,37,38] on the binding of anionic surfactants to polymers, T_2 was considered as the surfactant concentration corresponding to the polymer being saturated with bound surfactant and also sometimes the formation of free micelles in solution. In these circumstances T_2 could be estimated from plots such as EMF against concentration. For polymer/anionic surfactant systems it has been shown that the EMF of the surfactant electrode for both surfactant and surfactant plus polymer coincide at a very low surfactant concentration in the Nernstian region. At T_1, the EMF of the polymer/surfactant system starts deviating from that of the pure surfactant. The two EMF curves then diverge as more surfactant is added until a critical concentration is reached when the EMF of the surfactant and surfactant plus polymer are the same again. This critical concentration was generally referred as T_2. For anionic surfactant/polymer systems T_2 is regarded as the total surfactant concentration beyond which the polymer no longer has any influence on the surfactant aggregating process. In other words the polymer is fully saturated with bound

surfactant at T_2. Unfortunately in the present work we are unable to reach a sufficiently high surfactant concentration for the two EMF curves to coincide after the onset of binding. This observation was also made by Hoffmann and Huber[7].

We can however estimate T_2 again by reference to anionic surfactant/polymer interactions. According to Hall[12,19] a thermodynamic condition exists which can be used to estimate T_2. This theoretical consideration is related to equation (4-16) and can be expressed as follows

$$\log(m_1.\gamma_\pm) + (1-\alpha)\log(m_2.\gamma_\pm) \leq M \qquad (4\text{-}34)$$

The LHS of the above equation relate to m_1, m_2 and $\gamma_\pm$ in the binding region at surfactant concentrations exceeding T_1 and α for micellar CTAB as derived in section 4.2.5. The M value is the intercept of the plot shown in Figure 4-6 for micellar CTAB. In polymer/anionic surfactant mixtures the LHS equals the RHS at T_2. In Figures 4-16, 4-17 and 4-18 we have plotted the LHS of inequality (4-34) against total surfactant concentration in the binding region. The value M is also indicated. From this plot we have estimated T_2 at the surfactant concentrations shown in Table 4.10 for the different polymers.

Another interesting observation that we wish to report in relation to this work is that a plot m_1 against C_1 goes through a fairly pronounced maximum as shown in Figures 4-

Figure 4-13: The binding isotherm for CTAB/0.5%PPO system

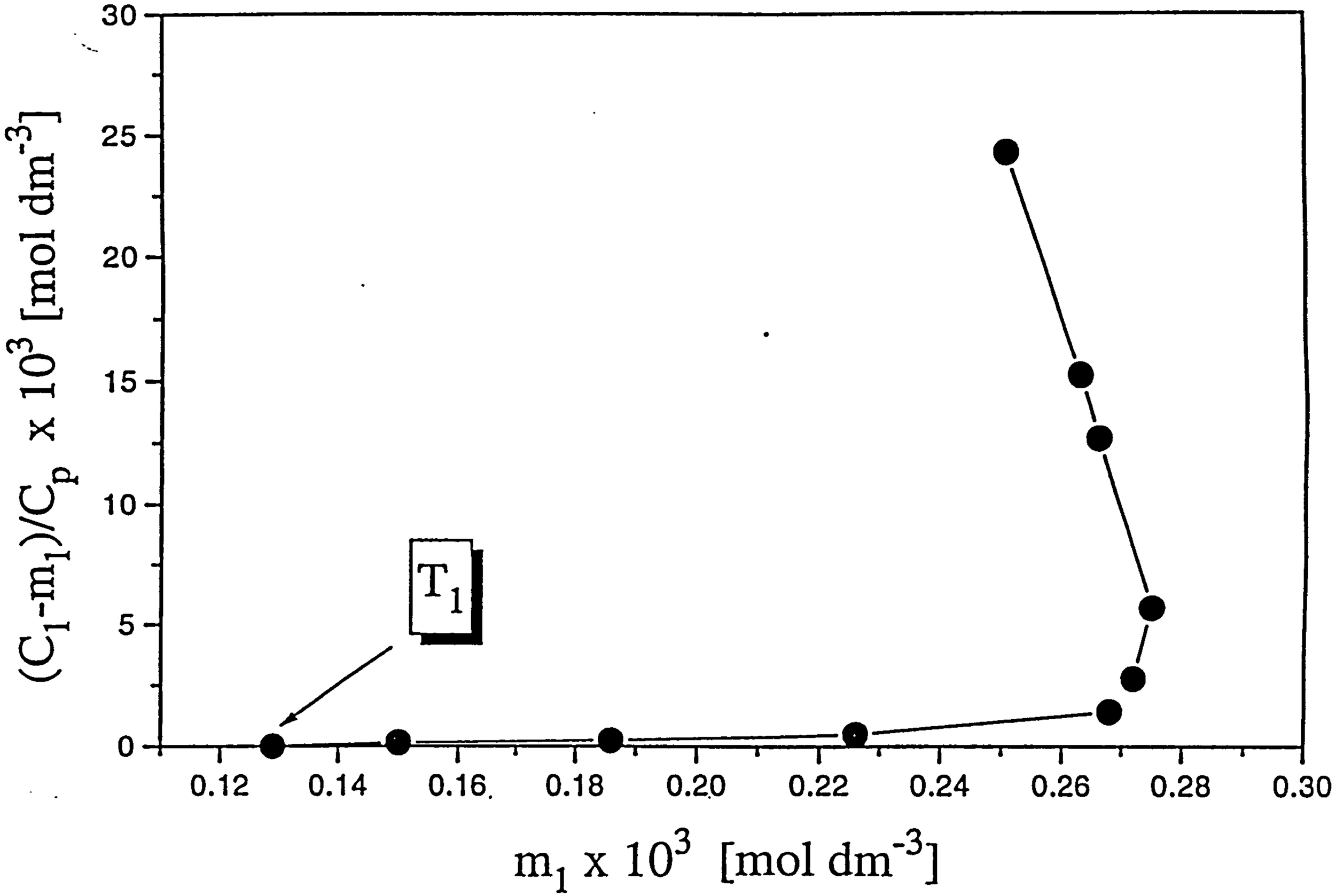

Figure 4-14: The binding isotherm for CTAB/0.5%PVME system

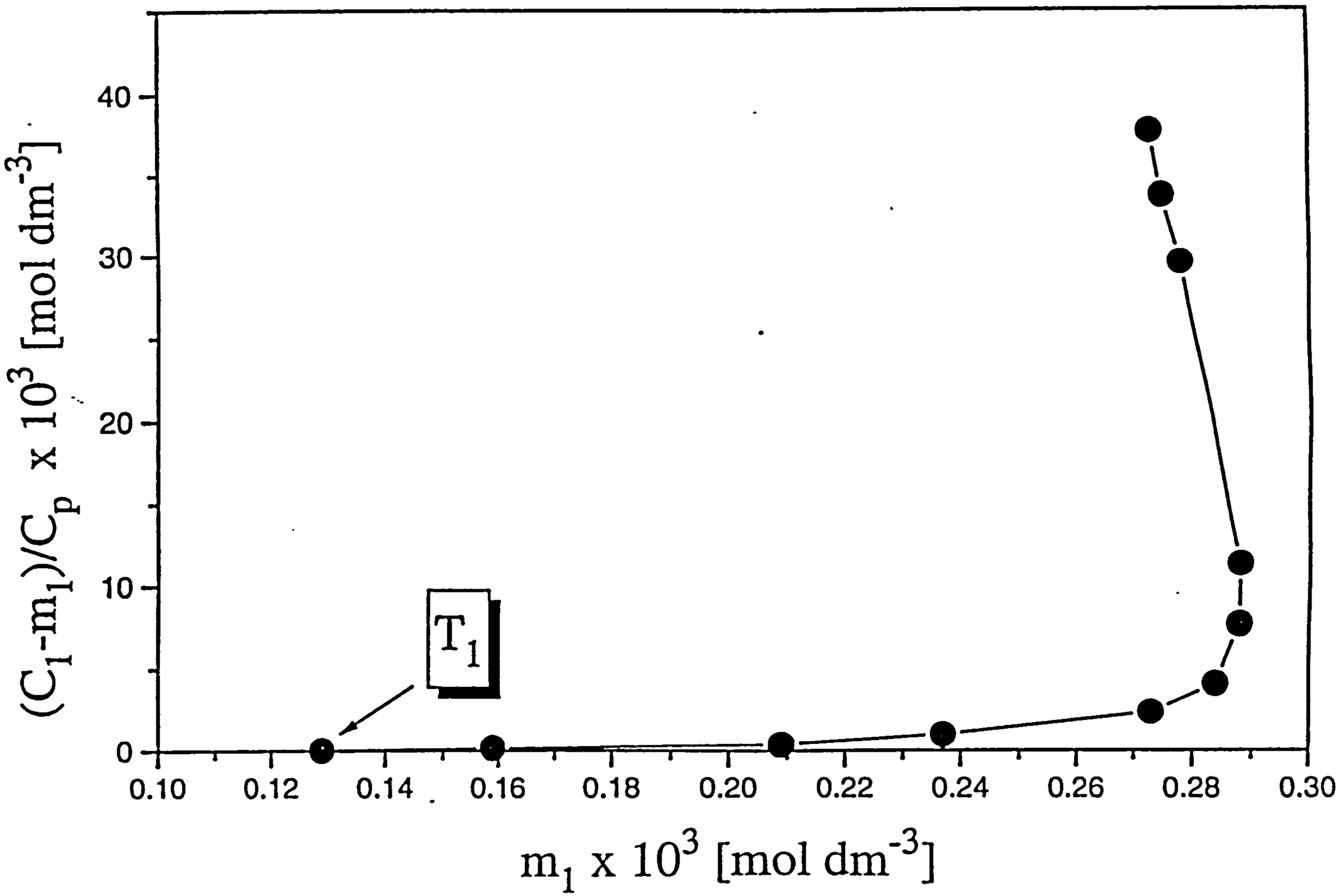

Figure 4-15: The binding isotherm for CTAB/0.5%EHEC system

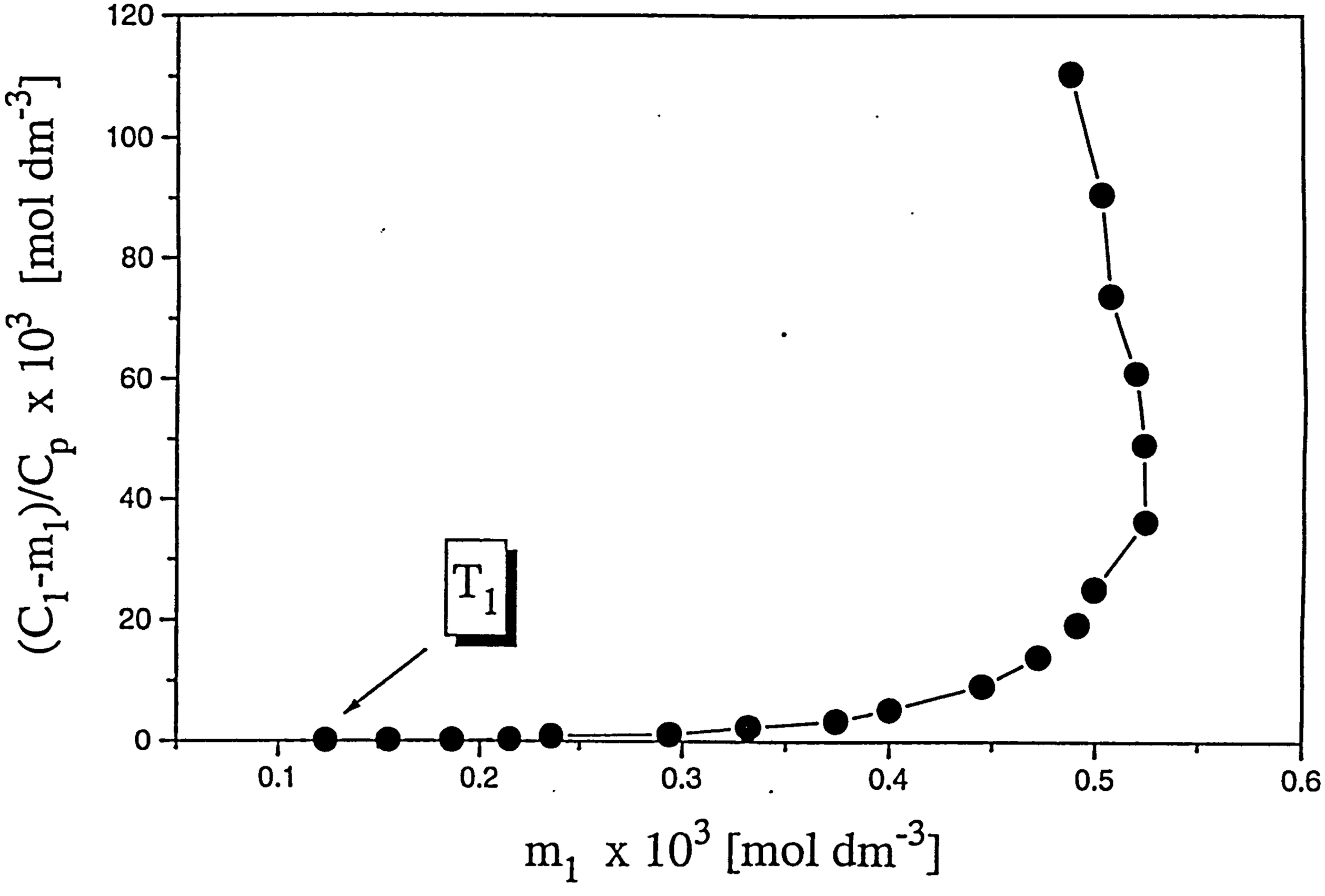

Figure 4-16: Estimation of T_2 from a plot $\log(m_1.\gamma_{\pm})+(1-\alpha).\log(m_2.\gamma_{\pm})$ versus C_1 for CTAB-PPO system

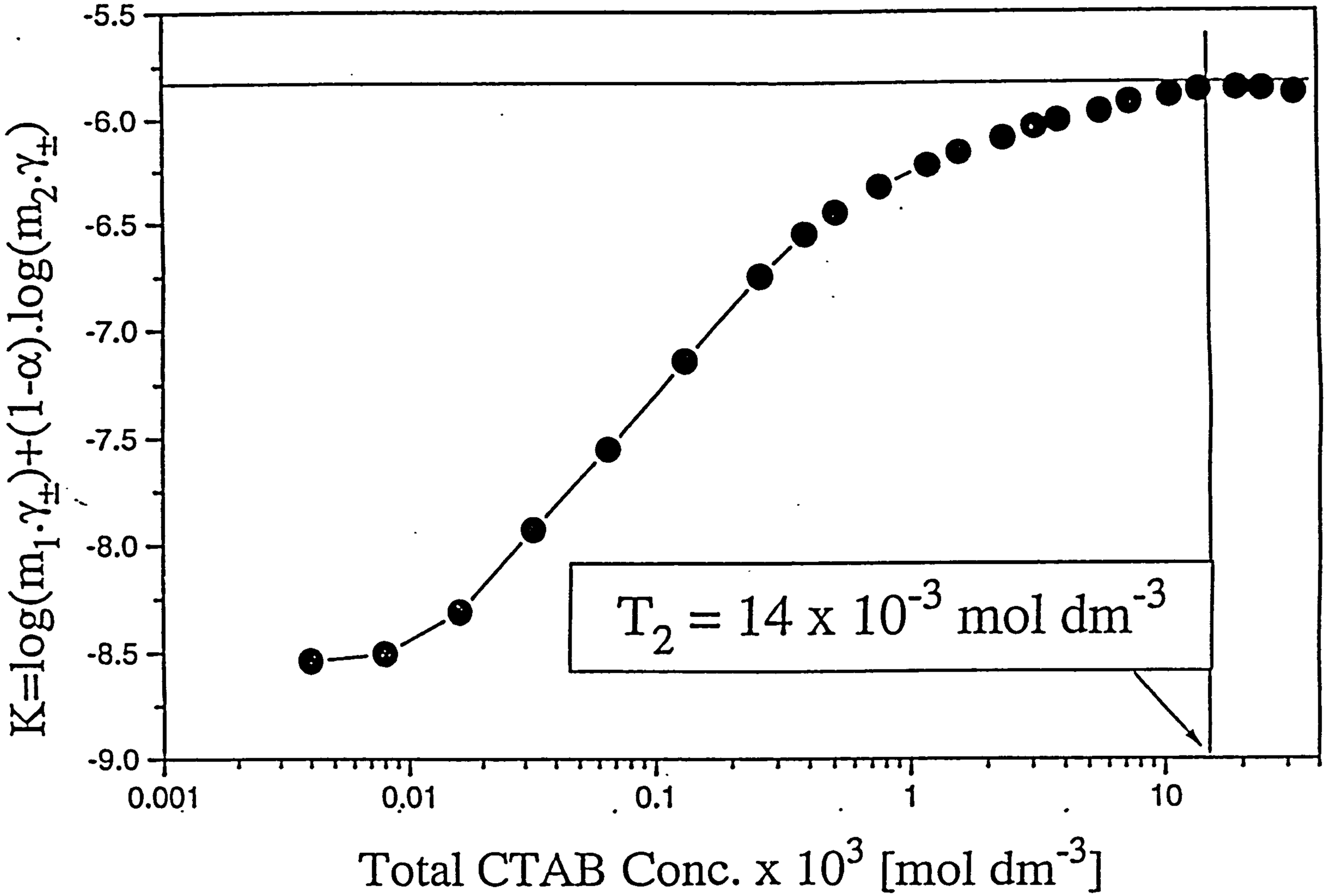

Figure 4-17: Estimation of T_2 from a plot $\log(m_1.\gamma_{\pm})+(1-\alpha).\log(m_2.\gamma_{\pm})$ versus C_1 for CTAB-PVME system

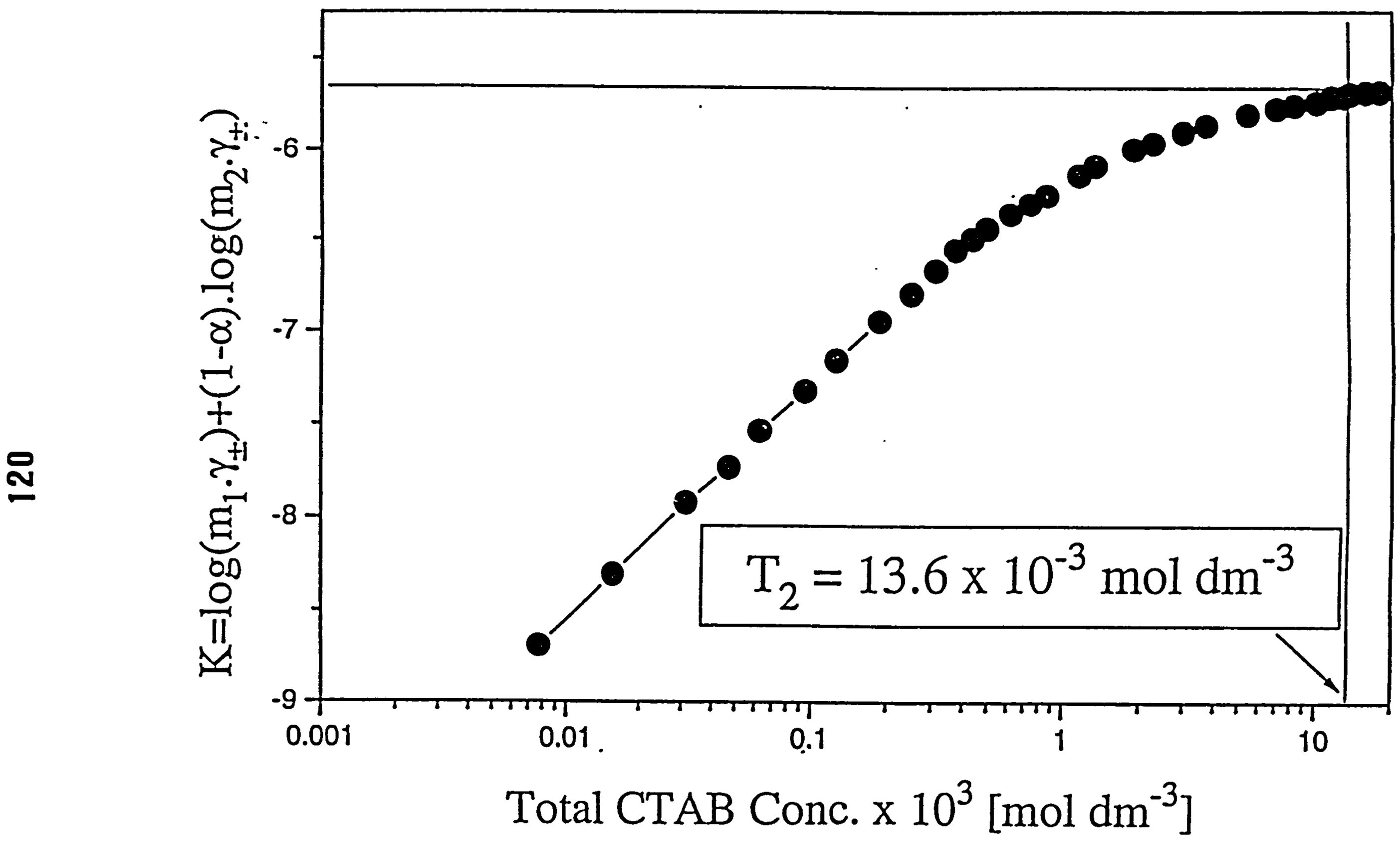

Figure 4-18: Estimation of T_2 from a plot $\log(m_1.\gamma_{\pm})+(1-\alpha).\log(m_2.\gamma_{\pm})$ versus C_1 for CTAB-EHEC system

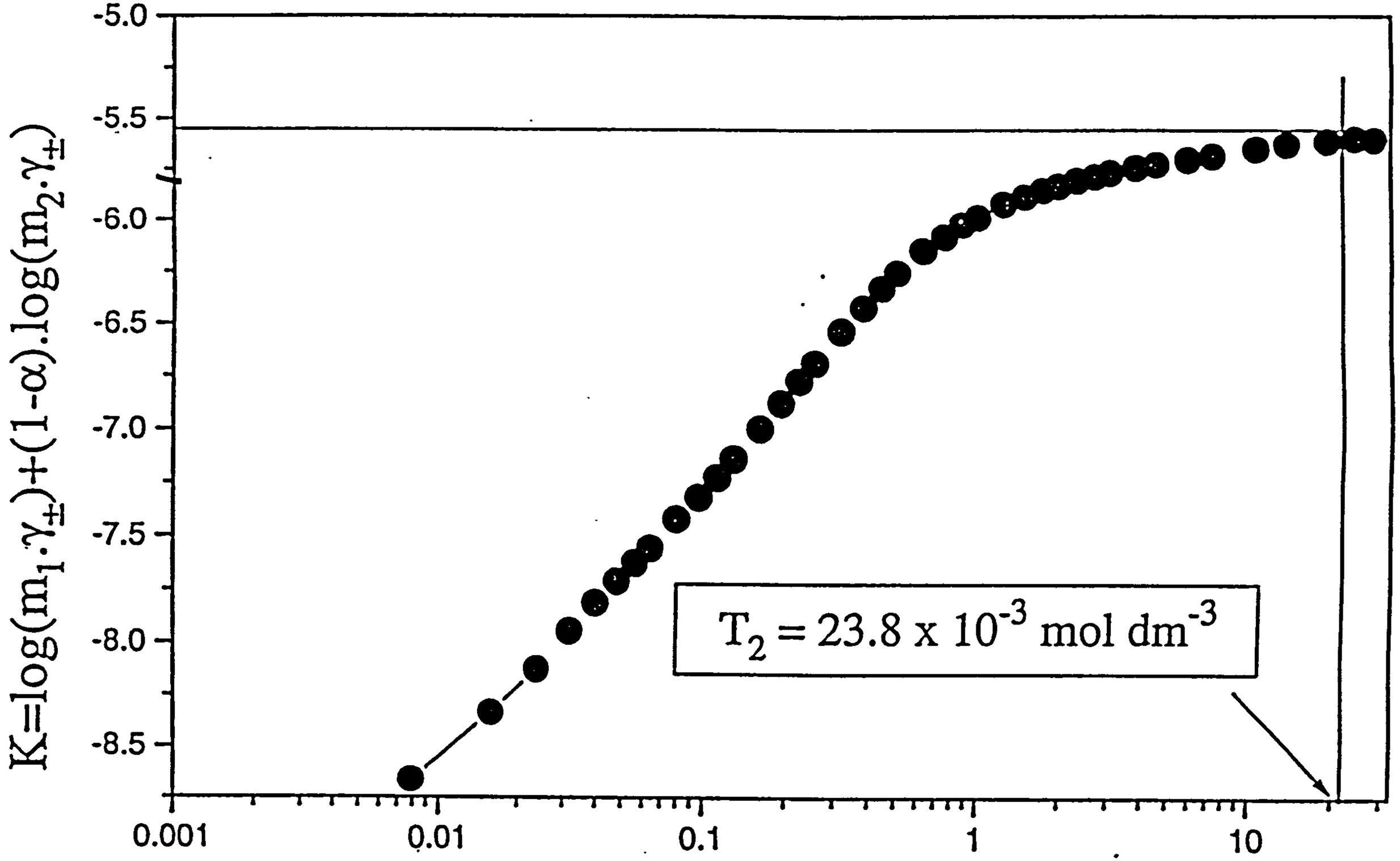

Figure 4-19: A plot m_1 against C_1 to determine maximum m_1 for CTAB/PPO system

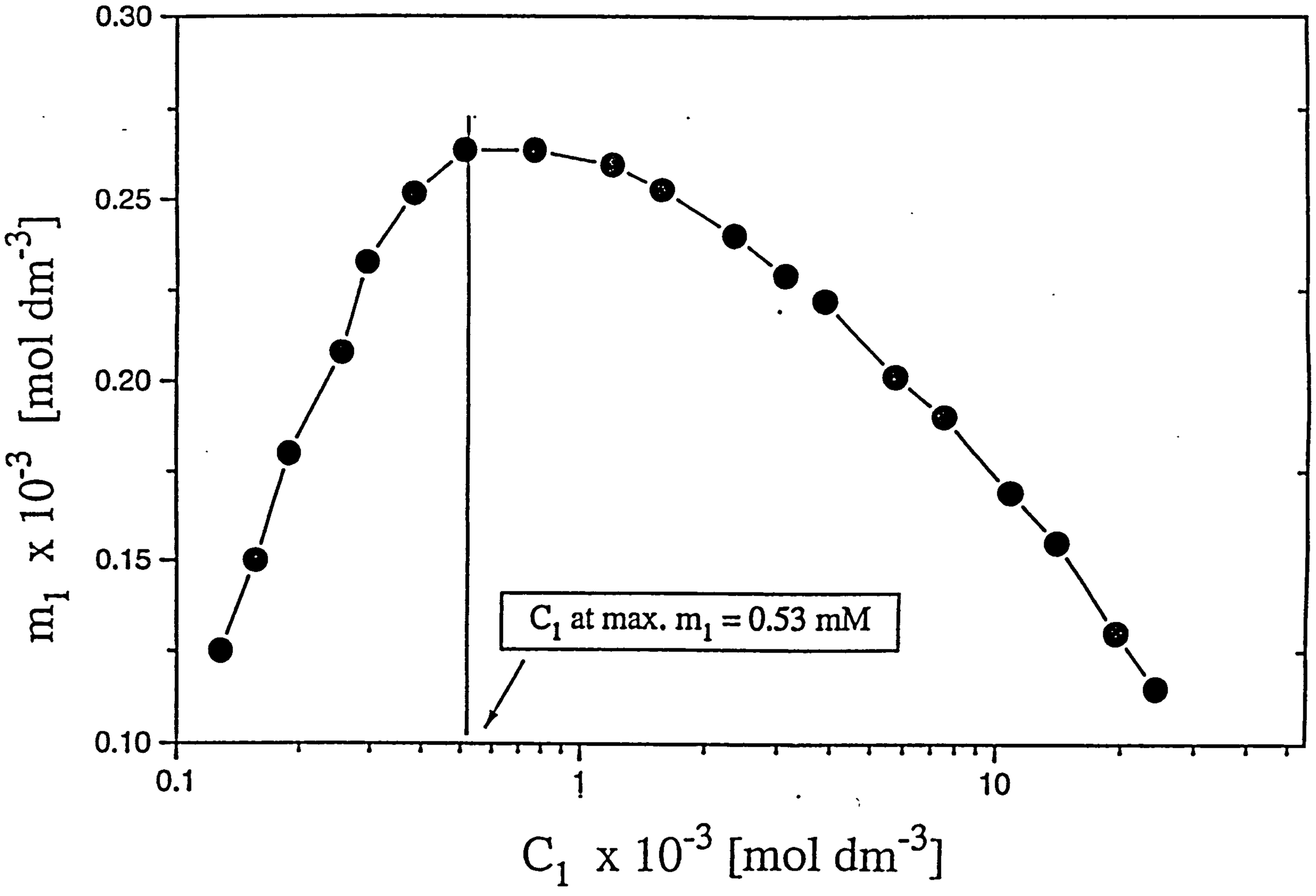

Figure 4-20: A plot m_1 against C_1 to determine maximum m_1 for CTAB/PVME system

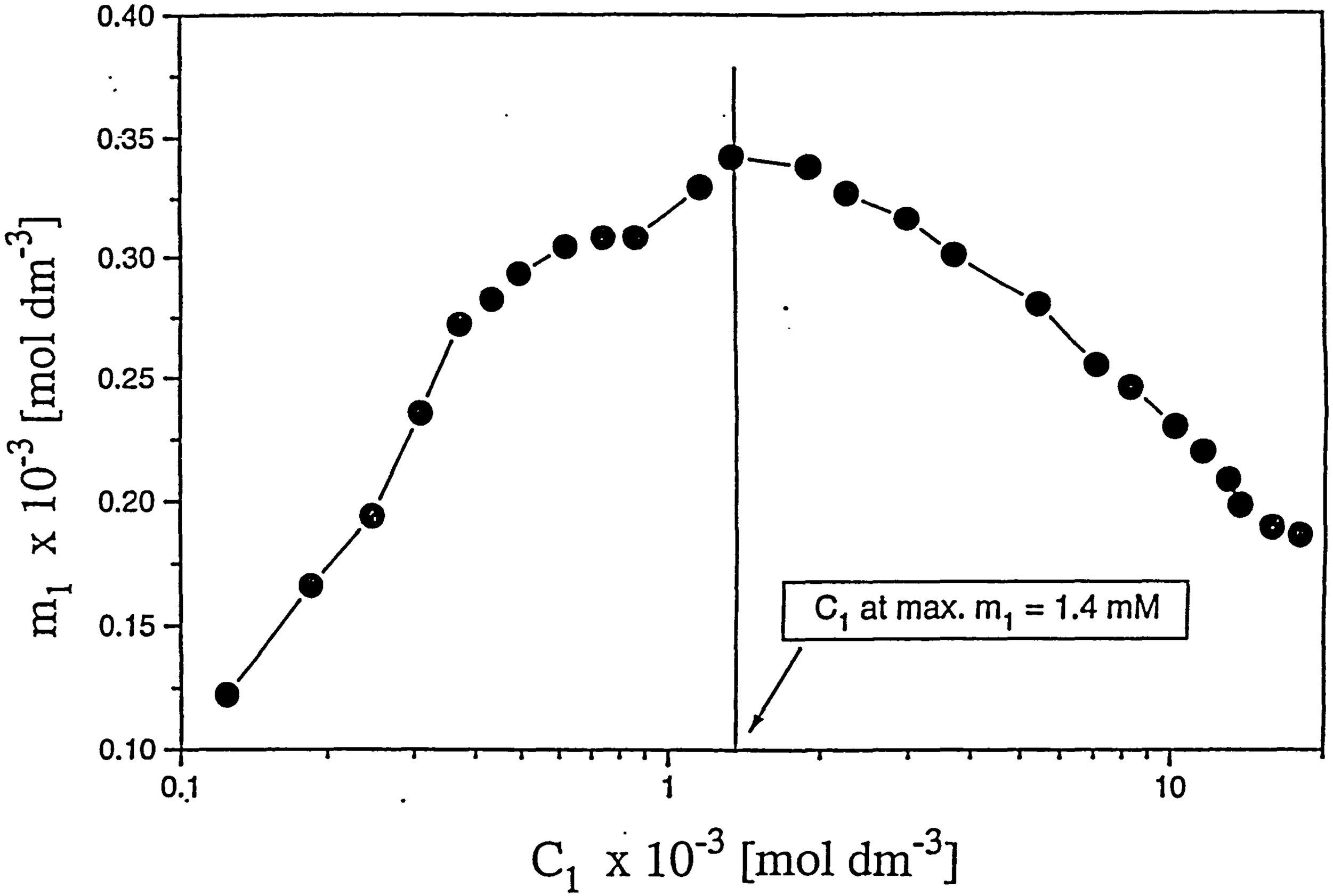

Figure 4-21: A plot m_1 against C_1 to determine maximum m_1 for CTAB/EHEC system

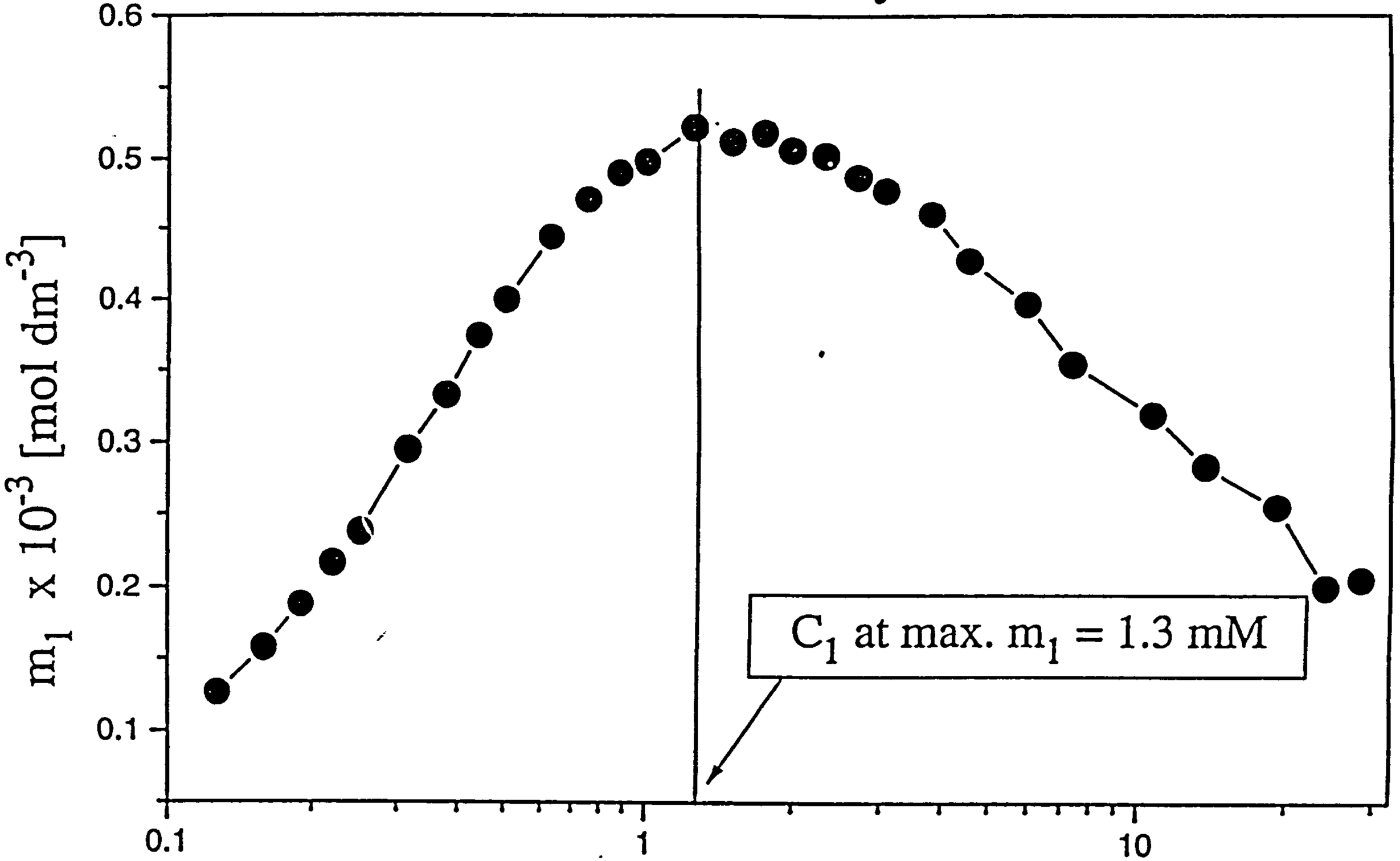

19, 4-20 and 4-21. This observation was also reported by Hoffmann *et al*[7]. In comparison with corresponding polymer/ anionic surfactant complexes this maximum is relatively sharp. The total surfactant concentration at which this maximum occur falls between the values of T_1 and T_2 and is an indication that two different aggregation mechanism having highly cooperative behaviour occur with one process being associated with m_1 increasing with increasing surfactant concentration and the second process having m_1 decreasing with increasing surfactant concentration. It must also be emphasized here that the electrode only measures m_1, we cannot distinguish whether the surfactant in aggregate form is present as a polymer-micelle complexes or free micelles. In anionic surfactant/polymer systems the aggregating process where m_1 increases with increasing concentration is the binding process whereas m_1 decreasing with increasing surfactant concentration is associated with micelle formation. When this maximum in m_1 occurs below T_2 this means that free micelles occur in solution before the polymer becomes fully saturated with bound surfactant. It is not possible to assess which of these processes is dominating and therefore the maximum in m_1 is only an indicator that both process occur. This means that the onset of micelle formation before T_2 definitely occur at the surfactant concentration corresponding to this maximum.

Table 4.10 C_1 at which polymer saturation occur (T_2)

	T_2 (mol dm^{-3})
PPO	14.0×10^{-3}
PVME	13.6×10^{-3}
EHEC	23.8×10^{-3}

Table 4.11 Polymer:micelle and polymer monomer:micelle ratio at T_2

Parameter	PPO/CTAB	PVME/CTAB	EHEC/CTAB
N at T_2 mol./mic.	33*	30*	50**
Polymer monomer:M	205:1	193:1	45:1
P:M at T_2	12:1	3:7	1:11

* approximated from reference 15.
** estimated for comparison purposes

At the surfactant concentrations corresponding to the saturation of polymers T_2 in Table 4.10, it is possible for PPO and PVME to estimate the limiting stoichiometry of the polymer-micelle complex P:M where P is the polymer and M correspond to the bound aggregate. This calculation is based on the presumption that at T_2 all the polymer molecules are involved in polymer-micelle complexes and P:M is therefore an average. In practice one would expect a distribution of polymer-micelle complexes to occur. These values are as listed in Table 4.11.

This rough calculation shows that in PPO we have a structure corresponding to a "hairy" polymer-micelle complex simply because the molecular weight is so low

(1000). A hairy polymer-micelle complex is a complex in which a number of polymer molecules bind into a micelle and some of their parts protrude at the surface of the micelle. This is expected mainly in polymer/surfactant systems involving polymers with low molecular weights. For PVME and presumably EHEC the structure of the complex must correspond to the bead-type model. For PPO this raises the question of how to differentiate between polymer binding and a normal solubilization process? Unfortunately the present measurement do not allow us to differentiate between these two extremes. In the present experiments we have approached the problem from the point of view of a binding experiment, that is, keeping the polymer concentration constant and gradually increasing the surfactant concentration. In a solubilization experiment one would keep the surfactant concentration above the cmc and vary the solubilizate (PPO in this case). Unfortunately we do not have a technique available in the laboratory to distinguish between 'free' and 'bound' PPO. In reality both binding and solubilization cannot be distinguished in the sense that one would expect a distribution of all species to occur in solution especially once micelle are formed.

4.3.5 DISCUSSION

The binding isotherms from EMF data measured using CTAB selective electrode show clearly that interactions between a cationic surfactant cetyltrimethylammonium bromide (CTAB) and neutral water-soluble hydrophobic polymers (PPO, PVME

and EHEC) take place. Critical aggregation concentrations T_1 listed in Table 4.9 for PPO, PVME and EHEC are within experimental confidence limit in agreement with T_1 from Hoffmann and Huber[7] PVAA/CTAB systems (0.2×10^{-3} mol dm^{-3}). These findings emphasize that T_1 appears to be independent of the polymer. The occurence of counterion binding is another clear evidence of the presence of polymer/CTAB interactions. In addition, observations by Brackman *et al*[15] which show the reduction in aggregation numbers for PPO/CTAB and PVME/CTAB support our findings.

According to Schwuger[39] polymers such as PPO, PVME and EHEC with etheric linkage oxygen atoms favour adsorption of the negatively charged surfactant ions. These interactions are enhanced further by hydrophobic interactions[39,40]. As a result anionic surfactants show strong interactions with these polymers. On the contrary, cationic surfactants experience electrical repulsions between their head groups and the partially protonated etheric linkage oxygen atoms[39]. These electrical repulsions account for the weak interactions between cationic surfactants and polymers. Brackman *et al*[41] agrees with Schwuger[39] that: (i) positive charges on the polymer, (ii) bulkiness of the cationic head group, and (iii) interactions of the head group with the hydration sheath of the polymer, are the main repulsive factors in polymer-cationic surfactant interactions. Nevertheless, strong CTAB hydrophobic interactions overcome these repulsive factors to form polymer-micelle complexes.

The orientation and shape of cationic polymer-micelle complexes is determined by these repulsive forces. It can be concluded from this conception that the polymer hydrophobic core will: (i) repel the CTAB head groups, and (ii) interact with CTAB hydrocarbon chain. The picture evolving from here is that: (i) CTAB head groups will avoid closeness with the polymer hydrophobic core, and (ii) CTAB hydrocarbon chain, whenever possible, will be closer to the polymer hydrophobic core. Interactions of cationic surfactants and CTAB in particular, therefore, do not involve head groups completely and they are dependent on the strength of their hydrophobicities. On the contrary, interactions of anionic surfactants, mostly sodium dodecylsulfate (SDS), to these polymers show that binding is at the micellar surface (the outer layer of the micelle)[35,36,41].

Polymer-micelle interactions depends on hydrophobicity[2,42,43] of both polymer and surfactant molecules. This hypothesis is demonstrated in interactions between cationic surfactants with PEO and PPO which are of the same family. Whereas PPO with a branched methyl group shows relatively strong interactions[15,44,45] to both cationic and nonionic surfactants, PEO fails to show any interactions[39,40]. The highly hydrophobic cationic cetyltrimethylammonium bromide (n_c = 16) and sufficiently hydrophobic uncharged water-soluble polymers (PPO, PVME and EHEC) lead to relatively stronger interactions as evidenced in our results.

PPO and PVME monomer units are similar in structure and size but differ in the position of the etheric linkage oxygen atom in their monomer units. Brackman et al[15,46,47] studies on these two polymers show very little differences indicating that the position of etheric linkage oxygen atom does not influence very much the interactions on both cationic[15] and nonionic[46,47] surfactants. Our results show similarity between PPO and PVME in their T_1 and T_2.

4.3.6 CONCLUSION

Polymer-micelle complex formation depends on several properties of the surfactant molecule: the chemical nature, geometry, and charge; as well as those of a polymer molecule: hydrophobicity and macromolecular nature. Charge and geometry of the trimethylammonium ion head group limit the extent of interaction between CTAB and polymers. The feature of the CTAB molecule favouring interaction is its higher hydrophobicity due to its long alkyl chain. Due to these limiting conditions in a CTAB molecule, the CTAB molecules undergo polymer-micelle complex formation on the premise that the polymer is: (i) sufficiently hydrophobic, and (ii) of reasonable molecular size.

4.4 REFERENCES

1. GODDARD, E.D. *Colloïds and Surfaces*, 19 (1986) 255.

2. SAITO, S. *Kolloid Z.*, 154 (1957) 1g

3. ZANA, R.; LANG. J. and LIANOS, P. *J. Phys. Chem.*, 89 (1985) 41.

4. PERRON, G.; FRANCOEUR, J.; DESNOYERS, J. and KWAK, J. *Can. J. Chem.*, 65 (1987) 990.

5. TAKAHARA, A.; ICHIMARU, K.; TASHITA, J.I.; KUMANO, A.; KAJIYAMA, T. and TAKANAYAGI, M. *Rep. Prog. Polym. Phys. Jpn.*, 26 (1983) 669.

6. WINNIK, F.; RINGSDORF, H. and VENZMER, J. *Langmuir*, 7 (1991) 905.

7. HOFFMANN, H. and HUBER, G. *Colloids Surf.*, 40 (1989) 181.

8. WINNIK, F.M.; WINNIK, M.A. and TAZUKE, S. *J. Phys. Chem.*, 91 (1987) 594.

9. DUYNSTEE, E.F.J. and GRUNWALD, E. *J. Am. Chem. Soc.*, 81 (1959) 4540.

10. PALEPU, R.; HALL, D.G. and WYN-JONES, E. *J. Chem. Soc., Faraday Trans. 1*, 86 (1990) 1535.

11. WAN-BADHI, W.A.; MWAKIBETE, H.; BLOOR, D.M.; PALEPU, R. and WYN-JONES, E.; *J. Phys. Chem.*, 96 (1992) 918.

12. HALL, D.G. and TIDDY, G.J.T. in *Anionic Surfactant: Physical Chemistry of Surfactant action*, 11, Ed. E.H. Lucassen-Reynders, Marcel Dekker, Inc., New York (1981) pp55-108.

13. DONG, W. and FLINT, C.D.; *J. Chem. Soc., Faraday Trans.*, 88 (1992) 705.

14. CLINT, J.H.; "*Surfactant Aggregation*", Chapman and Hall, New York (1991).

15. BRACKMAN, J.C. and ENGBERTS, J.B.F.N. *Langmuir*, 7 (1991) 2077.

16. BRANDRUP, J. and IMMERGUT, E.H. *Polymer Handbook*, 2nd Ed., Wiley, New York (1975).

17. GHARIBI, H.; PALEPU, R.; BLOOR, D.M.; HALL, D.G. and WYN-JONES, E. *Langmuir*, 8 (1992) 782.

18. HALL, D.G. *J. Chem. Soc. Faraday Trans. 2*, 73 (1977)

897.

19. HALL, D.G. *J. Chem. Soc. Faraday Trans. 1.*, 77 (1981) 1121.

20. MIJNLIEFF, P.F. *J. Colloid Interface Sci.*, 33 (1970) 255.

21. GHARIBI, H.; TAKISAWA, N.; BROWN, P.; THOMASON, M.A.; PAINTER, D.M.; BLOOR, D.M.; HALL, D.G. and WYN-JONES, E. *J. Chem. Soc., Faraday Trans. 1*, 87 (1991) 707.

22. WAN-BADHI, W.A.; PALEPU, R.; BLOOR, D.M.; HALL, D.G. and WYN-JONES, E.; *J. Phys. Chem.*, 95 (1991) 6642.

23. BUCKINGHAM., S.A.; GARVEY, C.J. and WARR, G.G. *J. Phys. Chem.*, 97 (1993) 10236.

24. BEŽAN, M.; MALAVAŠIČ, M. and VESNAVER, G. *J. Chem. Soc. Faraday Trans.*, 89 (1993) 2445.

25. LA MESA, C. *J. Phys. Chem.*, 94 (1990) 323.

26. MULLER, N. *Langmuir*, 9 (1993) 96.

27. LINDMAN, B. and WENNERSTRÖM, H. *Top. Curr. Chem.*, 87 (1980) 1 section 6.3.

28. EMERSON, M.F. and HOLTZER, A. *J. Phys. Chem.*, 69 (1965) 3718.

29. EVANS, D.F. and NINHAM, B.W. *J. Phys. Chem.*, 87 (1983) 5025.

30. WAN-BADHI, W.A. *PhD Thesis*, University of Salford, UK (1993).

31. HOLMBERG, C.; NILSSON, S.; SINGH, S.K. and SUNDLOF, L., *J. Phys. Chem.*, 96 (1992) 871.

32. MURATA, M. and ARAI, H. *J. Colloid Interface Sci.*, 44 (1973) 475.

33. WAN-BADHI, W.A.; WAN-YUNUS, W.M.Z.; BLOOR, D.M.; HALL, D.G. and WYN-JONES, E. *J. Chem. Soc. Faraday Trans.* 89(15) (1993) 2737.

34. ARAI, H.; MURATA, M. and SHINODA, K. *J. Colloid Interface Sci.*, 37 (1971) 223.

35. SHIRAHAMA, K. and IDE, N. *J. Colloid Interface Sci.*, 54 (1976) 223.

36. TOKIWA, F. and TSUJII, K. *Bull. Chem. Soc. Jpn.*, 46 (1973) 2684.

37. BLOOR, D.M.; WAN-BADHI, W.A.; HOLZWARTH, J.F. and WYN-JONES, E. *J. Phys. Chem.* 97 (1993) 5793.

38. TAKISAWA, N.; BROWN, P.; BLOOR, D.M.; HALL, D.G. and WYN-JONES, E. *J. Chem. Soc. Faraday Trans.1* 85(8) (1993) 2737.

39. SCHWUGER, M.J. *J. Colloid Interface Sci.*, 43 (1973) 491.

40. PLETNEV, M.YU. and TRAPEZNIKOV, A.A. *Kolloidn. Zh.*, 40 (1978) 948.

41. BRACKMAN, J.C. and ENGBERTS, J.B.F.N. *Chem. Soc. Reviews*, 22(3) (1993) 85

42. BREUER, M.M. and ROBB, I.D. *Chem. Ind. (London)*, 13 (1972) 530.

43. JONES, M.N. *J. Colloid Interface Sci.*, 30 (1969) 211.

44. WITTE, F.M. and ENGBERTS, J.B.F.N. *J. Org. Chem.*, 52 (1987) 4767.

45. WITTE, F.M. and ENGBERTS, J.B.F.N. *Colloids Surf.*, 36 (1989) 417.

46. BRACKMAN, J.C.; VAN OS, N.M. and ENGBERTS, J.B.F.N. *Langmuir*, 4 (1988) 1266.

47. BRACKMAN, J.C. and ENGBERTS, J.B.F.N. *Langmuir*, 8 (1992) 424

CHAPTER FIVE: INTRODUCTION TO CYCLODEXTRINS AND INCLUSION COMPLEXES

5.1 PREAMBLE

".....I realize that still very many questions remains unsolved. The answer to these I must leave to another, who, owing to more favorable external conditions, can deal with the subject more intensively...."

Schardinger (1911)[1] to end his early work on cyclodextrins.

"....(cyclodextrins will) continue to serve, delight, teach, and intrigue the carbohydrate chemist for many years to come...."

French (1957)[2] in his review of cyclodextrins.

Indeed, cyclodextrin (CD) chemistry delights and intrigues researchers today as it did 40 years ago. The current interest is not only carbohydrate chemistry but now applications cover a wider range of disciplines from organic chemists who use cyclodextrins for selective catalysis, analytical chemists who use CD's for chromatographic separation, to physical chemists, biologists and biochemists.

A multitude of studies have been carried out since Villier's discovery of cyclodextrins[3] and many of these have resulted in new areas of research being developed. Indeed cyclodextrin research is growing in breadth and depth. Notwithstanding the successful research on cyclodextrins carried out by Schardinger[1], French[2,4], Borchert[5], and Freudenberg[6] and many other early works; there are still many unanswered questions and many unknown factors which continue to intrigue researchers. As a result the above quotations by Schardinger and French will remain valid for

many years to come.

In this chapter and the following three chapters (6, 7 and 8) a contribution on 'cyclodextrin/surfactant inclusion complexes' is described.

5.2 CYCLODEXTRINS

Cyclodextrins are a group of doughnut-shaped, non-reducing macrocyclic oligosaccharides build up of six, seven, eight, or sometimes nine D-(+)-glucopyranose units joined together by an α-(1,4)-interglucose bonds and are named as α-, β-, γ- and δ-cyclodextrins respectively[1,3,7,8]. Whereas the first three are more common and abundant, δ-cyclodextrin is not common and is found in trace amounts during synthesis and separation of cyclodextrins[1]. The main cyclodextrins; α, β and γ (shown in Figure 5-1) were discovered in 1891 by Villiers[3], δ-cyclodextrin has been isolated recently and there is not much information available on this compound. The first detailed description of the preparation, isolation and some properties of α-, β- and γ-cyclodextrins were made in 1903 by Schardinger[1,7,8] and he was honoured by naming these compounds as Schardinger dextrins. They are also known as cycloamyloses or cycloglucoamyloses.

Preparation of cyclodextrins involves treatment of starch with a group of amylases known as cyclodextringluco-syltransferases (produced from microorganisms including, for example, *Bacillus macerans*)[1,7-9]. The starch helix is

hydrolysed off and its ends are joined together through α-(1,4)-linkages[10,11] to form cyclodextrins. During the preparation a mixture of cyclodextrins are obtained and as a result, separation and purification must be carried out to obtain pure compounds[9,12]. A process known as selective precipitation with appropriate organic compounds is used to separate these compounds from each other and from impurities. Higher cyclodextrin analogues consisting of up to 13 glucose units are traced in very small amounts in the mixtures. δ-cyclodextrin with nine glucose units is relatively significant compared to higher ones but very insignificant compared to α-, β- and γ-cyclodextrins. Cyclodextrins composed of less than six glucose units are not known due to steric hindrance[13] and the six-fold character of the starch helix[14].

Glucose units in the cyclodextrin molecules are all in a classical C1 chair conformation linked by α-(1,4)-bonds (Figure 5-2). This geometry gives cyclodextrins a shape of a truncated cone with a wider side formed by the secondary 2- and 3-hydroxyl groups and the narrower side by the primary 6-hydroxyl groups. The main difference between cyclodextrins is their dimensions and size of the cavities which are determined by the number of glucose units making the cyclodextrin molecules (Figure 5-3). As a result of the arrangement of functional groups in the cyclodextrin molecules, the cavities are hydrophobic and the exterior faces are hydrophilic (Figure 5-4).

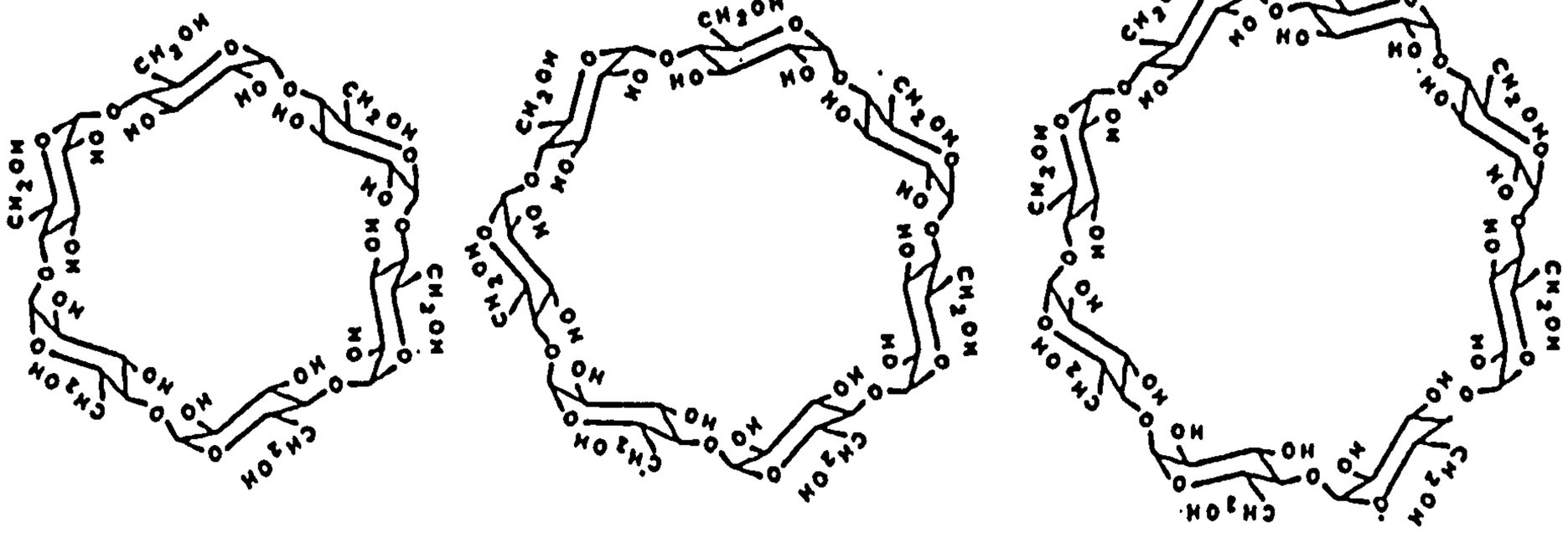

α-cyclodextrin β-cyclodextrin γ-cyclodextrin

Figure 5-1 Chemical structures for α-, ß- and γ-cyclodextrins

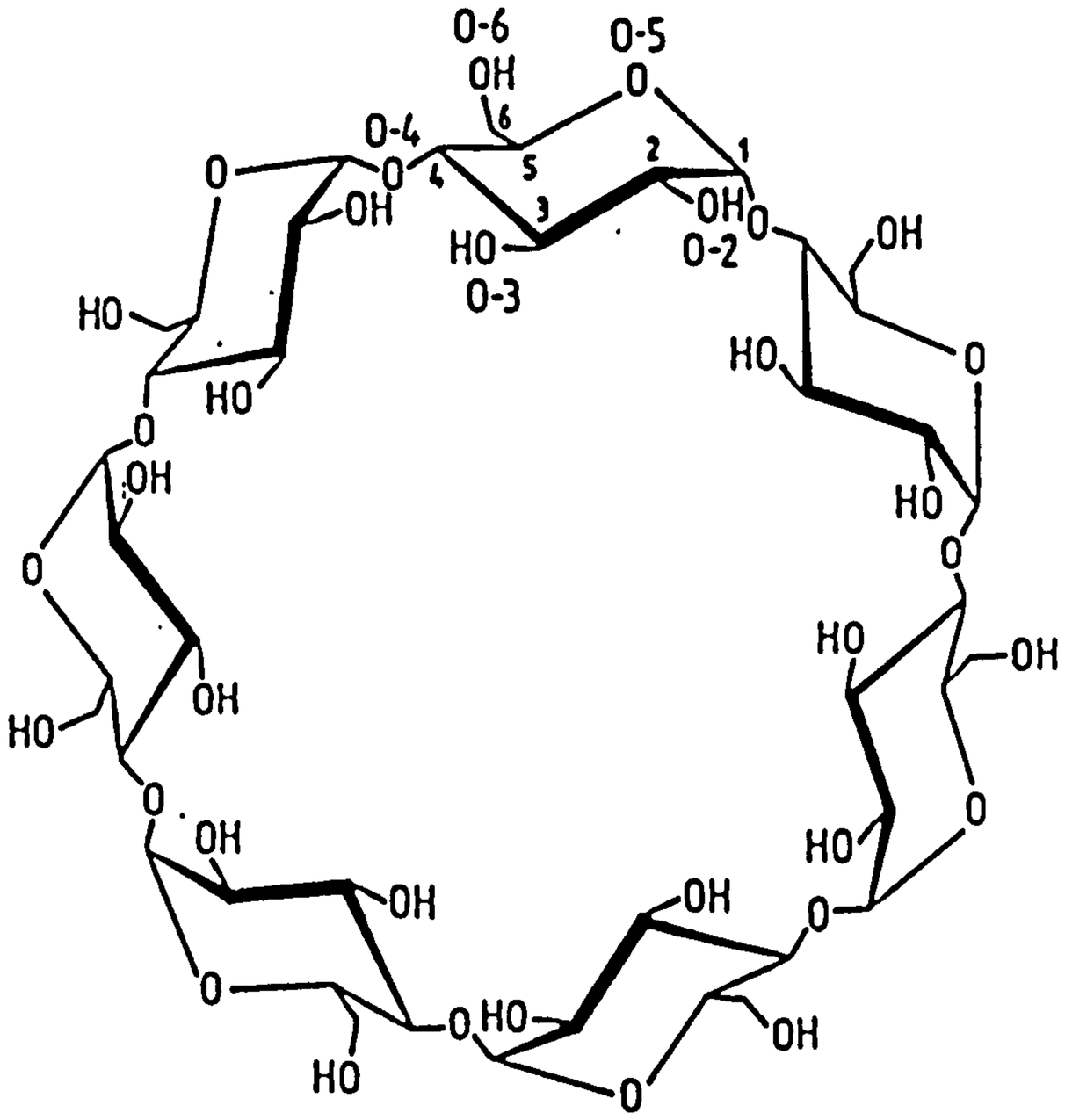

Figure 5-2 The α-(1,4)-linkage bonds and numbering of the atoms on glucose units in a ß-cyclodextrin molecule.

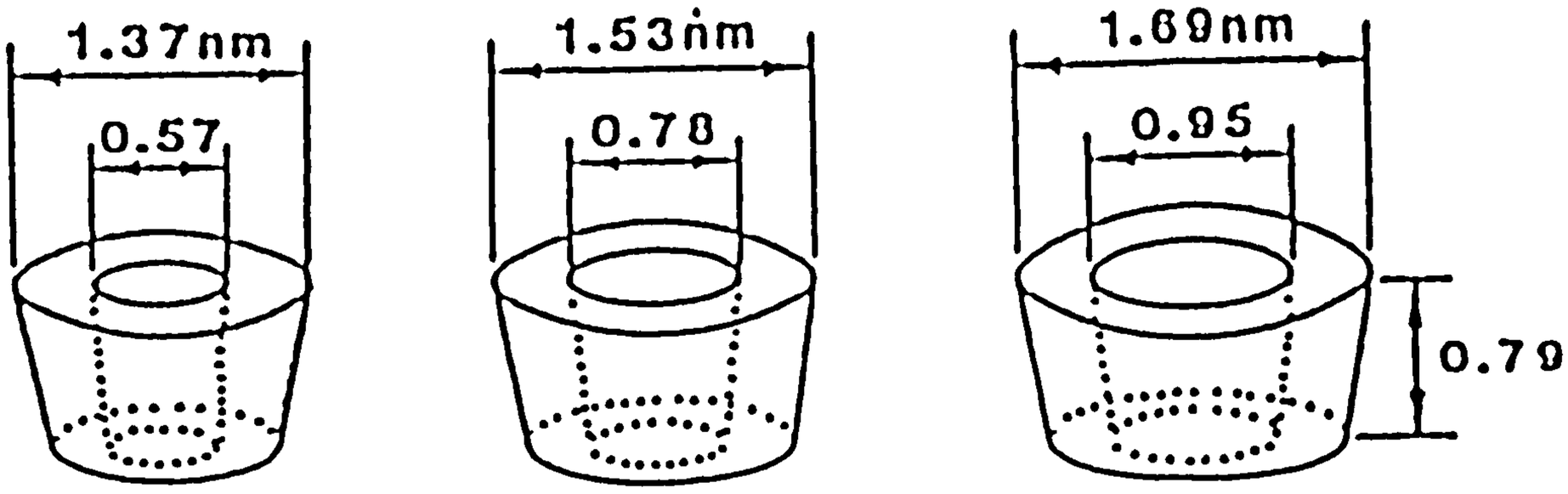

α-cyclodextrin β-cyclodextrin γ-cyclodextrin

Figure 5-3 Molecular dimensions of α-, ß- and γ-cyclodextrins.

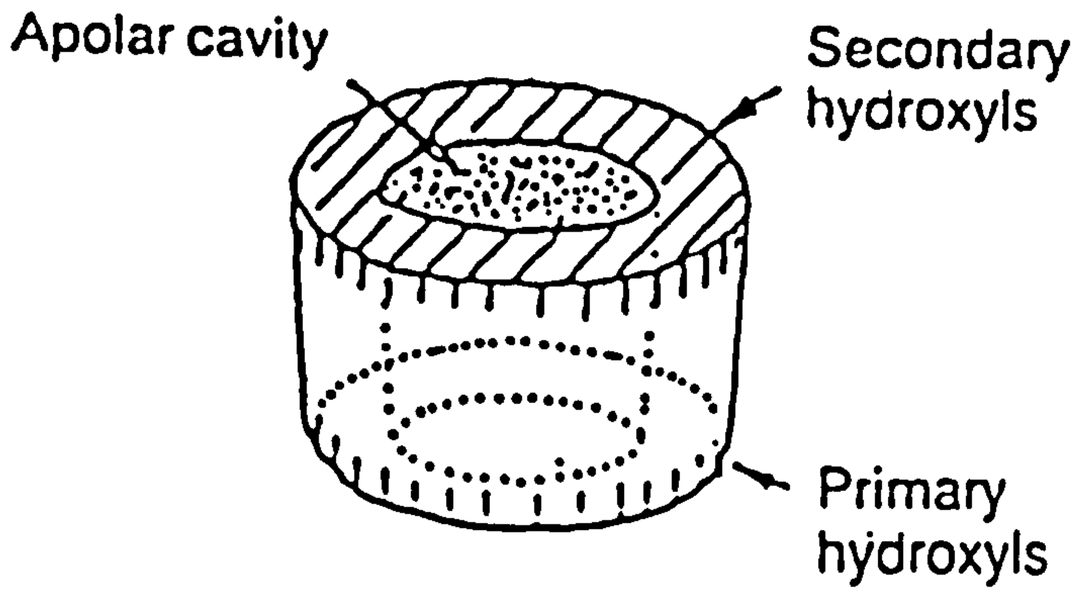

Figure 5-4 Functional structural scheme for a cyclodextrin molecule.

5.2.1 Characteristics of α-, ß- and γ-cyclodextrins

Cyclodextrins are not hygroscopic but they form numerous stable hydrates[9,15]. α-cyclodextrin absorbs around 4 to 6.6 molecules of water per molecule cyclodextrin (approximately 6.2 to 9.8% water by weight) at relative humidity 11 to 20%. The absorption remains constant around 6.6 molecules of water per molecule CD between relative humidities 20 to 95%. ß-cyclodextrin absorbs around 10 to 11 water molecules

per molecule CD (approx. 13.7 to 14.8% water by weight) at relative humidity of 50 to 70%. γ-cyclodextrin hydration is characterized by two phases, at 30 to 50% γ-CD absorbs around 7 molecules of water per molecule γ-CD and at around 70 to 90% γ-CD absorbs around 17 molecules of water per molecule γ-CD. Due to this hydration behaviour of cyclodextrins, it is important before using them in any analytical work to know the content of water in order to have correct CD concentration.

Solubility of cyclodextrins in water increases with temperature and are in the order: ß-CD < α-CD < γ-CD. Solubility in water (g/dm^3) at ambient temperature (T = 25°C) are 145.0, 18.5 and 232.0 for α-, ß- and γ-cyclodextrins respectively[9,16]. Aqueous solutions of cyclodextrins are not viscous. Cyclodextrins are fairly stable[16] in alkaline and weak acidic solutions (pH > 3.5) and temperatures lower than 60°C. In solutions with pH < 3.5 cyclodextrins are susceptible to partial acid hydrolysis producing glucose and a series of acyclic maltosaccharides[9,16]. However, at lower temperatures the effect of acid hydrolysis is low. Despite the observed cleavage of the 1,4-glucosidic bonds of ß- and γ-cyclodextrins by γ-irradiation, cyclodextrins are fairly resistive to the light within the UV-visible and IR ranges.

These characteristics and unique features of cyclodextrins can be attributed to their apolar internal structures and

polar external structures. The wider and narrower ends of the CD cylinder are lined with the secondary 2- and 3-hydroxyl groups and primary 6-hydroxyl groups respectively and therefore making the outer surface of the CD hydrophilic (polar). The cavity is lined with the hydrogen atoms and the glucosidic oxygen bridges making the cavity apolar as compared to water. In the cyclodextrin molecules, a ring of hydrogen bonds is also formed intramolecularly between the 2-hydroxyl and the 3-hydroxyl groups of adjacent glucose units. This hydrogen bonding ring gives the cyclodextrin a remarkably rigid structure.

5.3 CYCLODEXTRIN INCLUSION PROCESSES

A cyclodextrin molecule can be regarded as an empty 'capsule' of known molecular size. When this capsule is occupied by a molecule of another substance, the process in pharmaceutical and medical terms is called 'molecular encapsulation', it is also known as 'inclusion' or 'binding'. The product is termed an 'inclusion complex' (the process is diagramatically demonstrated in Figure 5-5).

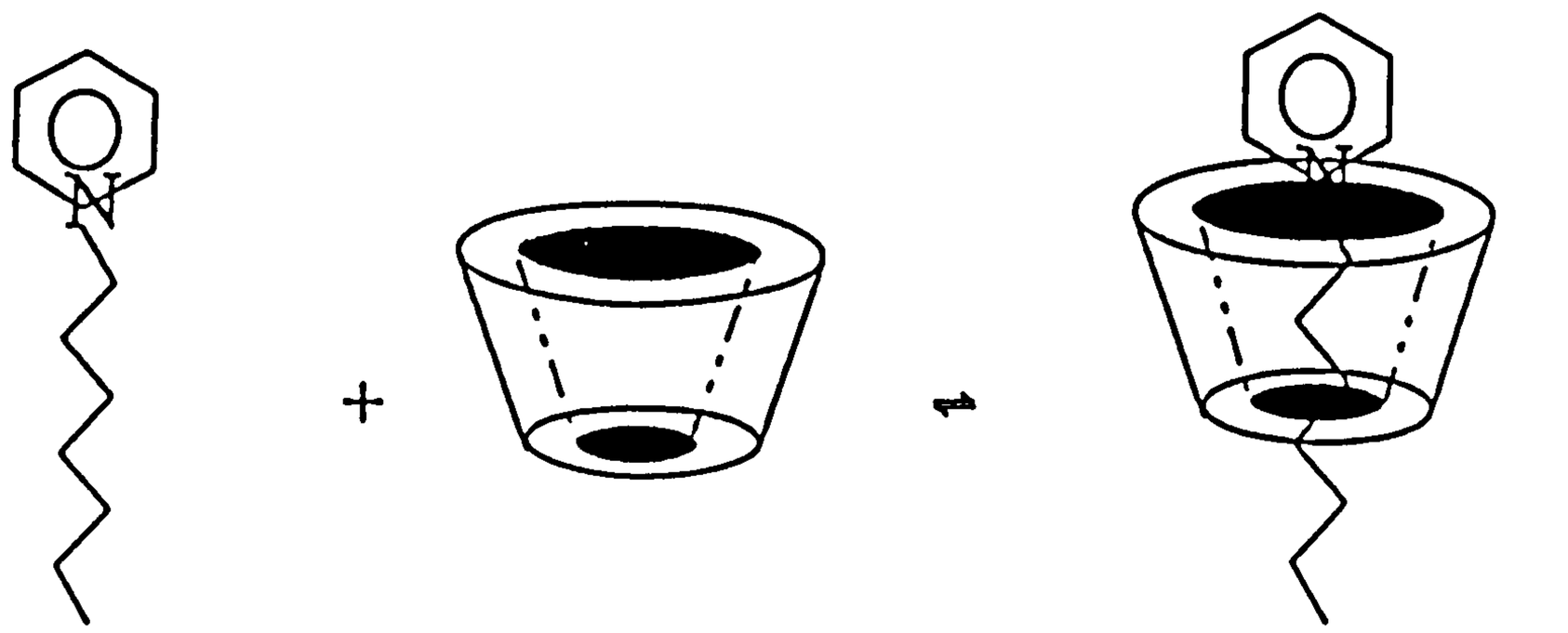

Figure 5-5: Host-Guest Inclusion Process

Inclusion complexes of two or more molecules, one of which, the 'receptor' (sometimes called 'host') hold the 'guest' molecule(s) within its cavity or partly, by non-covalent physical forces. The cavity and functional structure of cyclodextrins allows cyclodextrin to entrap, bind, cage, clathrate, or encapsulate organic compounds (surfactants, drugs, dyes, etc) and inorganic compounds in solution and some few in solid state.

5.3.1 Review of Surfactant/cyclodextrin work

As we have said previously the work described in Chapters 6, 7 and 8 is concerned with a study of the equilibrium properties of the inclusion complexes formed between cyclodextrins and surfactants.

It has been demonstrated that the addition of cyclodextrins to an aqueous solution of surfactant dramatically affects the physicochemical properties of the solution[17-31]. The reason for these changes is the ability of CD's to screen the hydrophobic moieties of surfactant molecules from contact with the surrounding aqueous media by the formation of an inclusion complex in which the hydrophobic chain of the surfactant is inserted into the CD cavity. As a result, surfactants are ideal guests which allow a systematic study of complexation with cyclodextrins since both their hydrophobic and hydrophilic moieties can be systematically changed. Indeed, the ability of cyclodextrins to modify the physicochemical properties of such aqueous solutions has

been used to study their complexation behaviour with surfactants, and a variety of experimental techniques have been used for this purpose. These techniques include conductivity[23], surface tension[25], UV and visible absorbance[17], NMR[18], scund velocity[27,33] and electrochemical[29,30] methods as well as dye inclusion studies using T-Jump and ultrasonic relaxation techniques[34]. A literature survey reveals that after an initial period that produced ambiguous and inconclusive information, it is now generally regarded that the existence of 1:1 and 2:1 cyclodextrin:surfactant inclusion complexes can occur[17-31]. Despite this progress there remains a serious question mark concerning the reliability of many of the binding constants that have been quoted. A typical example concerns the inclusion of sodium dodecylsulfate ($C_{12}OSO_3Na$) into ß-CD which are known to form both 1:1 and 2:1 ß-CD/$C_{12}OSO_3Na$ inclusion complexes according to the scheme

Scheme (1)

$$\text{ß-CD} + C_{12}OSO_3Na \overset{K_1}{\rightleftharpoons} \text{ß-CD}..C_{12}OSO_3Na$$

$$\text{ß-CD}..C_{12}OSO_3Na + \text{ß-CD} \overset{K_2}{\rightleftharpoons} (\text{ß-CD})_2..C_{12}OSO_3Na$$

The first step in the above scheme is the dominating equilibrium. The following values of K_1 (in units of [mol^{-1} dm^3]) have been quoted: 210[20], 356[22], 1300-7230[23], 3200-18000[24], 3630[22], 6600[26], 8360[25], 21000[30] and 25600[28]. At first sight this clearly represents a very unsatifactory state of affairs which when the present work was commenced still existed in

the current literature. In practice two different approaches are normally used to determine surfactant/cyclodextrin binding constants:

(a) The first relies on direct measurements of the "free" and "bound" surfactant in a solution containing a known amount of the cyclodextrin.

(b) The second approach takes advantage of the existence of any physically observable property that is proportional in some way to the extent of binding.

Table 5.1 EMF and FP Results for 1-alkyltrimethylammonium bromides (C_nTAB) and sodium dodecylsulfate ($C_{12}OSO_3Na$) inclusion complexes with ß-CD

	Jezequel[29] EMF	Park and Park[31] FP	Wan-Yunus[30] EMF	Park and Song[28] FP
$C_{12}TAB$	17785	22100	18100	-
$C_{14}TAB$	39811	44000	-	-
$C_{16}TAB$	70795	59800	-	-
$C_{12}OSO_3Na$	-	-	21000	25600

EMF = electromotive force using surfactant selective electrodes, FP = competitive binding using fluorescence probe.

A close inspection of the data published for the ß-CD/$C_{12}OSO_3Na$ system shows that the criteria spelled out under (a) above are only met by two independent studies; namely competitive binding using fluorescence probe studies (FP)[28] and electrochemical (EMF) methods[30] involving the use of a sodium dodecylsulfate membrane selective electrode. Interestingly enough, these two studies give values of K_1 and K_2 for scheme (1) which are very close, that is, K_1 =

25600 and 21000 [mol^{-1} dm^3] and K_2 = 220 and 210 [mol^{-1} dm^3] respectively. In Table 5.1 a comparison of equilibrium constants found from EMF and FP techniques for sodium dodecylsulfate and 1-alkyltrimethylammonium bromides (C_nTAB) inclusion complexes to ß-cyclodextrin are listed. It is encouraging to find that there is good general agreement between these independent studies.

All other techniques that have been used to study the above systems come under category (b) above. Whereas these methods have contributed to a better understanding of the solution properties of the system in the sense that the existence of both 1:1 and 2:1 ß-CD/$C_{12}OSO_3Na$ inclusion complexes occur, K_1 values ranging from 210 to 8360 [mol^{-1} dm^3] are clearly unacceptable.

The experimental evidence that is currently available suggests that cyclodextrins recognise surfactant in a specific manner. In order to measure such specificity, reliable binding constants for the inclusion compounds are required. In view of the current interest shown in these systems we wish to address the above problem concerning the consistency of experimentally determined complexation constants. Reliable values of K will serve to quantify the affinity of surfactants to cyclodextrins which in turn can lead to an understanding of the relationship between the surfactant chemical structure and its ability to form inclusion complexes. In theory, the key ingredients that

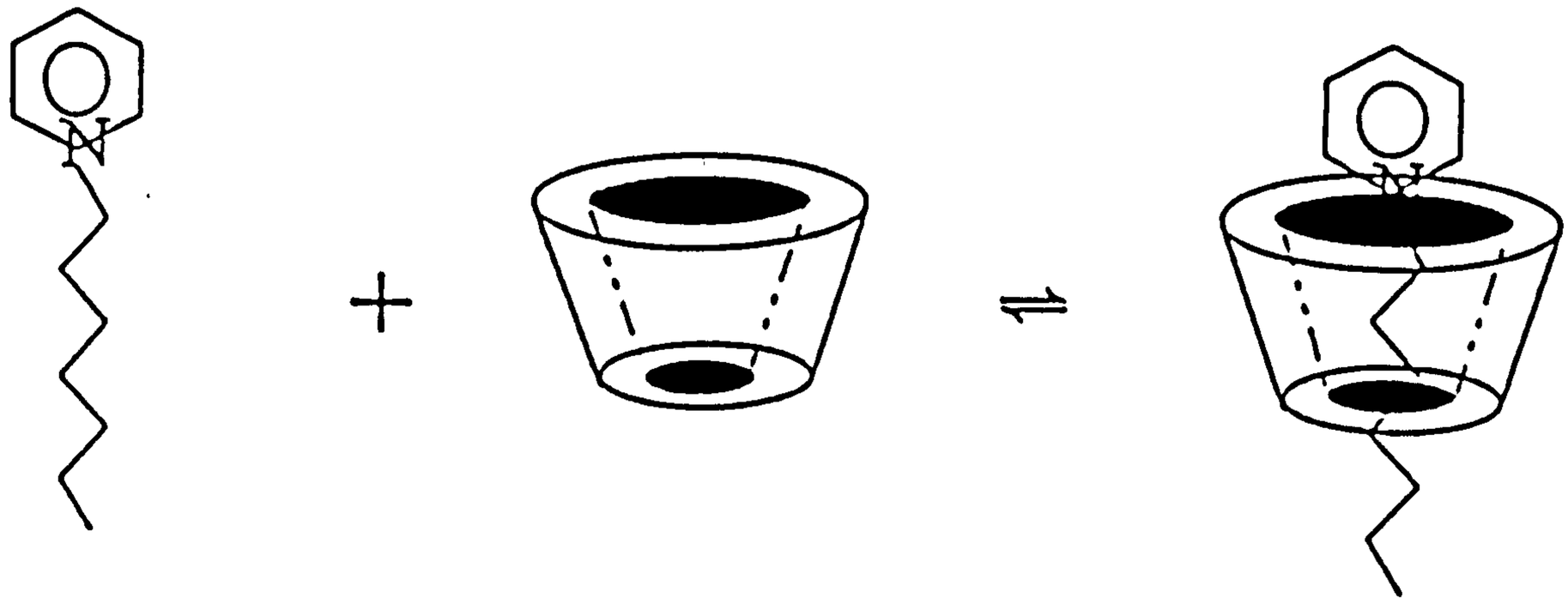

Surfactant molecule

cyclodextrin molecule

1:1 inclusion complex

Figure 5-6(a): Schematic representation of the formation of a 1:1 inclusion complex

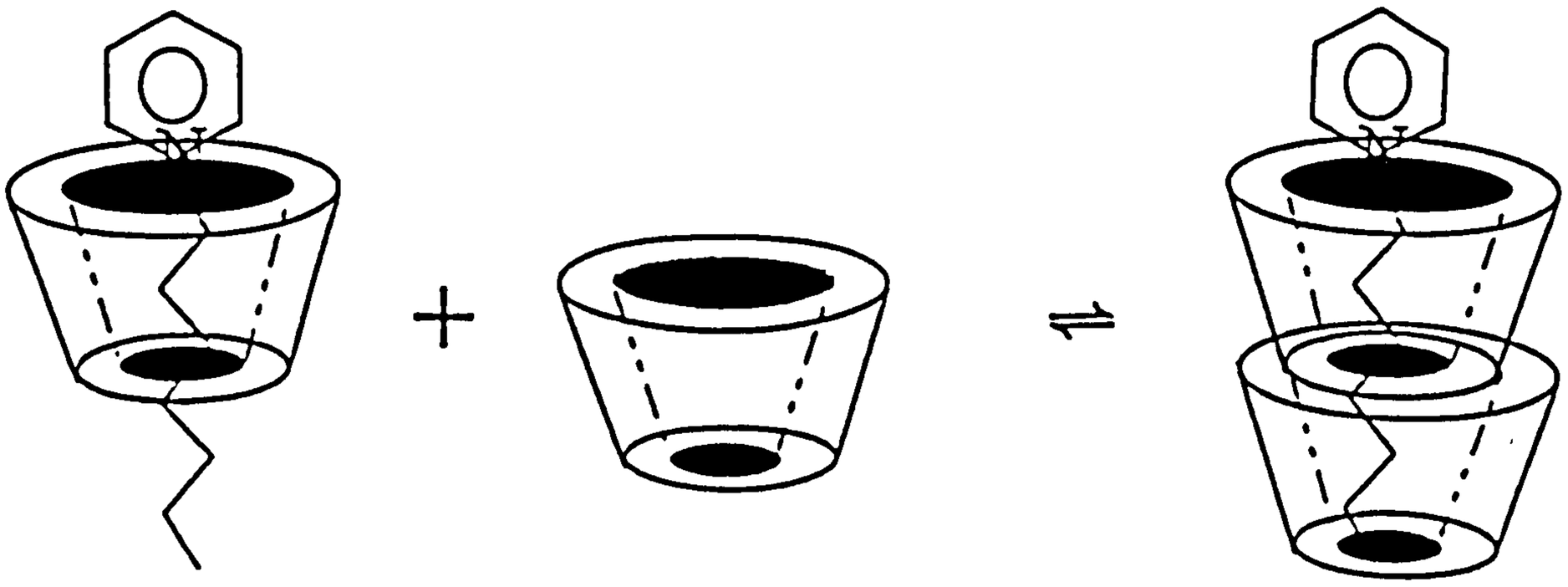

1:1 inclusion complex

cyclodextrin molecule

2:1 inclusion complex

Figure 5-6(b): Schematic representation of the formation of a 2:1 inclusion complex

are required to determine the equilibrium constants for scheme (1) are the equilibrium concentrations of the various species involved. On this basis and the evidence presented above, consistency of the K values can only be achieved conclusively if the experiments are carried out under the criteria spelled out in (a) above. With this in mind we have investigated the inclusion complexes of tetradecyltrimethylammonium bromide (C_{14}TAB) and also the homologous series 1-alkylpyridinium bromides (C_nPyBr) (n_c = 10, 12, 14 and 16) with α- and ß-cyclodextrins using the emf technique involving surfactant selective electrodes. These data are presented in Chapter 6. In addition we have used a new technique, hitherto not applied to surfactant/ cyclodextrin complexes, to study these systems. The technique is the Omega isothermal titration calorimetry and the data are presented in Chapter 7 for a wider range of surfactant/cyclodextrin systems.

5.3.2 General Guest-Host Inclusion Forces

The cyclodextrin/guest inclusion complexation system is made up of the solvent (water) and solutes (guest and cyclodextrin). According to Connors[37] the total free energy change contributions is given in equation (5-1):

$$\Delta G_T = \Delta G_{W/W} + \Delta G_{W/CD} + \Delta G_{W/G} + \Delta G_{G/CD} \qquad (5\text{-}1)$$

where $\Delta G_{W/W}$ is the contribution from solvent-solvent interactions, $\Delta G_{W/CD}$ from changes in CD solvation, $\Delta G_{W/G}$ from the changes in solvation of guest molecules and $\Delta G_{G/CD}$ is the

free energy changes contributed from solute-solute interactions (i.e. guest/cyclodextrin interactions). $\Delta G_{w/w}$ is negligible due to bulkiness of the system itself. The solvent-solute interactions ($\Delta G_{w/CD}$ and $\Delta G_{w/G}$) are expected to contribute significantly to ΔG_T.

The solvation of CDs is high due to two contributions, namely the exterior hydrophilic part and solvent in the cavity. The high energy water in the CD cavity is released from the cavity to the bulky water by the incoming guest molecule. The free energy change from the release of high energy water (ΔG^{o}_{hw})[16,38] is significant. The released high energy water (sometimes referred to as 'highly structured water' or 'icebergs') from the cyclodextrin cavity to the bulk water increases disorder and so the contribution is more or less entropic free energy[39-41]. The CD exterior hydrophilic contribution remains somehow undisturbed.

Solvation of guest which involves the hydrophilic moieties of the molecule ion very probable remain undisturbed by the inclusion process due to possible noninvolvement of the head groups in the inclusion complexation. As a result $\Delta G_{w/G}$ does not contribute much to the total free energy of complexation. Finally, $\Delta G_{G/CD}$ is the most important contributor to the inclusion complexation total free energy.

The forces involved in cyclodextrin/surfactant complexation

include: the hydrophobic interactions (ΔG°_{hp})[16,31,37,42,43] and the van der Waal's interactions (ΔG°_{vdW})[16,37,40,43] between the hydrophobic moiety of the guest molecules and the cyclodextrin cavity, the hydrogen bonding between the polar functional groups of the guest molecules and the hydroxyl groups of CD (ΔG°_{hb})[16,40,43] and the release of strain energy in the ring frame system of α-CD (ΔG°_{rse})[16,37] (It is sometimes referred to as relief of conformational strain and applies only to α-CD). The mechanism of inclusion complex formation from Saenger's Theory[44,45] with emphasize on release of strain energy in the ring frame of α-CD is shown in Figure 5-7.

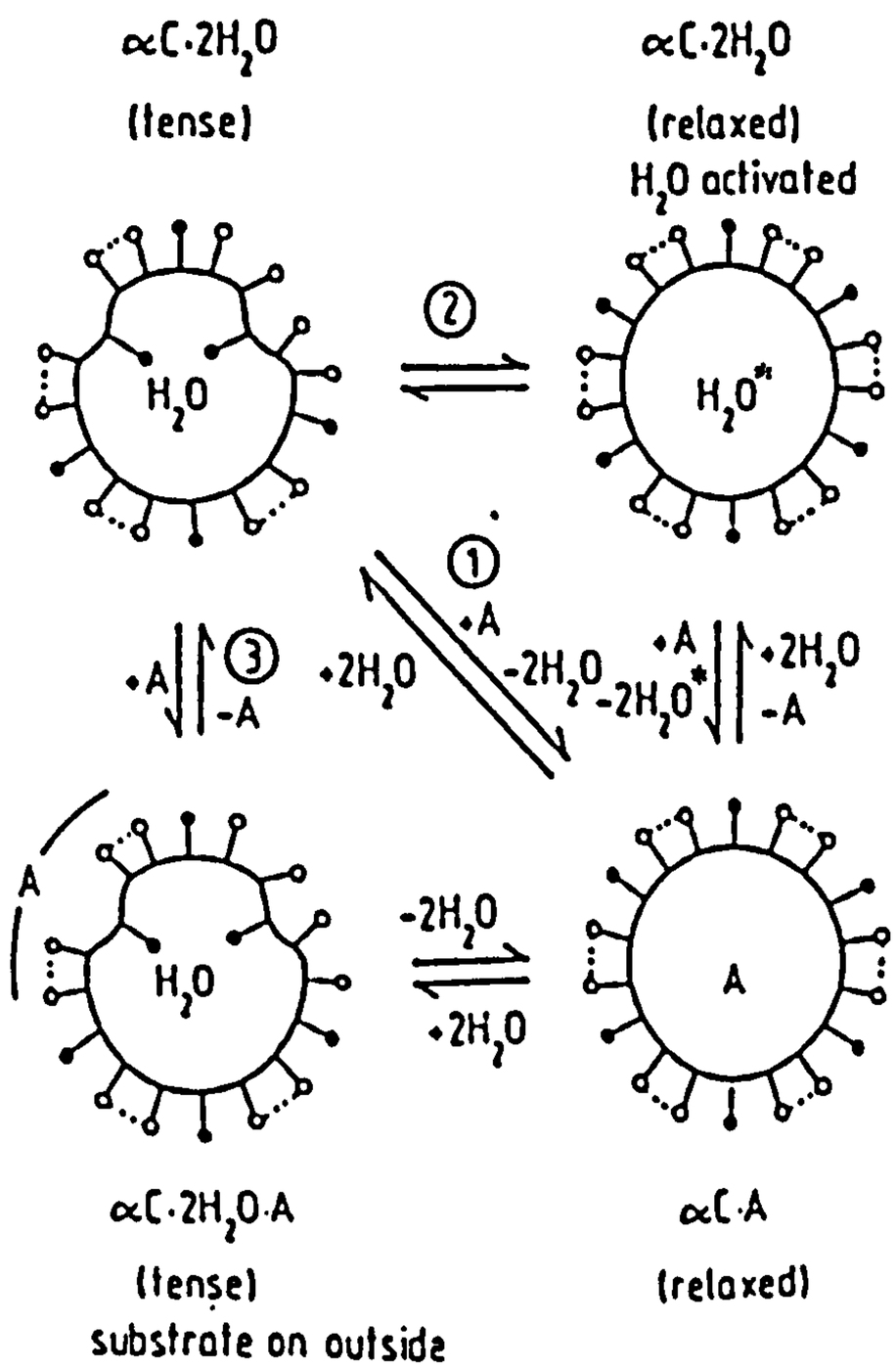

Figure 5-7: Schematic diagram[45] of Saenger's Theory of Formation of α-CD Inclusion Complex. In the diagram A = guest molecule, H_2O^* = "activated water", —● 6-hydroxyl group, —o 2- and 3-hydroxyl groups, -- hydrogen bonds. Equilibrium studies use path 1 which involves initial and final states only, but this model covers kinetics as well.

Despite the emphasis by many authors the role of hydrogen bonding is not universal, stable complexes have been found to form with guests such as benzene which can not form hydrogen bonds. The van der Waal's interactions (ΔG°_{vdW}) can be split further into electrostatic term (ΔG°_{el}) which includes mainly dipole-dipole and dipole-induced dipole forces (polarity of a guest molecule) and a steric term (ΔG°_{ster}) which depends on the surfactant molecular structure (bulkiness of a guest molecule). Finally, the total free energy of inclusion process can generally be approximated as[46]:

$$\Delta G^{\circ}_{T} = \Delta G^{\circ}_{hp} + \Delta G^{\circ}_{hb} + \Delta G^{\circ}_{el} + \Delta G^{\circ}_{ster} + \Delta G^{\circ}_{rhw} + \Delta G^{\circ}_{rsc} \quad (5\text{-}2)$$

Free energies ΔG°_{rhw} and ΔG°_{rsc} are constant and dependent on the individual cyclodextrin molecular structure. Free energies ΔG°_{hb}, ΔG°_{el} and ΔG°_{ster} are approximately constant for a given solvent, cyclodextrin and surfactant head group. It is only ΔG°_{hp} that vary with surfactant hydrophobic tail as summarized in the following equation:

$$\Delta G^{\circ}_{T} = A - (\Delta G^{\circ}(-CH_2-)).n_c \quad (5\text{-}3)$$

$$\Delta G^{\circ}_{hp} = - (\Delta G^{\circ}(-CH_2-)).n_c \quad (5\text{-}4)$$

where $\Delta G^{\circ}(-CH_2-)$ is the contribution per methylene group of the guest molecule (if it is a hydrocarbon amphiphilic compound). The term A include contributions from the guest molecule's polarity and bulkiness as well as hydrogen bonding. It includes specific constant contributions from CDs (ΔG°_{rhw} and ΔG°_{rsc}) as summed up in the following expression

$$A = \Delta G^{\circ}_{hb} + \Delta G^{\circ}_{el} + \Delta G^{\circ}_{ster} + \Delta G^{\circ}_{rhw} + \Delta G^{\circ}_{rse} \qquad (5\text{-}5)$$

A plot according to equation (5-3), ΔG°_{T} versus n_c, gives $\Delta G^{\circ}(-CH_2-)$ as slope which is the free energy change per methylene group and is the energy required to transfer one methylene group from bulky water into the CD cavity (hydrophobic environment).

5.3.3 Geometrical Considerations for Surfactant-Cyclodextrin Inclusion Complexes

The geometries of the host cyclodextrin cavities are well known[7,28] and theoretically it is possible to estimate the size of the guest molecules which can fit into cavities. Cavity geometrical dimensions such as; internal diameter (d), depth/height (h) and volume (V) for α-, ß- and γ-cyclodextrins are summarized in Table 5.2.

Table 5.2: Geometrical dimensions for cyclodextrin cavities

Parameter	α-CD	ß-CD	γ-CD
Internal diameter/nm	0.57	0.78	0.95
depth (height)/nm	0.79	0.79	0.79
Volume ($V=\pi(d^2h)/4$)/nm^3	0.20	0.38	0.56

The guest surfactant geometrical dimensions can also be estimated theoretically as described by Tanford[38]. The length (L) and the volume (V) of the fully extended hydrocarbon chain C_nH_{2n+1} are estimated as[30,38,39]:

$$L/nm = 0.1500 + 0.1265(n_c-1) \quad (5\text{-}6)$$

$$V/nm^3 = 0.0274 + 0.0269(n_c-1) \quad (5\text{-}7)$$

The chain length n_c-1 is applicable in micellar systems where the methylene group near the head group is in contact with water (very likely completely solvated), is not contained within the hydrophobic core[39] and therefore the hydrophobic core is one methylene group less. In cyclodextrin-surfactant inclusion complexation such a situation does not arise. Therefore, the number n_c-1 in equations (5-6) and (5-7) may be replaced by a full hydrocarbon chain length n_c. In cases like alkylsulfates (C_nH_{2n+1}-O-SO_3^-), the etheric oxygen atom of the sulfate head group bonding with hydrocarbon chain may be considered as an extra methylene group and so the chain length can be written as n_c+1, especially when compared to alkanesulfonates (C_nH_{2n+1}-SO_3^-)[28,30,38]. For systems studied in this work equations (5-6) and (5-7) may be rewritten as

$$L/nm = 0.1500 + 0.1265n_c \quad (5\text{-}8)$$

$$V/nm^3 = 0.0274 + 0.0269n_c \quad (5\text{-}9)$$

Fully extended length (L) involves a hydrocarbon chain in the all-*trans* configuration which exist only in a crystalline state and not in liquid or gaseous states[39]. Hydrocarbon chains in the liquid state are not fully extended and the true chain length is less than L in equations (5-6) and (5-8). A number of conformations occur to a surfactant hydrocarbon chain:

(1) A single *gauche* conformation in an all-*trans* hydrocarbon chain bends the chain. This creates steric hindrance to inclusion processes.

(2) A double-*gauche* conformation in opposite directions creates a 'kink'. A kink increases the number of carbon atoms which can be accommodated in a cyclodextrin cavity. The length (L) is decreased by 0.125 nm and the volume (V) increased by 0.02-0.05 nm^3. This phenomena may be thought to stabilize the complex or increase the feasibility of inclusion itself because a volume increase makes surfactant fit better into the cyclodextrin cavities if at all they can enter. It may be extrapolated that ß-cyclodextrin is the most suitable for this phenomenon.

For example, ß-CD can accommodate 4 carbon atoms of an all-*trans* hydrocarbon chain, 6 carbon atoms of a hydrocarbon with a single kink (*gauche/gauche* connections) and 8 carbon atoms hydrocarbon chain with double kinks (i.e. two *gauche/gauche* connections). Theoretical estimation of stoichiometries for all-*trans*, single kink and double kinks hydrocarbon chain conformations are shown in Table 5.3. H_c is taken as the depth in Table 5.2, L_c is calculated using equation (5-8) and L_K is given[30,38] (L_K = 0.125 nm, $2L_K$ = 0.25 nm).

The possibility of a *gauche* or *gauche/gauche* conformations to occur in a hydrocarbon chain depends on the chain

length. For example, it is not possible to have a kink for $n_c \leq 4$ and a double kink for $n_c \leq 6$. Theoretical assumptions using geometrical factors only leads to the following general conclusions:

(1) The C_{16}- and C_{18}- surfactants can form up to 3:1 complexes for an all-*trans* hydrocarbon chains but as conformations occur the 3:1 complex becomes less and less feasible.

(2) The C_{12}- and C_{14}- surfactants can form up to 2:1 complexes for an all-*trans* and presence of other conformations weakens the 2:1 complex leaving a stable 1:1 complex.

(3) The C_4-, C_6-, C_8- and C_{10}- surfactants either form automatically 1:1 complex or inclusion complexation do not occur.

Table 5.3 Estimated stoichiometries from surfactant hydrocarbon fully extended length L_c/nm = 0.15+0.1265n_c, $L_K \approx 0.125$ (a kink) and cyclodextrin height ($H_c \approx 0.78$ nm)

n_c -	L_c nm	L_c/H_c -	$(L_c-L_K)/H_c$	$(L_c-2L_K)/H_c$	max. CD accomm.	stoichiometry expected
4	0.66	0.84	0.68	-	1	1:1
6	0.91	1.17	1.01	0.85	1	1:1
8	1.16	1.49	1.33	1.17	1	1:1
10	1.42	1.81	1.65	1.49	1	1:1
12	1.67	2.14	1.98	1.82	2	1:1, 2:1
14	1.92	2.46	2.30	2.14	2	1:1, 2:1
16	2.17	2.79	2.63	2.47	3	1:1, 2:1, 3:1
18	2.43	3.11	2.95	2.79	3	1:1, 2:1, 3:1

In this work a diversified study is carried out on different surfactant homologous series with chain lengths ranging from n_c = 6 to n_c = 16. These studies will involve: (i) electrochemical work using surfactant selective electrodes (covered in Chapter 6) on 1-alkylpyridinium bromides (C_{10}-C_{16}) and 1-alkyltrimethylammonium bromide (C_{14}). (ii) thermochemical work using an isothermal titration calorimetry (ITC) covered in Chapter 7 on (a) sodium 1-alkylsulfates (C_6-C_{14}), (b) sodium 1-alkanesulfonates (C_8-C_{12}), (c) 1-alkylpyridinium bromides (C_{12}-C_{16}), and (d) 1-alkyltrimethylammonium bromides (C_8-C_{16}). Results from both the electrochemical work in Chapter 6 and the Omega ITC work in Chapter 7 will be compared to independent emf[29,30] and fluorescence probe[28,31] studies.

5.4 REFERENCES

1. SCHARDINGER, F. *Zentr. Bakteriol. Parasitek., Abt II*, 29 (1911) 188.

2. FRENCH, D. *Adv. Carbohydr. Chem.*, 12 (1957) 189.

3. VILLIERS, A.C.R. *Acad. Sci. Paris*, 112 (1891) 536.

4. FRENCH, D. and RUNDLE, R.E. *J. Am. Chem. Soc.*, 64 (1942) 1651.

5. BORCHERT, W. *Z. Naturforsch., Teil B*, 3 (1948) 464.

6. FREUDENBERG, K. and CRAMER, F. *Z. Naturforsch., Teil B*, 3 (1948) 464.

7. SCHARDINGER, F. *Z. Untersuch. Nahr. u. Genussm.*, 6 (1903) 865.

8. SCHARDINGER, F. *Wien. Klin. Nahr. Wochschr.*, 6 (1904) 207.

9. SZEJTLI, J. *J. Drug Dev.*, 4(Suppl 1) (1991) 3.

10. BENDER, H. *Carbohydrate Res.*, 65 (1978) 85.

11. PULLEY, A.O. and FRENCH, D. *Biochem. Biophys. Res. Commun.*, 5 (1961) 11.

12. SOPHIANOPOULOS, A.J. and WARNER, I.M. *Anal. Chem.*, 64 (1992) 2652.

13. SUNDARAJAN, P.R. and RAO, V.S.R. *Carbohydrate Res.*, 13 (1970) 351.

14. MURPHY, V.G.; ZASLOW, B. and FRENCH, A.D. *Biopolymers*, 14 (1975) 1487.

15. NAKAI, Y.; YAMAMOTO, K.; KAJIYAMA, A.; SASAKI, I. *Chem. Pharm. Bull.*, 34 (1986) 2178.

16. LI, S. and PURDY, W.C. *Chem. Rev.*, 92 (1992) 1457.

17. SASAKI, K.J.; CHRISTIAN, S.D. and TUCKER, E.E. *Fluid Phase Equilibria*, 49 (1989) 281.

18. FUNG, B.M.; GUO, W. and CHRISTIAN, S.D. *Langmuir*, 8 (1992) 446.

19. LIVERI, V.T.; CAVALLARO, G.; GIAMMONA, G.; PITERRESI, G.; PUGLISI, G. and VENTUNA, C. *Thermochimica Acta*, 199 (1992) 125.

20. OKUBO, T.; KITANO, H. and ISE, N. *J. Phys. Chem.*, 80 (1976) 2661.

21. SATAKE, I.; IKENOUE, T.; TAKESHITA, T.; HAYAKAWA, K. and MAEDA, T. *Bull. Chem. Soc. Jpn.*, 58 (1985) 2746.

22. SATAKE, I.; YOSHIDA, S.; HAYAKAWA, K.; MAEDA, T. and KUSUMOTO, Y. *Bull. Chem. Soc. Japan*, 59 (1986) 3991.

23. PALEPU, R. and REINSBOROUGH, V.C. *Can. J. Chem.*, 66 (1988) 325.

24. FUNASAKI, N.; YODO, H.; HADA, S. and NEYA, S. *Bull. Chem. Soc. Jpn.*, 65 (1992) 1323.

25. DHARMAWARDANA, J.R.; CHRISTIAN, S.D.; TUCKER, E.E.; TAYLOR, R.W. and SCAMEHORN, J.F. *Langmuir*, 9 (1993) 2258.

26. SAINT AMAN, E. and SERVE, D. *J. Colloid Interface Sci.* 183 (1990) 365.

27. JUNQUERA, D.; TARDAJOS, G. and AICART, D. *Langmuir*, 9 (1993) 1213.

28. PARK, J.W. and SONG, H.J. *J. Phys. Chem.*, 93 (1989) 6454.

29. JEZEQUEL, D.; MAYAFFRE, A. and LETELLIER, P. *Can. J. Chem.*, 69 (1991) 1865.

30. WAN-YUNUS, W.M.Z.; TAYLOR, J.; BLOOR, D.M.; HALL, D.G. and WYN-JONES, E. *J. Phys. Chem.*, 96 (1992) 8979.

31. PARK, J.W. and PARK, K.H. *J. Incl. Phenom.*(1994) In Press.

32. PALEPU, R.; RICHARDSON, J.E. and REINSBOROUGH, V.C. *Langmuir*, 5 (1989) 218.

33. JUNQUERA, D.; AICART, E. and TARDAJOS, G. *J. Phys. Chem.*, 96 (1992) 4533.

34. JOBE, D.J.; HOLZWARTH, J.F.; VERRALL, R.E. *Minutes of the 5th Int. Symposium on Cyclodextrins*, ed. DUCHENE, D., PARIS (1990).

35. MWAKIBETE, H.; BLOOR, D.M. and WYN-JONES, E. *Langmuir*, 10 (1994) 3328.

36. MWAKIBETE, H.; CRISTANTINO, R.; BLOOR, D.M.; HOLZWARTH, J.F. and WYN-JONES, E. *Langmuir* (1994) In press.

37. CONNORS, K.A. "*Binding Constants: The Measurements of Molecular Complex Stability*", John Wiley & Sons, New

York (1987).

38. TANFORD, C. "*The Hydrophobic Effect: Formation of Micelles and Biological Membranes*", 2nd Edition, John Wiley & Sons, New York (1980).

39. FRANK, H.S. and EVANS, M.W. *J. Chem. Phys.*, 13 (1945) 507.

40. LEWIS, E.A. and HANSEN, L.D. *J. Chem. Soc. Perkin Trans. 2*, (1973) 2081.

41. IKEDA, K.; UEKAMA, K. and OTAGIRI, M. *Chem. Pharm. Bull. (Tokyo)*, 23 (1975) 201.

42. SAINT AMAN, E. *J. Colloid Interface Sci.*, 132 (1990) 365.

43. GIORDANO, F. and LA MANNA, A. *J. Drug Dev.*, 4(Suppl.1) (1991) 13

44. CLARKE, R.J.; COATES, J.H.; and LINCOLN, S. *Adv. Carbohydr. Chem. & Biochem.*, 46 (1988) 205.

45. SAENGER, W.; NOLTEMEYER, M.; MANOR, P.C.; HINGERTY, B. and KLAR, B. *Bioorganic Chemistry*, 5 (1976) 187.

46. LUKAS, T.M., *PhD Thesis*, University of Salford (1991).

CHAPTER SIX: EQUILIBRIUM STUDIES ASSOCIATED WITH INCLUSION COMPLEXES OF CATIONIC SURFACTANTS TO α-, AND ß-CYCLODEXTRINS USING SURFACTANT SELECTIVE ELECTRODES

6.1 INTRODUCTION

The main section of this chapter describes a study on the inclusion complexes of the homologous series of 1-alkylpyridinium bromides (C_nPyBr) with α- and ß-cyclodextrins using surfactant selective electrodes. As far as we are aware there are very few studies on inclusion complexes for individual 1-alkylpyridinium bromides with ß-CD and none for α-CD. These include Jezequel *et al*[1] who carried out electrochemical studies on ß-CD/$C_{16}PyBr$ and Palepu *et al*[2] who used a conductometric method on the same system. During the course of this work we became aware of a paper submitted by Park and Park[3] describing fluorescence probe studies on the inclusion of 1-alkyltrimethylammonium bromides into ß-CD. The complexation constants of these systems were also measured independently by Jezequel *et al*[1] using surfactant selective electrodes. As a result of this work it was decided to measure the binding constants of the two surfactants $C_{14}TAB$ and $C_{16}TAB$ with α- and ß-CD in an effort to extend our examination on the reliability and consistency of binding constants as described in Chapter 5 section 5.3.1 page 141. The $C_{16}TAB$ complexes with α- and ß-CD were measured by a visiting student Cristantino and the present author measured $C_{14}TAB$ complexes with α- and ß-CD. These results are also described in this Chapter.

6.2 EXPERIMENTAL PROCEDURES

6.2.1 Synthesis of alkylpyridinium bromides

Most commercially available 1-alkylpyridinium bromides are impure and purification of these products is tedious and difficult. As a result we prepared these surfactants in the laboratory. The following 1-alkylpyridinium bromides $C_nH_{2n+1}PyBr$: decylpyridinium bromide ($C_{10}PyBr$), dodecylpyridinium bromide ($C_{12}PyBr$), tetradecylpyridinium bromide ($C_{14}PyBr$) and cetylpyridinium bromide ($C_{16}PyBr$)) were synthesized from the stoichiometric reaction between dried pyridine NC_5H_5 (> 99%, d = 0.978, Aldrich) and the corresponding 1-bromoalkanes $C_nH_{2n+1}Br$: 1-bromodecane (98%, d = 1.05, Aldrich), 1-bromododecane (97%, d = 1.04, BDH), 1-bromotetradecane (95%, d = 1.02, Sigma) and 1-bromohexadecane (99%, d = 1.00, Sigma) respectively. The preparation procedures were followed as described in literature[4-10].

$$C_nH_{2n+1}Br + NC_5H_5 \rightarrow C_nH_{2n+1}PyBr$$

1-bromoalkane dried pyridine 1-alkylpyridinium bromide

where Py = $\overset{+}{N}C_5H_5$.

The appropriate 1-bromoalkane and dried pyridine (Py) in a stoichiometric ratio of 1:1 were mixed with ethanol of AnalaR grade (more than half of the total reaction mixture volume) in a round bottomed flask. For example, to prepare 50 g of $C_{12}PyBr$, 38.689 g of 1-bromododecane and 12.045 g of dried pyridine were mixed with about 60 ml of ethanol. Anti-bumping granules were added to the mixture and the

mixture was refluxed overnight (at least 10 hours) in a fume cupboard. After completion the crude reaction mixture was poured into a round bottomed flask and rotary evaporated until it became viscous. The crude surfactant products were then extracted from the reaction mixture using hexane. C_{12}PyBr was also extracted successfully using diethyl ether[9] although diethyl ether failed to extract the other surfactants. Crude extracts for C_{10}PyBr, C_{12}PyBr and C_{14}PyBr are heavy oily liquids and they were separated from the organic layer using a separating funnel. A crude extract of C_{16}PyBr is a powdery solid and so it was separated repeatedly by shaking and decanting the extraction solvent.

Table 6.1: Comparison of physical characteristics from this work and literature

C_nPyBr	This work		Literature	
	cmc mmol dm^{-3}	m.p. °C	cmc mmol dm^{-3}	m.p. °C
C_{10}PyBr	45.50	36.0-38.0		36.5-37.8[f]
C_{12}PyBr	11.50	46.5-47.5	12.00[e]	47.0-47.4[f]
				44.5-45.5[b]
C_{14}PyBr	2.80	56.0-58.0	2.85[e,c]	58.9-59.5[f]
			2.82[d]	54.5-55.5[b]
				56.0-59.0[a]
C_{16}PyBr	0.74	60.0-62.0	0.67[c]	60.5-61.5[b,f]

[a](ref 4), [b](ref 5), [c](ref 7), [d](ref 8), [e](ref 10), [f](ref 11).

The crude extracted products were recrystallized from acetone for more than three times. Each recrystallization from acetone was followed by washing using cold acetone. Despite the efforts made, C_{16}PyBr did not reach the purity

required for the electrode work and so was purified further by column chromatography (25% CH_3OH : 75% $CHCl_3$). The purity of synthesized surfactants were checked by measuring the cmc and melting points. Table 6.1 lists the cmc and m.p. of synthesized surfactants which are in good agreement with literature.

Application of the Klevens plot, log(cmc) against n_c (Figure 6-1), yielded good Klevens parameters:

$\log(cmc) = 1.61 - 0.30n_c$, $r = -0.99997$ at 25°C (this work)

as compared to the literature Klevens equation[12-14]

$\log(cmc) = 1.72 - 0.31n_c$ at 30°C

which is a good indication that the 1-alkylpyridinium bromides prepared for this work are sufficiently pure.

6.2.2 Preparation of C_nPy^+ ions PVC-membranes

The preparation of PVC-membranes to construct selective electrodes for the 1-alkylpyridinium bromides ($C_{10}PyBr$, $C_{12}PyBr$, $C_{14}PyBr$ and $C_{16}PyBr$) was carried out as outlined in section 2.4.1 for $C_{16}TAB$. The PVC polymer with carboxylic ionic end groups (PVC-COO^-H^+) was used for conditioning $C_{10}PyBr$, $C_{12}PyBr$ and $C_{14}PyBr$. A special Montefibre PVC polymer with sulphonate ionic end groups (PVC-$SO_3^-H^+$) was used for conditioning $C_{16}PyBr$. The conditioning for all the surfactants was carried out using 500 ml of a 2 x cmc mol dm^{-3} aqueous surfactant solution to which a PVC-THF solution (500 mg PVC polymer dissolved in 30 ml of doubly distilled THF) was added gradually while stirred and left to stir for

48 hours. The polymeric plasticiser, Elvaloy 742, was used in casting. The detailed procedures are as outlined in section 2.4.1.

6.2.3 EMF Measurements in CD/Surfactant Systems

The EMF corresponding to the 1-alkylpyridinium ion (C_nPy^+) was measured using the corresponding 1-alkylpyridinium ion selective electrode relative to a standard sodium ion electrode (Kent, EIL) in a cell of type I:

1-alkylpyridinium ion selective electrode	test solution containing constant [NaBr] and [CD]	electrode reversible to sodium ion

The calibration was carried out for the 1-alkylpyridinium bromide systems in absence of cyclodextrins. The electrode characteristics are listed in Table 6.2. Figure 6-2 show typical calibration EMF versus $\log(C_1)$ plots of these surfactant membrane selective electrodes. The electrochemical experiment to measure the EMF in presence of constant amounts of CD was carried out by keeping the same concentration of α-CD or ß-CD in the test solution and the titrating solution. This allows a similar experiment to be carried out by measuring the EMF at different surfactant concentrations only. For each surfactant the experiments were repeated by changing the CD concentrations.

The possibility of bromide ions binding to cyclodextrin was checked by taking measurement of the EMF of a bromide ion electrode relative to standard calomel electrode (SCE) as

Figure 6-1: A Klevens plot log(cmc) versus n_c for the 1-alkylpyridinium bromides

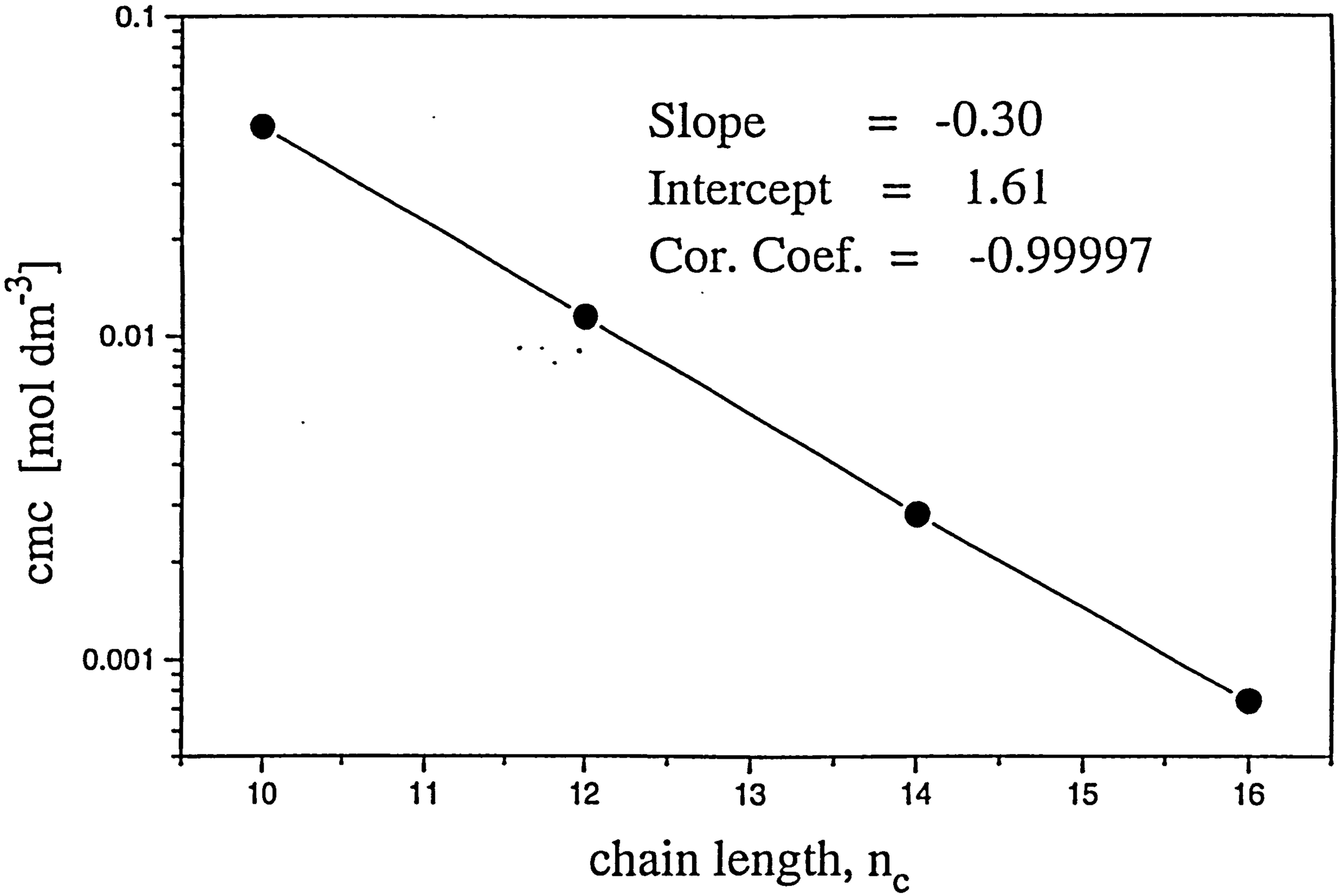

Figure 6-2: EMF versus log(C_1) plots for C_nPyBr homologous series

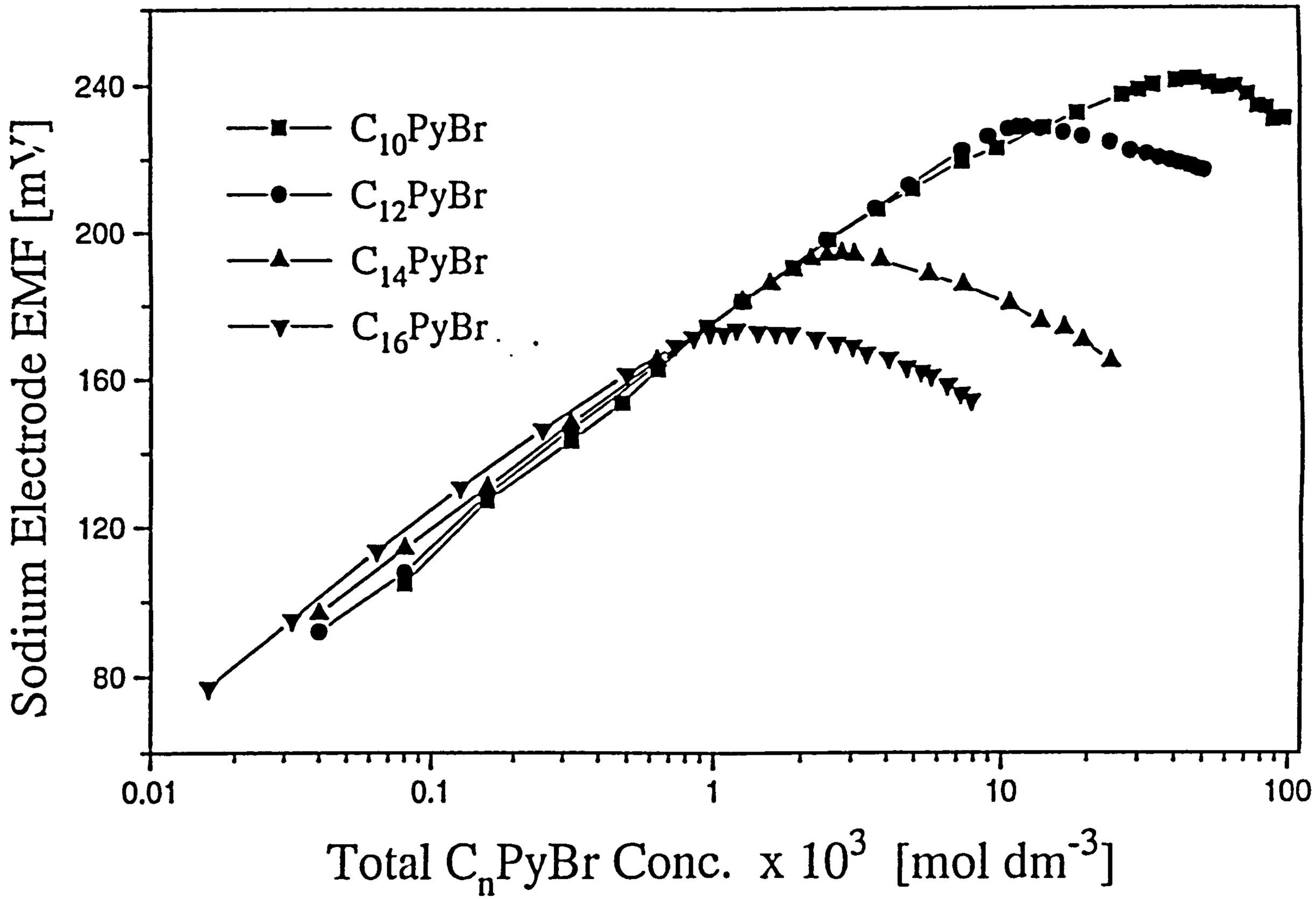

Figure 6-2a: EMF versus log(C_1) plot for C_{10}PyBr system

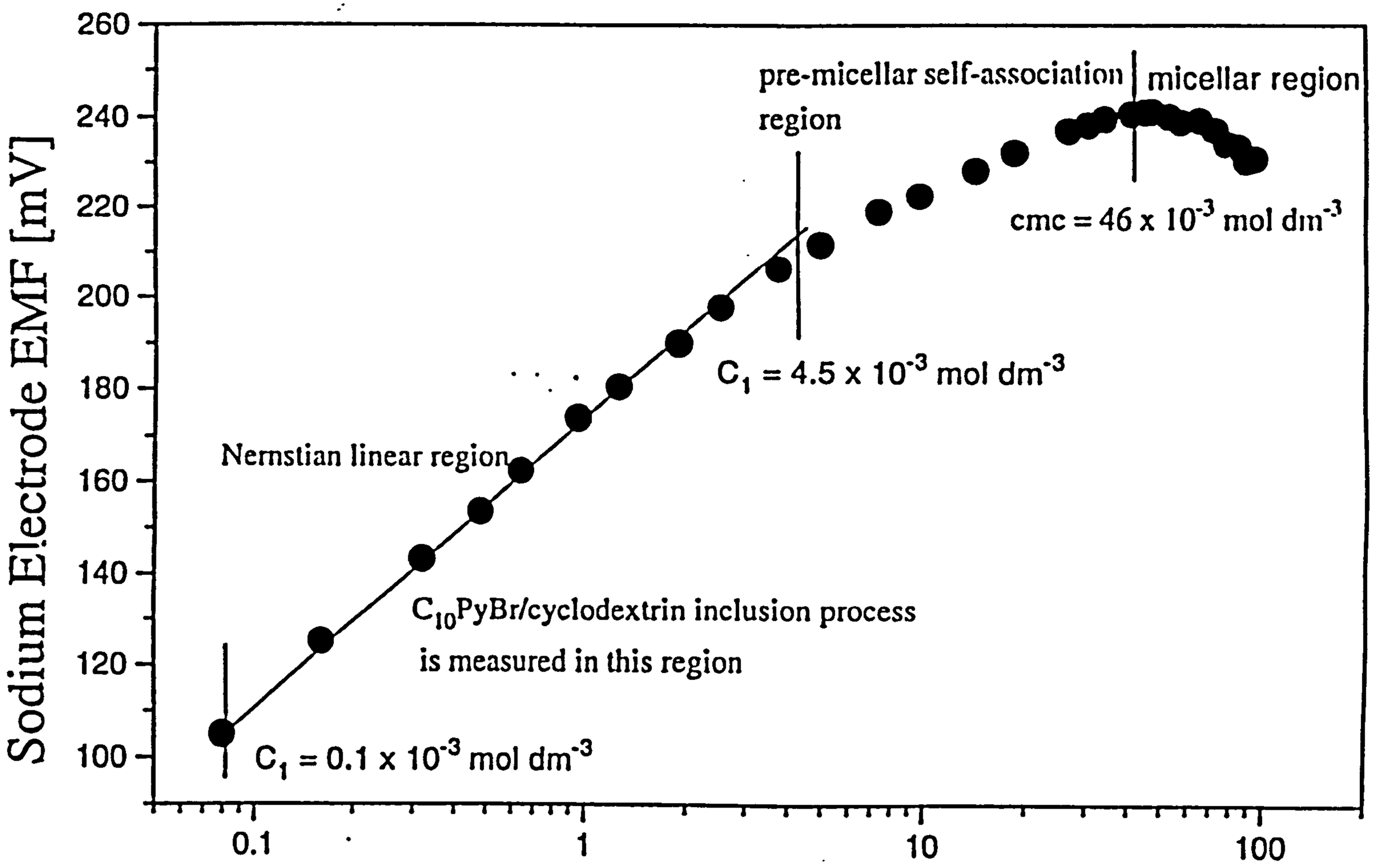

follows:

Bromide ion selective electrode	surfactant solution containing constant [NaBr] and [ß-CD]	standard calomel electrode

The data are shown in Table 6.3 and the EMF plot in Figure 6-3. These measurements showed a Nernstian response showing that no binding of bromide ions to the ß-cyclodextrins takes place.

Table 6.2: Characteristics of the 1-alkylpyridinium ion selective electrodes

	Electrode parameter			Micellar properties	
C_nPyBr	Linearity /mM	Slope mV/dec	Eo, mV	Pre-micellar /mM	cmc mM
C_{10}	0.10-4.50	58.0	186.0	4.50-46.00	46.00
C_{12}	0.04-3.00	58.1	341.0	3.00-11.50	11.50
C_{14}	0.04-1.30	56.6	362.2	1.30- 2.80	2.80
C_{16}	0.01-0.30	58.1	420.6	0.30- 0.75	0.75
$C_{14}TAB$	0.08-3.60	58.9	425.4	none	3.60

Table 6.3: Measurement of bromide ion in a surfactant-ß-cyclodextrin-0.1 mM NaBr system to check bromide ion binding

mmol dm^{-3}	mV	mmol dm^{-3}	mV	mmol dm^{-3}	mV
0.04	67.4	3.70	-17.8	24.24	-51.6
0.08	65.2	4.87	-24.5	28.57	-52.7
0.16	54.1	7.13	-34.6	32.43	-53.3
0.32	40.1	9.29	-40.7	35.89	-52.6
0.64	25.2	13.31	-45.5	39.02	-54.5
1.26	8.5	17.00	-49.1	41.86	-54.0
2.50	-8.4	19.35	-49.5	44.44	-54.5

The EMF plots in α-CD/C_nPyBr and ß-CD/C_nPyBr (n = 10, 12, 14 and 16), α-CD/C_{14}TAB and ß-CD/C_{14}TAB are shown in figures 6-4 to 6-13.

Figure 6-3: Examination of Counterion binding Bromide Electrode against StandardCalomel Electrode

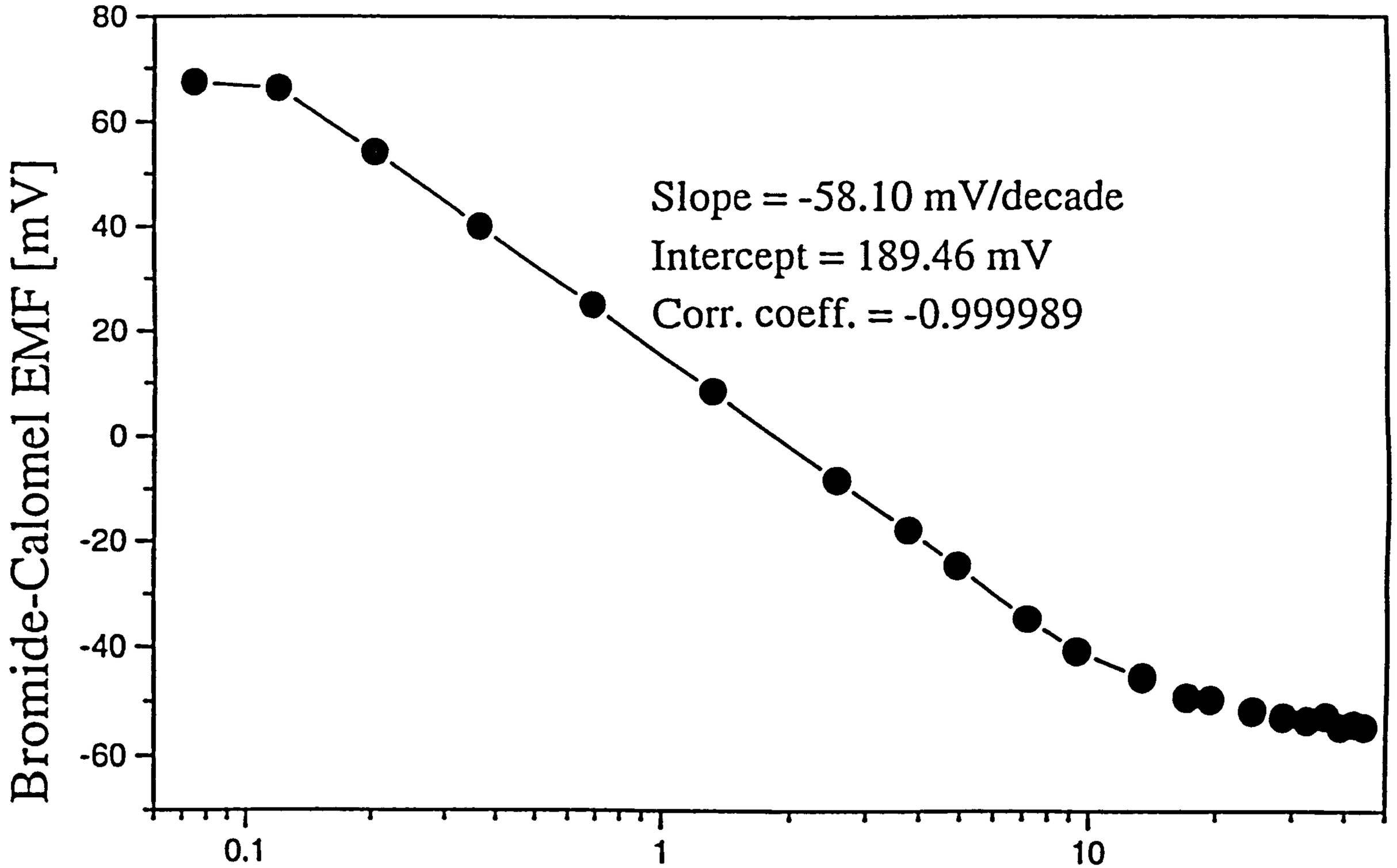

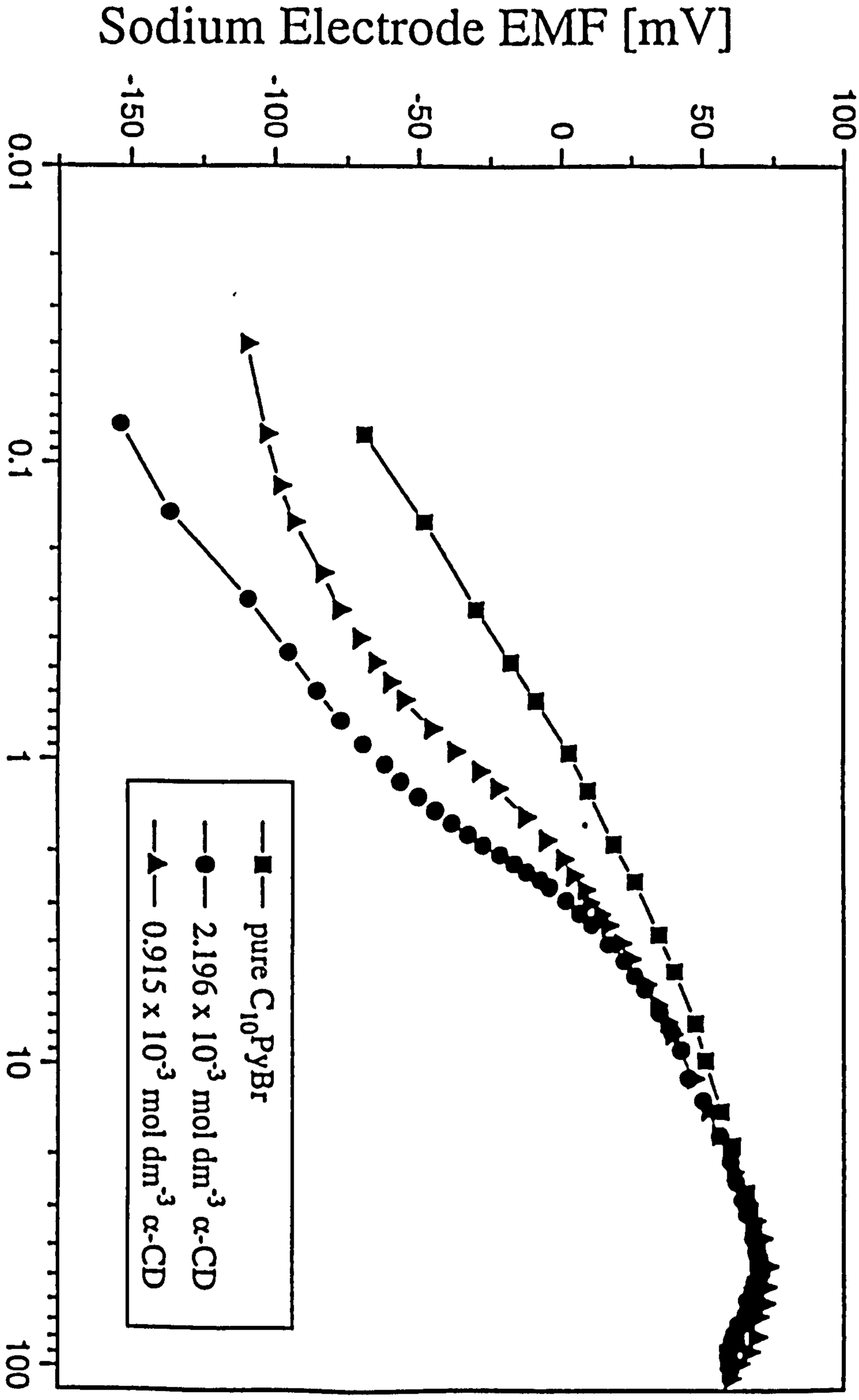

Figure 6-4: EMF versus log(C_{10}) plot for α-CD/C_{10}PyBr system

Figure 6-6: EMF versus log(C_1) plot for α-CD/C_{12}PyBr system

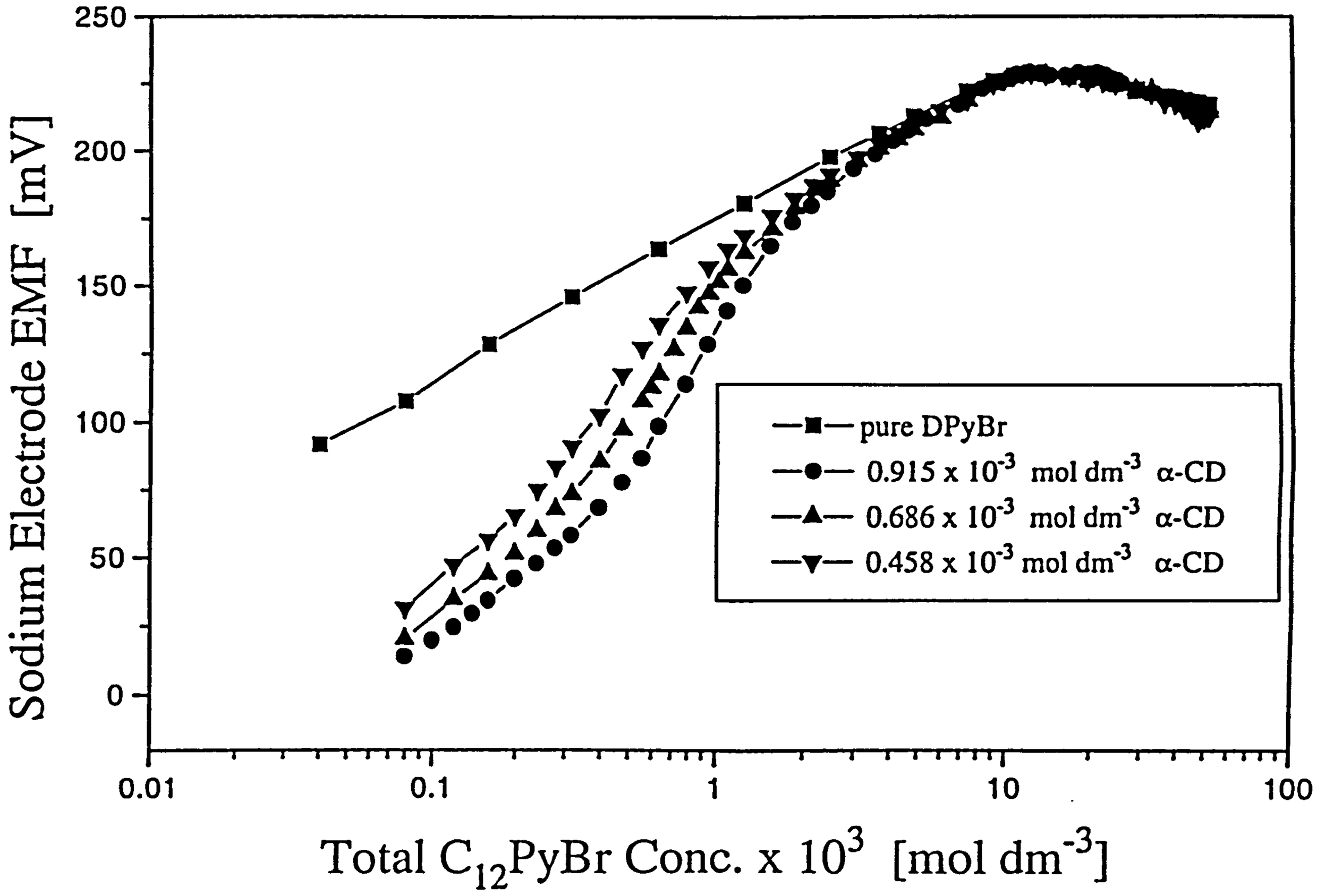

Figure 6-5: EMF versus log(C_1) plots for β-CD/C_{10}PyBr systems

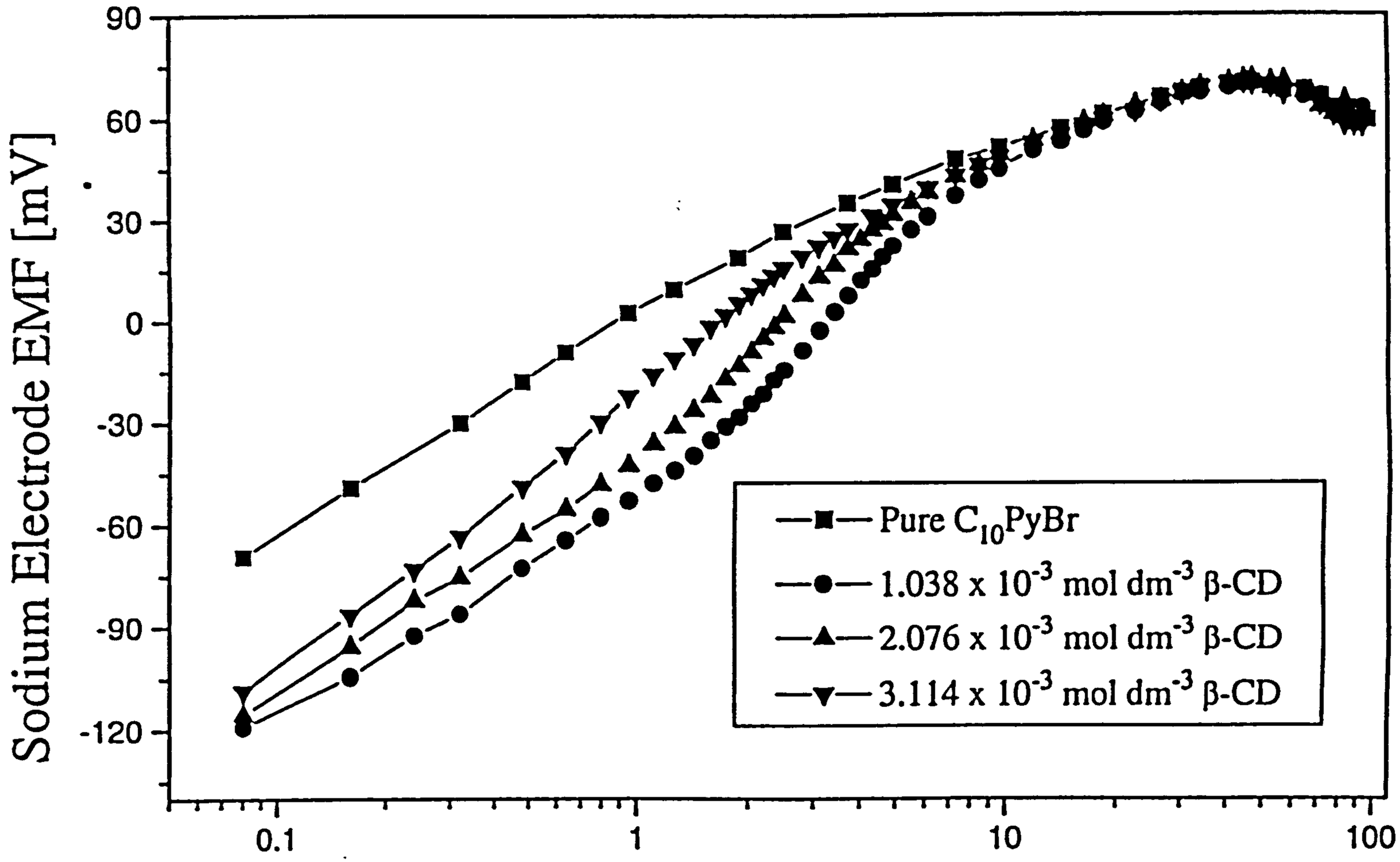

Figure 6-7: EMF versus log(C_1) plot for β-CD/C_{12}PyBr system

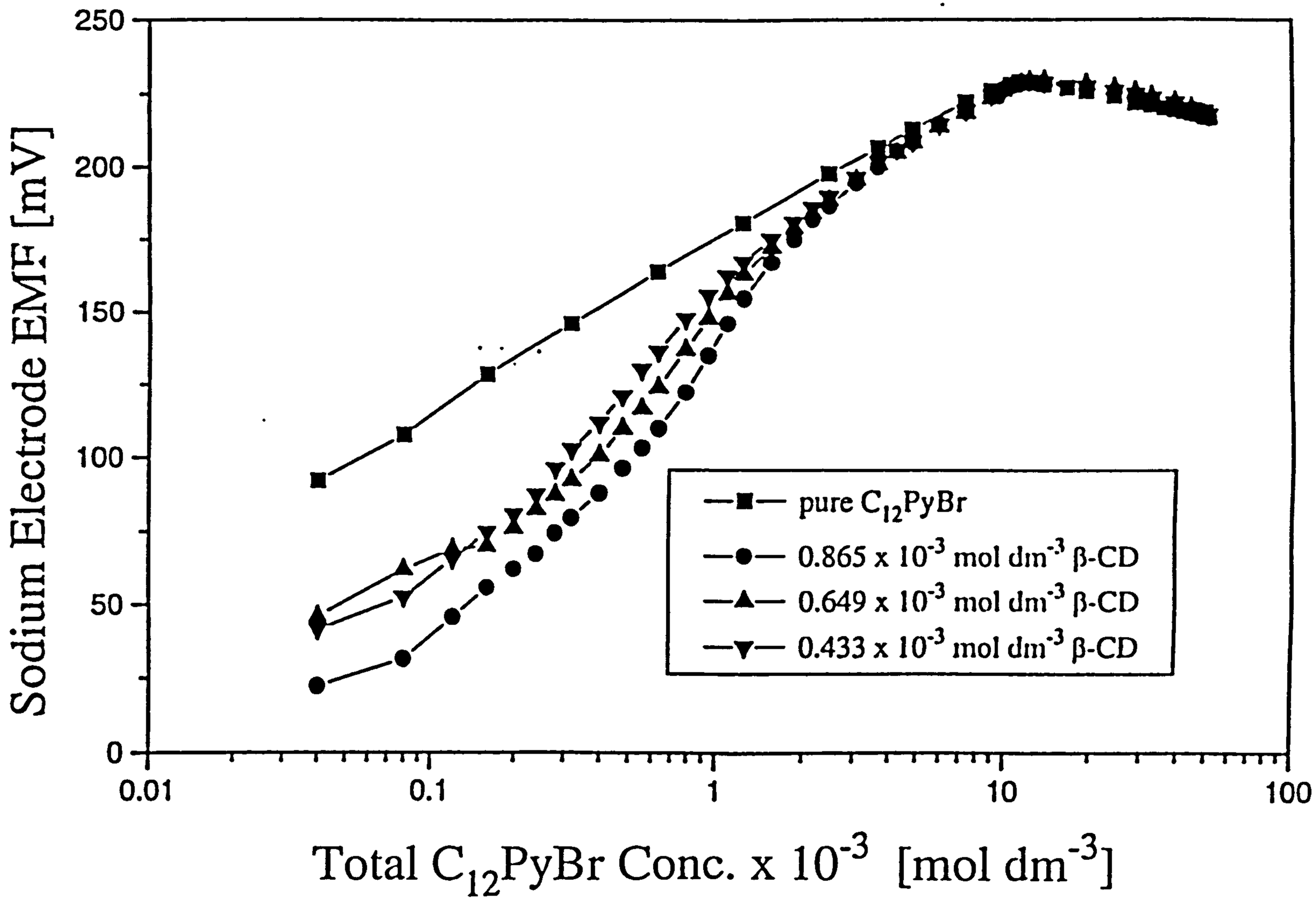

Figure 6-8: EMF versus log(C_1) plot for α-CD/C_{14}PyBr system

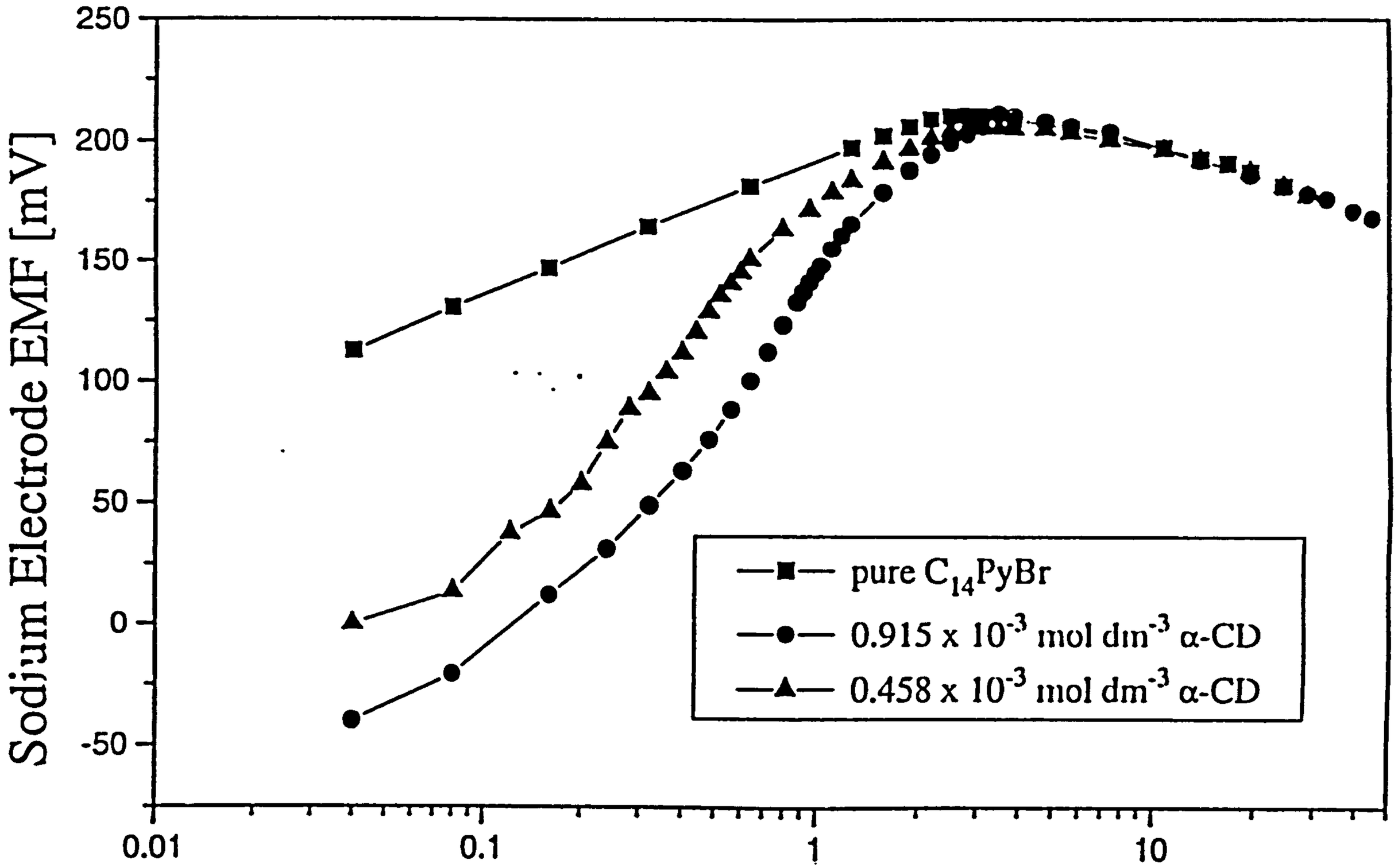

Figure 6-9: EMF versus log(C_1) plot for α-CD/C_{14}PyBr system

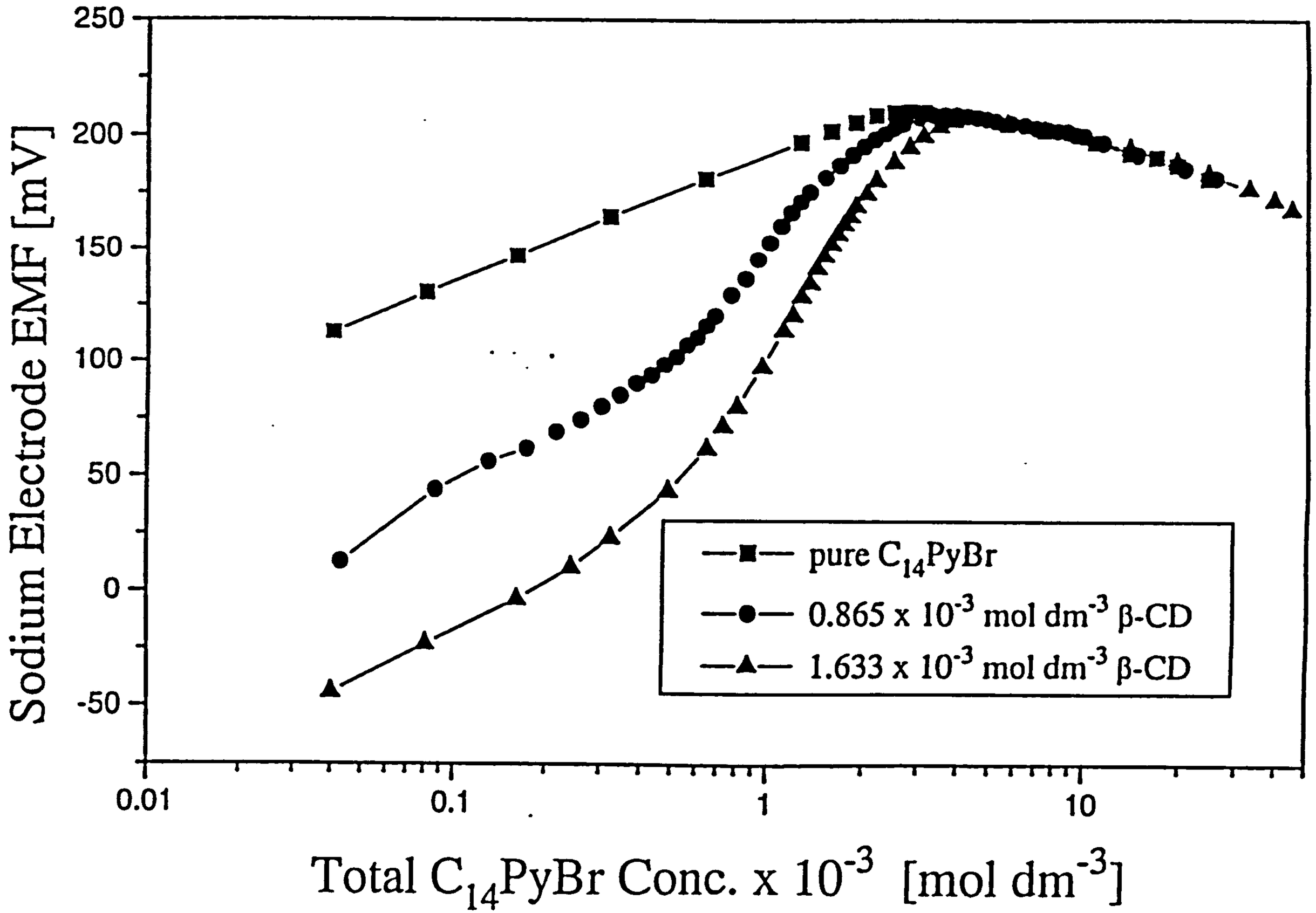

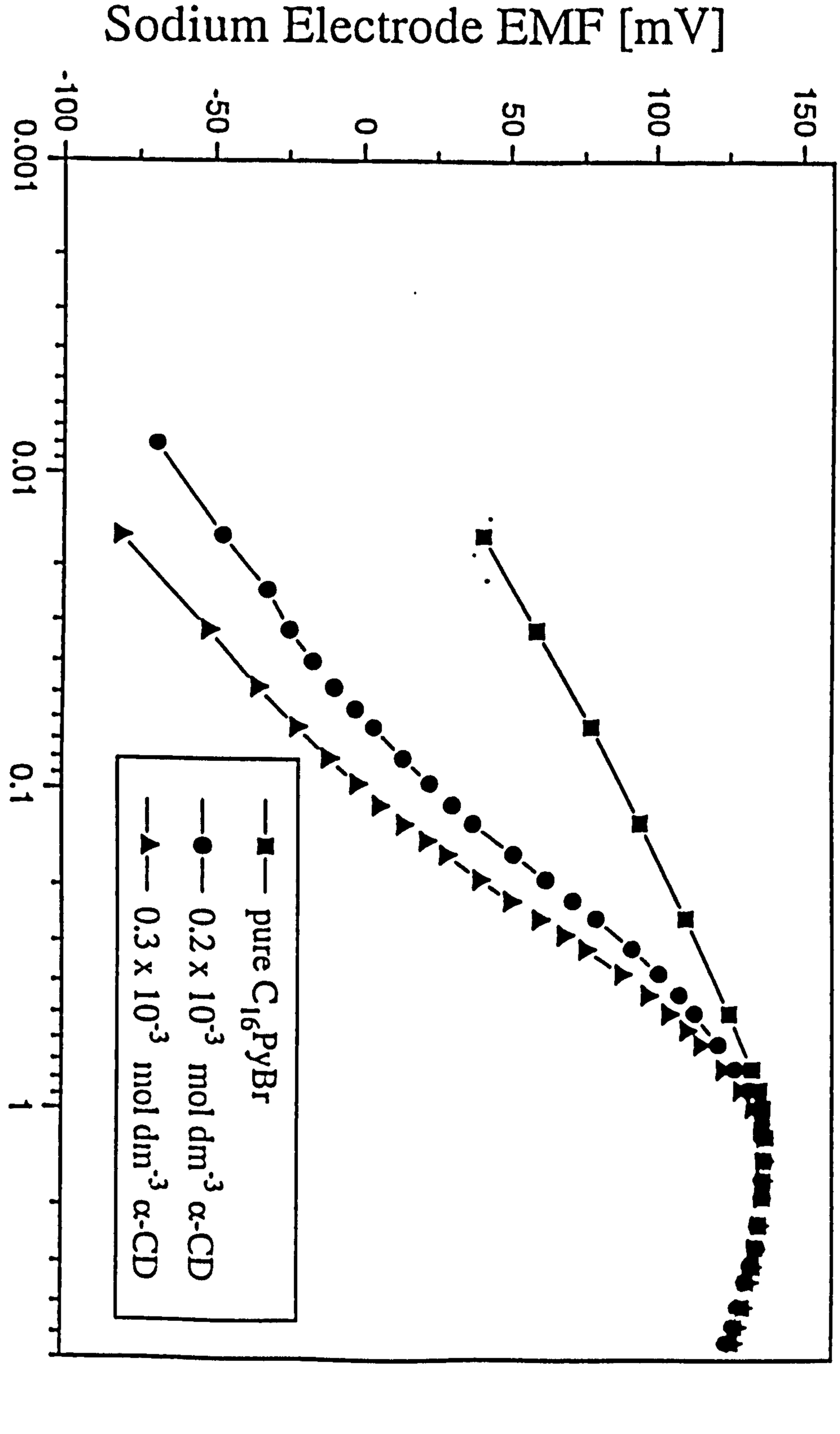

Figure 6-10: EMF versus log(C_1) plot for α-CD/C_{16}PyBr system

Figure 6-11: EMF versus log(C_1) plot for β-CD/C_{16}PyBr system

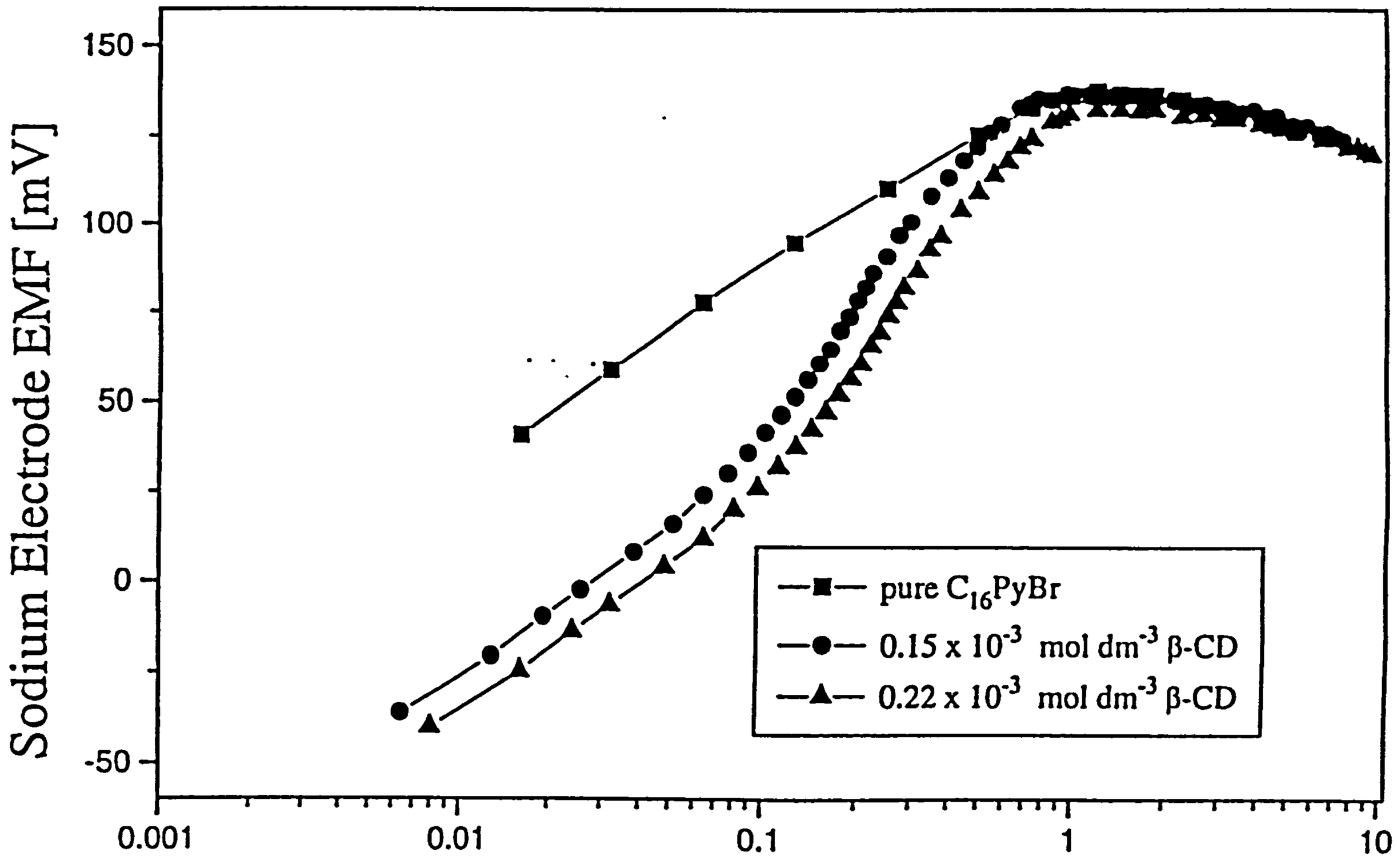

Figure 6-12: EMF versus log(C_1) plot for α-CD/C_{14}TAB systems

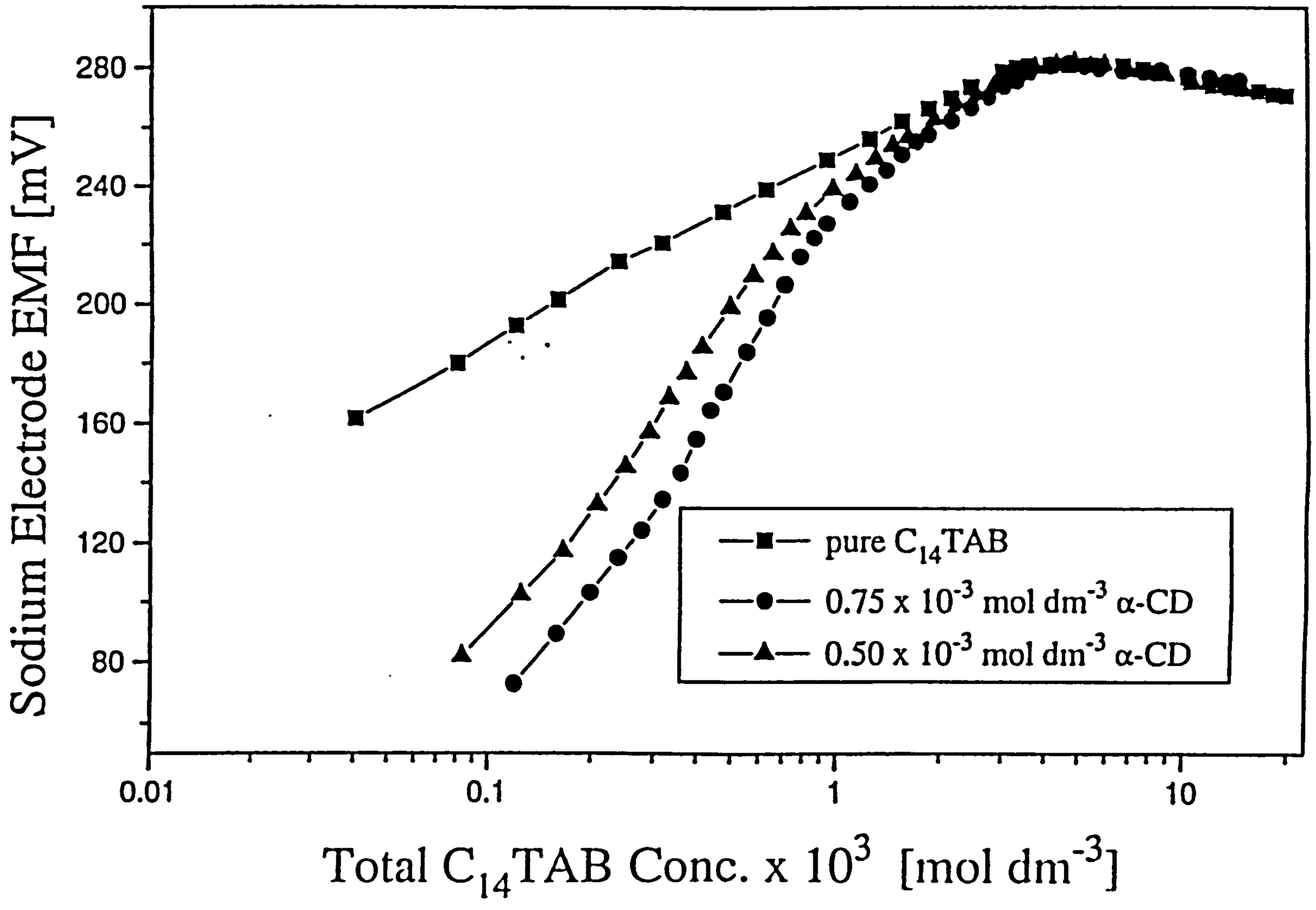

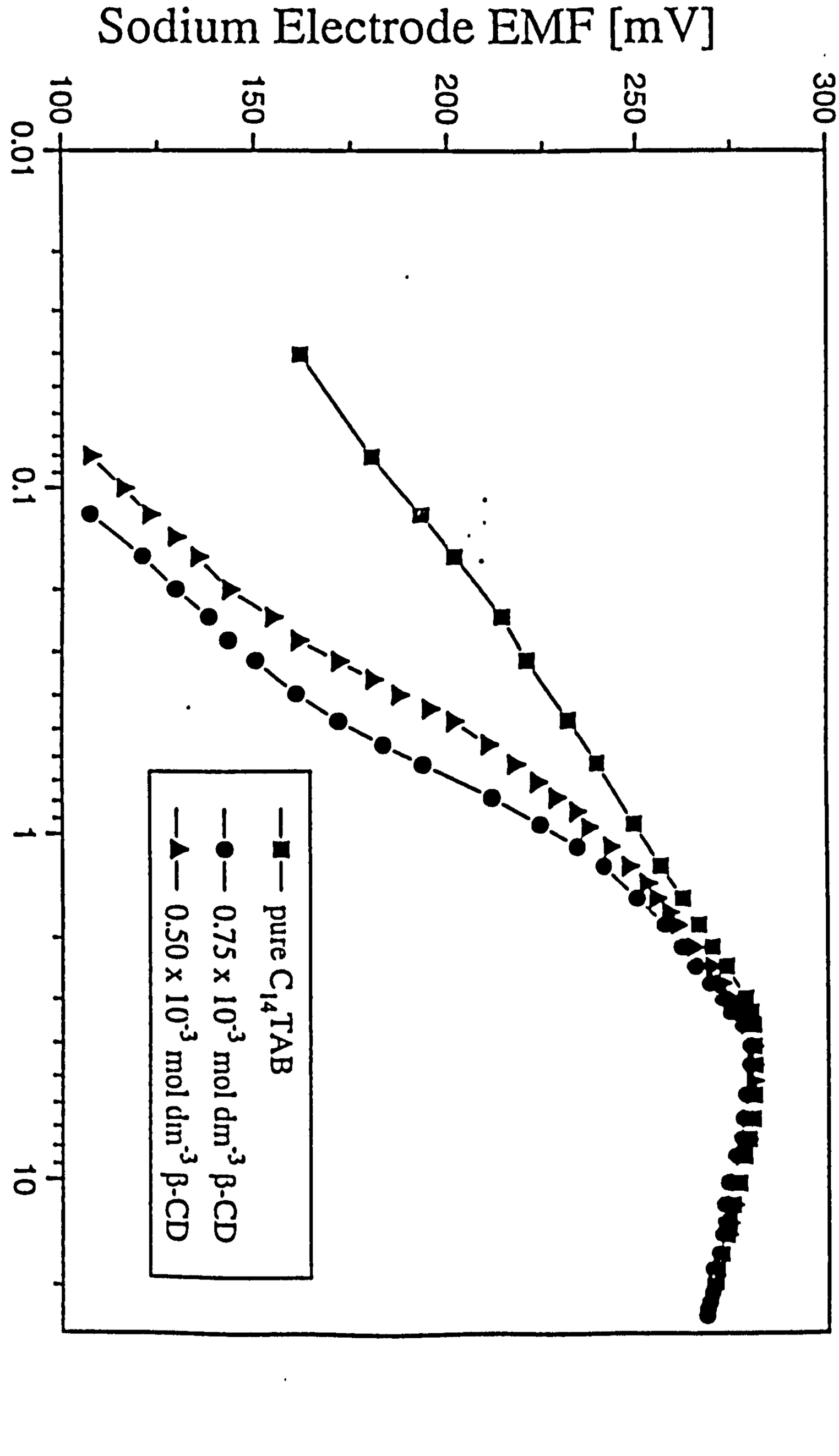

Figure 6-13: EMF versus log(C_1) plot for β-CD/C_{14}TAB systems

6.3 TREATMENT OF ELECTRODE DATA.

From the EMF plots described above it is possible to evaluate the monomer surfactant concentration m_1 at each total surfactant concentration in the presence of a constant amount of cyclodextrin. The second step is to analyse these data so that the described complexation constants can be measured.

The following assumptions are made[12]:

(a) cyclodextrin molecules exist in monomeric form in water (or any other solvent medium used),

(b) there is no interactions between cyclodextrin molecules with any other species other than surfactant in the system,

(c) the complex involves only one surfactant ion, and

(d) that the activity coefficients of ionic species of the same valency are the same and hence cancel.

It is important in the first instance to check whether the surfactant (S) and corresponding cyclodextrin (CD) form 1:1 inclusion complex according to scheme 1

scheme (1)

$$S + CD \overset{K_1}{\rightleftharpoons} S(CD)$$

In circumstances like these it is possible to derive K_1 using the Scatchard equation in the form[15]

$$\left(\frac{\Gamma}{m_1}\right) = K_1 - K_1\Gamma \qquad (6\text{-}1)$$

where m_1 = concentration of surfactant in monomeric form

$$\Gamma = \frac{\text{conc. of surfactant bound by CD}}{\text{total concentration of CD}} = \frac{C_1 - m_1}{C_c}$$

K_1 is the binding constant, C_1 and C_c are total surfactant and cyclodextrin concentrations respectively.

A plot of Γ/m_1 against Γ according to equation (6-1) is used to determine the equilibrium constant as slope ($-K_1$) and ordinate intercept (K_1). Typical Scatchard plots for CD/C_nPyBr systems studied in this work are shown in Figures 6-14 to 6-23. If the Scatchard plot according to equation (6-1) fails to give a straight line plot then we are certain of the existence of at least a second complex. It is clear from the data that the ratio (bound CD)/(bound S) consistently give values above unity which indicates presence of the complex involving one surfactant into two CD according to scheme (2).

scheme (2)

$$S(CD) + CD \overset{K_2}{\leftrightharpoons} S(CD)_2$$

In typical electrochemical experiment we keep the total concentration of cyclodextrin, C_c, constant, vary the surfactant concentration C_1, measure each corresponding value of monomer surfactant m_1 with surfactant selective

Figure 6-14: Scatchard Isotherms for α-CD/C_{10}PyBr systems

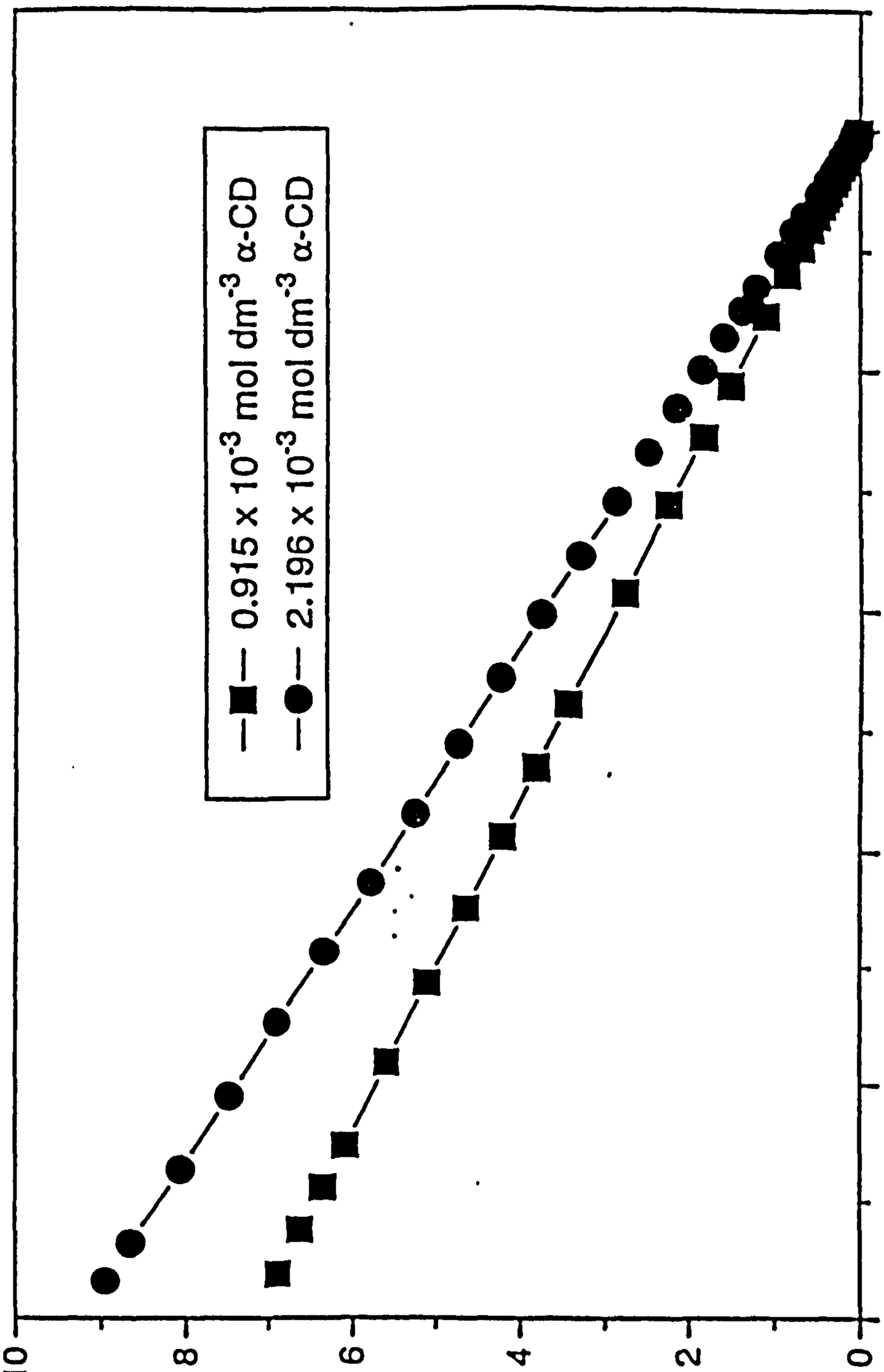

Figure 6-15: Scatchard Isotherms for β-CD/C_{10}PyBr systems

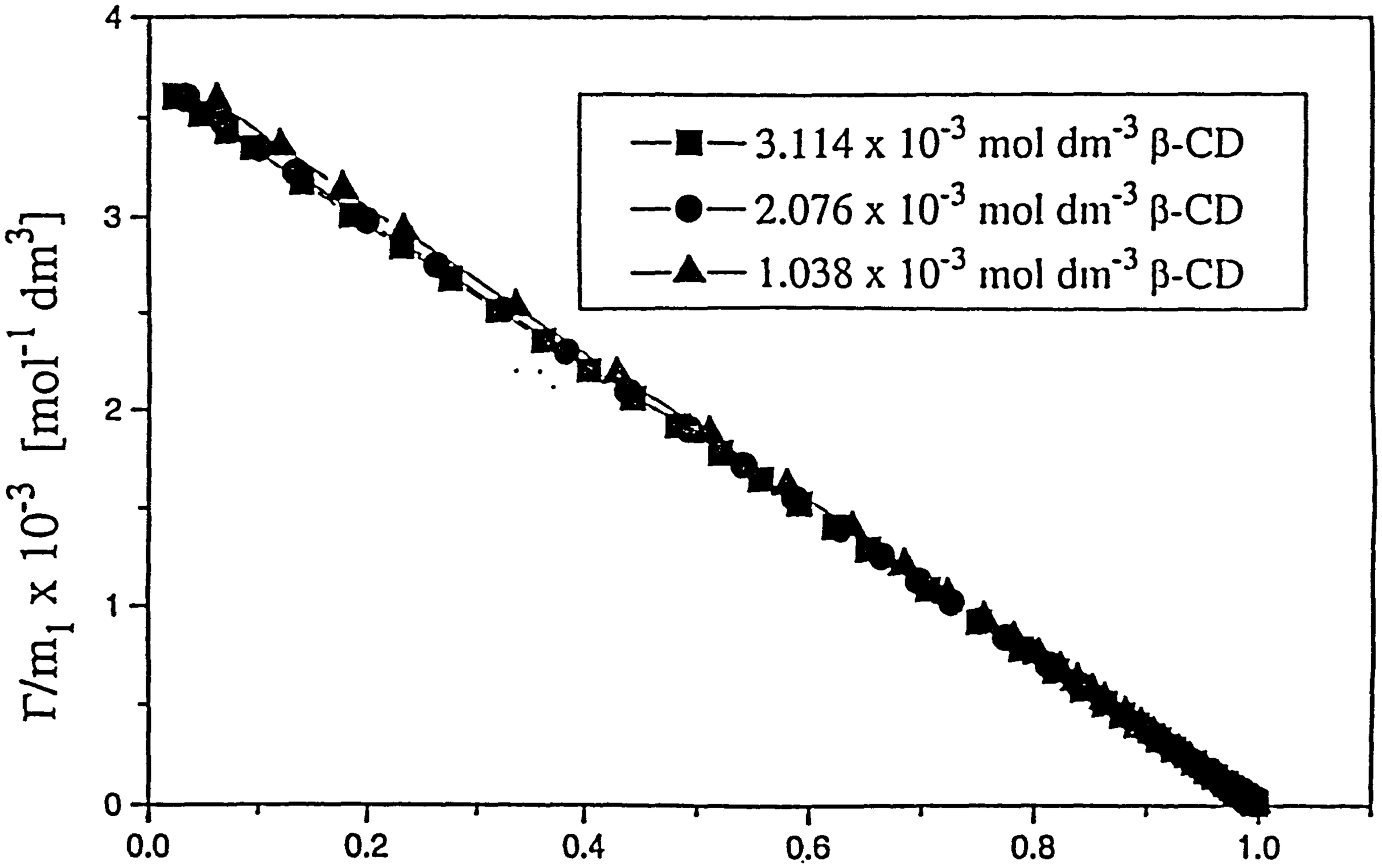

Figure 6-16: Scatchard Isotherms for α-CD/C_{12}PyBr systems

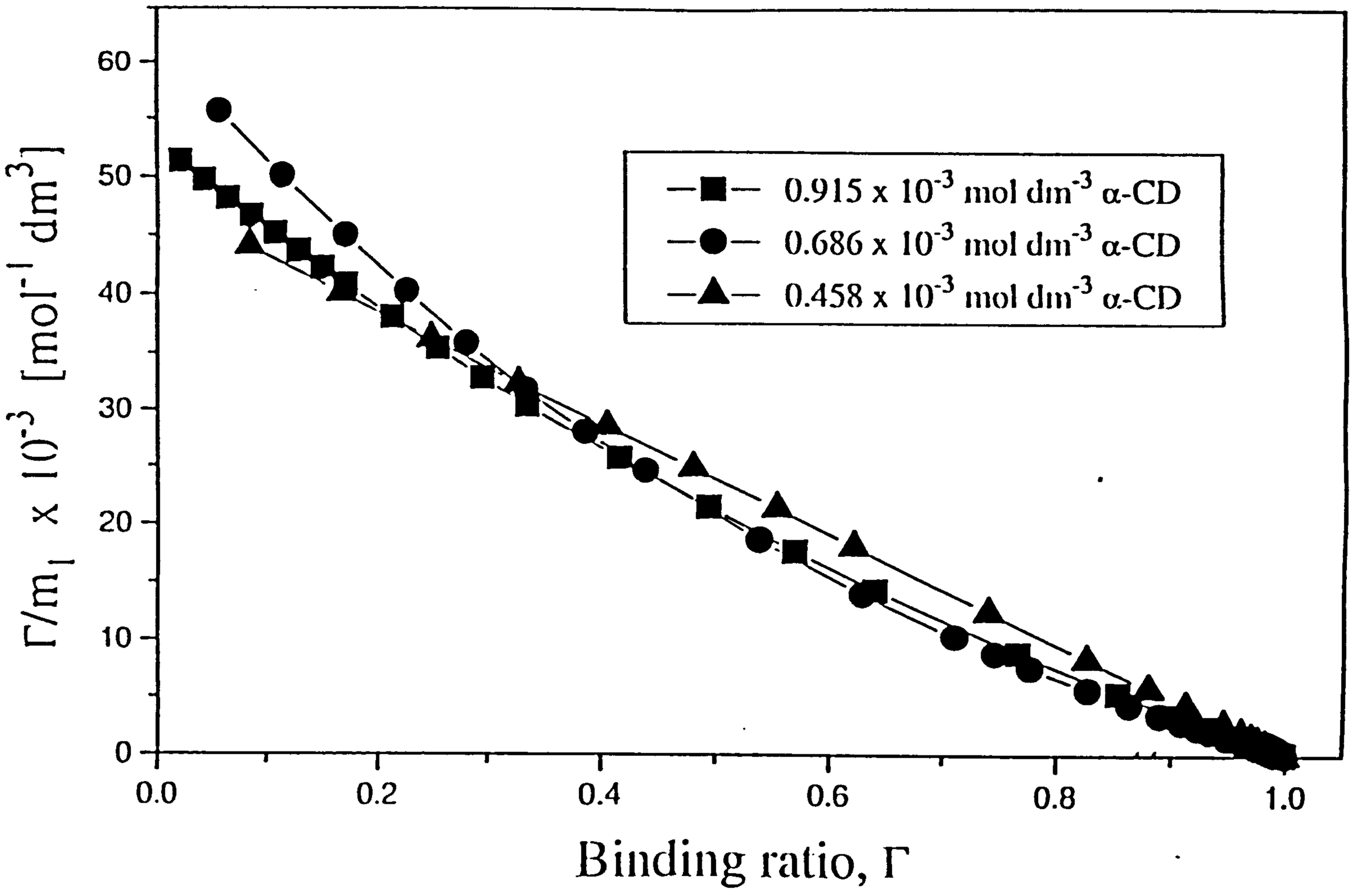

Figure 6-17: Scatchard Isotherms for β-CD/C_{12}PyBr systems

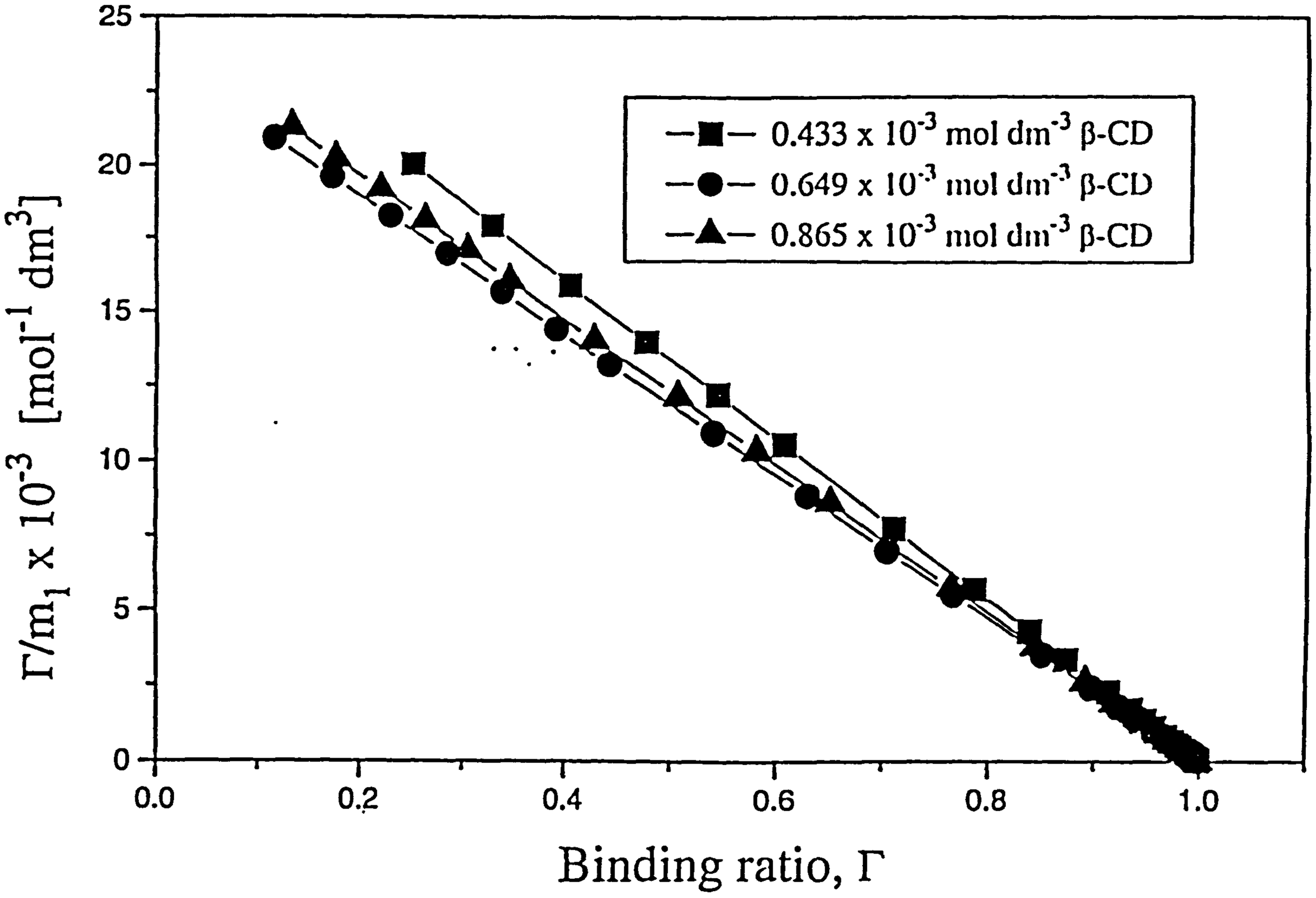

Figure 6-18: Scatchard Isotherm for α-CD/C_{14}PyBr systems

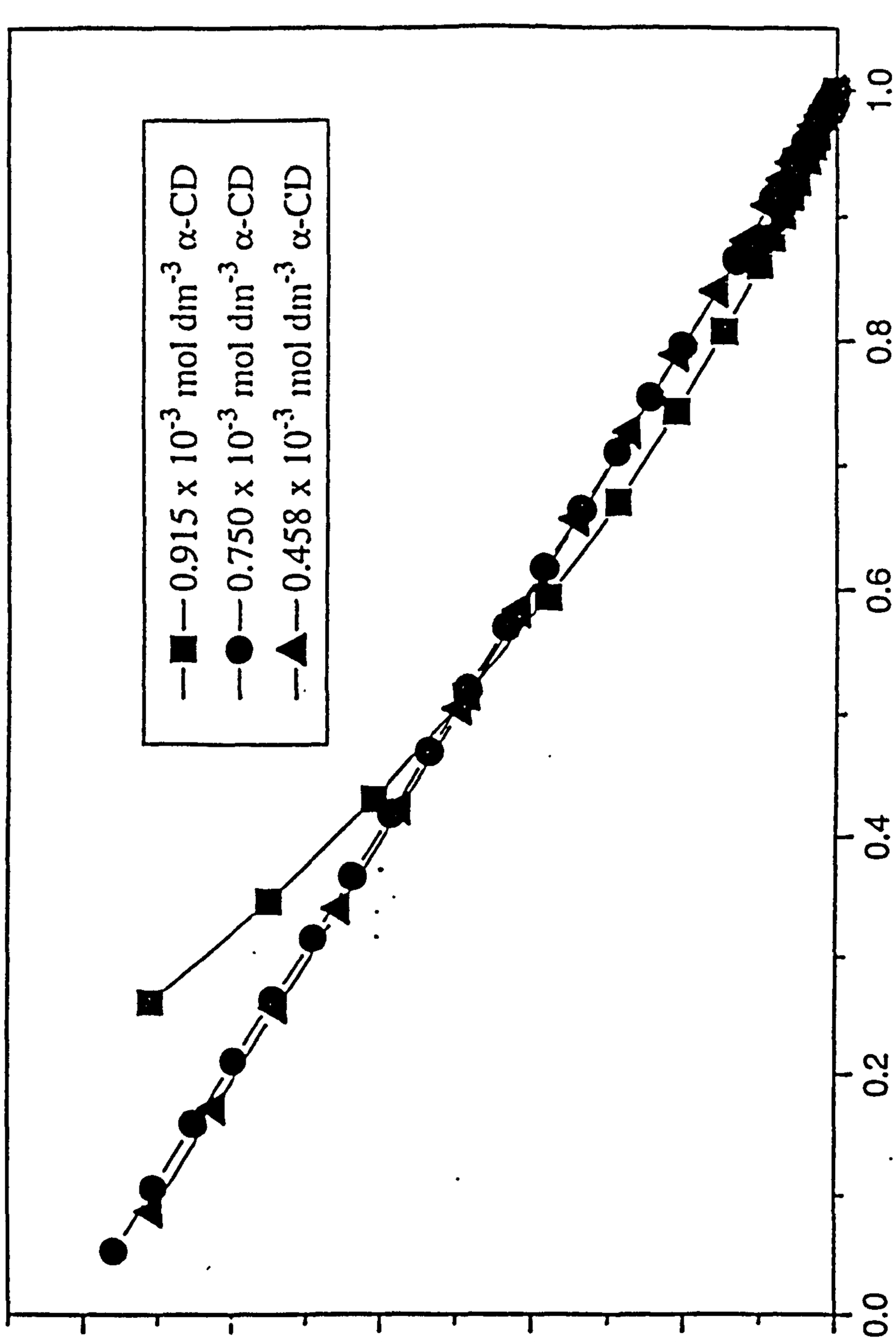

Figure 6-19: Scatchard Isotherms for β-CD/C_{14}PyBr systems

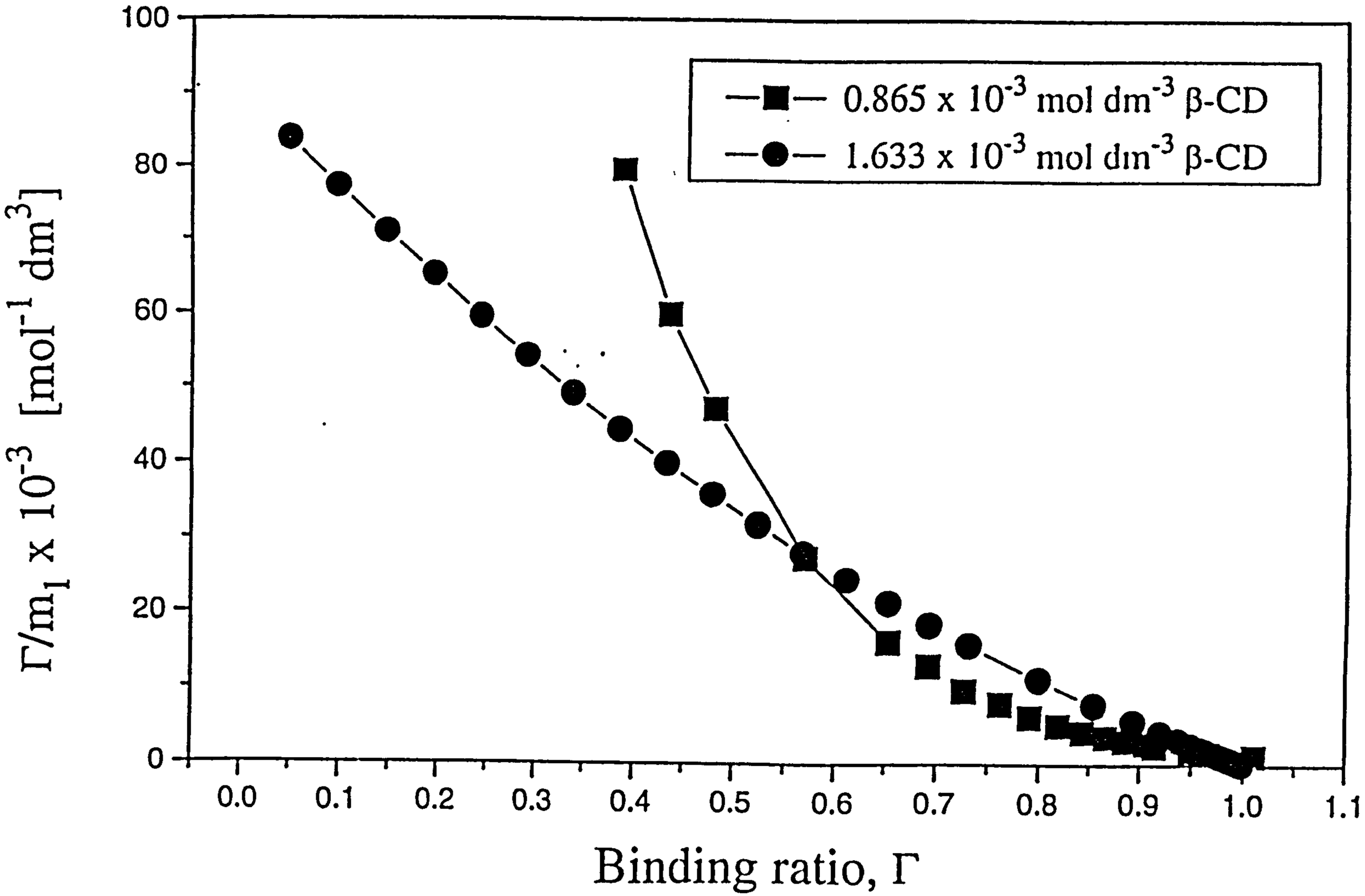

Figure 6-20: Scatchard Isotherm for α-CD/C_{16}PyBr systems

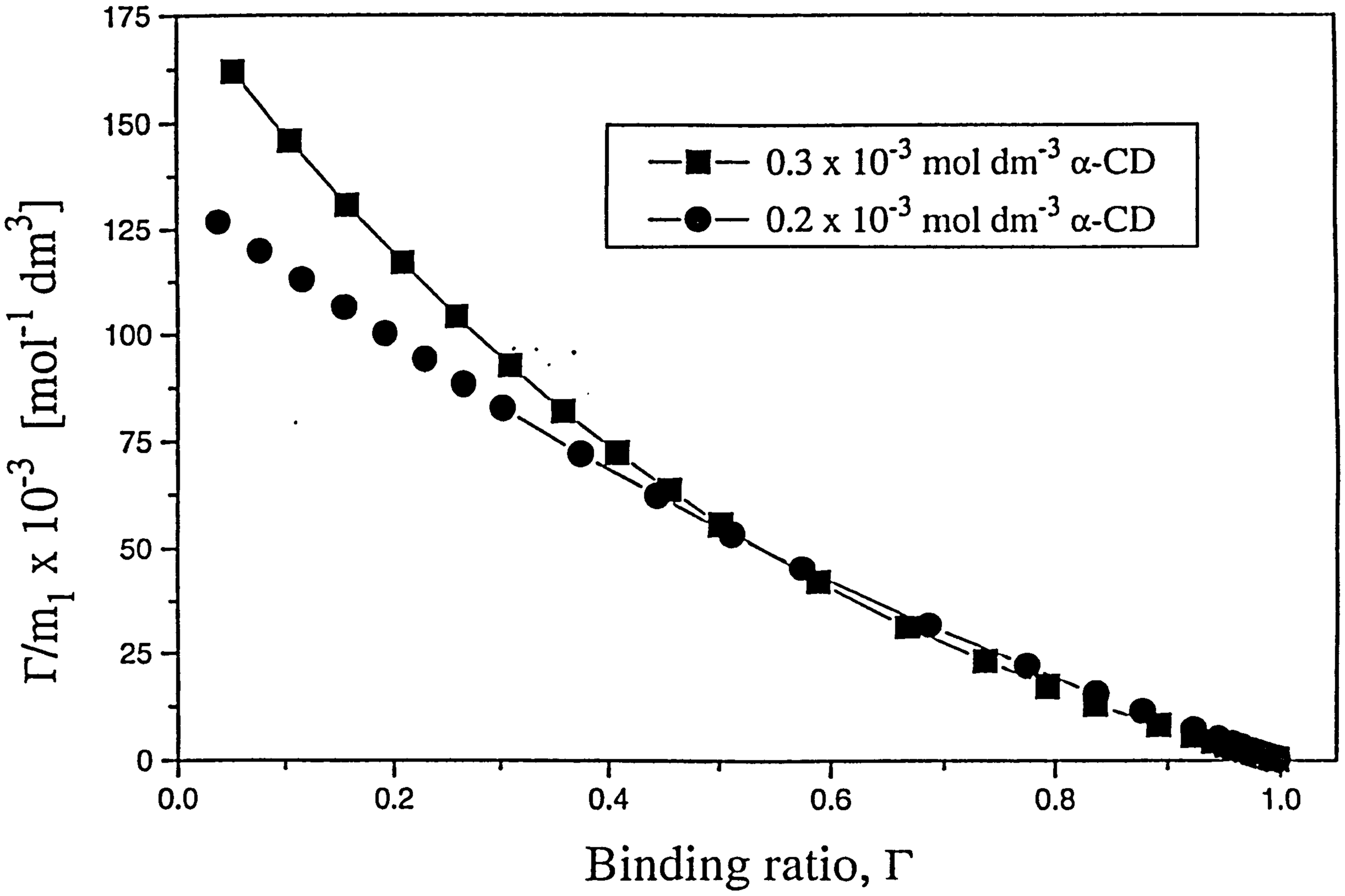

Figure 6-21: Scatchard Isotherm for β-CD/C_{16}PyBr systems

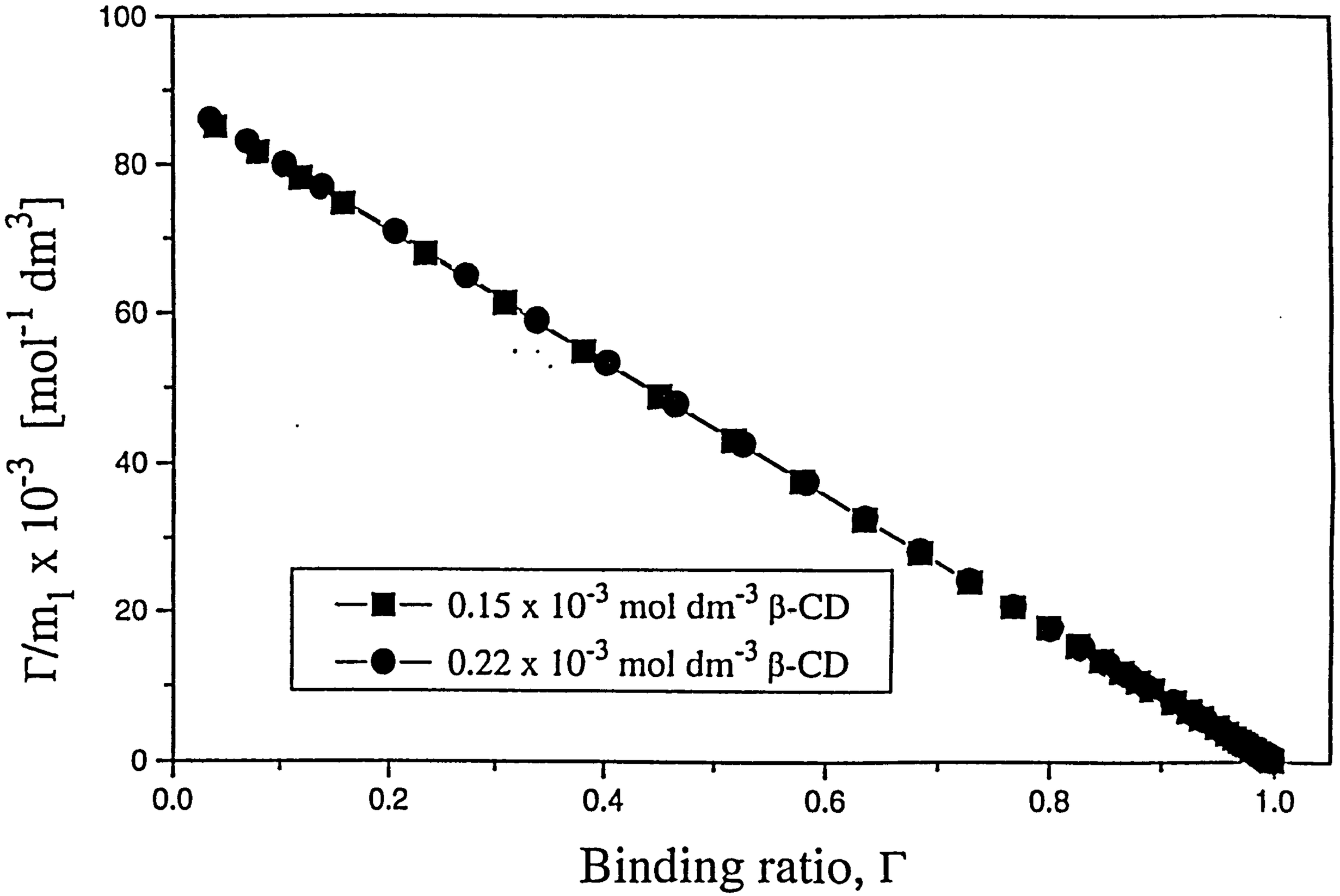

Figure 6-22: Scatchard Isotherm for α-CD/C_{14}TAB systems

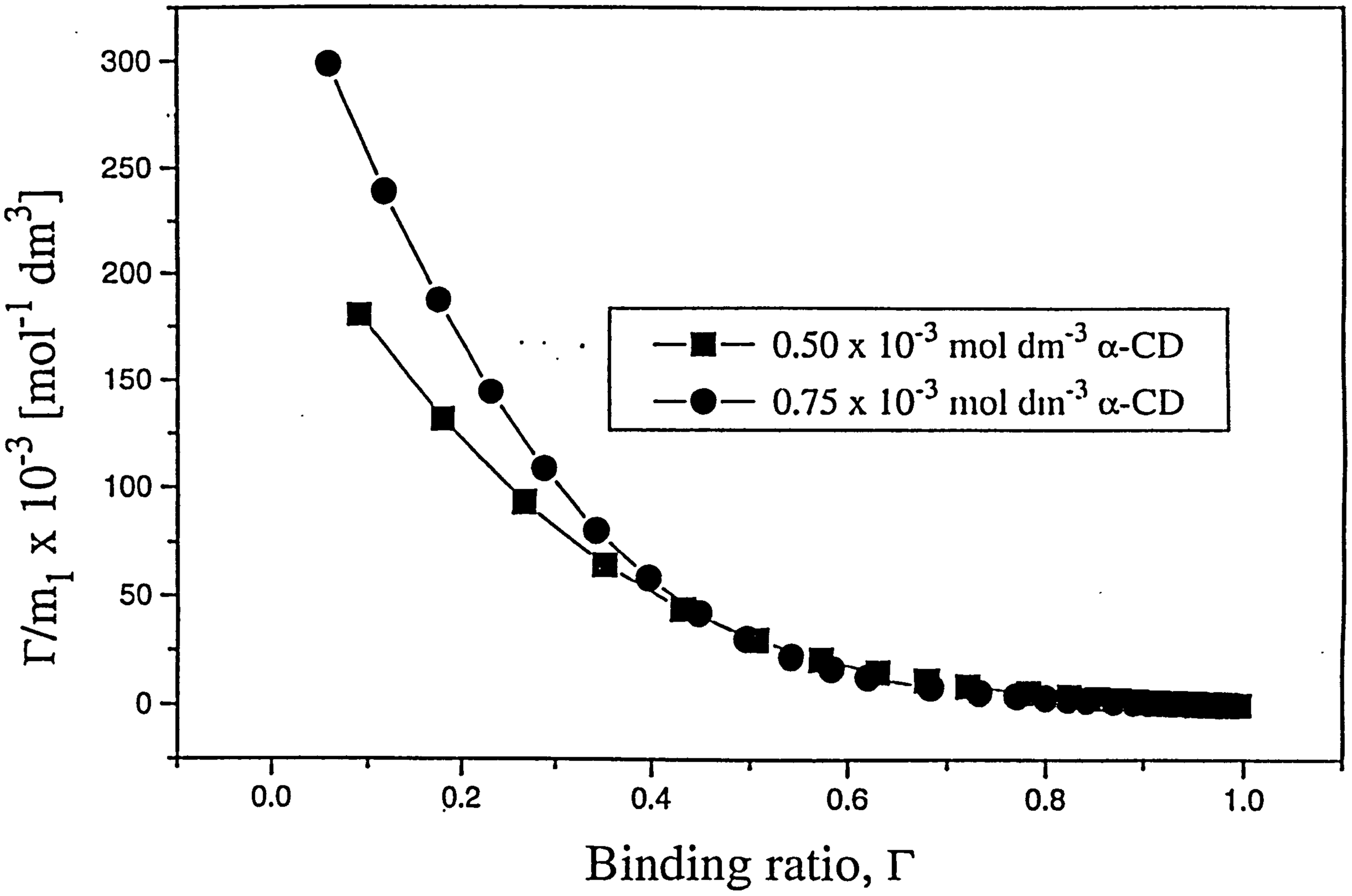

Figure 6-23: Scatchard Isotherm for β-CD/C_{14}TAB systems

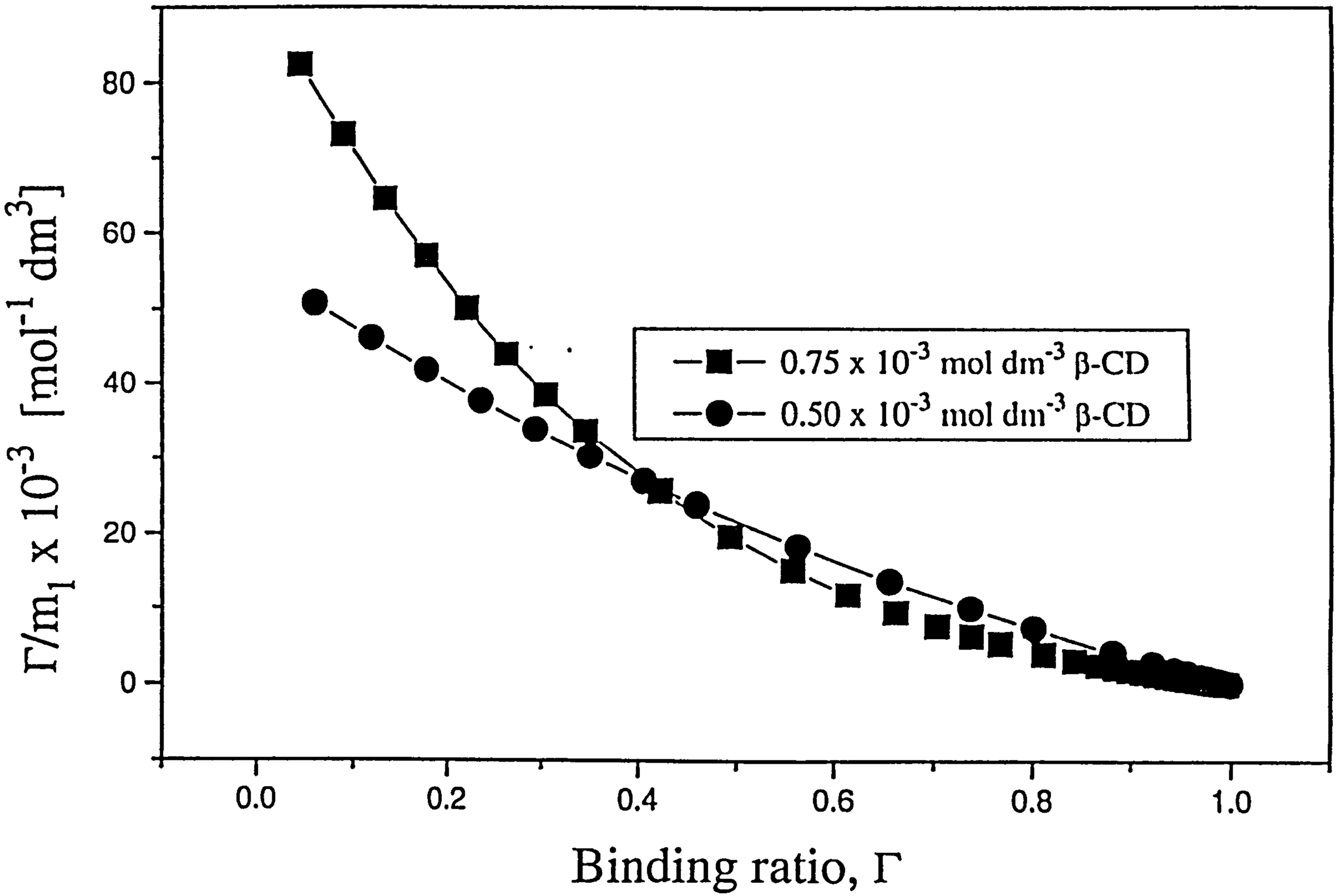

electrode. In schemes (1) and (2) let m_c be the monomer (i.e. uncomplexed) concentration of cyclodextrin, m′ and m˜ be the equilibrium concentrations of complexes S(CD) and $(S(CD)_2$ respectively. Therefore

$$K_1 = m'/m_1m_c,\ K_2 = m\tilde{}/m_cm',\ K_1K_2 = m\tilde{}/m_1m_c^2 \qquad (6\text{-}2)$$

Since $C_1 - m_1 = m' + m\tilde{}$ and $C_c - m_c = m' + 2m\tilde{}$ then

$$m' = 2(C_1-m_1) - (C_c-m_c) \qquad (6\text{-}3)$$

$$m\tilde{} = (C_c-m_c) - (C_1-m_1) \qquad (6\text{-}4)$$

Algebraic manipulation of equations (6-2), (6-3) and (6-4) lead to the following cubic equation in m_c[1,16-18]

$$m_c^3K_1K_2 + m_c^2(K_1+2K_1K_2C_1-K_1K_2C_c) + m_c(K_1C_1-K_1C_c+1) - C_c = 0 \qquad (6\text{-}5)$$

and m_1 follows from the equation

$$m_1 = \left(\frac{C_c-C_1-m_c}{K_1K_2m_c^2-1}\right) \qquad (6\text{-}6)$$

The value m_c is obtained from an iterative least mean squares computer fitting program using K_1 and K_2 as adjustable parameters. The 'goodness-of-fit' between values m_1 calculated from equation (6-6) using m_c value from equation (6-5) and the measured m_1 value (denoted as M_1) is tested using a least-squares procedure. The sum of squares of residuals (SS) is minimized[19]:

$$SS = \Sigma[(m_1-M_1)/m_1]^2 \qquad (6\text{-}7)$$

where m_1 is the monomer concentration calculated through equations (6-5) and (6-6) and M_1 is the experimental concentration of surfactant monomeric species obtained from EMF data ($M_1 = 10\exp[(E-E^o)/slope]$). The acceptable limit of the value SS in equation (6-7) depends on the nature of data and concentration range studied. It is important, however, to note that the value SS, whatever its magnitude, should correlate to the computer fitted plot of m_1 and M_1 versus C_1. Nevertheless in this work the limit of $0.0000 \leq SS \leq 0.0050$ correlate well with goodness-of-fit in most systems.

6.4 RESULTS

The results are listed in Table 6.4 for 1-alkyltrimethyl-ammonium bromides and Table 6-5 for 1-alkylpyridinium bromides and the computer fit plots comparing the measured and calculated monomer surfactant concentration are shown in Figures 6-24 to 6-33.

Table 6.4 Summary of binding constant K_1 and K_2 tetradecyl-trimethylammonium bromide (C_{14}TAB) to α- and ß-CDs

	CD	[CD]	$K_1/mol^{-1}dm^3$	mean±σ	$K_2/mol^{-1}dm^3$	mean±σ
C_{14}	α-CD	0.50	62030		6290	
				60700±1900		6900±860
		0.75	59290		7510	
	ß-CD	0.50	38230		3250	
				39750±2140		3060±280
		0.75	41260		2860	

Complexation constants K_1 and K_2 for the inclusion complexes of 1-alkylpyridinium bromides (C_nPyBr) to both α- and ß-

cyclodextrins are summarized in Table 6.4.

Table 6.5: Summary of binding constants for the inclusion complexes between 1-alkylpyridinium bromides with α- and ß-cyclodextrins derived from Equation (6-1) and the cubic equation (6-5)

			Scatchard Equation (6-1)			Cubic Equation (6-5)			
C_n	CD	[CD]	K_{slope}	K_{inter}	mean±std	K_1	mean±std	K_2	mean±std
		M	M^{-1}	M^{-1}	M^{-1}	M^{-1}	M^{-1}	M^{-1}	M^{-1}
C_{10}	α	0.915	7150	7150	8190±1040	7150	8190±1040	-	-
		2.196	9230	9230		9230		-	
	ß	1.038	3810	3810		3810		-	
		2.196	3720	3720	3740± 50	3720	3740± 50	-	-
		3.114	3690	3690		3690		-	
C_{12}	α	0.458	48100	48100		48100		1	
		0.686	45630	44490	46340±1300	41970	44200±2700	680	310±280
		0.915	46200	45500		42640		260	
	ß	0.433	26640	26640		26640		-	
		0.649	23620	23620	24920±1270	23620	24900±1300	-	-
		0.865	24500	24500		24480		-	
C_{14}	α	0.458	99020	99020		99010		0.09	
		0.915	15760	111840	106700±7520	100340	99700± 660	550	280±270
	ß	0.865	72040	70800		67240		400	
		1.633	89370	83150	78840±7750	65410	66300± 900	1250	830±420
C_{16}	α	0.200	12650	111240		109100		1140	
		0.300	13190	111620	112070±1580	111030	110070± 970	2050	1600±460
	ß	0.150	88610	88610		88600		0.9	
		0.220	89130	89120	88860± 256	89100	88850± 250	2.2	1.5±0.6

M = mol dm^{-3}, M^{-1} = mol^{-1} dm^3

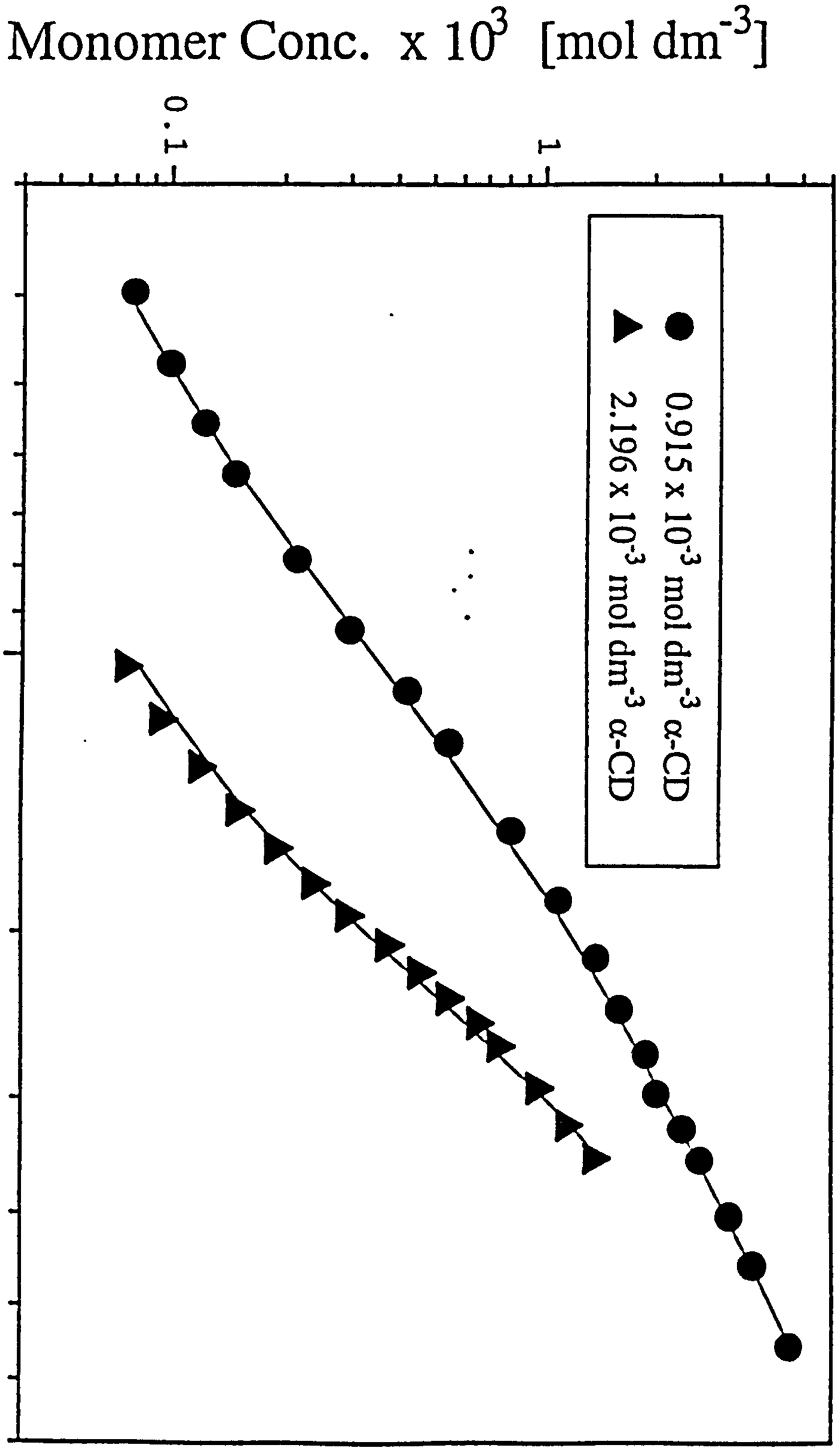

Figure 6-24: Computer fit plots for K_1 and K_2 in α-CD/C_{10}PyBr systems

Figure 6-25: Computer fit plots for K_1 and K_2 in β-CD/C_{10}PyBr systems

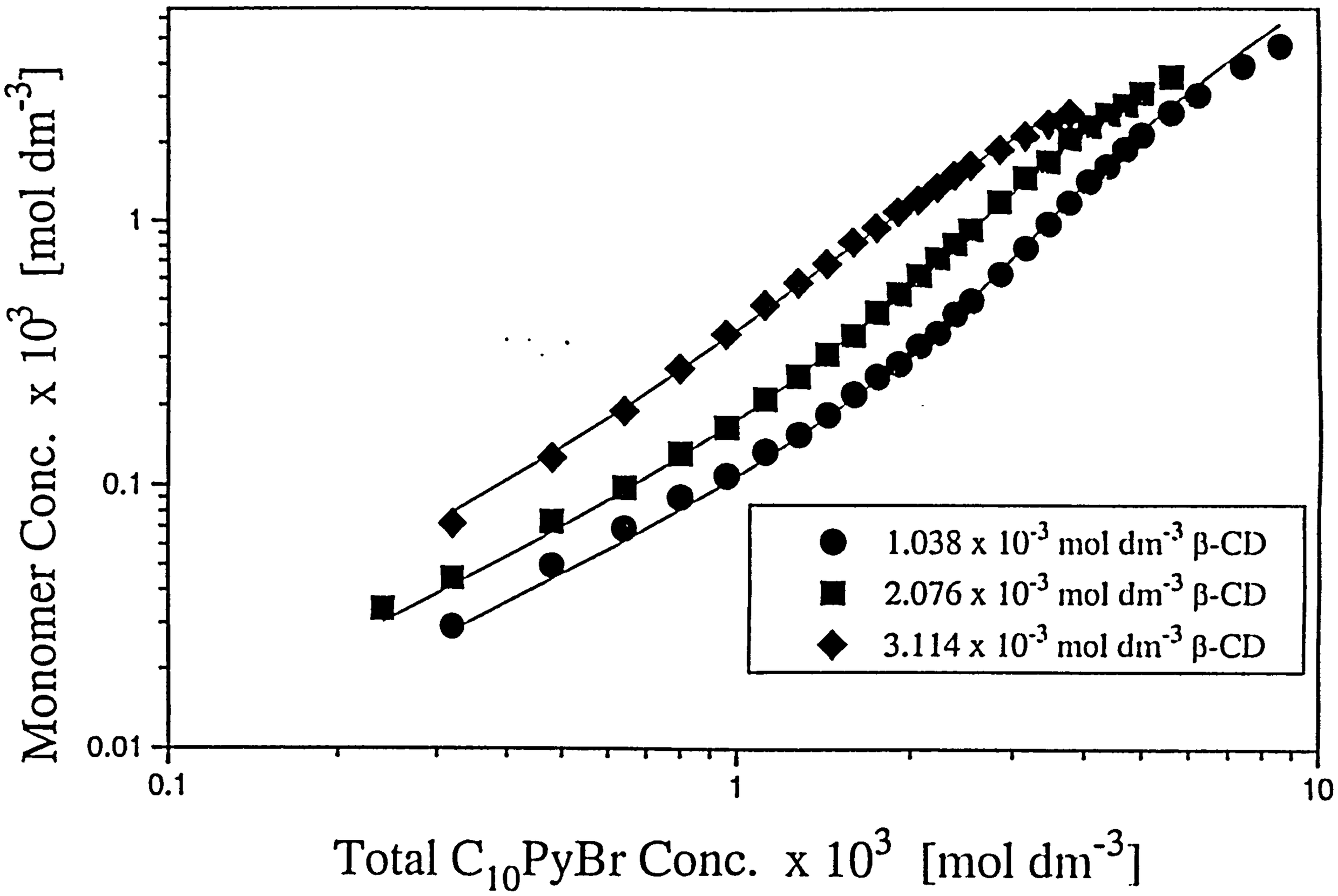

Figure 6-26: Computer fit plots for K_1 and K_2 in α-CD/C_{12}PyBr systems

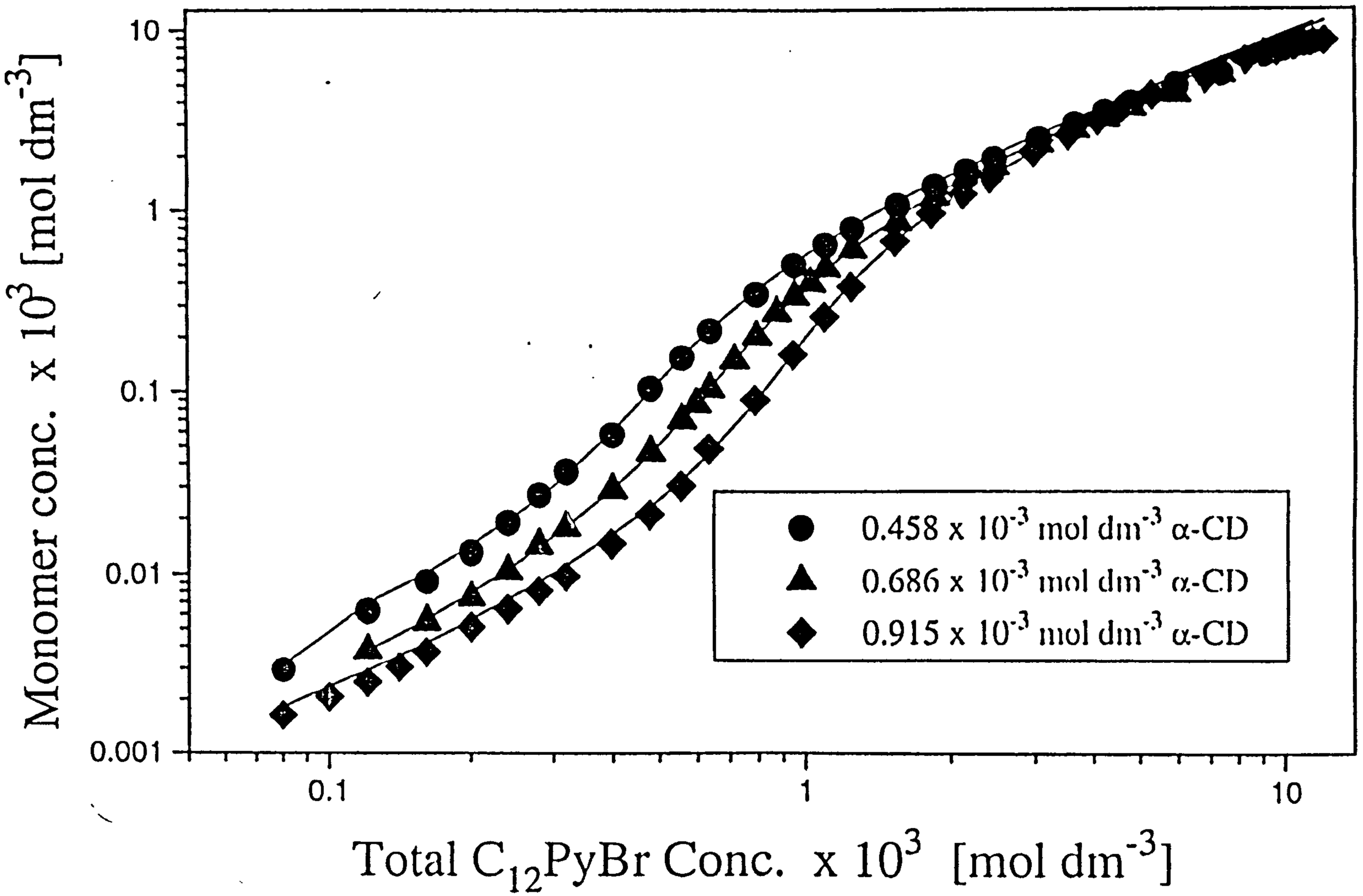

Figure 6-27: Computer fit plots for K_1 and K_2 in β-CD/C_{12}PyBr systems

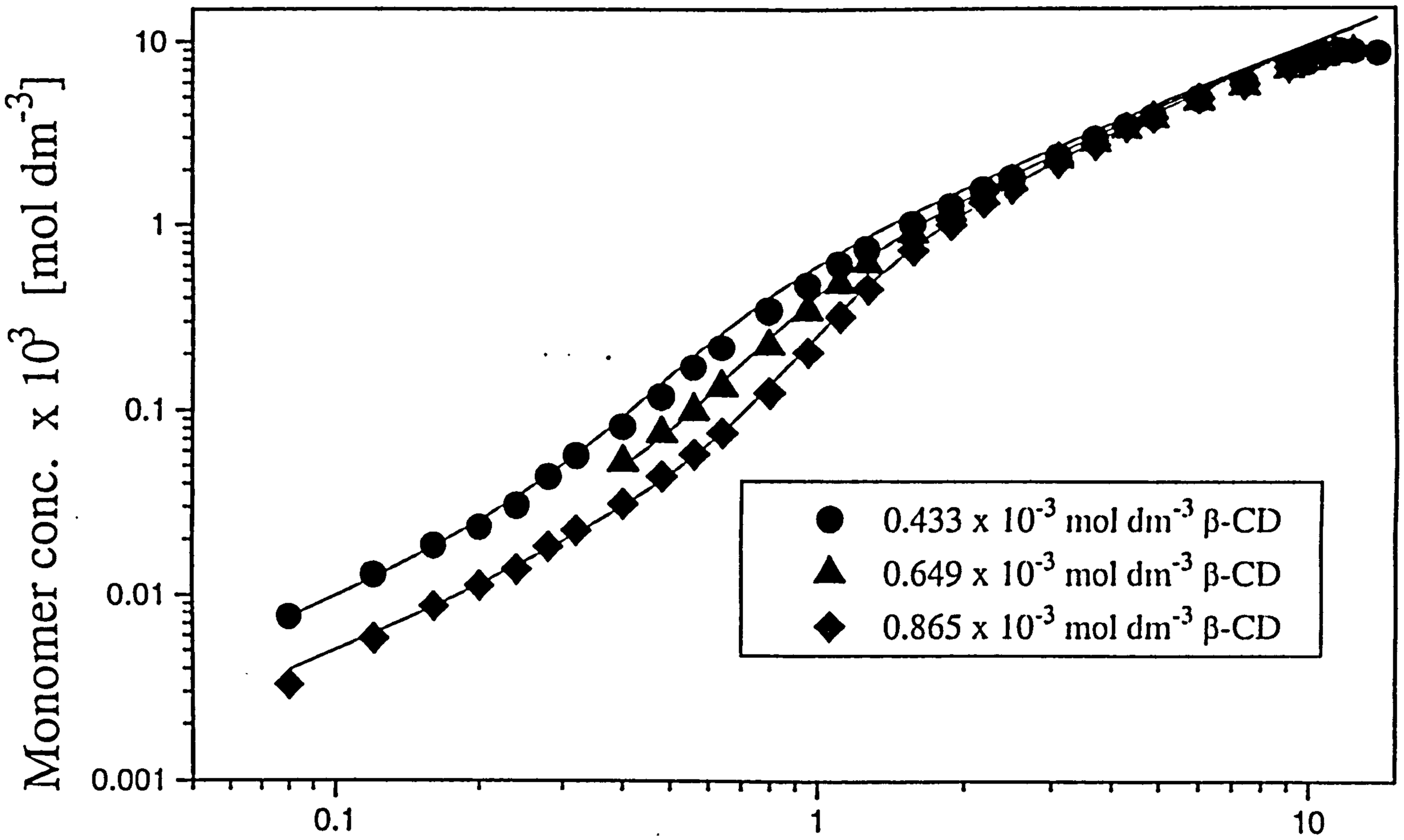

Figure 6-28: Computer fit plots for K_1 and K_2 in α-CD/C_{14}PyBr systems

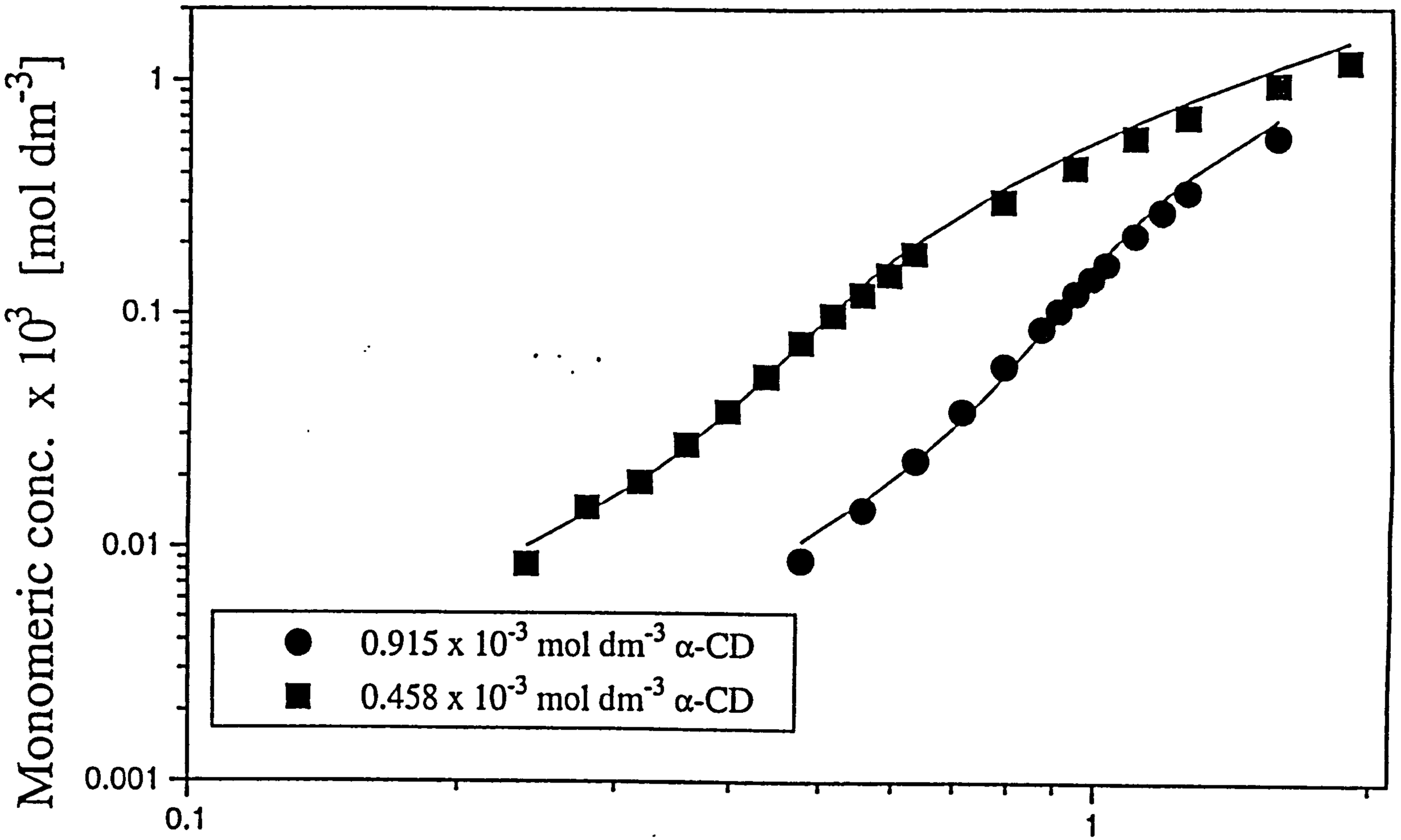

Figure 6-29: Computer fit plots for K_1 and K_2 in β-CD/C_{14}PyBr systems

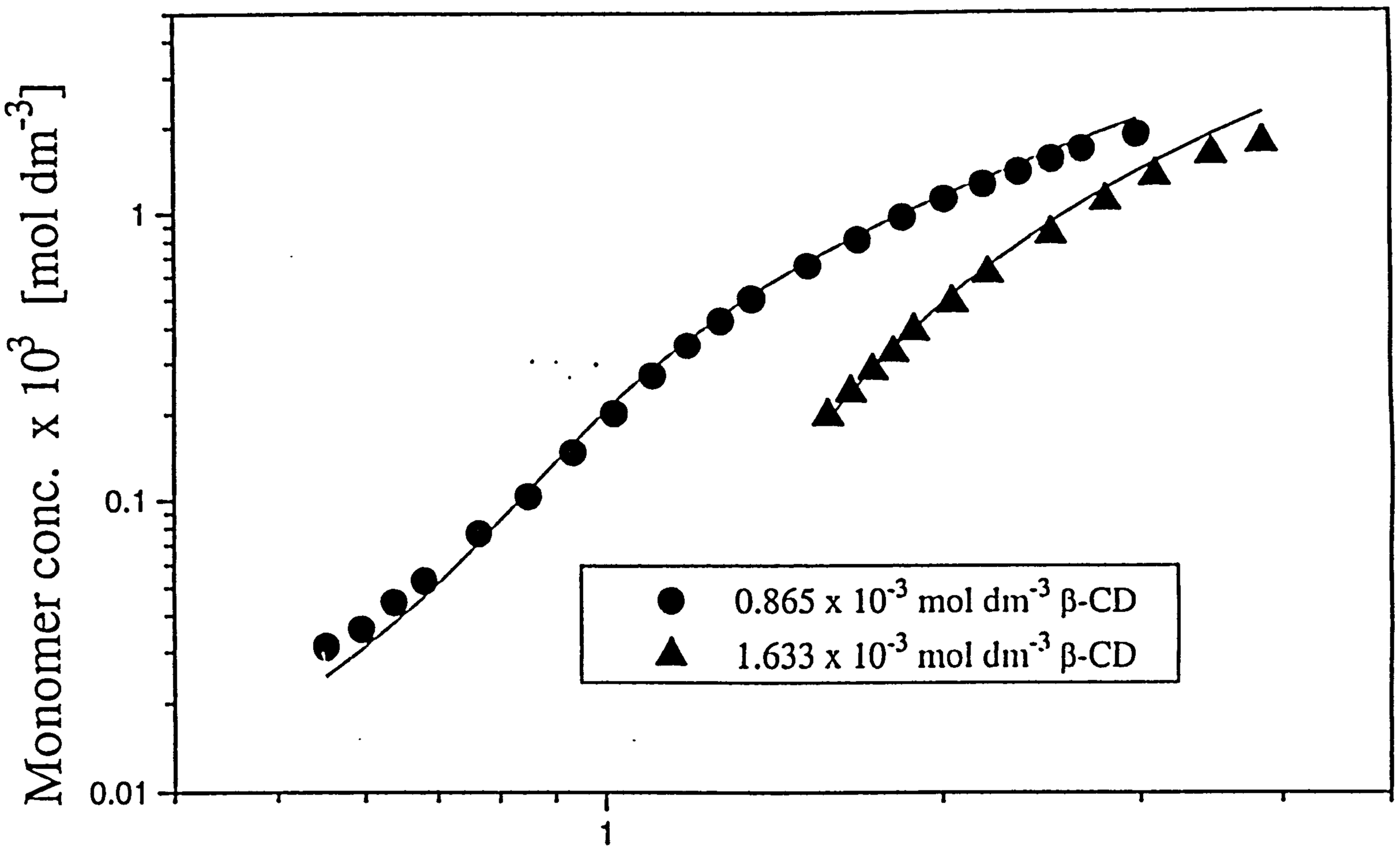

Figure 6-30: Computer fit plots for K_1 and K_2 in α-CD/C_{16}PyBr systems

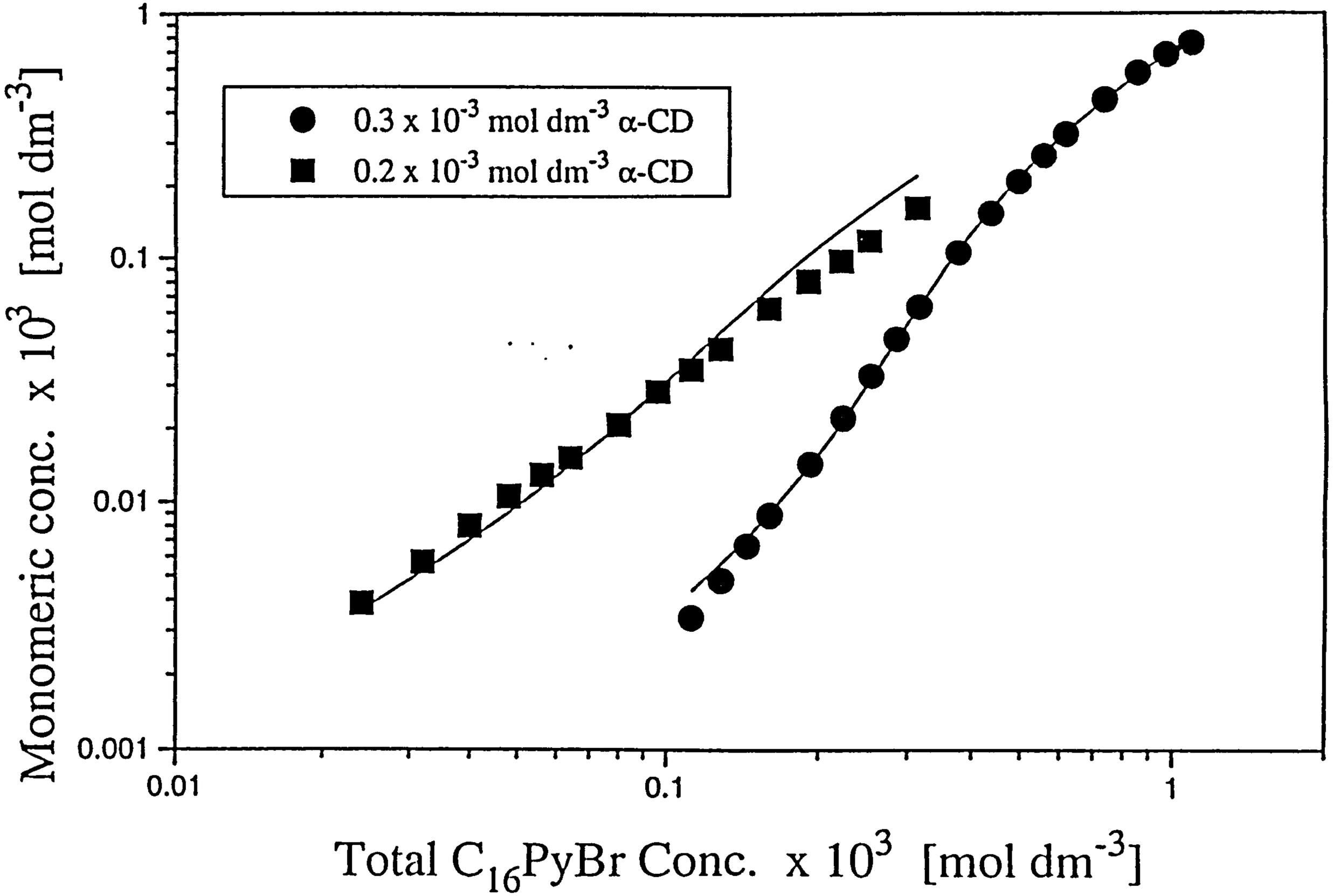

Figure 6-32: Computer fit plots for K_1 and K_2 in α-CD/C_{14}TAB systems

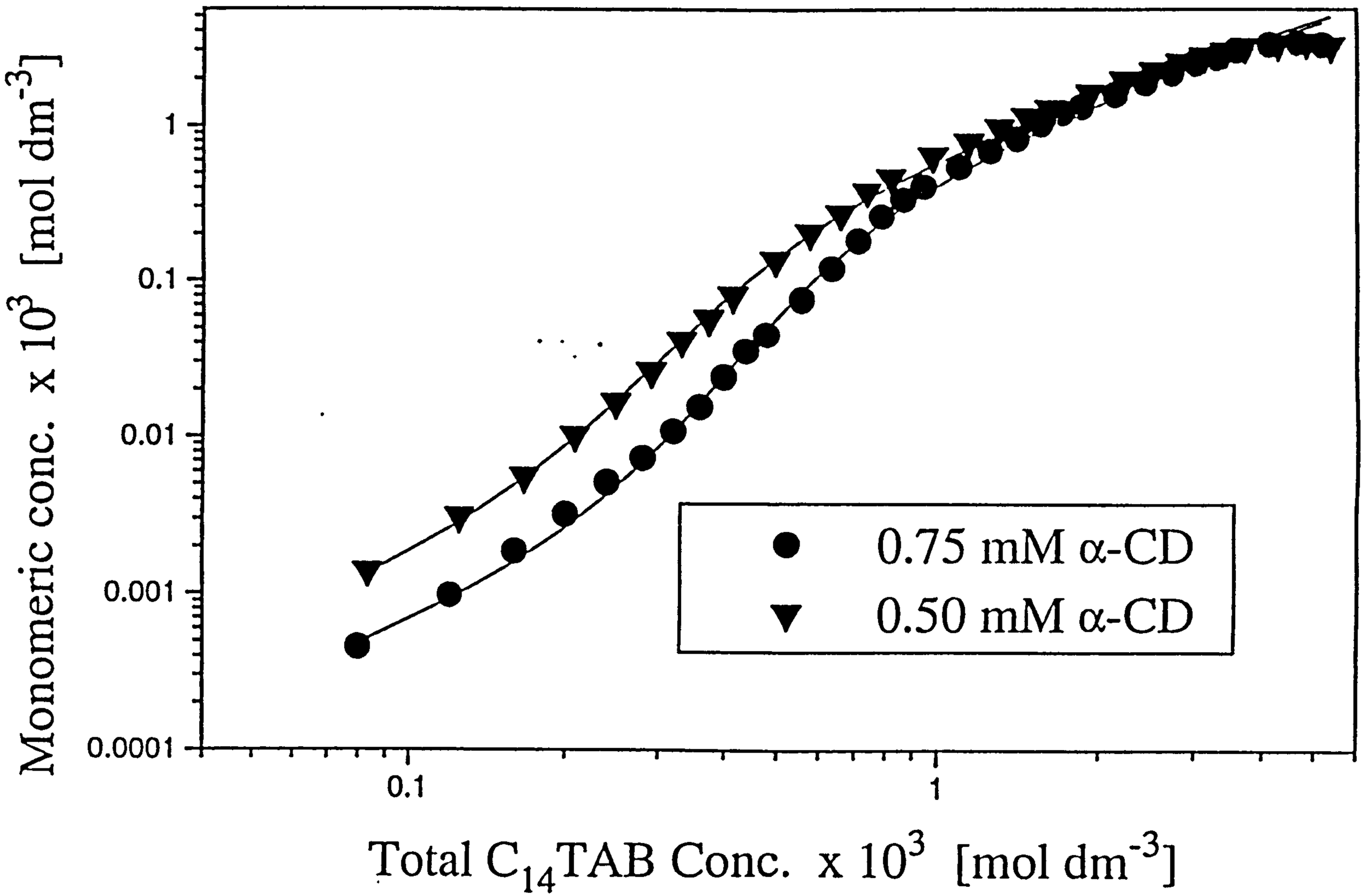

Figure 6-33: Computer fit plots for K_1 and K_2 in β-CD/C_{14}TAB system

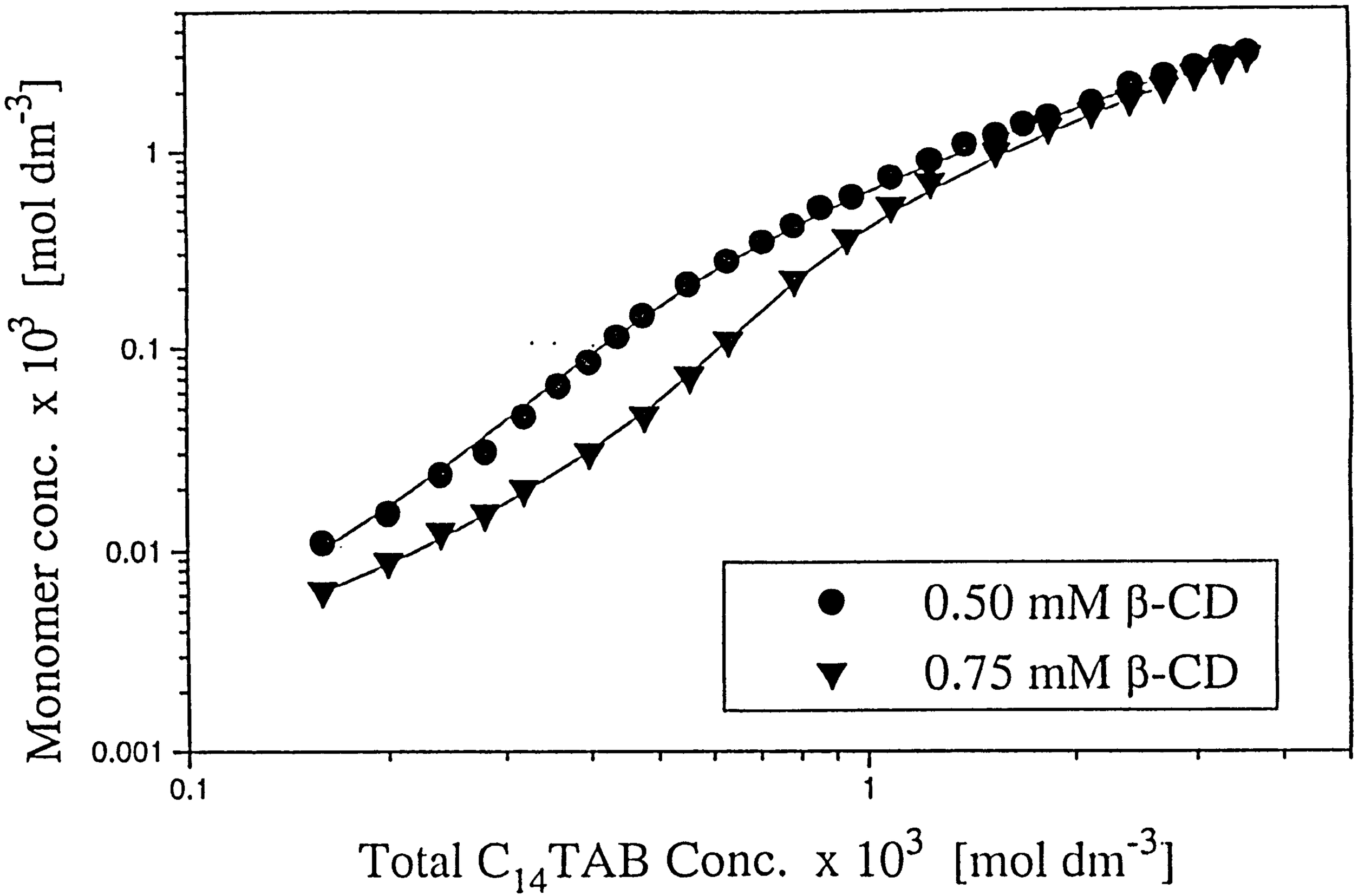

6.4.1 Decylpyridinium bromide ($C_{10}PyBr$)

α-CD/$C_{10}PyBr$

Both computer fitting of the cubic equation (6-5) and the Scatchard plots gave the same K_1 of magnitude 8190 mol^{-1} dm^3 for the system α-CD/$C_{10}PyBr$. The computer fit plots are shown in Figure 6-24 and the Scatchard plots in Figure 6-14.

ß-CD/$C_{10}PyBr$

The Scatchard plots for this system, shown in Figure 6-15, are linear and give average K_1 of magnitude 3740 mol^{-1} dm^3. The computer fit plots shown in Figure 6-25 give K_1 of the same magnitude as the Scatchard plots.

6.4.2 Dodecylpyridinium bromide ($C_{12}PyBr$)

α-CD/$C_{12}PyBr$

The Scatchard plots, Figure 6-16, are slightly curved giving an estimated K_1 of 46340 mol^{-1} dm^3. The computer fitting plots for the system α-CD/$C_{12}PyBr$ are shown in Figure 6-26 giving average K_1 and K_2 of magnitudes 44200 and 310 mol^{-1} dm^3 respectively.

ß-CD/$C_{12}PyBr$

The Scatchard plots shown in Figure 6-17 for this system are linear with an average K_1 of magnitude 24920 mol^{-1} dm^3. The computer fit plots in Figure 6-27 give K_1 of an average

magnitude of 24900 mol^{-1} dm^3.

6.4.3 Tetradecylpyridinium bromide ($C_{14}PyBr$)

α-CD/$C_{14}PyBr$

The Scatchard plots in Figure 6-18 are curved, consequently only an estimate K_1 of magnitude 106700 mol^{-1} dm^3 can be obtained. The computer fitting of the cubic equation for α-CD/$C_{14}PyBr$ system give average K_1 and K_2 of magnitudes 99700 and 280 mol^{-1} dm^3 respectively. The computer fit plots are shown Figure 6-28.

ß-CD/$C_{14}PyBr$

The average K_1 from the Scatchard plots, Figure 6-19, is 78840. The Scatchard plots are slightly curved. The average K_1 and K_2 for the system ß-CD/$C_{14}PyBr$ from the computer fitting of the cubic equation are 66300 and 830 mol^{-1} dm^3. The plot is shown in Figure 6-29.

6.4.4 Cetylpyridinium bromide ($C_{16}PyBr$)

α-CD/$C_{16}PyBr$

The Scatchard plots of this system in Figure 6-20 show curvatures with average K_1 of magnitude 112070 mol^{-1} dm^3. The computer fitting plots in Figure 6-30 for the system α-CD/$C_{16}PyBr$ give average K_1 and K_2 of magnitudes 110000 and 1600 mol^{-1} dm^3 respectively.

ß-CD/C_{16}PyBr

The Scatchard plots shown Figure 6-21 are linear and give average K_1 of magnitude 88860 mol^{-1} dm^3. The computer fitting plots for the system ß-CD/C_{16}PyBr are shown in Figure 6-31 with K_1 of average magnitude of 88850 mol^{-1} dm^3.

6.4.5 Tetradecyltrimethylammonium Bromide (C_{14}TAB)

α-CD/C_{14}TAB

The Scatchard plots in Figure 6-22 for this system shows pronounced curvatures and therefore cannot be applied. The Computer fitting plots, Figure 6-32, give average K_1 and K_2 of magnitudes 60700 and 6900 mol^{-1} dm^3.

ß-CD/C_{14}TAB

The Scatchard plots, Figure 6-23, show curvature and therefore cannot be used. The computer fitting of the cubic equation give average K_1 and K_2 of magnitudes 39750 and 3060 mol^{-1} dm^3.

A full discussion of these data will be given in Chapter 8 after considering the ITC measurements. For the sake of consistency a comparison of the independent data on both C_{14}TAB and C_{16}TAB is given in the following Table 6.6, agreement shows consistency for the experimental techniques under category (a).

Table 6.6: Equilibrium constants K_1 and K_2 (mol^{-1} dm^3) for $C_{14}TAB$ and $C_{16}TAB$ interactions with α- and ß-cyclodextrins

C_nTAB	CD	This work		Literature work		
		K_1	K_2	K_1	K_2	
$C_{14}TAB$	α-	61000	6900	42980 ±1440	3130 ±790	(ref. 20)
	ß-	39750	3060	39811	56	(ref. 1)
				44000	118	(ref. 3)
				51150 ±1260	-	(ref. 20)
$C_{16}TAB$	α-	99200	20400	-	-	
	ß-	67700	9600	70790	126	(ref. 1)
				59800	390	(ref. 3)

6.5 REFERENCES

1. JEZEQUEL, D.; MAYAFFRE, A. and LETELLIER, P. *Can. J. Chem.*, 69 (1991) 1865.

2. PALEPU, R.; RICHARDSON, J.E. and REINSBOROUGH, V.C. *Langmuir*, 5 (1989) 218.

3. PARK, J.W. and PARK, K.H. *Langmuir* (1994) In Press.

4. SHELTON, R.S.; VAN CAMPEN, M.G.; TILFORD, C.H.; LANG, H.C.; NISONGER, L.; BENDELIN, F.J. and RUBENKOENIG, H.L. *J. Am. Chem. Soc.*, 68 (1946) 755.

5. KOLLOFF, H.G.; WYSS, A.P.; HIMELICK, R.E. and MANTELE, F. *J. Am. Pharm. Assoc. Sci. Ed.*, 31 (1942) 51.

6. KNIGHT, G.A. and SHAW, B.D. *J. Chem. Soc.*, (1938) 682.

7. GHARIBI, H.; PALEPU, R.; BLOOR, D.M.; HALL, D.G. and WYN-JONES, E. *Langmuir*, 8 (1992) 782.

8. SHIRAHAMA, K.; OHISHI, M. and TAKISAWA, N. *Colloids Surf.*, 40 (1989) 261.

9. WAN-BADHI, W.A. *PhD Thesis*, University of Salford (1993)

10. PALEPU, R.; HALL, D.G. and WYN-JONES, E. *J. Chem. Soc. Faraday Trans. 1*, 86 (1990) 1535.

11. BREUSCH, F.L. and HERSEK, S. *Hoppe-Seylers Z. Physiol. Chem.*, 291 (1952) 1.

12. MYERS, D. "*Surfaces, Interfaces and Colloids: Principles and Applications*", VCH Publishers, New York (1991).

13. MYERS, D. "*Surfactant Science and Technology*", VCH Publishers, New York (1988).

14. ROSEN, M.J. "*Surfactants and Interfacial Phenomena*", 2nd Ed, John Wiley & Sons, New York (1989).

15. SCATCHARD, G. *Ann. N.Y. Acad. Sci.*, 51 (1949) 660.

16. WAN-YUNUS, W.M.Z.; TAYLOR, J.; BLOOR, D.M.; HALL, D.G. and WYN-JONES, E. *J. Phys. Chem.*, 96 (1992) 8979.

17. PARK, J.W. and SONG, H.J. *J. Phys. Chem.*, 93 (1989)6454.

18. LUKAS, T.M., *PhD. Thesis*, University of Salford (1991).

19. CONNORS, K.A. "*Binding Constants: The Measurements of Molecular Complex Stability*", John Wiley & Sons, New York (1987).

20. TOMINAGA, T.; HACHISU, D. and KAMADO, M. *Langmuir* (1994) In Press.

CHAPTER SEVEN: THE OMEGA ISOTHERMAL TITRATION CALORIMETRY (ITC) STUDIES ASSOCIATED WITH CYCLODEXTRIN/ SURFACTANTS INCLUSION COMPLEXES

7.1 INTRODUCTION

The ITC technique essentially measures directly the energetics (enthalpy changes) associated with the binding of ligands to macromolecules at constant temperature. In favourable conditions, enthalpies can be measured at different molar ratios leading to enthalpy profiles which in turn can be analysed to produce binding constants and the stoichiometry associated with the process in question. As a result of a link between the group at Salford and the Physical Chemistry Department, Fritz-Haber-Institut, Berlin we were able to use their ITC technique to carry out preliminary work on cyclodextrin/surfactant inclusion complexes.

Table 7.1 ITC, EMF and FP Results for ß-CD inclusion complexes with dodecyltrimethylammonium bromide and dodecylpyridinium bromide systems

	ITC	EMF	FP
C_{12}TAB	23700	18100[1], 17795[2]	22100[3]
C_{12}PyBr	18700	24900[4]	-

In the preliminary work the complexation constants of the 1:1 inclusion complex of C_{12}TAB and C_{12}PyBr with ß-CD were determined. These results are compared with emf[1,2,4] and Fluorescence-Probe (FP)[3] data in Table 7.1. The agreement between the ITC and the other independent methods were so encouraging that the author visited the Fritz-Haber-

Institut Laboratories, Berlin, Germany to carry out an extensive study of surfactant/cyclodextrin complexes. The surfactant inclusion complexes with both α- and ß-cyclodextrins studied by ITC in this work include: 1-alkyltrimethylammonium bromides (C_8, C_{10}, C_{12}, C_{14} and C_{16}TAB), 1-alkylpyridinium bromides (C_{12}, C_{14} and C_{16}PyBr), sodium 1-alkylsulfates (C_6, C_8, C_{10}, C_{12} and $C_{14}OSO_3Na$) and sodium 1-alkanesulfonates (C_8, C_{10}, $C_{12}SO_3Na$). In this chapter, we wish to present a summary of Omega ITC working theory, experimental procedures and a description of the results. A discussion of these results together with results from electrochemical work in Chapter 6 is given in Chapter 8.

7.2 WORKING THEORY OF THE OMEGA ITC

The target for the design and functional improvement of an isothermal titration calorimeter (ITC) was to attain a calorimeter of high sensitivity[5] and which can use small amounts of material. Two of the most critical aspects of high sensitivity titration microcalorimeters have been (i) the design of efficient, low-energy stirring mechanism, and (ii) the provision of a low-volume, thermally equilibrated injection system. The newly designed ITC still incorporates some features found in other commercial microcalorimeters[6-8]. They include: (i) the adiabatic shielding, (ii) the differential heat detection, and (iii) the slow thermal scanning for examination of the thermal process. In recent years, the ITC has been developed to include: (i) the use of combined titration and stirring assembly, (ii) a

reaction cell made of metal (Hastelloy-C alloy), (iii) a small sample volume (1.3575 ml for the cell used for this work); (iv) elimination of gas space in the reaction cell; and (v) computer automation and data collection.

In this section we wish to discuss how these new features have improved performance of the Omega ITC calorimeter as compared to other microcalorimeters. Also theoretical and experimental aspects in relation to similarities and differences between an ITC and heat conduction calorimeters are described.

7.2.1 General Principles of Calorimeters

Calorimeters are generally classified into two groups: (i) adiabatic calorimeters, and (ii) heat-conduction calorimeters. The main difference between them, is that, in adiabatic calorimeters there is no heat exchange between the calorimeter cell and the surroundings.

The heat quantity Q released from the system or absorbed into the system gives rise to a temperature change ΔT which is proportional to the heat capacity of the calorimeter cell as follows[9]:

$$Q = \epsilon.\Delta T = \epsilon.(T_C - T_B) \qquad (7\text{-}1)$$

where ϵ is the proportionality constant (the calibration constant), T_C and T_B are temperatures in the calorimeter cell and the calorimeter block respectively, and ϵ is

referred to as a practical heat capacity value for the overall calorimetric system. Therefore, in an adiabatic calorimeter it is ΔT which is measured.

In an ideal heat-conduction calorimeter, heat is quantitatively transferred from reaction cell to a heat sink and vice versa. The quantity Φ, which is proportional to the heat flow, is measured. Heat-conduction calorimeters involve time integrals which are proportional to the heat quantity Q evolved or absorbed, that is:

$$Q = \text{const.} \int \Phi dt \qquad (7\text{-}2)$$

The quantity Φ is proportional to the heat (P) evolved or absorbed during a chemical process.

Since a thermopile heat-conduction calorimeter was the basis for the construction of the Omega isothermal titration calorimeter (ITC), a brief account of the theory underlying heat flow will help in the understanding of the ITC operation. In a thermopile heat-conduction calorimeter there is a controlled transfer of heat from the calorimeter cell to the surroundings. This is attained by having a thermopile wall between the cell and the surrounding heat sink. For each thermocouple, both voltage (v) and heat flow (dq/dt) are proportional to ΔT between calorimeter walls and the heat sink, that is: $v = k_1 \Delta T$ and $dq/dt = k_2 \Delta T$, where k_1 and k_2 are constants of proportionality respectively. Simple arithmetic leads to $v/k_1 = \Delta T$ and

$(dq/dt)/k_2 = \Delta T$ which implies $v/k_1 = (dq/dt)/k_2$ and finally the following equation is obtained:

$$v = c\left(\frac{dq}{dt}\right) \qquad (7\text{-}3)$$

where $k_2/k_1 = c$. However, in a real practical situation a number of thermocouples are used and equation (7-3) can be rewritten as $v_1 + v_2 + v_3 + \ldots = c(dq_1/dt) + c(dq_2/dt) + c(dq_3/dt) + \ldots$ and we know $V = v_1 + v_2 + v_3 + \ldots$ and $Q = q_1 + q_2 + q_3 + \ldots$, therefore, equation (7-3) becomes

$$V = c\left(\frac{dQ}{dt}\right) \qquad (7\text{-}4)$$

where V is the thermopile voltage and dQ/dt is the total heat flow through a thermopile.

In this derivation it has been assumed that all heat outlets or inlets are through a thermopile, whereas in a real situation heat passages can be through: (i) air gaps, (ii) mechanical supports between cell and heat sink, (iii) leads to the calibration heater, and (iv) insulation material in the thermopile. There are a number of outlets and inlets other than a thermopile and these change equation (7-3). The values c and dq should include these unrecorded passages of heat. Let dq″/dt be the heat gained or lost through other dissipation mechanism and dq′/dt a normal heat flow through a thermopile. Utilizing these new definitions equation (7-3) becomes,

$$v = c' \left(\frac{dq'' + dq'}{dt}\right) \qquad (7\text{-}5)$$

and equation (7-4) becomes

$$V = c' \left(\frac{dQ}{dt}\right) \qquad (7\text{-}6)$$

where c′ is the effective proportionality constant covering all possible outlets and inlets of heat and dQ = dq″ + dq′. Although it is not possible to cover everything that can take out heat or bring in heat, c′ covers most expectations. To avoid more ways of taking out or letting in heat a wall of the calorimeter cell should have a high thermal conductivity so that there is uniformity.

Integration and rearrangement of equation (7-6) yields a fundamental heat-conduction calorimeter time-integral[8,9],

$$Q = (1/c')\int V dt \qquad (7\text{-}7)$$

where Q is the heat quantity evolved from the reaction cell or absorbed into the reaction cell over a period of time. This concludes that, the surface area under the voltage curve is proportional to heat evolved or absorbed and it is this same principle which is modified to make ITC, a more sensitive and efficient calorimeter.

7.2.2 An ITC Operational Theory

An ITC system consists of a reaction cell (C) and a reference cell (R) surrounded by a calorimeter block (B). A schematic representation is shown in Figure 7-1. The cells are thermally connected to the calorimeter block through thermopiles.

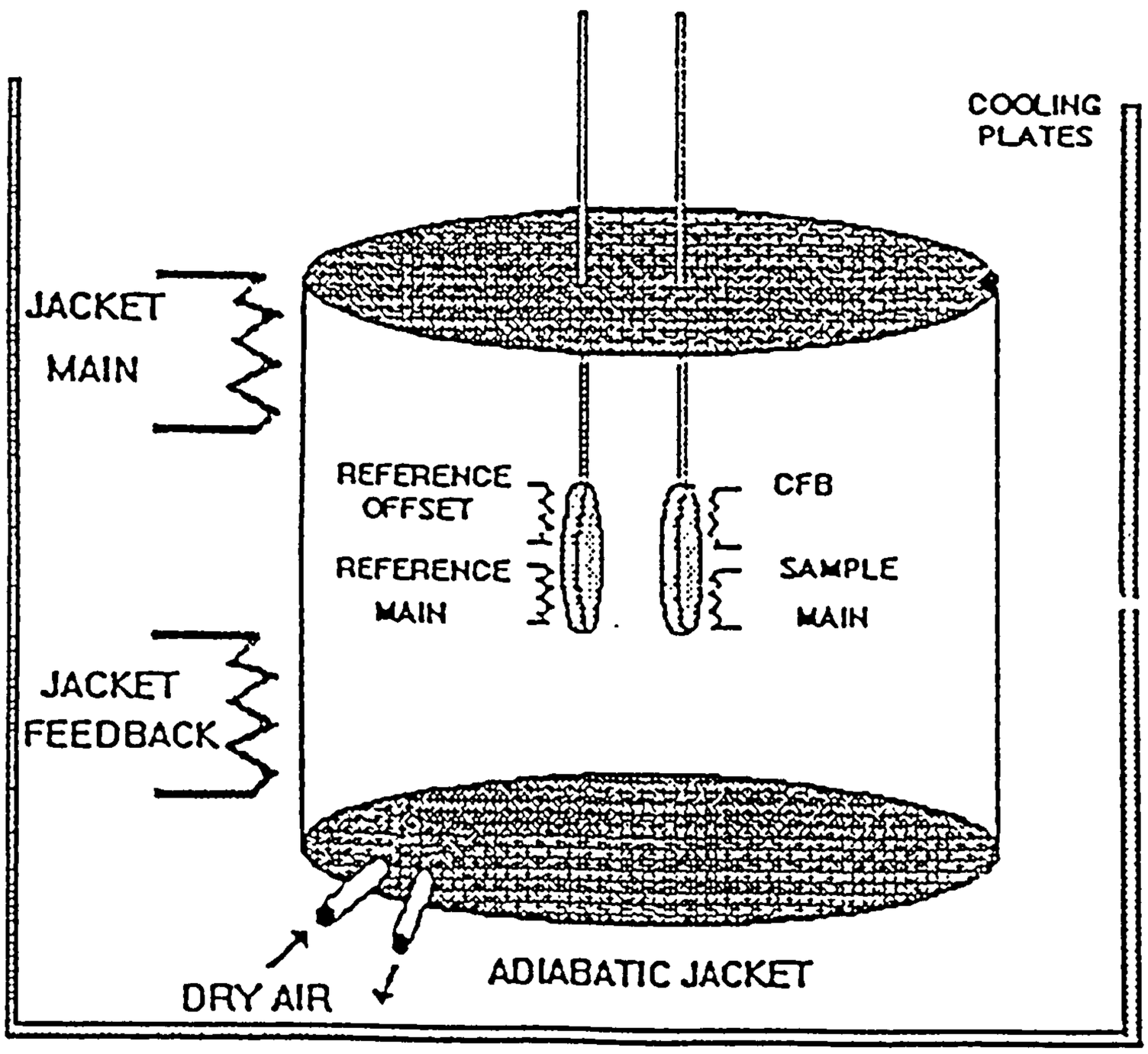

Figure 7-1: Schematic diagram of an Isothermal Titration Calorimeter.

The equality of heat capacities of the cells ($C_C \sim C_R$) and thermal conductivities between each cell and the block ($K_C \sim K_R$) forms the basis of the ITC's working mechanism. The rates of energy change in each cell due to various thermal processes form the basis of measurements. Within a time

increment (Δt) a change of energy of the reaction cell due to electrical power to the heater (P_C), chemical reaction (dQ_C) and heat conduction through a thermopile $K_C.(T_C-T_B)$ is equal to the change in temperature of the cell (dT_C) multiplied by the heat capacity of the cell (C_C)[5,8]

$$C_C.dT_C = P_C.\Delta t + dQ_C - K_C.(T_C-T_B).\Delta t \qquad (7\text{-}8)$$

The analogous equation to equation (7-8) for the reference cell (R) does not include a chemical reaction contribution term (i.e. $dQ_R=0$). Thus for the reference cell:

$$C_R.dT_R = P_R.\Delta t - K_R.(T_R-T_B).\Delta t \qquad (7\text{-}9)$$

At an infinitesimal time t, the increment Δt can be approximated to dt. Also in an ITC cell $C_C = C_R = C$, $K_R = K_C = K$ and combination of (7-8) and (7-9) by subtraction yields

$$C.d(T_C-T_R) = (P_C-P_R).dt + dQ_C - K.(T_C-T_R).dt \qquad (7\text{-}10)$$

The change of energy due to a chemical reaction in the reaction cell is the only one in the system and so it is possible to eliminate subscript 'C' ($dQ_C = dQ$) and equation (7-10) becomes

$$C.d(T_C-T_R) = (P_C-P_R).dt + dQ - K.(T_C-T_R).dt \qquad (7\text{-}11)$$

Integration of the term on the LHS, $C\int d(T_C-T_R)$, over a period of time t of the experiment, where the initial and final values of T_C-T_R are equal, is zero. Elimination of the LHS terms leaves the integral on RHS terms which gives an

ITC operating equation

$$Q = \int K.(T_C-T_R).dt + \int (P_C-P_R).dt \qquad (7\text{-}12)$$

where the temperature difference T_C-T_R is measured by the voltage (V) of the thermopiles, connected in opposition, multiplied by calibration constant α. The power (P_C-P_R) is given as I^2R where I is the current and R is the resistance of each cell heater. After these considerations a fundamental practical ITC operating equation is given as

$$Q = \int \alpha KV.dt + \int (P_C-P_R).dt \qquad (7\text{-}13)$$

The two integrals in equation (7-13) play different but important roles. A pure heat-conduction calorimeter does not involve any electrical power input which means $P_R = P_C$ = 0 implying that $\int (P_C-P_R).dt = 0$ leaving the first integral only which is similar to the integral in equation (7-7) where $(1/c') = \alpha K$.

7.2.3 Improved Response Times and Experimental Signal Interpretation

Generally speaking, isothermal titration calorimeters are similar to heat conduction calorimeters with added power control (sometimes this is referred to as 'power compensation'). According to McKinnon[5] the role of power control is: (i) to shorten the time t, (ii) to minimize the effect of baseline drift, and (iii) to control the first integral. This exercise requires simultaneous measurement of the second integral using a computer-controlled,

constant-current source. In order to achieve this there must be a power supply to the reaction cell at all times. The reference cell power is fixed at P_R (simple cases use P_R = 0).

If P'_C and P_R are chosen as the initial power to the reaction and reference cells respectively then a system will be allowed to reach an initial steady state temperature difference T'_C-T'_R (ΔT) with thermopile voltage V'. Before addition of reactants, the initial steady state voltage is given by $\alpha K V' = P'_C - P_R$ and equation (7-13) becomes

$$Q = \alpha K . \int (V-V') . dt + \int (P_C - P_R) . dt \qquad (7\text{-}14)$$

where the calorimeter constant αK is obtained in the absence of any chemical reaction. A simple control strategy requires that changes in the control power (P_C-P'_C) be negatively proportional to the output voltage (V-V'). This is the effective way of shortening recovery time. If a chemical reaction generates heat within the reaction cell, then the output voltage (V-V') becomes positive, the power P_C is reduced to the reaction cell so that a second integral provides a positive contribution to the measurement of the heat effect Q and vice versa. In practice, the current source is controlled at a chosen value of power for given time period.

In the Omega ITC, ΔT, the temperature difference between

the cell and the heat sink, is the centre of the functioning mechanism. At all times the cell is working at $\Delta T \sim 0$ and is controlled by a cell feedback (CFB) and jacket feedback (JFB). Rapid time responses are achieved by controlling electric power, increasing or decreasing the power as required to maintain $\Delta T \sim 0$. In cases where the heat conduction losses are negligibly small, the heat of reaction is given by the integration of the change of power with time (second integral of equation (7-14))[6]. In case the heat conduction through the thermopile to the sink is significant then one must measure this heat contribution by integration of changes of the thermopile voltage with time (first integral in equation (7-14)). In this exercise we find that: (i) the second integral is given by the sum of these finite energy quantities, and (ii) the evaluation of the first integral is determined by the sum of the mean voltage readings.

7.3 OMEGA ITC EXPERIMENTAL PROCEDURES

7.3.1 Preparation of Solutions for an ITC Experiment

The ITC experimental procedures define a 'macromolecule' as a host molecule and a 'ligand' as a guest molecule. Under normal circumstances (in an ITC experiment, for example, in biochemical systems) a macromolecule should be kept in the reaction cell and a ligand should be injected into the reaction cell. In surfactant/cyclodextrin studies there are limitations on the surfactant concentrations since the experiments have to be carried out below the cmc. This must

be done to avoid complications with micelles. In some cases the surfactant solutions are kept in the cell. To avoid confusion on definitions the subscripts 'm' and 'i' will be used to denote the solution kept in the cell and the injectant (titrant) solution respectively.

The molar ratio C_i/C_m is very important when planning ITC experiments. If a 1:1 inclusion complex is expected then the molar ratio should reach at least 2.5 to 3 to get a sigmoidal enthalpy profile and this requires injectant concentration to be at least 4 to 5 times higher than macromolecule concentration in the cell. This will provide a good sigmoidal enthalpy profile and allow accurate curve fitting to derive K, n and ΔH°. If 1:1 and 2:1 inclusion complexes are expected then C_i/C_m should reach a value of 4 or more to allow accurate fitting of n_1, n_2, K_1, K_2, ΔH°_1 and ΔH°_2 which means that the injectant concentration should be 8 to 10 times higher than the macromolecule concentration.

In order to obtain good signals and an enthalpy profile which can be confidently analysed, a parameter c according to equation[10]

$$c = K.C_m.n \qquad (7\text{-}15)$$

is used to estimate the total macromolecule concentration required in the cell for the experiment. In equation (7-15); K is the estimated equilibrium constant of the inclusion process, C_m is the concentration of the

macromolecule (or simply the concentration of a solution in the reaction cell) and n is the number of binding sites in the macromolecule.

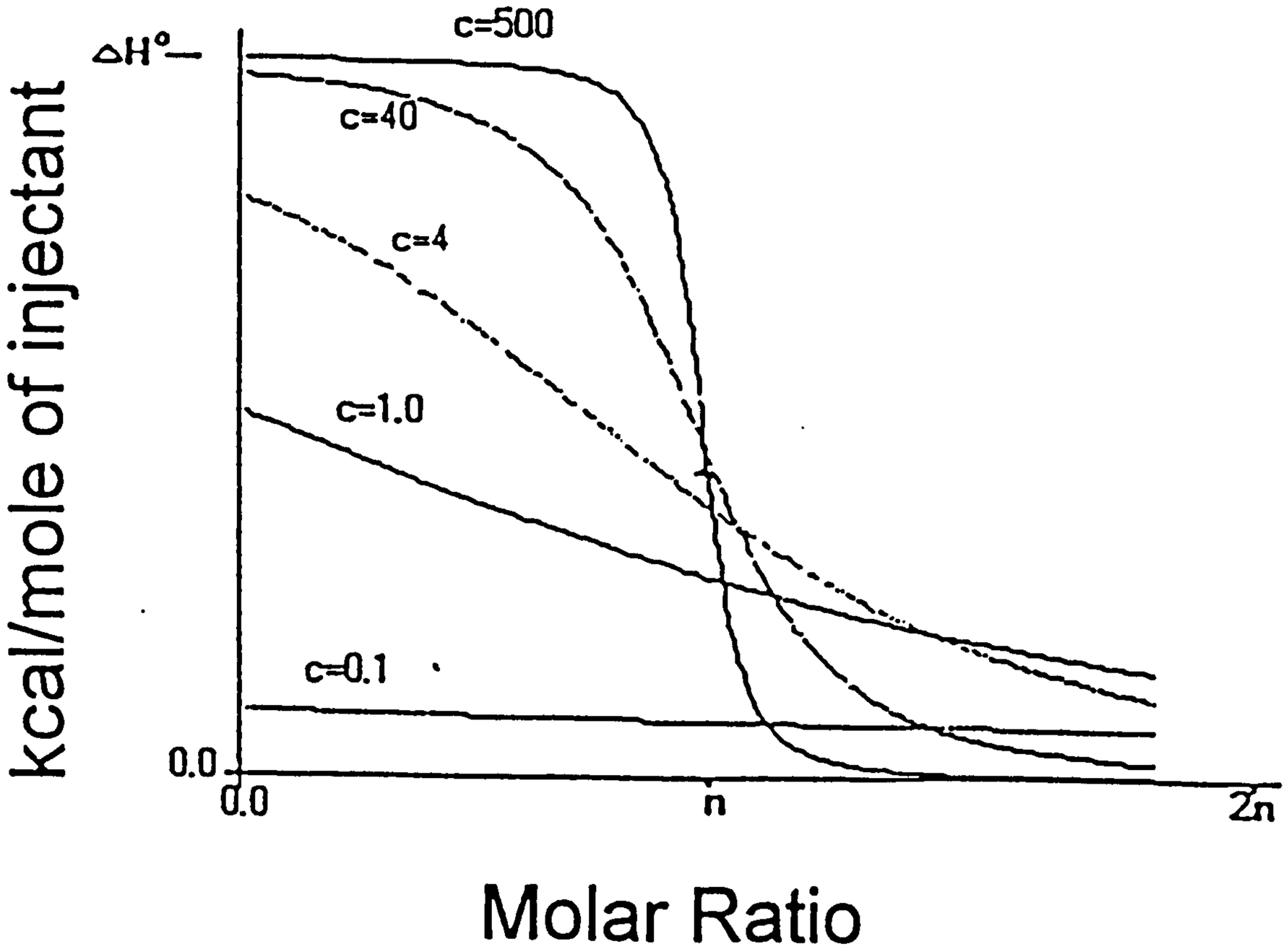

Figure 7-2: Simulated enthalpy profiles for various values of the parameter c.

The range of c values $5 < c < 500$ are thought to be most ideal for measuring K (Figure 7-2). For $c < 5$ profiles are featureless and most probably will not have good fits. Very large c (>500) are not good either, they lead to a very tight binding and the enthalpy profiles are rectangular. Although they provide accurate ΔH°, they fail to fit K and n. Lower c values (c=4, c=1 and c=0.1 in Figure 7-2) give inaccurate ΔH° due to broadened equivalence region and marginalizes sigmoidal tails at both ends of the profile which are very necessary in order to obtain reliable ΔH° values. To obtain good values for K, ΔH° and n, a balance of

factors should be considered very carefully for each system.

In circumstances where no information is available on the system equation (7-15) cannot be used. However, for surfactant systems it is possible sometimes to use K from other experiments on surfactant systems of the same charge and alkyl chain length for estimation purpose. Otherwise a trial and error method is used in which a number of experiments are carried out until the enthalpy profile of measured data fits correctly.

7.3.2 Setting $\Delta T \approx 0$ (The Control Module)

The cell temperature drops to around 11°C ~ 12°C overnight. Cooling water is thermostatted at 8°C using HAAKE F3-CH External Water Bath. The temperature has to be raised to the working temperature, 25°C for this particular work. The main **POWER** for the Omega ITC cell controls is switched on at least two hours before the experiment to warm up the system (at FHI the cell is permanently switched on). The **RUN** switch is switched on to **SCAN ENABLE**. The RUN switch turns on the cell heaters and temperature rises until the set **TEMPERATURE SHUT-OFF** (around one tenth of a degree above working temperature). The RUN switch is now switched to **BASELINE ENABLE** which starts the process of thermal equilibriation between the reaction and reference cells, that is, to reach $\Delta T \approx 0$ (0.0 to 0.2°C is acceptable). During this period the **JACKET FEEDBACK (JFB) METER** shows a

rise to maximum of the order +138.9 ~ +139 when the two cells are at thermal equilibrium. At this point the reading drops monotonously to a constant +30 ~ +35. The JFB controls the power to the jacket heater which maintains temperature equilibrium between the cells. The reading on the JFB should always read positive during the experiment. A nanovolt preamplifier (an ultralow noise dc amplifier) is switched on and the CELL FEEDBACK (CFB) METER readings drops or rises to reach the set baseline. Sometimes the CFB METER gave a persistent reading of ±141.2 this is an indication of charge saturation. To correct this it was found necessary to start out the input to the nanovolt preamplifier for a few seconds to eliminate this charge. A non-injection experiment is run by the computer to check noise levels. Noise levels of magnitudes below 5 x 10^{-3} rms are tolerable.

7.3.3 Setting an Omega ITC Reaction Cell for Experiment

A reaction cell is cleaned each time before starting a new experiment by filling and emptying with triply distilled water using a 5000 μl Hamilton gas-tight emptying syringe (Hamilton Bonaduz, AG, CH-7402 Bonaduz) four or five times and then rinsed with the sample solution. Finally the reaction cell is filled with the sample solution using a 2500 μl Hamilton gas-tight filling syringe (Hamilton Bonaduz, AG, CH-7402 Bonaduz) up to the top of the cell (Cell volume is 1.3595 ml) and any extra sample solution is emptied out to make sure that only the required volume is

left in the reaction cell. This is also a way of making sure that no gases get into the reaction cell.

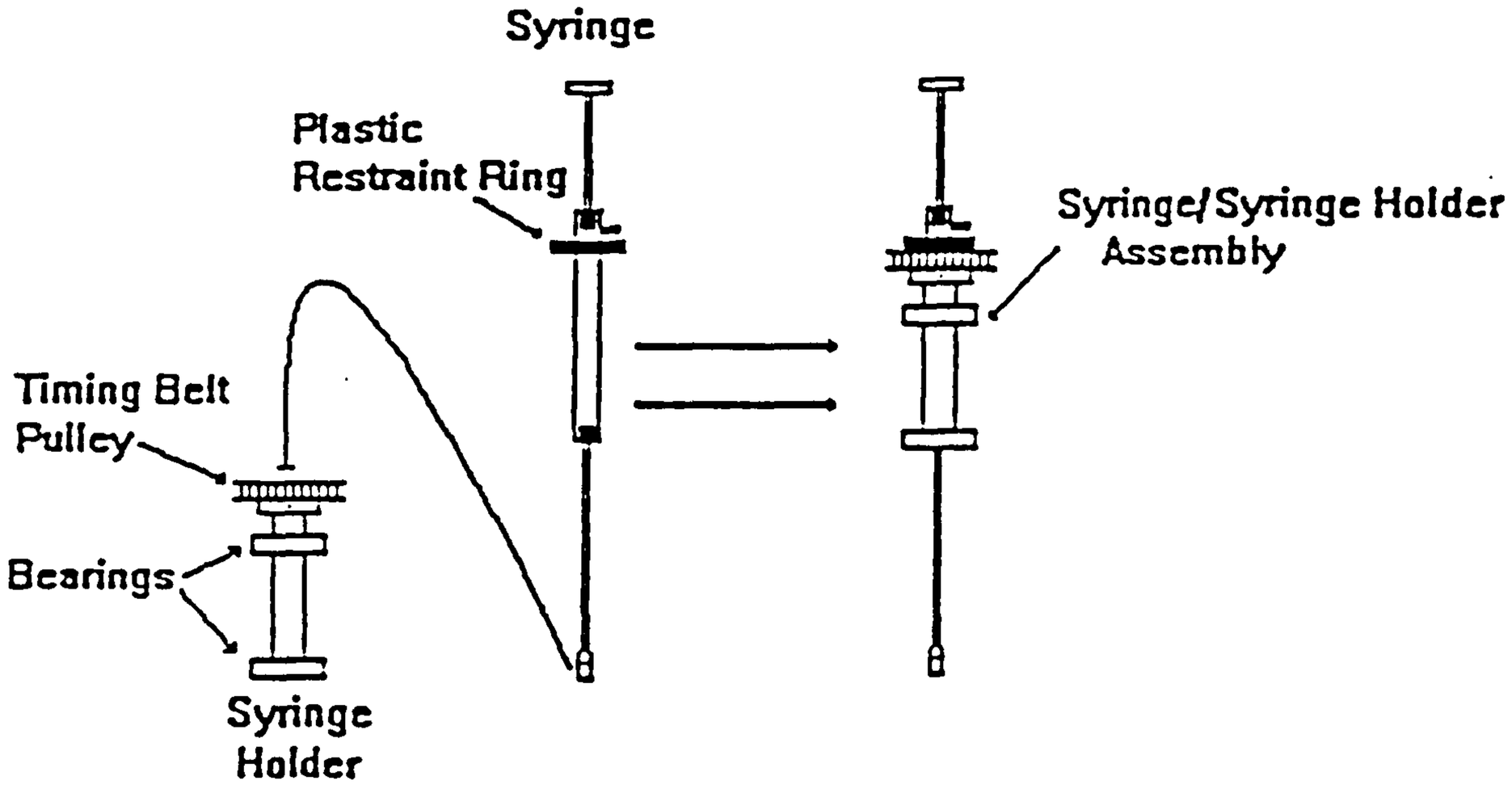

Figure 7-3 Setting the Syringe on the Syringe Holder

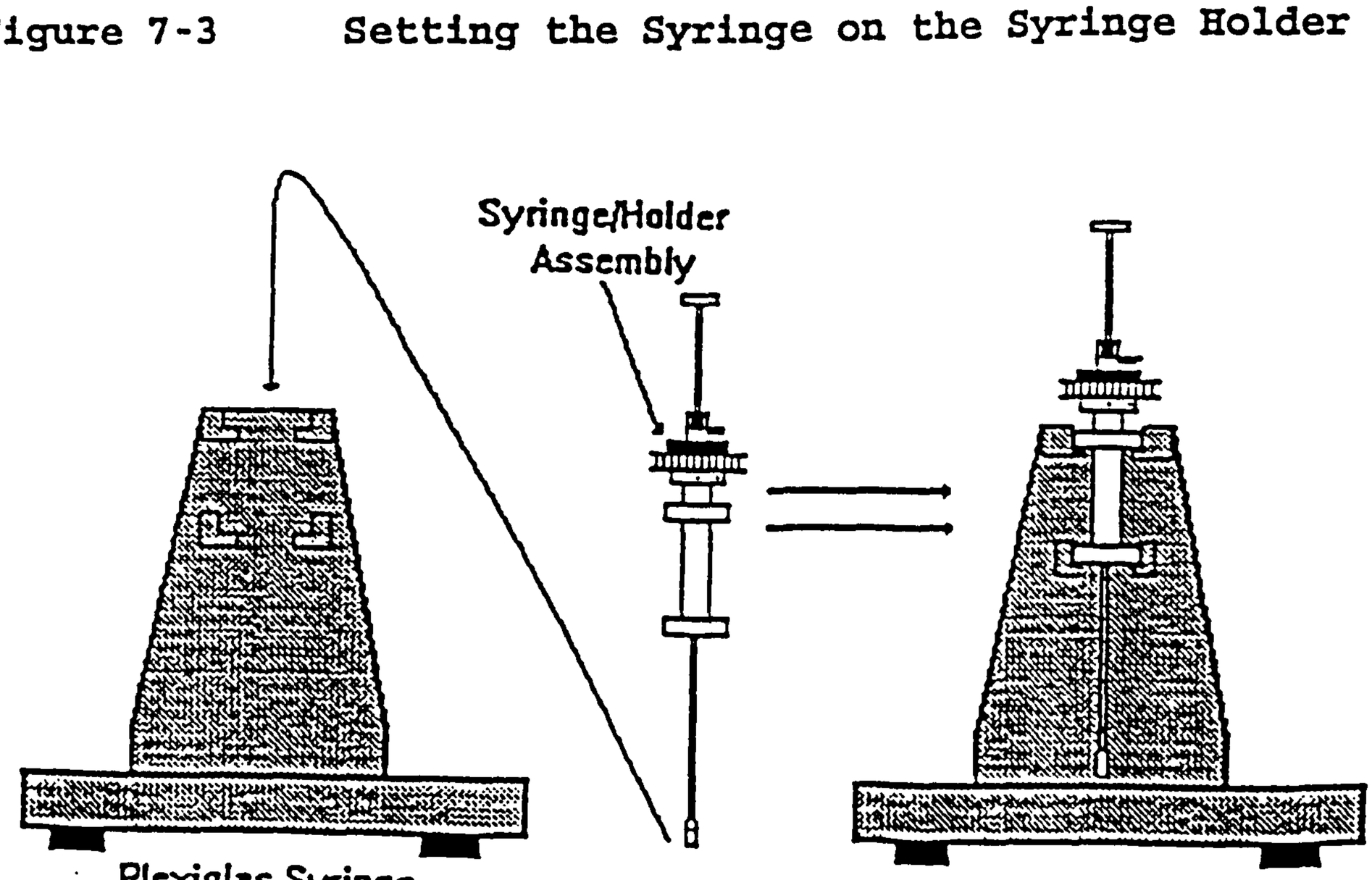

Figure 7-4 Setting the Syringe/Holder Assembly on the Plexiglas Syringe Stand

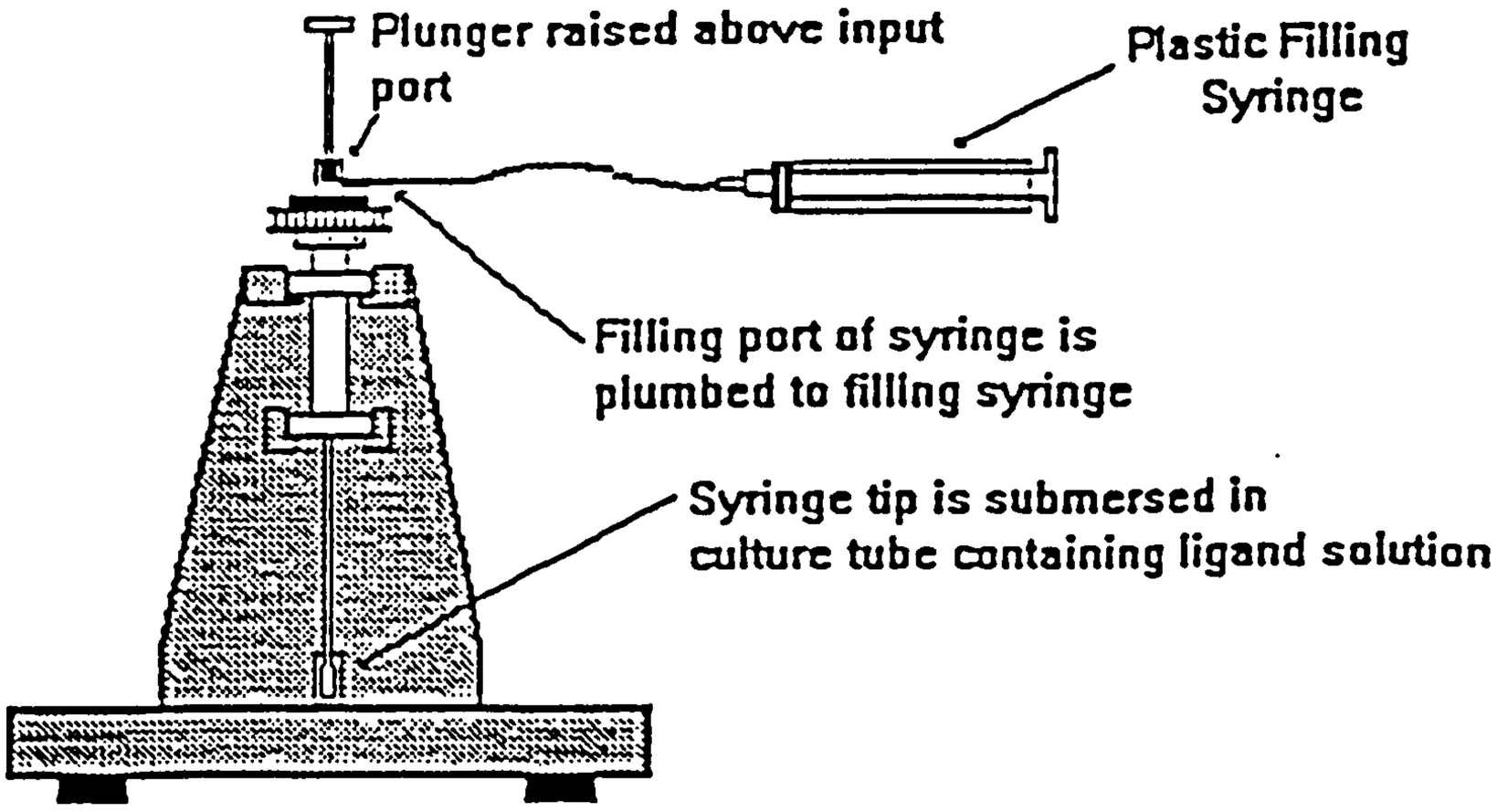

Figure 7-5 Filling the Syringe with the sample

The injectant (titrant) is filled into an injection syringe with the support of a white plastic (Delrin) syringe holder and a Plexiglas syringe stand as shown in Figures 7-3, 7-4 and 7-5. The plunger is raised above the input port and the filling syringe sucks in the injectant solution until no bubbles are seen in the injection syringe. The plunger is then lowered enough to close the input port and the filling syringe taken out.

The whole set is taken out of the Plexiglas syringe and inserted into the reaction cell. A belt connecting the stirring mechanism is set in place and the whole injection set is fixed by a screw so that it does not shake during stirring. A computer injection control program (Microcal software) is now applied. The plunger injection controller is lowered down on top of the plunger. The rpm of the stirrer is chosen depending on the experiment in question (in this work a 400 rpm was used in all experiments).

Higher rpm introduces excessive noise into the baseline and therefore affects the accuracy of the measurements.

7.3.4 Setting the Injection Matrix for an Omega ITC Experiment

A computer injection matrix controls and runs the ITC experiment. The setting up of a computer injection matrix, depends on: (i) spacing of data with respect to injectant concentration, (ii) rates of chemical reaction to reach equilibrium, and (iii) to attain a good ITC injection signal. As a result, a computer injection matrix is set using the following factors:

(i) Injection Syringe Volume (V): The injection syringe carries the maximum amount of injectant that is possible to be injected. At The Fritz-Haber-Institut (FHI) three types of syringes are used: (1) 250 μl, (2) 100 μl, and (3) 50 μl. Selection of these syringes depends on: (i) the extent of reaction, (ii) size and accuracy of injection volume, and (iii) size of the signal to be measured.

(ii) Number of injections (N): A MicroCal ITC software sets a maximum number of 50 injections. This number depends on: (i) injection volume required, and (ii) injection syringe used.

(iii) Injection volume (v): This is the volume injected per single injection. This depends on the Injection syringe volume and number of injections ($v = V/N$).

(iv) Injection time: This is dependent on (i), (ii) and (iii). Higher injection volumes requires higher injection times to allow smooth interactions leading to good measurement of heat effects. Whereas slower reactions needs longer injection times, faster reactions need shorter injection times.

(v) Time between injections: This is the time taken to restore the baseline before another injection. The time integrals need good separation between injection peaks.

Table 7.2: Examples of Injection Matrices used in this work

Experiment	I	II	III
Injection Syringe volume (μl)	250	250	250
Number of Injections	50	38	25
Injection Volume (μl)	5	7.5	10
Injection Time (secs.)	30	30	30
Time between Injections (mins.)	3	3	3
Time before Injections (mins.)	1	1	1
Total Experimental Time (mins.)	151	115	76

(vi) Time before first injection: This time is important to establish a smooth baseline before injections. (Table 7.2 show examples of injection matrices).

7.4 OMEGA ITC DATA ANALYSIS

Upon binding of a surfactant molecule into a cyclodextrin cavity heat will be released or absorbed accompanying the binding event. The heat effects associated with each injection (addition) of injectant solution represent the experimentally observable response in an Omega ITC experiment. For each injection, the heat released or absorbed is given by[11]

$$q = V_o.\Delta H^\circ.\Delta(C_i-m_i).n \qquad (7\text{-}16)$$

where q is the heat associated with the change in bound injectant concentration, $\Delta(C_i-m_i)$ is the change in the bound injectant concentration, C_i and m_i are the injectant's total and monomer concentrations, ΔH° is the enthalpy of binding (mol injectant)$^{-1}$, V_o is the active reaction volume, and n is the stoichiometric number (number of binding sites). The parameter q is directly proportional to the increase in the bound surfactant concentration resulting from each injection, and as a result decreases as the fractional saturation of the system is titrated stepwise to completion.

The total cummulative heat released or absorbed is directly proportional to the total amount of bound injectant

$$Q = V_o.\Delta H^\circ.n.\Sigma\Delta(C_i-m_i) \qquad (7\text{-}17)$$

where $Q = \Sigma q$ and $\Sigma\Delta(C_i-m_i) = C_i-m_i$. If we define the

fractional saturation $\Gamma = (C_i - m_i)/C_m$ then $\Sigma\Delta(C_i - m_i) = C_i - m_i = \Gamma C_m$ and equation (7-17) becomes[11,12]

$$Q = V_o.\Delta H^o.n.\Gamma C_m \qquad (7\text{-}18)$$

where C_m is the macromolecule concentration (for convenience we define a solution kept in the cell as a macromolecule). The experimental parameter measured in the isothermal titration calorimeter is the differential heat dQ/dC_i (in practice: $\Delta Q/\Delta C_i$ = change in heat content/change of injectant concentration). In an ITC experiment the total injectant concentration C_i is the independent variable under experimental control. Since ΔC_i is known and controlled, we wish to concentrate on elaborating on how ΔQ relate to real experimental data and to equations (7-16), (7-17) and (7-18).

7.4.1 Single Binding Site Systems

For the reaction of 1:1 stoichiometry in a single binding site systems according to scheme:

scheme (1)

$$S + CD \rightleftharpoons S(CD)$$

the following equations describe the binding equilibrium in scheme (1)

$$K = \left[\frac{\Gamma}{(1-\Gamma)m_i}\right] \qquad (7\text{-}20)$$

$$C_i = m_i + \Gamma C_m \qquad (7\text{-}21)$$

Algebraic manipulation of equations (7-20) and (7-21) gives quadratic equations in Γ and m_i respectively

$$\Gamma^2 - \Gamma[1 + C_i/C_m + 1/KC_m] + C_i/C_m = 0 \qquad (7\text{-}22)$$

and

$$Km_i^2 + m_i[1 + KC_m - KC_i] - C_i = 0 \qquad (7\text{-}23)$$

The Omega ITC computer data fitting used in this work use the only positive root of the quadratic equation (7-22)

$$\Gamma_s = \left(\frac{-b-(b^2-4c)^{1/2}}{2}\right) \qquad (7\text{-}24)$$

where $b = 1 + C_i/C_m + 1/KC_m$ and $c = C_i/C_m$, together with equation (7-18)

$$Q = \left(\frac{\Delta H^\circ . V_o . C_m}{2}\right) . \Gamma_s \qquad (7\text{-}25)$$

where Γ_s is the root of the quadratic equation (7-22) given in equation (7-24). The dependent variable Q can be calculated for any designated n, K and ΔH° at the end of each ith injection and designated Q_i. The variable Q_i calculated in equation (7-25) do not represent the total heat released or absorbed. Due to the cell set-up the displaced solution from the cell contribute about half as much heat effect as an equivalent volume in the active cell volume V_o. Therefore, the correct expression for the change in heat content from the end of (i-1)th injection to the completion of ith injection is given as[13]

$$\Delta Q_i = Q_i + \left(\frac{dV_i}{V_o}\right) \cdot \left[\frac{Q_i + Q_{i-1}}{2}\right] - Q_{i-1} \qquad (7\text{-}26)$$

where ΔQ_i is the heat released or absorbed from the ith injection and dV_i is the injection volume.

The Omega ITC computer fitting procedure of experimental data involves:

(i) initial guesses for n, K and ΔH°. For reactions of 1:1 stoichiometries the Origin computer software initial estimate are accurate enough, for 2:1 stoichiometries initial guesses should be fed into the computer program;

(ii) calculation of ΔQ_i according to equation (7-25) and (7-26) for each injection and comparison of these values with the measured heat for the corresponding experimental injection;

(iii) improvement in the initial values by standard Marquardt method and least-squares minimization of the measured heat ΔQ_m and calculated heat ΔQ_c;

(iv) an iteration of the above procedure is carried out until no further improvement in fit occurs with continued iteration; and

(v) the sum of squares of the differences between the measured heat content ΔQ_m and calculated heat content ΔQ_c i.e. $(\Delta Q_m - \Delta Q_c)^2$ is used as a criteria for goodness-of-fit.

7.4.2 Two-Consecutive Binding Sites Systems

In systems involving straight chain surfactants and cyclodextrins, binding sites are rarely identical because one of the site in the surfactant molecule must be near the head group and the other near the tail. The influence of the head group to the site will differ and that will make them nonidentical. Again binding sites can rarely be independent because for surfactant with bulky head groups there is only one path to binding and therefore one CD will bind first followed by the second as described in the following scheme:

scheme (2)

$$S + CD \rightleftharpoons S(CD)$$

$$S(CD) + CD \rightleftharpoons S(CD)_2$$

We refer this binding mechanism as "consecutive binding". Apart from the hindrance of binding caused by bulkiness of the head groups, it is well known that the inclusion of the polar head group is disfavoured by the large desolvation energy[14-17]. Automatically in circumstances like this the first CD to bind will influence the second and this explains the dependence of the second CD on the first CD. As a result, most CD/surfactant inclusion complexation systems fall under "nonidentical consecutive binding sites". In very rare cases where head groups are small and has little influence, there is a possibility of having "identical and independent binding sites". This category of systems are treated as "single binding site systems"

(section 7.4.1).

As a result the Omega ITC data were treated using the cubic equation (6-5) for "two consecutive binding site systems" used for electrochemical data.

$$K_1K_2m_i^3 + [K_1 + 2K_1K_2C_m - K_1K_2C_i]m_i^2 + [K_1C_m - K_1C_i + 1]m_i - C_i = 0 \quad (7\text{-}27)$$

The solution m_i is obtained from an iterative non-linear least-squares Omega ITC computer program using K_1, K_2 as adjustable parameters. C_i and C_m are the experimentally controlled variables. The value m_i obtained as a solution for equation (7-27) is used to estimate fractional saturation variables Γ_1 and Γ_2 as follows

$$\Gamma_1 = \left(\frac{K_1m_i}{1 + K_1m_i}\right) \quad (7\text{-}28)$$

$$\Gamma_2 = \left(\frac{K_2m_i}{1 + K_2m_i}\right) \quad (7\text{-}29)$$

which are then used in the fit to derive enthalpies of binding ΔH°_1 and ΔH°_2 in the following equation

$$Q = C_m.V_o.[\Gamma_1\Delta H^\circ_1 + \Gamma_2\Delta H^\circ_2] \quad (7\text{-}30)$$

An iterative procedure involving equations (7-27), (7-28), (7-29) and (7-30) is used to derive thermodynamic parameters K_1, K_2, ΔH°_1 and ΔH°_2. A least-mean squares minimization of the measured heat content (ΔQ_m) and the

calculated heat content (ΔQ_c) is used to improve these parameters. Improvement in fits is carried out with continued iteration until no further improvement on the fit can be attained. The algorithm of the iterative procedures used in sections 7.4.1 and 7.4.2 is referred to as Marquardt method[18,19]. Strictly speaking one should include n_1 and n_2 in the above equation but this introduces too many adjustable parameters.

7.5 OMEGA ITC RESULTS

The period spent at the Fritz-Haber-Institut, Berlin carrying out the ITC experiments on surfactant/cyclodextrin work was four weeks. As far as we are aware this work describes the first set of comprenhensive data using ITC on the systems. The strategy used in this short time available was to investigate as many different surfactant/cyclodextrin systems as possible. In order to find out the scope and limitation of the technique it was necessary to carry out an extensive set of experiments under different conditions and the most suitable option was to look on as many surfactant as possible. In many of the systems a predetermined value of the best equivalent conditions was not possible due to lack of information. In addition the choice of concentrations was also limited due to the cmc of the surfactants and the solubility of the cyclodextrins. We give below a typical survey of the type of results obtained in this brief interlude.

In this particular work a plot of "molar enthalpy" per injection as a function of "molar ratio" will be referred to as the "enthalpy profile".

Table 7.3 Parameter c and molar ratio C_i/C_m for different Omega ITC CD/surfactant systems

Surfactant	K	C_m	n	c (=K.C_m.n)	C_i/C_m
ß-CD/C_8TAB	441	0.0055	1.31	3.18	9.10
ß-CD/C_{10}TAB	3770	0.0055	1.13	23.43	7.50
ß-CD/C_{12}TAB	22900	0.002	1.00	45.80	11.00
ß-CD/C_{14}TAB	51600	0.001	0.86	44.43	11.00
ß-CD/C_{12}PyBr	24000	0.00165	1.07	42.37	5.80
ß-CD/C_6OSO_3Na	851	0.0055	1.07	5.01	4.50
ß-CD/C_8OSO_3Na	1740	0.0033	1.15	6.60	6.10
ß-CD/$C_{10}OSO_3Na$	11000	0.0033	1.03	37.39	6.10
ß-CD/$C_{12}OSO_3Na$	19900	0.006	1.01	120.59	1.80
ß-CD/C_8SO_3Na	1640	0.0022	1.17	4.22	4.50
ß-CD/$C_{10}SO_3Na$	10900	0.0019	1.10	22.78	4.80
ß-CD/$C_{12}SO_3Na$	18400	0.0011	1.03	20.85	9.10
α-CD/C_8TAB	1920	0.00424	0.96	7.78	4.72
α-CD/C_{10}TAB	5830	0.003	1.16	20.29	6.67
α-CD/C_6OSO_3Na	1880	0.004125	1.25	9.69	4.85
α-CD/C_8OSO_3Na	7770	0.001	2.11	16.39	20.00
α-CD/C_8SO_3Na	1920	0.003	2.11	9.69	6.67
α-CD/$C_{10}SO_3Na$	1650	0.0015	2.19	5.42	13.33

A good example of Omega ITC data which allows a non-linear least-mean-squares analysis to obtain stoichiometry number (n), equilibrium constant (K) and enthalpy of binding (ΔH°)

is provided in Figure 7-6 for ß-CD/C_{12}TAB. The enthalpy profile has a sigmoidal shape. It is not possible to derive the parameter ΔH° if the enthalpy profile does not conform to a sigmoidal shape but it is possible to derive n and K if profiles have good equivalence region. Problems and constraints which lead to non-sigmoidal enthalpy profiles are as described in section 7.3.1.

A typical example of Omega ITC data with very low values of parameter c is demonstrated in Figure 7-7 for ß-CD/C_8TAB, the enthalpy profile is almost linear. With this type of enthalpy profiles it is difficult to derive an accurate ΔH° which ideally requires both tails of the sigmoidal profile.

Another example is provided by the system ß-CD/$C_{10}OSO_3Na$ in Figure 7-8 which show non-sigmoidal enthalpy profile. In this case the parameter C_i/C_m is low and the reaction fails to reach the upper sigmoidal tail. Although in this case the lower sigmoidal tail is available, the profile does not yield an accurate ΔH°. Another situation is found for high C_i/C_m, where there are not enough data for the lower sigmoidal tail. In all cases if the equivalence region is wide enough it is possible to obtain reasonably accurate n and K from the fitting procedure.

The above constraints can be solved and improved to yield a sigmoidal enthalpy profile mainly by trial and error. Table 7.3 lists the parameter c and C_i/C_m values obtained in

the present work.

7.5.1 1:1 α- and ß-CD/surfactant Inclusion complexes

The parameters n and K derived from non-sigmoidal ITC enthalpy profiles are listed in Table 7.4. Omega ITC results for nonionic surfactant tetraethylene glycol mono n-octyl ether $C_8(OE)_4$ inclusion complexes with α-, ß- and γ-cyclodextrins are also summarized in Table 7.4. The results (n, K and ΔH°) derived from complete sigmoidal ITC enthalpy profiles are tabulated in Table 7.5.

Table 7.4 The Stoichiometric number (n) and binding constant (K) derived from non-sigmoidal ITC data

System	N	K/mol^{-1} dm^3
ß-CD/C_8TAB	1.310±0.028	441± 53
ß-CD/C_{12}PyBr	1.070±0.013	24000±4500
ß-CD/C_6OSO_3Na	1.070±0.018	851± 150
ß-CD/C_8OSO_3Na	1.150±0.015	1740± 210
ß-CD/$C_{10}OSO_3Na$	1.030±0.006	11000±1700
ß-CD/$C_{12}OSO_3Na$	1.010±0.007	19900±1700
ß-CD/C_8SO_3Na	1.170±0.039	1640± 450
ß-CD/$C_{10}SO_3Na$	1.100±0.019	10900±2000
α-CD/C_8TAB	0.956±0.011	1920± 200
α-CD/C_6OSO_3Na	1.250±0.011	1880± 180
α-CD/C_8SO_3Na	2.110±0.057	1920± 260
α-CD/$C_{10}SO_3Na$	2.190±0.050	1650± 310
α-CD/$C_8(OE)_4$	1.270±0.037	5150±1400
ß-CD/$C_8(OE)_4$	1.200±0.069	2270± 680
γ-CD/$C_8(OE)_4$	1.010±0.049	600± 270

7.5.2 1:1 and 2:1 CD/surfactant Inclusion Complexes

The inclusion of cationic and anionic surfactants into α-CD cavity to form 1:1 and 2:1 lead to inclusion complexes with higher K_1 and K_2 as compared to the corresponding ß-CD inclusion complexes. For $C_{10}OSO_3Na$ and $C_{12}SO_3Na$, both K_1 and K_2 were obtained directly from the computer fitting of the Omega ITC data. In all other systems the K_1 derived from electrode data was used as a fixed parameter in the fitting procedure to obtain estimates of K_2, ΔH°_1 and ΔH°_2. The results are summarized in Table 7.6. An example of a sigmoidal enthalpy profile for systems involving 1:1 and 2:1 inclusion complexes is shown in Figure 7-9 for α-CD/C_{16}TAB system.

Table 7.5 Omega ITC results for 1:1 CD/surfactant inclusion complexes

System	N	K/mol^{-1}dm^3	ΔH°/cal mol^{-1}
ß-CD/C_{10}TAB	1.130±0.013	3770± 440	-1675± 26
ß-CD/C_{12}TAB	1.000±0.003	22000± 890	-2307± 11
ß-CD/C_{14}TAB	0.861±0.005	51600±3500	-3111± 24
ß-CD/$C_{12}SO_3Na$	1.030±0.012	18400±2000	-2344± 36
α-CD/C_{10}TAB	1.160±0.005	5830± 300	-6280± 43
α-CD/C_8OSO_3Na	2.110±0.011	7770± 280	-9529± 87

Figure 7-6

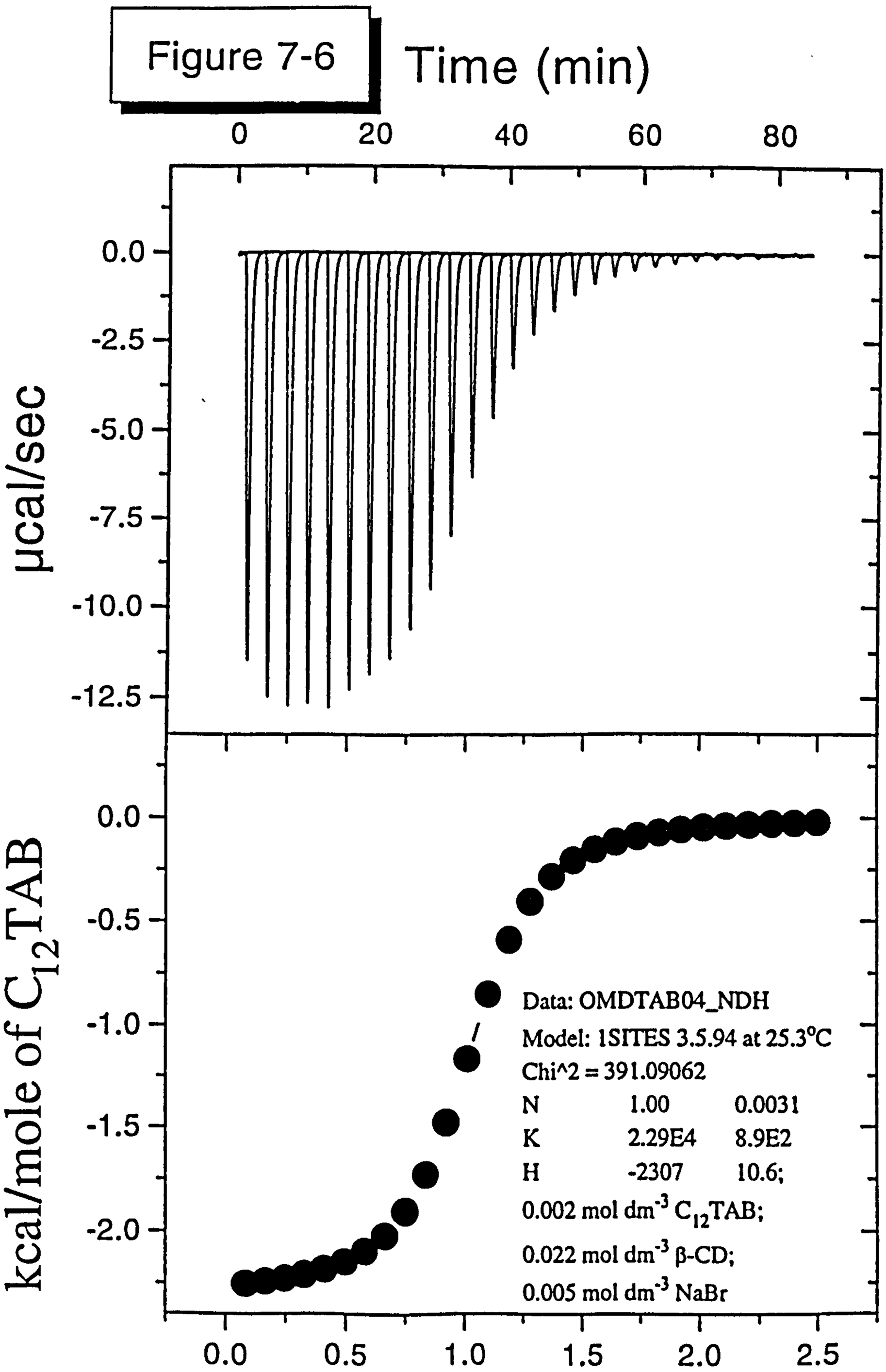
Time (min)
0
20
40
60
80
0.0
-2.5
-5.0
-7.5
-10.0
-12.5
µcal/sec
0.0
-0.5
-1.0
-1.5
-2.0
kcal/mole of C_{12}TAB
Data: OMDTAB04_NDH
Model: 1SITES 3.5.94 at 25.3°C
Chi^2 = 391.09062
N 1.00 0.0031
K 2.29E4 8.9E2
H -2307 10.6;
0.002 mol dm^{-3} C_{12}TAB;
0.022 mol dm^{-3} β-CD;
0.005 mol dm^{-3} NaBr
0.0
0.5
1.0
1.5
2.0
2.5
Molar Ratio

Figure 7-7

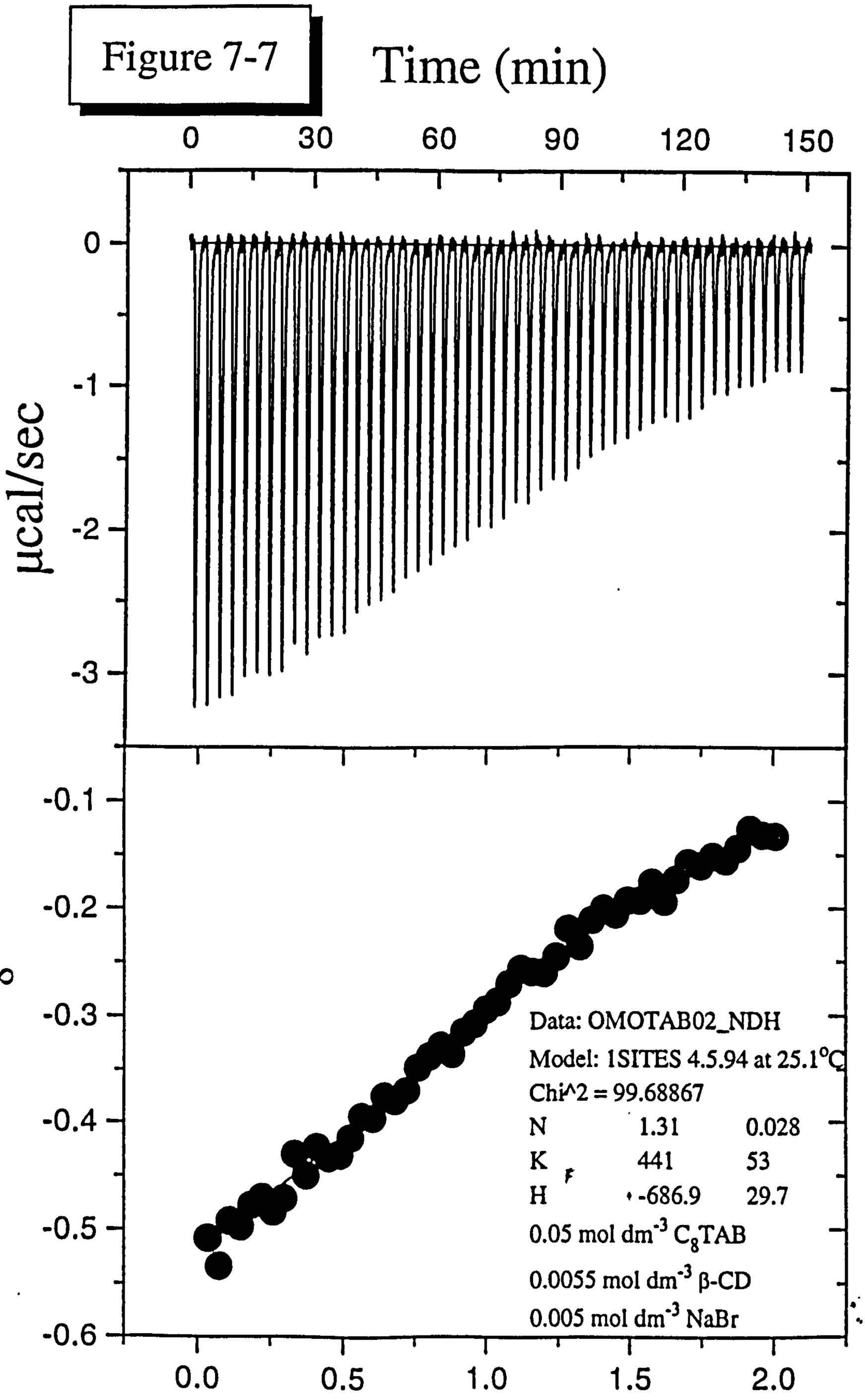
Time (min)
0
30
60
90
120
150
0
-1
-2
-3
µcal/sec
-0.1
-0.2
-0.3
-0.4
-0.5
-0.6
kcal/mole of C8TAB
Data: OMOTAB02_NDH
Model: 1SITES 4.5.94 at 25.1°C
Chi^2 = 99.68867
N 1.31 0.028
K 441 53
H -686.9 29.7
0.05 mol dm-3 C8TAB
0.0055 mol dm-3 β-CD
0.005 mol dm-3 NaBr
0.0
0.5
1.0
1.5
2.0
Molar Ratio

Figure 7-8

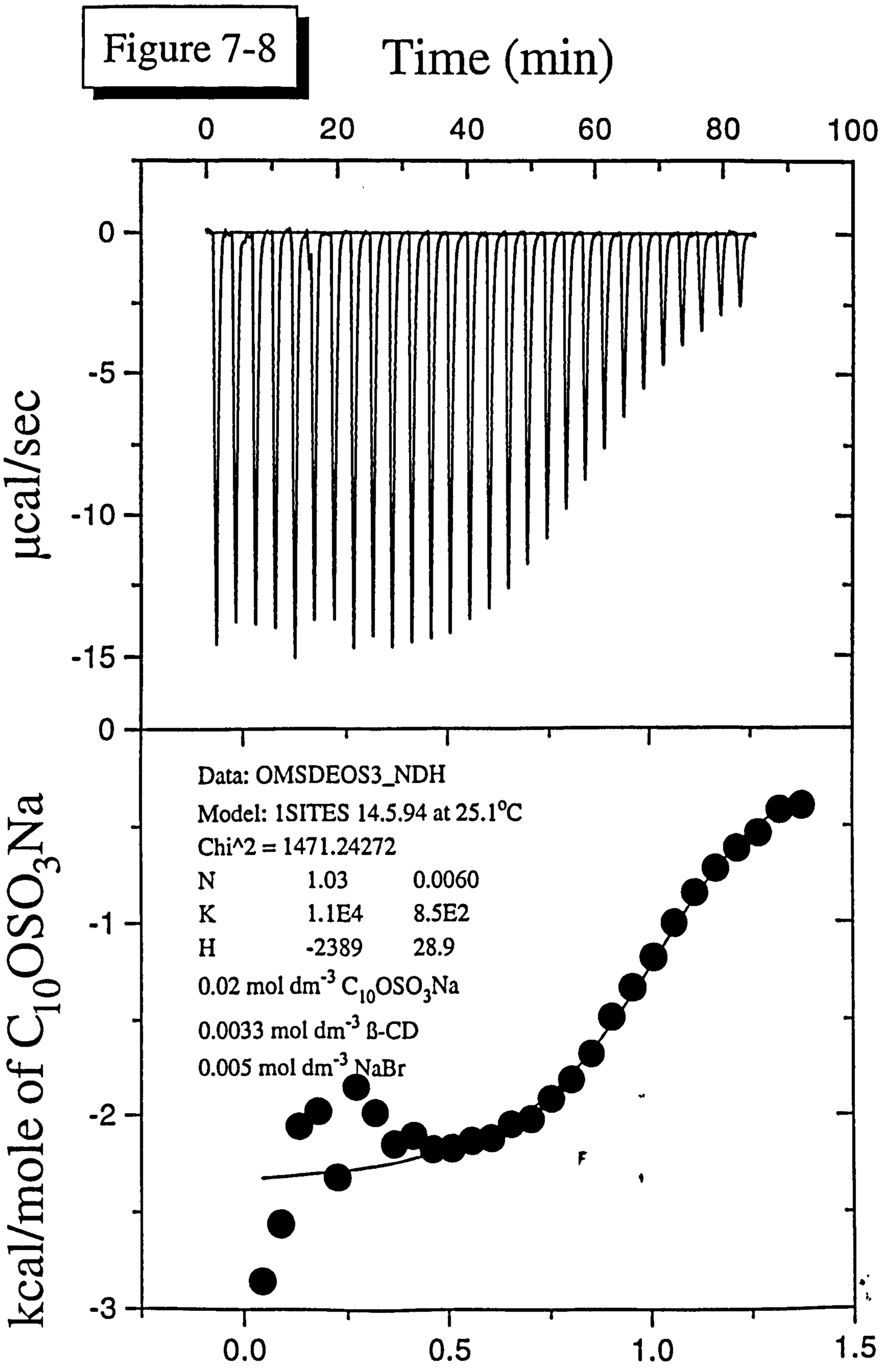
Time (min)
0
20
40
60
80
100
0
-5
-10
-15
µcal/sec
Data: OMSDEOS3_NDH
Model: 1SITES 14.5.94 at 25.1°C
Chi^2 = 1471.24272
N 1.03 0.0060
K 1.1E4 8.5E2
H -2389 28.9
0.02 mol dm-3 C10OSO3Na
0.0033 mol dm-3 ß-CD
0.005 mol dm-3 NaBr
0
-1
-2
-3
kcal/mole of C10OSO3Na
0.0
0.5
1.0
1.5
Molar Ratio

Figure 7-9 : A Two-Site Consecutive Fit for α-CD/C_{16}TAB system

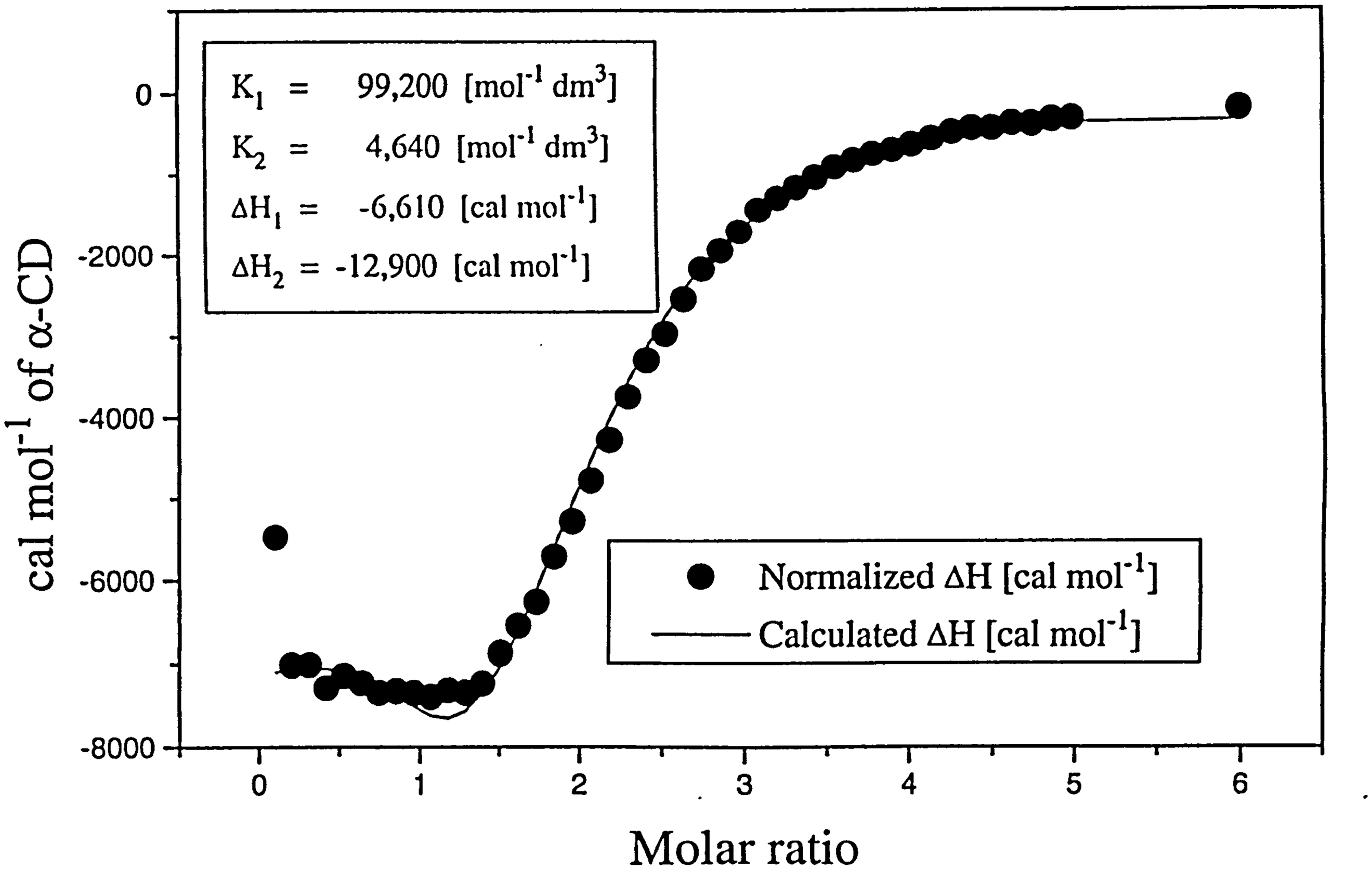

Table 7.6 Omega ITC results for both 1:1 and 2:1 α- and ß-CD/surfactant inclusion complexes

System	K_1	K_2	ΔH°_1	ΔH°_2
α-CD/C_{12}TAB	17000	368	-7510	-10500
α-CD/C_{14}TAB	60700	1760	-7300	-11100
α-CD/C_{16}TAB	99200	4640	-6610	-12900
α-CD/C_{12}PyBr	44200	797	-7180	-8320
α-CD/C_{14}PyBr	99700	2180	-6900	-10700
α-CD/C_{16}PyBr	110000	8110	-7700	-12600
α-CD/$C_{10}OSO_3Na$	15000	4230	-1800	-22000
α-CD/$C_{14}OSO_3Na$	49300	11000	-5000	-16900
α-CD/$C_{12}SO_3Na$	19100	2360	-6400	-11400
ß-CD/C_{16}TAB	65300	33.1	-3180	-22700
ß-CD/$C_{14}OSO_3Na$	48300	32.8	-3030	-44400

Units: K_1 and K_2 [mol^{-1} dm^3]; ΔH°_1 and ΔH°_2 [cal mol^{-1}]

7.6 REFERENCES

1. WAN-YUNUS, W.M.Z.; TAYLOR, J.; BLOOR, D.M.; HALL, D.G. and WYN-JONES, E. *J. Phys. Chem.*, 96 (1992) 8979.

2. JEZEQUEL, D.; MAYAFFRE, A. and LETELLIER, P. *Can. J. Chem.*, 69 (1991) 1865.

3. PARK, J.W. and PARK, K.H. *J. Incl. Phenom.* (In Press).

4. MWAKIBETE, H.; BLOOR, D.M. and WYN-JONES, E. *Langmuir*, 10 (1994) 3328.

5. McKINNON, I.R.; FALL, L.; PARODY-MORREALE, A. and GILL, S.J. *Anal. Biochem.*, 139 (1984) 134.

6. RUDOLF, S.A.; BOYLE, S.G.; DRESDEN, C.F. and GILL, S.J. *Biochemistry*, 11 (1972) 5344.

7. CHRISTENSEN, J.J. "*Bioenergetics and Thermodynamics: Model Systems*", edited by A. Braibanti (D. Reidel, Boston, 1980), p.75

8. SPOKANE, R.B. and GILL, S.J. *Rev. Sci. Instrum.*, 52 (1981) 1781.

9. SPINK, C. and WADSÖ, I. *Methods of Biochemical Analysis*, 23 (1976) 1.

10. WISEMAN, T.; WILLISTON, S.; BRANDTS, J.F. and LIN, L-N. *Anal. Biochem.*, 179 (1989) 131.

11. FREIRE, E.; MAYORGA, O.L. and STRAUME, M. *Anal. Chem.*, 62 (1990) 950.

12. MYERS, M.; MAYORGA, O.L.; EMTAGE, J. and FREIRE, E. *Biochemistry*, 26 (1987) 4309.

13. *ITC Data Analysis in Origin*, Tutorial Guide, Version 2.9, MicroCal Inc., May 1993.

14. PARK, J.W. and SONG, H.J. *J. Phys. Chem.*, 93 (1989) 6454.

15. BENDER, M.L.; KOMIYAMA, M. *Cyclodextrin Chemistry*; Springer-Verlage: New York (1977).

16. HARATA, K. *Bull. Chem. Soc. Jpn.*, 49 (1976) 2066.

17. HARATA, K. *Bull. Chem. Soc. Jpn.*, 49 (1976) 1493.

18. BEVINGTON, P.R. "*Data Reduction and Error Analysis for the Physical Sciences*", p235, McGraw-Hill, New York (1969)

19. MARQUARDT, D.W. *J. Soc. Ind. Appl. Math.*, 11 (1963) 431.

CHAPTER EIGHT: DISCUSSION ON ELECTROCHEMICAL AND OMEGA ITC RESULTS ON CYCLODEXTRIN/SURFACTANT INCLUSION COMPLEXES

8.1 INTRODUCTION

The consistency and reliability of the experimental techniques used in investigating CD/surfactant inclusion complexes have been discussed in Chapter 5 (section 5.3.1 page 141). We have established that certain experimental techniques can be considered to give reliable binding constants, these include: (i) the electrochemical technique using surfactant selective electrodes (EMF)[1-3], and (ii) the fluorescence-probe studies involving competitive binding (FP)[4,5].

We have also established the type of agreement that can be expected from the results of EMF and FP techniques. Tables 5.1, 6.6 and 7.1 show the agreement of the first binding constant K_1 according to the scheme:

scheme (1)

$$S + CD \rightleftharpoons S(CD)$$

for CD/surfactant systems such as ß-CD/C_nTAB[1-3,5], ß-CD/$C_n OSO_3Na$[4] and ß-CD/$C_n SO_3Na$[2,4]. For example, the system ß-CD/C_{14}TAB has been studied independently by three different investigators and has K_1 values in [mol^{-1} dm^3] units of: 39811 (EMF)[1], 44000 (FP)[5] and 39750 (EMF this work) which are considered in acceptable agreement.

The second issue we wish to address in this discussion is the Omega ITC results described in Chapter 7. Although the Omega ITC technique comes under category (b) techniques described in Chapter 5 (section 5.3.1 page 141) the early results shown in Table 7.1 (page 209) are promising when compared with results from EMF and FP techniques. In the present work the equilibrium constants obtained from the Omega ITC 1:1 inclusion complexes results are compared to EMF and FP results as listed in Table 8.1.

Table 8.1 Omega ITC, EMF and FP equilibrium constants for 1:1 ß-CD/surfactant inclusion complexes

Surfactant	ITC	EMF	FP
C_{10}TAB	3770	3981[a]	-
C_{12}TAB	22000	17780[a], 18100[b]	22100[c]
C_{14}TAB	51600	49100-52500[d] 39750[f], 39810[a]	44000[c]
C_{12}PyBr	24000	24900[f]	-
C_8OSO_3Na	2390	-	2560[e]
$C_{10}OSO_3Na$	11000	-	8750[e]
$C_{12}OSO_3Na$	19900	21000[b]	25600[e]
C_8SO_3Na	1640	-	1180[e]
$C_{10}SO_3Na$	10900	-	5360[e]
$C_{12}SO_3Na$	18400	-	16100[e]

[a](ref 1), [b](ref 2), [c](ref 5), [d](ref 3), [e](ref 4), [f](this work)

With a few exceptions the data again show acceptable agreement.

However, there is a problem with the Omega ITC technique on

systems which exhibit both 1:1 and 2:1 inclusion complexes according to the scheme:

scheme (2)

$$S + CD \rightleftharpoons S(CD)$$

$$S(CD) + CD \rightleftharpoons S(CD)_2$$

The fact that the number of adjustable parameters in the equation are 6 means that the computer fitting procedure with a limited amount of points covering the sigmoidal curve is not reliable. In some cases, however, if K_1 is known from other experimental techniques and we fix $n_1 = n_2 = 1$ then the problem is reduced to a three parameter fit in ΔH°_1; ΔH°_2 and K_2. This can sometimes lead to useful data which are listed in Table 7.6 (page 243). Finally if no complementary data are available the best one can achieve is to estimate K_1 from the bank of data available in this work and other sources[1-6].

The surfactant membrane selective electrodes used for the electrochemical work showed good Nernstian parameters as summarized in Table 6.2 (page 164). A possibility of CD complexing with Br^- ion in the cationic surfactants was checked by measuring the EMF of a bromide ion electrode against a standard calomel electrode. The EMF data gave a very good Nernstian plot shown in Figure 6-3 (page 167) with slope = 58.1 mV/decade, intercept = 189.5 mV and a correlation coefficient of 0.9999. This indicates that within experimental confidence limit there is no inclusion

compounds with Br^- ions.

The complexation constants K_1 and K_2 for the systems α-CD/C_nPyBr, ß-CD/C_nPyBr, α-CD/C_{14}TAB and ß-CD/C_{14}TAB were determined using an EMF technique. Tables 6.4 (page 191) and 6.5 (page 192) list these results for C_nPyBr and C_{14}TAB systems.

8.2 THE FIRST BINDING CONSTANT K_1

In this section the first binding constants K_1 derived from electrochemical work for cationic surfactants and the Omega ITC work for 1:1 CD/Surfactant inclusion complexes are discussed.

8.2.1 ß-CD/Surfactant Systems

The 1:1 inclusion complexes for ß-CD/C_nPyBr according to scheme (1) show dominance in the systems: ß-CD/C_{10}PyBr and ß-CD/C_{12}PyBr with K_1 in [mol^{-1} dm^3] units: 3740 and 24900 respectively. The Scatchard plots for these systems in Figures 6-15 and 6-17 respectively confirms only 1:1 inclusion complexes. The Omega ITC data for ß-CD/C_{12}PyBr, despite having a non-sigmoidal enthalpy profile, gave K_1 value of magnitude 24000 mol^{-1} dm^3 which agrees very well with the electrochemical K_1 value (24900 mol^{-1} dm^3).

Unexpectedly we also observed a 1:1 inclusion complex for ß-CD/C_{16}PyBr with K_1 of magnitude 88850 (in [mol^{-1} dm^3] units). The Scatchard plot for this system in Figure 6-21 (page

187) is clearly linear. The computer fit based on the cubic equation (6-5) for these systems shown in Figures 6-25 and 6-27 respectively are smooth with acceptable minimization criteria. One could have easily concluded the dominance of 1:1 inclusion complexes for the whole ß-CD/C_nPyBr systems but the system ß-CD/C_{14}PyBr showed relatively strong 1:1 and 2:1 inclusion complexes with K_1 and K_2 of magnitudes in [mol^{-1} dm^3] units: 66300 and 830 respectively. The Scatchard plots in Figure 6-19 (page 185) are slightly curved. According to the observed trend, especially results on ß-CD/C_{16}PyBr, we feel K_2 of magnitude 830 mol^{-1} dm^3 for ß-CD/C_{14}PyBr system might be a product of error from either experimental or the computer fitting procedure.

With the exception of the K_1 value for ß-CD/C_{10}PyBr (3740 mol^{-1} dm^3) which agrees very well with the corresponding K_1 value found by Jezequel *et al*[1] for ß-CD/C_{10}TAB (3981 mol^{-1} dm^3), other K_1 values of: 24900, 66300 and 88850 mol^{-1} dm^3 for ß-CD inclusion complexes with C_{12}PyBr, C_{14}PyBr and C_{16}PyBr respectively are higher than those found for the corresponding series ß-CD/C_nTAB: C_{12}TAB (17780[1], 22100[5] and 18100[2]), C_{14}TAB (39750, 39800[1], 44000[5] and 49100-52500[3]) and C_{16}TAB (65250[7], 70800[1] and 59800[5]). This observation on pyridinium-containing surfactants was also reported by Palepu *et al*[8] in their conductimetric work. It is undoubtedly the pyridinium moiety that helps to ensure a closeness-of-fit of the surfactant hydrocarbon tail within the ß-CD cavity. However, it is not very clear what really

happens, whether it is influenced by electronic factors due to the presence of the aromatic ring or steric factors due to the bulkiness of the head group. Despite these observations, Jezequel *et al*[1] work on ß-CD/C_{16}PyBr and ß-CD/C_{16}TAB show K_1 of the same magnitude 70800 mol^{-1} dm^3 and relatively lower than our K_1 for ß-CD/C_{16}PyBr (88850 mol^{-1} dm^3); these values are however within ±15% of each other.

The Omega ITC data for 1:1 ß-CD/C_nTAB give K_1 values (in [mol^{-1} dm^3] units): 441, 3770, 22000 and 51600 respectively for C_8TAB, C_{10}TAB, C_{12}TAB and C_{14}TAB. The K_1 value for ß-CD/C_{10}TAB (3770 mol^{-1} dm^3) is in acceptable agreement with Jezequel's[1] electrochemical K_1 value (3981 mol^{-1} dm^3). The Omega ITC K_1 value for ß-CD/C_{12}TAB, 22000 mol^{-1} dm^3, show good agreement with K_1 values from EMF (18100[2], 17795[1]); FP (22100)[5] and an earlier ITC work (23700)[7]. Electrochemical work on ß-CD/C_{14}TAB gave an average K_1 of magnitude 39750 mol^{-1} dm^3. The K_1 value derived here is found to agree very well with other EMF and FP literature results: 39800[1] and 44000[5] but not as well with Tominaga's[3] recent EMF data where K_1 values in the range 49100-52500 were reported and only 1:1 complexation was observed.

We observed very weak 2:1 ß-CD/surfactant inclusion complexes for all surfactants with alkyl chain lengths n_c > 12. Our Omega ITC data confirm the predominance of 1:1 inclusion complexes for ß-CD/C_nPyBr but the fitting procedure failed to reach an acceptable minimization

criteria for ß-CD/C_{14}PyBr and ß-CD/C_{16}PyBr.

A similar case was observed by Lewis *et al*[9] on the ß-CD/hydrocinnamic acid complex which was reported by Pauli *et al*[10] to have a binding constant K = 200 mol^{-1} dm^3. However no measurable interaction was detected using calorimetric measurement. This was explained by Lewis *et al*[9] to be caused by non-enthalpic interaction of the complexation process and so cannot be detected by calorimetric methods. What we might conclude from the Lewis work is that probably the first or the second CD binding in ß-CD systems with C_{14}PyBr and C_{16}PyBr might not involve much enthalpy change.

The Omega ITC data again failed to give a satisfactory answer for 1:1 and 2:1 inclusion complexes for ß-CD/C_{14}TAB but fitted well for 1:1 inclusion complex to give: n = 0.86, K = 51600 mol^{-1} dm^3 and ΔH° = -13.0 kJ mol^{-1}. A K_1 of magnitude 51600 mol^{-1} dm^3 is higher than our electrochemical value for K_1 (39750 mol^{-1} dm^3) and those from studies by Jezequel *et al*[1] (39810 mol^{-1} dm^3) and Park and Park[5] (44000 mol^{-1} dm^3) but agree very well with Tominaga's[3] EMF K_1 values in the range 49100-52500 mol^{-1} dm^3 over a ß-CD concentration range from 1 x 10^{-3} to 1.2 x 10^{-2} mol dm^{-3}. Nonetheless a value for n = 0.86 is low and could very likely indicate some irregularity. Fitting of the ß-CD/C_{16}TAB data using K_1 = 65300 mol^{-1} dm^3 from electrode data[7] and fixing $n_1 = n_2 = 1$ gives K_2 = 33.1 mol^{-1} dm^3, ΔH°_1 = -13.3 and ΔH°_2 = -94.9 kJ mol^{-1}. This observation supports dominance of 1:1 inclusion

complexes for ß-CD/C_nTAB.

The Omega ITC data for 1:1 ß-CD/anionic surfactant inclusion complexes for the systems: ß-CD/C_8OSO_3Na, ß-CD/$C_{10}OSO_3Na$, ß-CD/$C_{12}OSO_3Na$, ß-CD/C_8SO_3Na and ß-CD/$C_{12}SO_3Na$ show K_1 values which are in acceptable agreement with FP data by Park and Song[4] shown in Table 8.1. Unexpectedly the Omega ITC data shows a K_1 value of magnitude 10900 mol^{-1} dm^3 for ß-CD/$C_{10}SO_3Na$ which is much higher than FP data (5360 mol^{-1} dm^3). The K_1 values for the system ß-CD/$C_{12}OSO_3Na$ in [mol^{-1} dm^3] from all methods: EMF (21000)[2], FP (25600)[4] and ITC (19900) are in acceptable agreement.

8.2.2 α-CD/Surfactant Systems

The K_1 values for α-CD/C_nPyBr systems: 8190, 44200, 99700 and 110070 mol^{-1} dm^3 for C_{10}PyBr, C_{12}PyBr, C_{14}PyBr and C_{16}PyBr respectively, are higher compared to their corresponding values for the series ß-CD/C_nPyBr. This trend in K_1 values was also observed by Funasaki *et al*[11] using surface tension work. Wan-Yunus *et al*[2] carried out electrochemical measurements on α- and ß-CD inclusion complexes with C_{12}TAB and $C_{12}OSO_3Na$ and found K_1 values of approximately the same magnitude for both systems. A study of inclusion complexation involving phenyl-containing compounds by Takisawa *et al*[12,13] and the author's earlier work[14,15] show that K_1 for ß-CD > α-CD. A possible explanation[4] for this are the differences in the goodness-of-fit within the CD cavity to different guest molecules. Whereas the hydrocarbon tail of

a surfactant molecule fits snugly into α-CD, it rattles around inside the ß-CD. Phenyl moieties do not rattle around in ß-CD cavity instead they lead to stronger complexes compared to their counterparts with α-CD.

The Omega ITC K_1 values for 1:1 α-CD/C_nTAB inclusion complexes are 1920 and 5830 mol^{-1} dm^3 respectively for C_8TAB and C_{10}TAB. The K_1 value for α-CD/C_{14}TAB (60700 mol^{-1} dm^3) was derived from our electrochemical work. The trend in K_1 values for α-CD/C_nTAB systems is completed by results taken in this laboratory by Wan-Yunus[2] and Cristantino[7] on C_{12}TAB (K_1 = 17000) and C_{16}TAB (K_1 = 99700) respectively.

8.3 THE SECOND BINDING CONSTANT K_2

The K_2 values derived from electrochemical and ITC techniques together with other literature values from EMF and FP techniques are summarized in Table 8.2.

In effect the procedures to derive K_2 from the experimental data using both EMF and ITC experiments involve a least mean squares computer fitting procedure involving three unknown parameters in the EMF work (K_1, K_2, m_c) and four unknown parameters in the ITC experiment (ΔH°_1, ΔH°_2, K_1, K_2). In the EMF work we can get good fits to the data with K_1 values being consistent to ±15% but the K_2 value can differ by up to 100%. On the other hand in the ITC experiment we can still get good fits to the data but the goodness of fit criterion satisfies such a large range of both K_1 and K_2

values that in effect makes the exercise meaningless. This arises mainly because of the limited amount of raw experimental data available. If we fix K_1 from other independent experiments (e.g. EMF, FP) this reduces the fitting procedure to three unknowns. Although good fits are obtained the magnitudes of K_2 are still rather incosistent. The main conclusion which we can make is that the K_2 values are much smaller than the K_1 values. Indeed in many cases the error in the K_1 value is comparable with the magnitude of K_2. This is a situation which possibly accounts for the difficulties found in the fitting methods.

Table 8.2 The second binding constant K_2 for α- and ß-cyclodextrin systems

Surfactant	α-cyclodextrin			ß-cyclodextrin		
	EMF	ITC	Lit.	EMF	ITC	Lit.
$C_{12}PyBr$	310	797	-	-	-	-
$C_{14}PyBr$	280	2180	-	830	-	-
$C_{16}PyBr$	1600	8110	-	-	-	178[a]
$C_{12}TAB$	-	368	1000[b]	-	-	25[a], 52[c]
$C_{14}TAB$	6900	1760	2390-4340[d]	3060	-	56[a], 118[c]
$C_{16}TAB$	-	4640	20400[e]	-	33.1	9600[e], 126[a] 390[c]
$C_{10}OSO_3Na$	-	4230	-	-	-	-
$C_{14}OSO_3Na$	-	11000	15200[f]	-	32.8	290-600[g]
$C_{12}SO_3Na$	-	2360	-	-	-	-

[a](ref 1), [b](ref 2), [c](ref 5), [d](ref 3), [e](ref 7), [f](ref 17) and [g](ref 4)

The K_2 values are tabulated in Table 8.2 for both α- and ß-CD/surfactant systems. The consistency and reliability

observed for K_1 values from EMF, FP and ITC techniques is not observed for K_2 values. As discussed in our earlier publications[6,7] and by Wan-Yunus *et al*[2] there is too much uncertainty in these values to consider them quantitatively but however they have a qualitative value as indicators of the presence of 2:1 inclusion complexes. Nonetheless, the K_2 values always seem to increase with the alkyl chain of the surfactant.

8.4 INCLUSION COMPLEXES OF TETRAETHYLENE GLYCOL MONO N-OCTYL ETHER WITH α-, ß- and γ-CDs

A study of the inclusion complexation of a nonionic surfactant tetraethylene glycol mono n-octyl ether,

$$CH_3(CH_2)_7(-O-CH_2CH_2)_4-OH$$

with α-, ß- and γ-CDs was also carried out using the Omega ITC method. Tetraethylene glycol mono n-octyl ether is abbreviated as $C_8(OE)_4$.

The Omega ITC enthalpy profiles for the systems α-CD/$C_8(OE)_4$, ß-CD/$C_8(OE)_4$ and γ-CD/$C_8(OE)_4$ are non-sigmoidal and therefore considered unsuitable to derive inclusion enthalpies ΔH°. However, their equivalence region are wide which means that reasonably reliable n and K values can be derived.

The K_1 values tabulated in Table 7.4 (page 237) for α-CD/$C_8(OE)_4$, ß-CD/$C_8(OE)_4$ and γ-CD/$C_8(OE)_4$ show that by

increasing the size (radius) of the hydrophobic cavity (α-CD < ß-CD < γ-CD) there is a trend toward less stable complexes[18]. As expected, the tighter the fit of the surfactant molecule in the CD cavity, the more stable the complex. The trend in the binding constants of complexes of the nonionic surfactant $C_8(OE)_4$: α-CD > ß-CD > γ-CD; in Table 7.4 agrees with Funasaki's[11] surface tension data on another nonionic surfactant dodecyl maltoside. The fit of the surfactant hydrocarbon tail in the CD cavity which was described by Park and Song[4] as snugly in α-CD and rattling around in ß-CD could be fairly described as floating in γ-CD. Using Clarke's[19] description of this phenomenon, in α-CD there is the highest loss of motional freedom of a guest molecule due to 'tightness-of-fit'. This tendency decreases respectively in the ß-CD and γ-CD cavities.

The K_1 value of 5150 mol^{-1} dm^3 for α-CD/$C_8(OE)_4$ is higher compared to the α-CD/C_8 inclusion complexation of corresponding ionic surfactants: C_8TAB (K_1 = 1920) and C_8SO_3Na (K_1 = 1920) but is relatively close to the K_1 observed for α-CD/C_8OSO_3Na (7770 mol^{-1} dm^3). In order to explain these differences with other surfactants, it is the linear nature of the $C_8(OE)_4$ head group where one expects very little steric hindrance. If there is anything to inhibit the head group not being bound by a CD molecule, then probably it is the electronic effect of the etheric linkage oxygen and the hydroxyl group. For example, according to Park and Song[4], the more pronounced stability

of alkylsulfates inclusion complexes is due to the presence of this type of oxygen linking the sulfate group effectively making the alkyl chain longer. Therefore, to explain this discrepancy, it could be concluded that some parts of the head group participates in the binding process to make $C_8(OE)_4$ behaves like a C_9 hydrocarbon chain which is approximately one extra methylene group.

The K_1 value of 2270 mol^{-1} dm^3 for the ß-CD/$C_8(OE)_4$ inclusion complex compares well with the anionic surfactants: C_8OSO_3Na (K_1 = 1740) and C_8SO_3Na (K_1 = 1640) but higher compared to the cationic surfactants: C_8TAB (K_1 = 780). There is very little data to compare with the γ-CD/$C_8(OE)_4$ inclusion complex (600 mol^{-1} dm^3); however the trend is obvious.

8.5 THERMODYNAMIC PARAMETERS FOR INCLUSION COMPLEX FORMATION

8.5.1 1:1 Inclusional Complexes

The Omega ITC measurements provide a wider thermodynamic characterization of inclusion complex formation. In theory the stoichiometry number (n), equilibrium constant (K) and enthalpy (ΔH°) are obtained directly from a single Omega ITC experiment. The remaining thermodynamic parameters e.g. the free energy (ΔG°) and entropy (ΔS°) of inclusion are calculated as: $\Delta G^\circ = -RT\ln(55.55K)$ and $\Delta S^\circ = (\Delta H^\circ - \Delta G^\circ)/T$ respectively.

The enthalpy profiles for ß-CD 1:1 inclusion complexes with

C_{10}TAB, C_{12}TAB, C_{14}TAB and $C_{12}SO_3Na$; and α-CD 1:1 inclusion complexes with C_{10}TAB and C_8OSO_3Na exhibit good sigmoidal shapes. These systems satisfy the conditions for accurate non-linear least-squares computer fitting for the parameters n, K and ΔH°. Table 8.3 lists the thermodynamic parameters for these systems.

Table 8.3 Thermodynamic parameters for 1:1 α- and ß-CD:surfactant inclusion complexes

System	K	ΔH°	ΔG°	ΔS°	$-T\Delta S^\circ$
ß-CD/C_{10}TAB	3770	-7.0	-30.4	+78.4	-23.4
ß-CD/C_{12}TAB	22000	-9.6	-34.8	+84.2	-25.1
ß-CD/C_{14}TAB	51600	-13.0	-36.9	+80.0	-23.9
ß-CD/$C_{12}SO_3Na$	18400	-9.8	-34.3	+82.2	-24.5
α-CD/C_{10}TAB	5830	-26.3	-31.5	+17.5	-5.2
α-CD/C_8OSO_3Na	7770	-39.8	-32.2	-25.7	+7.7

The contribution of the entropy term ($-T\Delta S^\circ$) to the free energy (ΔG°) is larger than the enthalpy term (ΔH°) for ß-CD/surfactant inclusion complexes. This is clear evidence that the main contributing factor to inclusion complexation for ß-CD/surfactant systems is the release of 'high energy' and 'low entropy' water molecules which gain motional freedom in the bulk water leading to high entropy. Thus the ß-CD/surfactant systems in Table 8.3 are entropically driven.

The ß-CD/surfactant systems C_{10} to C_{12} show inclusional entropies with magnitudes lying within the range +82.2±2.2

J mol^{-1} K^{-1}. The almost constant values of these entropies indicate that probably the same amount of high energy water molecules are released into the bulk water by the different surfactants. The systems α-CD/C_{10}TAB and α-CD/C_8OSO_3Na show lower entropy changes (+17.5 and -25.7 J mol^{-1} K^{-1} respectively) whereas the inclusional process for α-CD/C_8OSO_3Na system is entropically unfavourable and is effectively a negative contribution to the free energy of the system. The system α-CD/C_{10}TAB shows a positive entropic contribution to the free energy of the system, but the contribution $T\Delta S^\circ$ (-5.2 kJ mol^{-1}) is smaller compared to ΔH° (-26.3 kJ mol^{-1}). Although it is well known that the main difference between ß-CD and α-CD inclusion complexes with surfactants is mainly attributed to goodness-of-fit, the relief of conformational strain can be attributed to high enthalpies in α-CD/surfactant systems.

A careful inspection of Table 8.3 show that inclusional enthalpies for ß-CD/surfactant systems increase in magnitude with the alkyl chain lengths as demonstrated by C_{10}TAB, C_{12}TAB and C_{14}TAB: -7.0, -9.6 and -13.0 kJ mol^{-1} respectively. This is opposed to the entropies which remain constant. We also observe that for the same alkyl chain length the enthalpies do not change much for surfactants with different head groups. For example the enthalpies for ß-CD/C_{12}TAB and ß-CD/$C_{12}SO_3Na$ have values of -9.6 and -9.8 kJ mol^{-1} respectively which are very close.

8.5.2 1:1 and 2:1 Inclusion Complexes

Due to difficulties with estimating the K_2 values from the fitting procedures the second CD binding thermodynamic parameters are only considered as rough estimates. However they are considered useful enough to explain the overall trend in the thermodynamic behaviour. The discussion in this section is based on the enthalpies measured using the Omega ITC technique.

Table 8.4 Apparent thermodynamic parameters for 1:1 and 2:1 α- and ß-CD/surfactant inclusion complexes

	K_1	K_2	ΔH°_1	ΔH°_2	ΔG°_1	ΔG°_2	ΔS°_1	ΔS°_2
α-CD/C_{12}TAB	17000	368	-31.4	-43.9	-34.1	-24.6	+9.1	-64.7
α-CD/C_{14}TAB	60700	1760	-30.5	-46.4	-37.3	-28.5	+22.6	-50.0
α-CD/C_{16}TAB	99200	4640	-27.6	-53.9	-38.5	-30.9	+36.4	-77.2
α-CD/C_{12}PyBr	44200	797	-30.0	-34.8	-36.5	-26.5	+21.7	-27.7
α-CD/C_{14}PyBr	99700	2180	-28.8	-44.7	-38.5	-29.0	+32.4	-52.7
α-CD/C_{16}PyBr	110000	8110	-32.2	-52.7	-38.7	-32.3	+21.9	-68.4
α-CD/$C_{10}OSO_3Na$	15000	4230	-7.5	-91.9	-33.8	-30.7	+88.1	-205.6
α-CD/$C_{14}OSO_3Na$	49300	11100	-20.9	-70.6	-36.8	-30.0	+53.2	-136.2
α-CD/$C_{12}SO_3Na$	19100	2360	-26.8	-47.7	-34.4	-29.2	+25.9	-61.9
ß-CD/C_{16}TAB	65300	33.1	-13.3	-94.9	-37.4	-18.6	+81.0	-255.8
ß-CD/$C_{14}OSO_3Na$	48300	32.8	-12.7	-185.6	-36.7	-18.6	+80.6	-560.1

Bearing in mind the possible error in the thermodynamic parameters ΔG°_2 and ΔS°_2 which result from the difficulties in estimating the values of K_2, any discussion concerning the results on Table 8.4 is meaningless. However it is possible to arrive at general conclusions in reference to the trends in the results tabulated in Table 8.4:

(a) The inclusional enthalpies ΔH°_1 are less in magnitude than ΔH°_2 for all systems. Moreover the quotients $\Delta H^\circ_2/\Delta H^\circ_1$ for ß-CD inclusion complexes systems are higher than the corresponding α-CD systems. Whereas ΔH°_2 values are observed to increase with the alkyl chain length in α-CD/C_nTAB and α-CD/C_nPyBr, ΔH°_1 is almost constant for the same systems. The trends in these parameters for the CD/anionic surfactant systems are not as clear as in the CD/cationic surfactant systems.

(b) The inclusional entropies ΔS°_1 are positive and similar to those observed for 1:1 inclusion complexes. On the other hand ΔS°_2 values are negative. Both increase in magnitude with the alkyl chain length. ΔS°_1 and ΔS°_2 for ß-CD systems are higher in magnitude compared to the corresponding α-CD systems. The second entropy term dominates the contribution to the total entropy of the system.

(c) The Free energies ΔG°_1 and ΔG°_2 can be described in a similar manner as K_1 and K_2 in relation to magnitude and dependence on the alkyl chain length.

The 1:1 ß-CD/surfactant systems can be concluded to be entropy deriven whereas on the other hand their counterparts 1:1 α-CD/surfactant systems are enthalpy driven. All CD/surfactant systems involving both 1:1 and 2:1 inclusion complexes are enthalpy driven.

8.6 ALKYL CHAIN DEPENDENCE OF INCLUSION COMPLEX FORMATION

The first binding constant K_1 for the 1:1 surfactant inclusion complexes with both α- and ß-cyclodextrins increases with alkyl chain length but the rate of increase slows down for the higher alkyl chain length surfactants. In the linear region the parameters A and B according to $\Delta G^\circ_1 = A - Bn$, where $\Delta G^\circ_1 = -RT\ln(55.55K_1)$ and n is the alkyl chain length, are summarized in Table 8.5. It must be emphasized that these parameters are only rough estimates.

Table 8.5 Dependence parameters for first cationic inclusion complexes with α- and ß-CDs

System	n	A	B	r	Method
		$\Delta G^\circ_1 = A - Bn$			
α-CD/C_nPyBr	10,12,14	-17.2	1.6	-0.9835	EMF
ß-CD/C_nPyBr	10,12,14	-12.9	1.8	-0.9805	EMF
α-CD/C_nTAB	8,10,12	-17.3	1.4	-0.9993	ITC
ß-CD/C_nTAB	8,10,12,14	-5.8	2.4	-0.9984	ITC
		$\Delta G^\circ_2 = A - Bn$			
α-CD/C_nPyBr	12,14,16	-11.2	1.0	-0.8391	EMF
α-CD/C_nPyBr	12,14,16	-9.1	1.4	-0.9970	ITC
α-CD/C_nTAB	12,14,16	-5.0	1.9	-0.9871	EMF
α-CD/C_nTAB	12,14,16	-6.0	1.6	-0.9910	ITC

The slope of the straight line part of the graph gives an estimate of the free energy change of a methylene group from water into the cyclodextrin cavity. The estimates of free energies of transfer of methylene groups are higher

Figure 8-1: $-\Delta G^{o}_{1}$ dependence on alkyl chain length for C_nPyBr

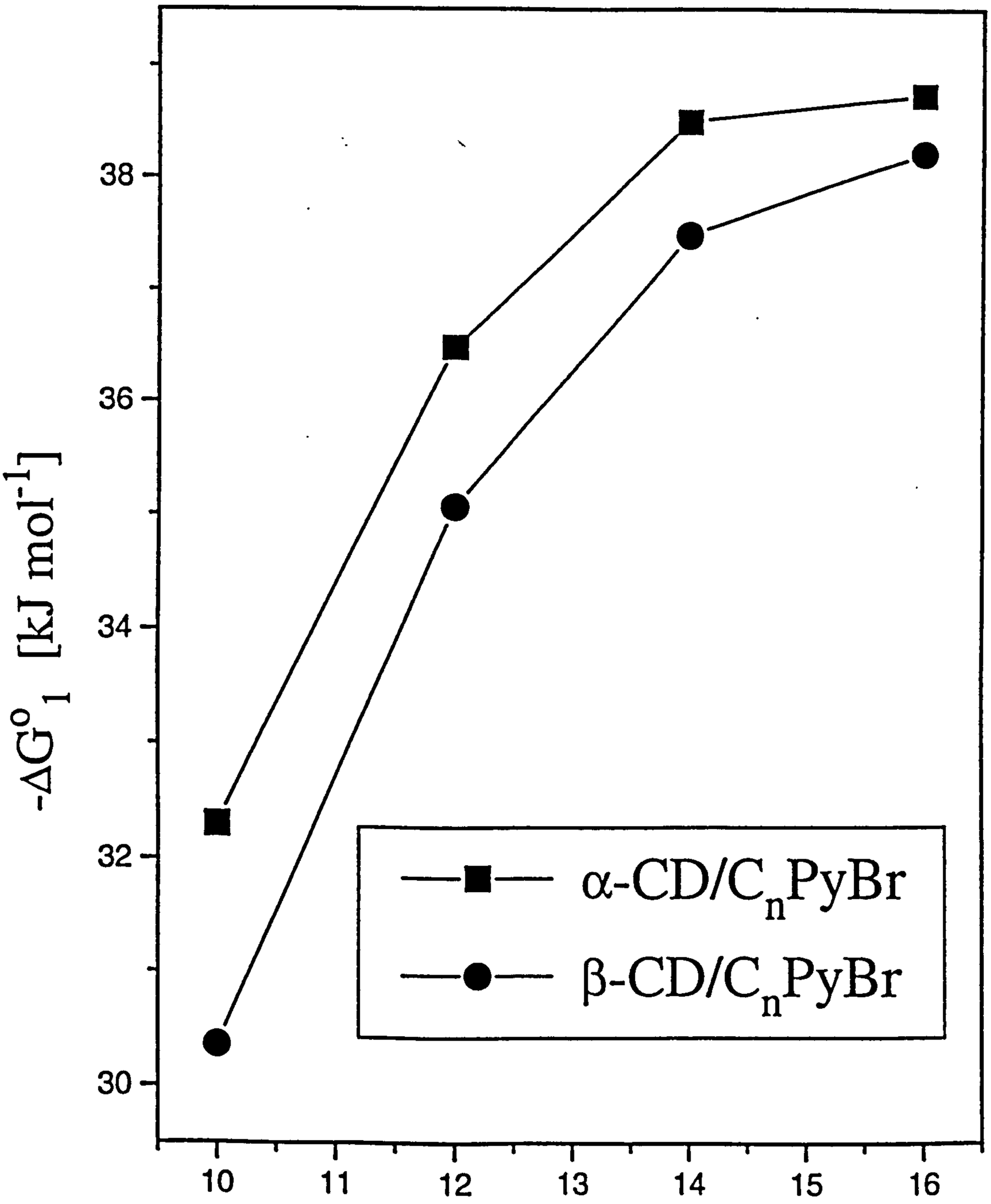

Figure 8-2: ΔG^{o}_{1} dependence on alkyl chain length for C_nTAB

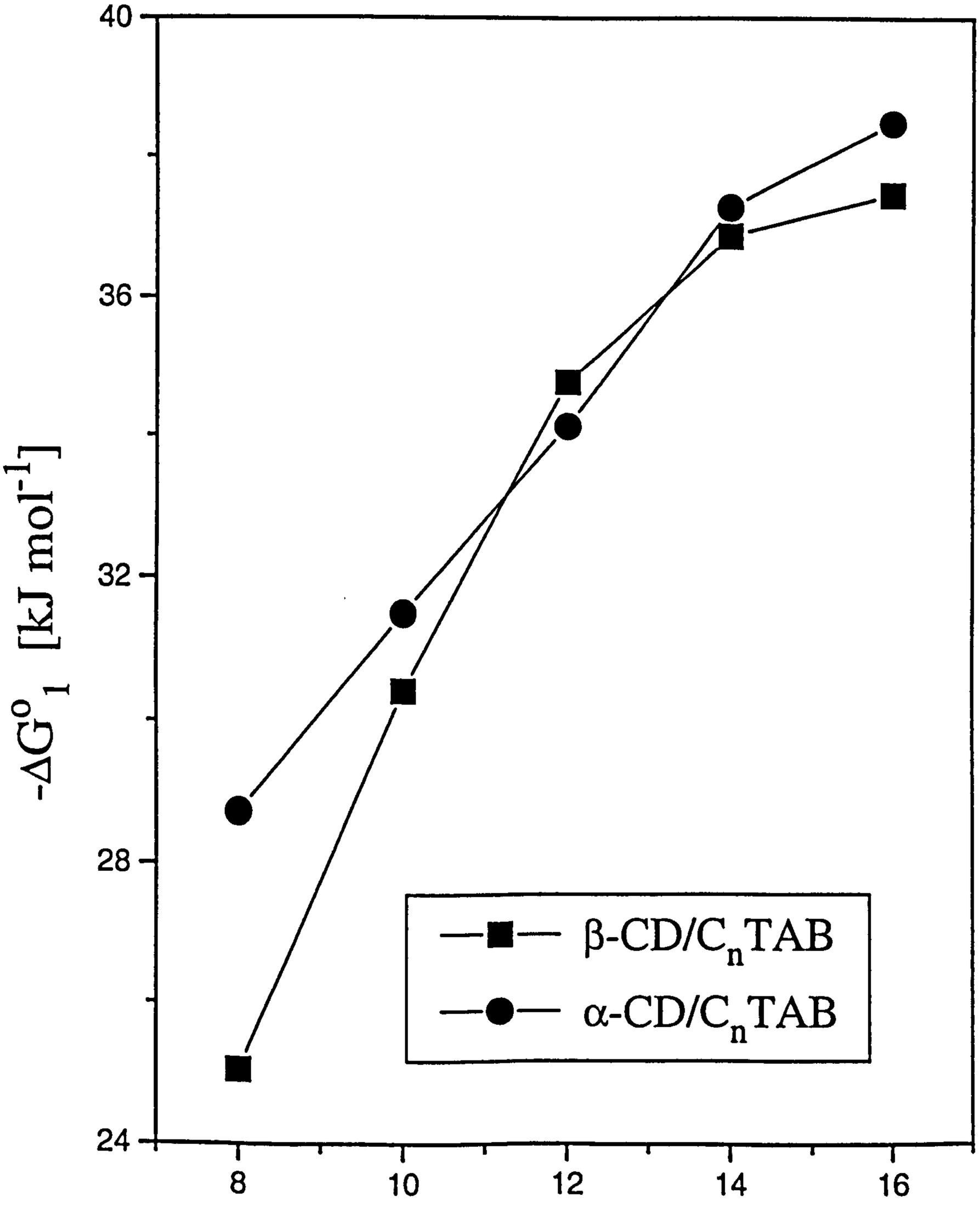

Figure 8-3: ΔG^{o}_{2} dependence on alkyl chain length for α-CD systems

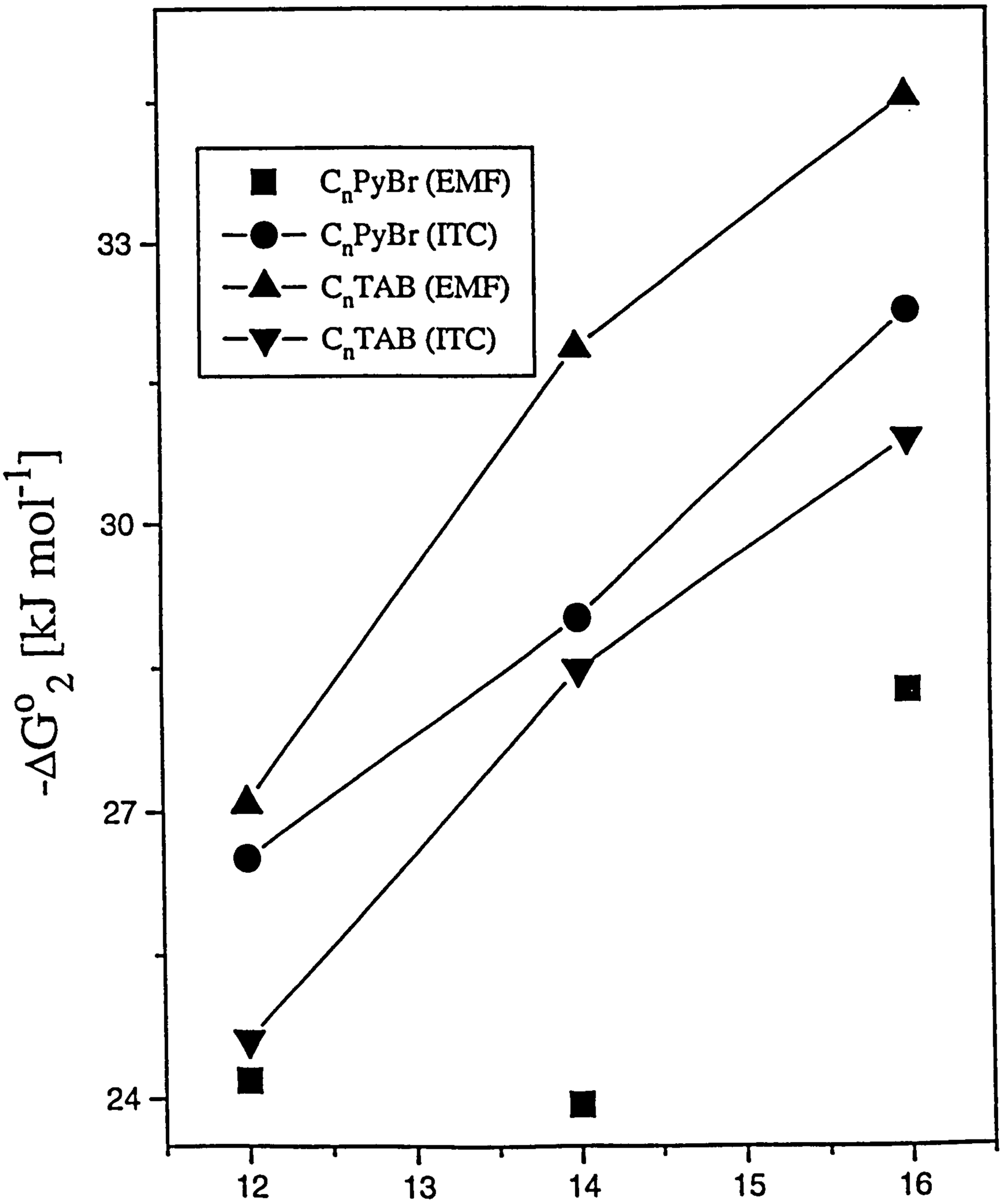

for ß-CD/C_nPyBr and ß-CD/C_nTAB (-1.8 and -2.4 kJ mol^{-1}) as compared to α-CD/C_nPyBr and α-CD/C_nTAB (-1.6 and -1.4 kJ mol^{-1}). This leads to the conclusion that the binding constants K_1 for ß-CD increase more rapidly than that of α-CD with increasing chain length. This observation is in agreement with the data of Satake *et al*[20,21] on α- and ß-CD inclusion complexes with sodium 1-alkanesulfonates. Whereas the K_1 values for both α- and ß-CD/C_nPyBr systems show a levelling-off at C_{14}, the K_1 for α- and ß-CD/C_nTAB level-off at C_{12} and C_{14} respectively. This suggests that for inclusion complex formation in a homologous series of surfactants, the hydrophobic cavity of ß-CD is supposed to accomodate the hydrocarbon tail in a similar manner to α-CD even though the degree of interactions is different. The plots of ΔG°_1 against n are shown in Figures 8-1 and 8-2 for C_nPyBr and C_nTAB systems respectively.

The K_2 values for the α-CD/cationic surfactant systems increase with the alkyl chain length giving rough estimates of the free energy of transfer of magnitudes ≈-1.8 and -1.4 kJ mol^{-1} for α-CD/C_nTAB and α-CD/C_nPyBr respectively. The magnitudes of these rough estimates are close to those observed for the K_1 values. This observation in a way indicates: (i) the presence of a "consecutive binding mechanism" rather than "independent binding mechanism", (ii) that the second CD binding is also driven by hydrophobic forces i.e. dependent on alkyl chain length. The plots of ΔG°_2 against n are shown in Figure 8-3.

8.7 REFERENCES

1. JEZEQUEL, D.; MAYAFFRE, A. and LETELLIER, P. *Can. J. Chem.*, 69 (1991) 1865.

2. WAN-YUNUS, W.M.Z.; TAYLOR, J.; BLOOR, D.M.; HALL, D.G. and WYN-JONES, E. *J. Phys. Chem.*, 96 (1992) 8979.

3. TOMINAGA, T.; HACHISU, D. and KAMADO, M. *Langmuir* (1994) In press.

4. PARK, J.W. and SONG, H.J. *J. Phys. Chem.*, 93 (1989) 6454.

5. PARK, J.W. and PARK, K. H. *J. Incl. Phenom.* (1994) In Press.

6. MWAKIBETE, H.; BLOOR, D.M. and WYN-JONES, E. *Langmuir*, 10 (1994) 3328.

7. MWAKIBETE, H.; CRISTANTINO, R.; BLOOR, D.M.; HOLZWARTH, J.F. and WYN-JONES, E. *Langmuir* (1994) In Press.

8. PALEPU, R.; RICHARDSON, J.E. and REINSBOROUGH, V.C. *Langmuir*, 5 (1989) 218.

9. LEWIS, E.A. and HANSEN, L.D. *J. Chem. Soc. Perkin Trans. II* (1973) 2081.

10. PAULI, W.A. and LACH, J.L. *J. Pharm. Sci.*, 54 (1965) 1745.

11. FUNASAKI, N.; YODO, H.; HADA, S. and NEYA, S. *Bull. Chem. Soc. Jpn.*, 65 (1992) 1323.

12. TAKISAWA, N.; HALL, D.G.; WYN-JONES, E. and BROWN, P. *J. Chem. Soc. Faraday Trans. 1*, 84 (1988) 3059.

13. TAKISAWA, N.; SHIRAHAMA, K. and TANAKA, I. *Colloid Polym. Sci.*, 271 (1993) 499.

14. MWAKIBETE, H.; BLOOR, D.M. and WYN-JONES, E. *J. Incl. Phenom.* 10 (1991) 497.

15. THOMASON, M.A.; MWAKIBETE, H. and WYN-JONES, E. *J. Chem. Soc. Faraday Trans.*, 86 (1990) 1511.

16. HERSEY, A.; ROBINSON, B.H. and KELLY, H.C. *J. Chem. Soc., Faraday Trans. 1*, 82 (1986) 1271.

17. LUKAS, T.M. PhD Thesis, UNIVERSITY OF SALFORD (1991).

18. LIVERI, V.T.; CAVALLARO, G.; GIOMMONA, G.; PITARRESI, G.; PUGLISI, G. and VENTURA, C. *Thermochimica Acta*, 199 (1992) 125.

19. CLARKE, R.J.; COATES, J.H. and LINCOLN, S. *Adv. Carbohydr. Chem. & Biochem.*, 46 (1988) 205.

20. SATAKE, I.; YOSHIDA, S.; HAYAKAWA, K.; MAEDA, T. and KUSUMOTO, Y. *Bull. Chem. Soc. Jpn.*, 59 (1986) 3991.

21. SATAKE, I.; IKENOUE, T.; TAKESHITA, T.; HAYAKAWA, K. and MAEDA, T. *Bull. Chem. Soc. Jpn.*, 58 (1986) 3991.

APPENDIX 4: Electrochemical data for CTAB/SALT and POLYMER/CTAB/SALT systems

Table 4.A1: m_1, m_2 and $\gamma_\pm$ in CTAB/10^{-5} mol dm^{-3} NaBr system

C_1 mM	$E_{cell,I}$ mV	$E_{cell,II}$ mV	m_1 mM	m_2 mM	$\gamma_\pm$
0.888	390.3	201.3	0.601	2.137	0.958976
1.014	388.6	202.3	0.559	2.417	0.957336
1.186	388.4	203.0	0.554	2.524	0.956656
1.575	388.1	204.7	0.547	2.781	0.955040
1.961	387.3	205.1	0.529	2.937	0.954175
2.344	386.1	205.6	0.503	3.174	0.952899
3.101	383.3	206.1	0.447	3.680	0.950295
6.716	373.6	204.0	0.296	5.095	0.943746
7.407	372.2	207.2	0.279	6.373	0.938049
10.714	368.1	204.8	0.234	6.788	0.936499
13.793	364.9	203.4	0.205	7.304	0.934531
19.355	361.4	204.3	0.176	8.961	0.928448
24.242	358.6	202.9	0.157	9.476	0.926729
28.571	357.1	201.5	0.147	9.444	0.926869

	Slope (mV/dec.)	Inter. (mV)	Cor. Coef.
Sodium Electrode:	55.2	346.9	0.9998
Bromide Electrode:	110.7	489.4	0.9996

Table 4.A2: m_1, m_2 and $\gamma_\pm$ in CTAB/10^{-4} mol dm^{-3} NaBr system

C_1 mM	$E_{cell,I}$ mV	$E_{cell,II}$ mV	m_1 mM	m_2 mM	$\gamma_\pm$
1.130	191.6	181.9	1.090	1.380	0.960221
1.360	191.7	184.0	1.100	1.500	0.959343
1.580	191.4	185.3	1.090	1.600	0.958724
1.800	190.5	185.7	1.050	1.680	0.958392
2.100	190.3	186.1	1.040	1.780	0.958162
2.450	189.6	186.8	1.010	1.830	0.957668
2.780	189.0	186.7	0.987	1.860	0.957579
3.450	187.4	187.2	0.926	2.030	0.956878
5.080	183.2	187.7	0.784	2.450	0.955042
6.650	180.6	188.2	0.707	2.780	0.953470
8.160	177.7	188.5	0.630	3.170	0.951616
9.620	176.6	188.9	0.603	3.380	0.950615

	Slope (mV/dec.)	Inter. (mV)	Cor. Coef.
Sodium Electrode:	58.0	363.3	0.9997
Bromide Electrode:	115.5	519.9	0.9998

Table 4.A3: m_1, m_2 and $\gamma_\pm$ in CTAB /5×10^{-4} mol dm^{-3} NaBr system

C_1	$E_{cell,I}$	$E_{cell,II}$	m_1	m_2	$\gamma_\pm$
mM	mV	mV	mM	mM	
0.794	284.5	156.5	0.675	1.260	0.961269
0.951	284.6	158.8	0.677	1.370	0.960405
1.11	285.3	158.7	0.696	1.330	0.960580
1.26	185.5	159.3	0.702	1.350	0.960386
2.50	284.7	162.0	0.680	1.550	0.958104
4.87	281.3	164.8	0.595	1.980	0.956734
7.41	276.9	165.7	0.501	2.450	0.954346
10.70	271.8	166.5	0.411	3.100	0.950992
13.80	269.1	166.9	0.370	3.520	0.948920

	Slope (mV/dec.)	Inter. (mV)	Cor. Coef.
Sodium Electrode:	58.5	470.7	0.9981
Bromide Electrode:	112.6	498.4	0.9941

Table 4.A4: m_1, m_2 and $\gamma_\pm$ in CTAB/10^{-3} mol dm^{-3} NaBr system

C_1	$E_{cell,I}$	$E_{cell,II}$	m_1	m_2	$\gamma_\pm$
mM	mV	mV	mM	mM	
0.636	175.0	54.8	0.486	2.950	0.948671
0.794	180.0	61.7	0.603	3.130	0.947103
0.990	181.3	64.5	0.637	3.310	0.945996
1.110	183.6	65.5	0.704	3.110	0.946656
1.230	184.3	65.9	0.725	3.070	0.946778
1.480	184.6	66.4	0.734	3.090	0.946618
1.960	185.0	67.5	0.747	3.170	0.946121
2.910	184.6	67.6	0.734	3.240	0.945833
3.850	183.4	67.8	0.698	3.450	0.944995
5.660	179.8	68.3	0.597	4.130	0.942208
7.410	178.2	68.7	0.558	4.510	0.940657
10.700	173.3	69.5	0.452	5.810	0.935578
13.800	169.5	69.8	0.384	6.980	0.931281
16.700	166.0	70.0	0.330	8.260	0.926917
23.100	161.8	71.0	0.275	10.400	0.920045
28.600	159.2	71.1	0.246	11.800	0.916067
35.500	153.6	72.0	0.194	16.000	0.905443
41.176	151.5	72.3	0.177	17.800	0.901104

	Slope (mV/dec.)	Inter. (mV)	Cor. Coef.
Sodium Electrode:	56.5	375.3	0.9989
Bromide Electrode:	113.9	432.8	0.9991

Table 4.A5: m_1, m_2 and $\gamma_\pm$ in 0.5%PPO/CTAB/10^{-4} mol dm^{-3} NaBr system

C_1 mM	$E_{cell,I}$ mV	$E_{cell,II}$ mV	m_1 mM	m_2 mM	$\gamma_\pm$
0.383	365.4	178.8	0.268	0.479	0.976640
0.509	365.8	184.6	0.272	0.605	0.974965
0.762	366.0	193.2	0.275	0.844	0.972156
1.190	365.2	200.1	0.266	1.160	0.968982
1.570	364.9	203.7	0.263	1.360	0.967097
2.340	363.8	207.2	0.251	1.650	0.964683
3.100	361.4	211.0	0.227	2.140	0.960994
3.850	360.6	212.7	0.220	2.380	0.959318
5.660	357.1	215.9	0.191	3.160	0.954345
7.410	356.4	218.2	0.185	3.590	0.951809
10.700	353.0	220.0	0.161	4.480	0.947048
13.800	350.1	222.1	0.143	5.550	0.941896
19.400	346.4	225.2	0.123	7.450	0.933932
24.200	341.9	226.0	0.103	9.390	0.926888
32.400	340.1	227.6	0.095	10.900	0.921956
39.000	334.5	225.5	0.075	12.800	0.916469

	Slope (mV/dec.)	Inter. (mV)	Cor. Coef.
Sodium Electrode:	56.1	565.9	0.9998
Bromide Electrode:	114.0	572.8	0.9985

Table 4.A6: m_1, m_2 and $\gamma_\pm$ in 0.5%PVME/CTAB/10^{-4} mol dm^{-3} NaBr system

C_1 mM	$E_{cell,I}$ mV	$E_{cell,II}$ mV	m_1 mM	m_2 mM	$\gamma_\pm$
0.589	148.8	142.4	0.261	0.847	0.972279
0.686	149.2	146.2	0.265	0.982	0.970790
0.784	149.5	149.2	0.268	1.104	0.969515
0.977	150.2	154.0	0.276	1.321	0.967376
1.169	149.9	157.1	0.272	1.530	0.965545
1.361	150.0	160.6	0.273	1.774	0.963498
1.551	149.9	162.6	0.272	1.944	0.962165
1.929	149.7	166.5	0.270	2.324	0.959358
2.304	149.3	168.9	0.266	2.625	0.957304
2.675	148.6	171.0	0.258	2.964	0.955139
3.042	148.5	172.9	0.257	3.236	0.953459
3.821	148.7	175.7	0.259	3.630	0.951122
4.375	147.8	177.4	0.250	4.066	0.948759
5.726	148.0	180.0	0.252	4.524	0.946343
8.282	145.4	183.9	0.227	6.012	0.939443

	Slope (mV/dec.)	Inter. (mV)	Cor. Coef.
Sodium Electrode:	56.8	396.6	0.9990
Bromide Electrode:	112.9	559.8	0.9993

Table 4.A7: m_1, m_2 and $\gamma_\pm$ in 0.5%EHEC/CTAB/10^{-4} mol dm^{-3} NaBr system

C_1 mM	$E_{cell,I}$ mV	$E_{cell,II}$ mV	m_1 mM	m_2 mM	$\gamma_\pm$
0.754	160.6	150.0	0.472	1.050	0.968034
0.878	161.6	153.9	0.491	1.200	0.966512
1.000	162.0	156.2	0.499	1.310	0.965511
1.250	163.2	160.4	0.524	1.500	0.963710
1.496	162.7	162.8	0.513	1.700	0.962197
1.741	163.0	164.9	0.519	1.840	0.961065
1.985	162.4	166.4	0.507	2.020	0.959870
2.318	162.2	168.2	0.503	2.200	0.958586
2.694	161.4	169.5	0.488	2.410	0.957273
3.067	160.9	170.8	0.478	2.600	0.956044
3.804	160.0	172.5	0.461	2.910	0.954188
4.530	158.1	173.8	0.428	3.340	0.951846
5.949	156.2	175.6	0.397	3.910	0.948800
7.326	153.3	177.1	0.354	4.720	0.944864
10.596	150.6	179.7	0.318	5.940	0.939370
13.641	147.6	181.5	0.282	7.310	0.933851
19.142	144.9	182.9	0.254	8.730	0.928657
23.976	138.6	184.5	0.198	12.300	0.917429

	Slope (mV/dec.)	Inter. (mV)	Cor. Coef.
Sodium Electrode:	58.2	353.9	0.9980
Bromide Electrode:	107.4	490.0	0.9988

APPENDIX 6 Electrochemical data for Inclusion complexation between 1-alkylpyridinium bromide and Tetradecyltrimethylammonium bromide with α- and ß-cyclodextrin systems

DATA-A11: Decylpyridinium bromide/α-CD C_c = 0.915 mol dm^3

C_1/mM	E_{Na} (mV)	C_1/mM	E_{Na} (mV)	C_1/mM	E_{Na} (mV)
0.0399	-81.5	2.12	29.2	22.7	89.5
0.0798	-74.7	2.41	32.8	27.9	93.5
0.120	-69.9	2.69	36.9	32.9	96.8
0.159	-65.0	2.96	38.6	37.6	99.1
0.239	-55.2	3.24	42.6	46.3	101.0
0.317	-49.4	3.50	45.3	54.2	100.5
0.396	-42.5	4.03	49.9	61.3	100.0
0.474	-36.9	4.54	53.3	67.7	97.8
0.552	-31.6	5.52	58.9	79.1	97.3
0.630	-26.8	6.44	62.9	88.7	95.0
0.784	-17.3	7.32	66.3	97.0	91.7
0.938	-9.2	8.00	68.2	104.0	88.0
1.09	-0.4	11.1	75.5	109.0	88.7
1.24	6.0	14.1	80.7		
1.54	15.7	17.1	84.4		
1.83	23.1	19.9	88.0		

E°=-3.9, Slope=57.4, Inter.=189.4, Cor. Coef.=0.999, SS=0.0015.

DATA-A12: Decylpyridinium bromide/α-CD C_c = 2.196 mol dm^3

C_1/mM	E_{Na} (mV)	C_1/mM	E_{Na} (mV)	C_1/mM	E_{Na} (mV)
0.0739	-160.8	2.626	-10.8	37.71	61.3
0.1478	-143.4	2.913	-4.8	41.37	62.4
0.2955	-116.3	3.199	0.0	43.48	63.0
0.4429	-102.2	3.485	4.3	46.19	63.8
0.5901	-92.3	4.053	10.4	48.81	63.7
0.7370	-84.2	4.618	16.0	52.85	61.6
0.8837	-76.5	5.179	19.7	60.00	59.1
1.030	-68.8	5.736	23.3	66.41	58.7
1.176	-63.3	6.841	28.5	72.20	55.9
1.322	-57.2	7.933	32.8	77.44	54.5
1.468	-51.3	9.011	35.9	82.22	53.6
1.614	-45.5	11.13	38.6	86.60	53.3
1.759	-39.7	13.19	43.7	89.84	53.1
1.904	-34.4	17.18	49.4		
2.049	-15.7	20.99	53.2		
2.194	-23.3	24.63	55.3		
2.338	-18.9	27.93	57.6		
2.482	-14.1	31.45	59.2		

E°=6.8, Slope=58.0, Inter.=177.3, Cor. Coef.=0.998, SS=0.0076.

DATA-B11: Decylpyridinium bromide/ß-CD C_c = 1.038 mol dm^3

C_1/mM	E_{Na} (mV)	C_1/mM	E_{Na} (mV)	C_1/mM	E_{Na} (mV)
0.0799	-115.7	2.372	6.2	22.69	54.6
0.1598	-93.6	2.528	8.5	26.63	57.5
0.2397	-80.3	2.839	11.9	30.39	59.5
0.3194	-70.4	3.149	15.0	33.99	61.1
0.4788	-56.0	3.459	17.6	40.76	62.1
0.6379	-45.9	3.768	20.0	44.72	62.5
0.7968	-36.7	4.382	24.1	47.00	62.2
0.9554	-29.2	4.992	27.2	52.78	61.3
1.114	-22.8	6.202	32.2	57.14	59.6
1.272	-17.9	7.396	35.8	64.86	60.0
1.430	-13.6	8.576	39.0	71.79	56.2
1.587	-8.7	9.741	41.3	78.08	53.3
1.745	-5.4	12.03	45.4	83.72	50.4
1.902	-1.9	14.26	47.9	88.89	50.6
2.059	0.9	16.45	50.6	93.62	50.3
2.215	3.6	20.03	52.2		

E°=7.2, Slope=58.0, Inter.=177.3, Cor. Coef.=0.998, SS=0.0067.

DATA-B12: Decylpyridinium bromide/ß-CD C_c = 2.076 mol dm^3

C_1/mM	E_{Na} (mV)	C_1/mM	E_{Na} (mV)	C_1/mM	E_{Na} (mV)
0.0799	-122.2	2.372	-8.6	14.26	48.5
0.1598	-102.5	2.528	-5.4	16.45	51.8
0.2397	-88.8	2.839	0.8	20.03	56.6
0.3194	-82.0	3.149	6.2	26.63	58.1
0.4788	-69.4	3.459	9.8	30.39	60.3
0.6379	-62.1	3.768	14.8	33.99	61.8
0.7968	-54.8	4.075	17.6	40.76	63.0
0.9554	-49.1	4.382	20.3	44.72	63.9
1.114	-42.8	4.688	22.3	47.00	64.0
1.272	-37.9	4.992	24.9	52.78	63.1
1.430	-33.0	5.599	28.4	57.14	63.4
1.587	-28.9	6.202	31.5	64.86	60.2
1.745	-23.7	7.396	36.1	71.79	56.3
1.902	-19.8	8.576	39.5	78.08	54.1
2.059	-15.7	9.741	42.5	83.72	57.8
2.215	-11.8	12.03	46.6	88.89	55.0
				93.62	55.0

E°=6.7, Slope=58.0, Inter.=177.3, Cor. Coef.=0.998, SS=0.0023.

DATA-B13: Decylpyridinium bromide/ß-CD C_c = 3.114 mol dm^{-3}

C_1/mM	E_{Na} (mV)	C_1/mM	E_{Na} (mV)	C_1/mM	E_{Na} (mV)
0.0799	-127.9	2.528	-23.2	20.03	50.2
0.1598	-113.0	2.839	-17.3	22.69	53.0
0.2397	-101.1	3.149	-11.5	26.63	55.7
0.3194	-94.6	3.459	-6.0	33.99	58.7
0.4788	-81.1	3.768	-1.2	40.76	60.0
0.6379	-72.9	4.075	3.4	44.72	60.9
0.7968	-66.2	4.382	6.8	47.00	61.2
0.9554	-61.5	4.688	10.5	57.14	59.6
1.114	-56.3	4.992	13.7	64.86	57.4
1.272	-52.6	5.599	18.6	71.79	57.2
1.430	-48.2	6.202	22.4	78.08	52.5
1.587	-43.7	7.396	28.7	64.86	54.2
1.745	-39.8	8.576	33.2	71.79	53.1
1.902	-37.0	9.741	36.5	93.62	53.9
2.059	-33.0	12.03	41.9		
2.215	-30.2	14.26	44.4		
2.372	-26.1	16.45	47.6		

E°=8.6, Slope=58.0, Inter.=177.3, Cor. Coef.=0.998, SS=0.0035.

DATA-A21: Dodecylpyridinium bromide/α-CD C_c = 0.458 mmol dm^{-3}

C_1/mM	E_{Na} (mV)	C_1/mM	E_{Na} (mV)	C_1/mM	E_{Na} (mV)
0.0399	23.5	1.2638	168.7	12.2807	228.2
0.0799	28.6	1.5748	176.3	13.7931	227.6
0.1199	47.3	1.8838	182.4	16.6667	227.1
0.1597	56.7	2.1909	187.2	19.3548	225.3
0.1996	65.8	2.4961	191.2	21.8750	225.0
0.2394	75.2	3.1008	197.5	24.2424	224.2
0.2792	84.0	3.6980	202.4	28.5714	223.0
0.3189	91.4	4.2879	206.5	32.4324	220.7
0.3984	103.0	4.8706	209.4	35.8974	217.5
0.4777	117.8	6.0150	214.8	39.0244	217.0
0.5588	127.5	7.4074	218.5	41.8605	215.1
0.6359	136.2	9.0909	224.3	44.4444	213.2
0.7937	147.7	9.9099	225.8	46.8085	210.5
0.9509	157.0	10.7143	227.4	48.9796	211.5
1.1076	163.5	11.5044	228.3	50.9804	212.2

E°=0, Slope=57.7, Inter.=347.9, Cor. Coef.=0.999, SS=0.0028.

DATA-A22: Dodecylpyridinium bromide/α-CD C_c = 0.686 mmol dm^{-3}

C_I/mM	E_{Na} (mV)	C_I/mM	E_{Na} (mV)	C_I/mM	E_{Na} (mV)
0.0399	-42.9	0.8723	93.0	9.0909	175.1
0.0799	-28.8	0.9509	98.1	9.9099	176.3
0.1199	-14.2	1.0293	102.4	10.7143	177.6
0.1597	-5.0	1.1076	107.0	11.5044	178.7
0.1996	2.5	1.2638	113.2	12.2807	179.1
0.2394	11.0	1.5748	122.0	13.7931	179.1
0.2792	19.1	1.8838	130.0	19.3548	176.6
0.3189	24.6	2.1909	136.6	24.2424	174.7
0.3984	36.7	2.4961	139.9	28.5714	173.2
0.4777	48.5	3.1008	147.1	32.4324	163.0
0.5569	58.8	3.6980	151.7	39.0244	169.5
0.5964	63.9	4.2879	155.2	44.4444	168.3
0.6359	68.7	4.8706	158.9	48.9796	165.1
0.7149	77.7	6.0150	163.2	50.9804	165.0
0.7937	85.4	7.4074	169.4		

E°=49.1, Slope=57.7, Inter.=347.9, Cor. Coef.=0.999, SS=0.0013.

DATA-A23: Dodecylpyridinium bromide/α-CD C_c=0.915 mmol dm^{-3}

C_I/mM	E_{Na} (mV)	C_I/mM	E_{Na} (mV)	C_I/mM	E_{Na} (mV)
0.0199	-23.5	0.6319	91.4	8.3333	215.4
0.0399	-12.6	0.7874	106.9	9.6774	218.1
0.0599	-0.9	0.9419	121.3	10.9375	220.9
0.0798	6.8	1.0954	133.5	12.1212	221.6
0.0998	12.6	1.2480	143.0	13.2352	221.5
0.1197	17.4	1.5503	157.6	14.2857	220.3
0.1396	22.3	1.8489	166.6	16.2162	220.3
0.1594	27.1	2.1439	172.8	17.9487	221.4
0.1992	35.1	2.4353	177.9	19.5121	220.9
0.2388	40.7	3.0075	186.5	20.9302	221.4
0.2784	46.5	3.5661	191.5	22.2222	220.6
0.3179	51.2	4.1116	196.3	23.4042	219.1
0.3968	61.4	4.6444	200.3	24.4897	218.5
0.4754	70.7	5.3571	204.5	25.4901	217.1
0.5537	79.8	6.8965	209.8		

E°=7.3, Slope=57.7, Inter.=347.9, Cor. Coef.=0.999, SS=0.0012.

DATA-B21: Dodecylpyridinium bromide/α-CD C_c = 0.433 mmol dm^3

C_1/mM	E_{Na} (mV)	C_1/mM	E_{Na} (mV)	C_1/mM	E_{Na} (mV)
0.0399	-13.5	1.2638	112.1	12.2807	174.2
0.0799	-2.3	1.5748	120.2	13.7931	173.5
0.1199	10.8	1.8838	126.1	19.3548	172.2
0.1597	20.0	2.1909	131.1	24.2424	170.7
0.1996	25.8	2.4961	134.8	28.5714	169.7
0.2394	32.4	3.1008	141.3	32.4324	168.3
0.2792	41.4	3.6980	146.9	39.0244	166.7
0.3189	48.0	4.2879	150.9	44.4444	164.9
0.3984	57.1	4.8706	153.7	48.9796	164.0
0.4777	66.3	6.0150	159.3	50.9804	162.7
0.5568	75.4	7.4074	164.1		
0.6359	81.5	9.0909	169.3		
0.7937	92.8	9.9099	170.4		
0.9509	100.6	10.7143	173.3		
1.1076	107.3	11.5044	174.4		

E°=54.9, Slope=57.7, Inter.=347.9, Cor. Coef.=0.999, SS=0.0167.

DATA-B22: Dodecylpyridinium bromide/α-CD C_c = 0.649 mmol dm^3

C_1/mM	E_{Na} (mV)	C_1/mM	E_{Na} (mV)	C_1/mM	E_{Na} (mV)
0.0399	-17.8	1.2638	99.0	12.2807	165.2
0.0799	-1.6	1.5748	108.4	13.7931	165.3
0.1199	5.4	1.8838	115.3	19.3548	164.0
0.1597	6.6	2.1909	120.5	24.2424	162.7
0.1996	12.7	2.4961	124.9	28.5714	161.5
0.2394	18.8	3.1008	131.9	32.4324	160.0
0.2792	23.6	3.6980	137.1	39.0244	158.0
0.3189	28.5	4.2879	141.2	44.4444	156.1
0.3984	37.2	4.8706	144.6	48.9796	154.1
0.4777	46.2	6.0150	150.0	50.9804	152.8
0.5568	53.1	7.4074	154.6		
0.6359	60.4	9.0909	159.6		
0.7937	73.3	9.9099	162.0		
0.9509	84.0	10.7143	163.4		
1.1076	92.4	11.5044	164.5		

E°=63.7, Slope=57.7, Inter.=347.9, Cor. Coef.=0.999, SS=0.0046.

DATA-B23: Dodecylpyridinium bromide/α-CD C_c = 0.865 mmol dm^{-3}

C_I/mM	E_{Na} (mV)	C_I/mM	E_{Na} (mV)	C_I/mM	E_{Na} (mV)
0.0399	-54.8	1.2638	77.4	12.2807	151.2
0.0799	-45.7	1.5748	89.7	13.7931	150.8
0.1199	-31.4	1.8838	97.8	19.3548	148.8
0.1597	-21.3	2.1909	104.8	24.2424	147.2
0.1996	-14.9	2.4961	109.4	28.5714	146.0
0.2394	-9.7	3.1008	117.4	32.4324	145.2
0.2792	-2.6	3.6980	122.8	39.0244	143.0
0.3189	2.5	4.2879	128.2	44.4444	140.9
0.3984	10.7	4.8706	131.2	48.9796	139.6
0.4777	19.2	6.0150	137.2	50.9804	139.2
0.5568	26.1	7.4074	141.5		
0.6359	32.7	9.0909	146.6		
0.7937	45.1	9.9099	148.9		
0.9509	57.7	10.7143	150.3		
1.1076	68.8	11.5044	151.0		

E°=77.2, Slope=57.7, Inter.=347.9, Cor. Coef.=0.999, SS=0.0020.

DATA-A31: Tetradecylpyridinium bromide/α-CD C_c=0.458 mol dm^{-3}

C_I/mM	E_{Na} (mV)	C_I/mM	E_{Na} (mV)	C_I/mM	E_{Na} (mV)
0.0399	4.9	0.517	140.2	2.799	210.3
0.0799	18.7	0.557	145.3	3.101	210.2
0.120	42.5	0.596	150.0	3.475	209.9
0.159	51.4	0.636	155.3	3.846	209.6
0.199	62.7	0.794	168.2	4.762	209.5
0.239	80.0	0.951	176.4	5.660	207.9
0.279	93.6	1.108	183.6	7.407	204.8
0.319	99.8	1.264	188.5	10.714	200.7
0.359	108.9	1.575	196.0	13.793	196.6
0.398	116.9	1.884	201.5	19.355	191.7
0.438	125.3	2.191	205.7	24.242	185.9
0.478	133.5	2.496	208.7	28.571	181.9

E°=-4.9, Slope=56.6, Inter.=362.2, Cor. Coef.=0.999, SS=0.0091.

DATA-A32: Tetradecylpyridinium bromide/α-CD C_c=0.915 mol dm^{-3}

C_1/mM	E_{Na} (mV)	C_1/mM	E_{Na} (mV)	C_1/mM	E_{Na} (mV)
0.0399	-41.6	0.912	135.2	2.799	201.0
0.0799	-22.2	0.951	139.3	3.101	203.9
0.1597	10.9	0.990	142.9	3.475	209.4
0.239	29.6	1.029	146.4	3.846	208.4
0.319	47.4	1.108	153.5	4.762	206.1
0.398	61.5	1.186	159.2	5.660	204.2
0.478	74.4	1.264	163.9	7.407	201.7
0.557	86.6	1.575	177.1	13.793	190.2
0.636	98.6	1.575	177.1	19.355	184.1
0.715	110.6	1.884	186.3	24.242	179.5
0.794	121.5	2.191	192.8		
0.872	130.8	2.496	197.6		

E°=1.5, Slope=56.6, Inter.=362.2, Cor. Coef.=0.999, SS=0.0094.

DATA-B31: Tetradecylpyridinium bromide/ß-CD C_c=0.865 mol dm^{-3}

C_1/mM	E_{Na} (mV)	C_1/mM	E_{Na} (mV)	C_1/mM	E_{Na} (mV)
0.0427	9.8	1.0152	149.9	4.8780	203.8
0.0854	40.9	1.0989	157.3	5.1864	203.0
0.1280	52.9	1.1824	163.3	5.7971	201.9
0.1706	58.6	1.2658	168.1	6.4000	201.1
0.2132	66.0	1.3491	172.3	6.9952	199.8
0.2553	71.3	1.5152	178.8	7.5829	199.0
0.2983	77.1	1.6807	184.1	8.1633	198.5
0.3407	82.0	1.8456	188.6	8.7363	198.2
0.3831	87.1	2.0101	192.2	9.3023	196.8
0.4255	90.7	2.1739	195.2	9.8613	196.2
0.4679	95.3	2.3372	197.6	11.3636	193.2
0.5102	98.8	2.5000	200.1	14.5985	188.1
0.5525	104.1	2.6622	202.0	20.4081	182.1
0.5947	107.5	2.9851	204.8	25.4777	178.1
0.6369	112.8	3.3058	205.9		
0.6791	117.0	3.6244	205.7		
0.7634	126.2	3.9409	205.7		
0.8475	133.4	4.2553	205.1		
0.9314	142.3	4.5677	204.5		

E°=3.1, Slope=56.6, Inter.=342.5, Cor. Coef.=0.999, SS=0.0029.

DATA-B32: Tetradecylpyridinium bromide/ß-CD C_c=1.635 mol dm^3

C_1/mM	E_{Na} (mV)	C_1/mM	E_{Na} (mV)	C_1/mM	E_{Na} (mV)
0.0399	-49.6	1.4196	136.2	4.2146	201.2
0.0799	-28.5	1.4972	141.9	4.5802	200.9
0.1597	-9.1	1.5748	147.1	4.9429	200.4
0.2394	5.2	1.6522	151.7	5.3030	200.0
0.3189	17.8	1.7296	156.1	5.6604	199.5
0.4777	38.1	1.8067	159.6	7.4074	196.6
0.6359	56.3	1.8838	164.0	13.7931	188.6
0.7149	66.1	2.0376	169.5	19.3548	182.7
0.7937	74.5	2.1909	175.2	24.2424	177.7
0.9509	92.0	2.4961	183.1	32.4324	171.3
1.1076	108.4	2.7994	189.5	39.0244	166.3
1.1858	115.2	3.1008	194.4	44.4444	162.2
1.2638	123.5	3.4749	198.6		
1.3418	129.4	3.8462	200.9		

E°=5.2, Slope=56.6, Inter.=362.2, Cor. Coef.=0.999, SS=0.0045.

DATA-A41: Cetylpyridinium bromide/α-CD C_c = 0.2 mol dm^3

C_1/mM	E_{Na} (mV)	C_1/mM	E_{Na} (mV)	C_1/mM	E_{Na} (mV)
0.008	-80.0	0.315	68.6	3.400	119.6
0.016	-58.3	0.377	81.0	4.076	117.2
0.024	-43.0	0.438	90.2	4.700	115.4
0.040	-35.5	0.499	97.1	5.277	113.0
0.048	-27.6	0.620	102.3	5.714	110.9
0.056	-20.5	0.740	110.4	6.486	108.6
0.064	-13.5	0.858	116.2	7.179	108.1
0.080	-7.2	0.974	120.9	7.805	105.6
0.096	2.8	1.203	124.4	8.372	104.2
0.111	11.8	1.426	125.4	8.889	102.8
0.127	19.4	1.645	126.0		
0.159	26.5	1.858	125.2		
0.190	40.4	2.270	125.3		
0.222	51.2	2.663	123.9		
0.253	60.5	3.039	121.2		

E°=10.8, Slope=55.3, Inter.=308.2, Cor. Coef.=0.998, SS=0.0009.

DATA-A42: Cetylpyridinium bromide/α-CD C_c = 0.3 mol dm^3

C_1/mM	E_{Na} (mV)	C_1/mM	E_{Na} (mV)	C_1/mM	E_{Na} (mV)
0.016	-89.3	0.284	60.3	1.645	128.1
0.032	-60.4	0.315	67.7	1.858	127.5
0.048	-43.5	0.377	80.0	2.270	126.7
0.064	-30.3	0.438	89.1	2.663	125.5
0.080	-19.7	0.499	96.2	3.039	124.5
0.096	-10.3	0.560	102.2	3.400	123.3
0.111	-2.7	0.620	107.0	4.076	121.4
0.127	5.6	0.740	114.7	4.700	119.5
0.143	13.4	0.858	120.6	5.277	118.2
0.159	20.2	0.974	124.7		
0.190	31.6	1.089	127.3		
0.222	42.2	1.203	128.3		
0.253	51.8	1.426	128.4		

E°=8, Slope=55.3, Inter.=308.2, Cor. Coef.=0.998, SS=0.0007.

DATA-B41: Cetylpyridinium bromide/ß-CD C_c = 0.15 mol dm^3

C_1/mM	E_{Na} (mV)	C_1/mM	E_{Na} (mV)	C_1/mM	E_{Na} (mV)
0.016	108.1	0.560	296.5	4.70	292.2
0.032	160.8	0.620	299.8	5.28	290.6
0.048	179.0	0.740	304.1	5.71	289.4
0.064	193.1	0.858	305.6	6.49	287.2
0.080	203.0	0.974	304.9	7.18	285.6
0.096	211.4	1.09	304.7	7.81	283.9
0.111	220.1	1.20	304.4	8.37	283.0
0.127	225.9	1.43	303.5	8.89	281.9
0.159	239.8	1.65	302.3	9.36	280.7
0.190	248.2	1.86	301.9	9.80	280.0
0.222	256.6	2.07	301.3		
0.253	263.8	2.27	300.8		
0.315	274.1	2.66	299.0		
0.377	281.6	3.04	297.5		
0.438	286.9	3.40	296.1		
0.499	292.6	4.08	293.9		

E°=-77.9, Slope=58.1, Inter.=320.2, Cor. Coef.=0.999, SS=0.0046.

DATA-B42: Cetylpyridinium bromide/ß-CD C_c = 0.22 mol dm^3

C_1/mM	E_{Na} (mV)	C_1/mM	E_{Na} (mV)	C_1/mM	E_{Na} (mV)
0.006	41.8	0.20	156.0	1.30	213.7
0.013	57.2	0.21	159.7	1.50	214.1
0.019	68.0	0.23	163.8	1.80	212.3
0.026	75.4	0.25	168.6	2.10	212.7
0.038	85.7	0.28	174.8	2.40	211.3
0.051	93.7	0.30	178.5	2.70	211.4
0.064	101.8	0.35	186.0	3.30	209.9
0.076	107.9	0.40	191.1	3.60	209.2
0.089	113.7	0.45	195.9	3.90	209.7
0.10	119.3	0.50	199.5	4.20	207.8
0.11	124.2	0.54	203.6	4.60	208.2
0.13	129.1	0.59	205.8	5.20	205.5
0.14	133.9	0.69	210.8	5.70	205.3
0.15	138.4	0.73	211.7	6.20	203.2
0.16	142.5	0.78	213.1	6.70	203.3
0.18	147.7	0.96	214.2	7.10	202.1
0.19	151.4	1.10	214.2	7.50	201.2

E°=-82, Slope=56.6, Inter.=313.4, Cor. Coef.=0.998, SS=0.0105.

DATA-A51: Tetradecyltrimethylammonium bromide/α-CD C_c = 0.5 mol dm^3

C_1/mM	E_{Na} (mV)	C_1/mM	E_{Na} (mV)	C_1/mM	E_{Na} (mV)
0.042	20.3	0.739	223.6	3.70	278.8
0.083	80.3	0.820	229.0	4.27	278.9
0.125	100.7	0.980	237.2	4.82	279.5
0.166	115.6	1.14	242.4	5.42	278.2
0.207	131.0	1.30	247.8	5.67	278.6
0.249	143.7	1.46	252.1	6.90	276.8
0.290	155.3	1.61	255.0	7.87	275.8
0.331	167.0	1.92	260.7	8.79	275.5
0.372	175.2	2.27	265.4	10.50	272.7
0.413	183.8	2.53	268.7	12.10	271.4
0.495	197.2	2.83	273.0	13.60	270.8
0.577	207.6	3.13	274.2	14.70	270.3
0.658	215.1	3.42	276.0		

E°=1.8, Slope=58.9, Inter.=427.2, Cor. Coef.=0.999, SS=0.0051.

DATA-A52: Tetradecyltrimethylammonium bromide/α-CD C_c = 0.75 mol dm^3

C_1/mM	E_{Na} (mV)	C_1/mM	E_{Na} (mV)	C_1/mM	E_{Na} (mV)
0.04	-10.1	0.787	211.1	3.57	273.4
0.08	48.7	0.865	217.7	4.11	275.6
0.12	68.1	0.942	222.6	4.64	276.3
0.16	84.8	1.10	230.1	5.10	275.5
0.24	98.5	1.25	236.1	5.67	274.8
0.278	110.4	1.40	240.8	6.66	274.0
0.32	119.5	1.55	246.2	7.60	273.9
0.357	138.7	1.70	250.5	8.50	273.8
0.397	149.9	1.85	252.8	10.20	272.4
0.436	159.8	2.14	257.4	12.00	271.4
0.475	165.9	2.44	261.6	13.10	270.2
0.554	179.1	2.72	265.2	14.30	270.5
0.632	190.9	3.01	268.7		
0.71	201.7	3.33	270.7		

E°=4.8, Slope=58.9, Inter.=427.2, Cor. Coef.=0.999, SS=0.0059.

DATA-B51: Tetradecyltrimethylammonium bromide/ß-CD C_c = 0.5 mol dm^3

C_1/mM	E_{Na} (mV)	C_1/mM	E_{Na} (mV)	C_1/mM	E_{Na} (mV)
0.02	30.5	0.554	208.7	3.33	275.3
0.04	74.5	0.632	215.5	3.57	276.9
0.06	95.5	0.710	221.4	4.11	278.4
0.08	105.4	0.787	226.3	4.64	278.5
0.10	114.1	0.865	231.7	5.10	278.3
0.12	120.9	0.942	234.9	5.67	278.1
0.14	127.5	1.10	240.9	6.66	277.1
0.16	133.3	1.25	246.0	7.60	276.9
0.20	141.6	1.40	250.7	8.50	275.3
0.24	152.8	1.55	253.2	10.20	274.0
0.278	159.5	1.70	256.5	12.00	273.2
0.32	169.8	1.85	258.7	13.20	272.1
0.357	178.7	2.14	262.9	14.30	271.7
0.397	185.6	2.44	267.8		
0.436	193.4	2.72	270.3		
0.475	199.6	3.01	272.6		

E°=1.6, Slope=58.9, Inter.=427.2, Cor. Coef.=0.999, SS=0.0019.

DATA-B52: Tetradecyltrimethylammonium bromide/ß-CD C_c = 0.75 mol dm^{-3}

C_1/mM	E_{Na} (mV)	C_1/mM	E_{Na} (mV)	C_1/mM	E_{Na} (mV)
0.02	44.6	0.554	184.1	3.33	273.2
0.04	69.7	0.632	195.2	3.57	275.1
0.06	81.5	0.710	203.6	4.11	277.0
0.08	90.2	0.787	210.5	4.64	277.5
0.10	99.7	0.865	218.1	5.10	277.1
0.12	108.4	0.942	223.9	5.67	276.7
0.14	113.7	1.10	231.8	6.66	276.6
0.16	118.8	1.25	238.3	7.60	275.0
0.20	127.4	1.40	242.4	8.50	274.1
0.24	136.9	1.55	247.0	10.20	272.2
0.278	143.5	1.70	251.2	12.00	271.0
0.32	148.2	1.85	254.6	13.20	270.5
0.357	154.9	2.14	260.0	14.30	269.7
0.397	160.5	2.44	264.3		
0.436	166.1	2.72	267.7		
0.475	173.5	3.01	270.6		

E°=-0,9, Slope=58.9, Inter.=427.2, Cor. Coef.=0.999, SS=0.0027.

Appendix 7

Figures 7-A series: Omega ITC computer fits for 1:1 α- and ß-CD/surfactant inclusion complexes

Figures 7-B series: Omega ITC computer fits for 1:1 inclusion complexes for the systems α-CD/$C_8(OE)_4$, ß-CD/$C_8(OE)_4$ and γ-CD/$C_8(OE)_4$

Figures 7-C series: Two-Consecutive Sites computer fits for 1:1 and 2:1 inclusion complexes Omega ITC data for α- and ß-CD/surfactant systems

Figures 7-D series: Two-Independent Sites Omega ITC computer fits for 1:1 and 2:1 inclusion complexes for α- and ß-CD/surfactant systems (NOT USED IN THE DISCUSSION)

Figure 7-A1

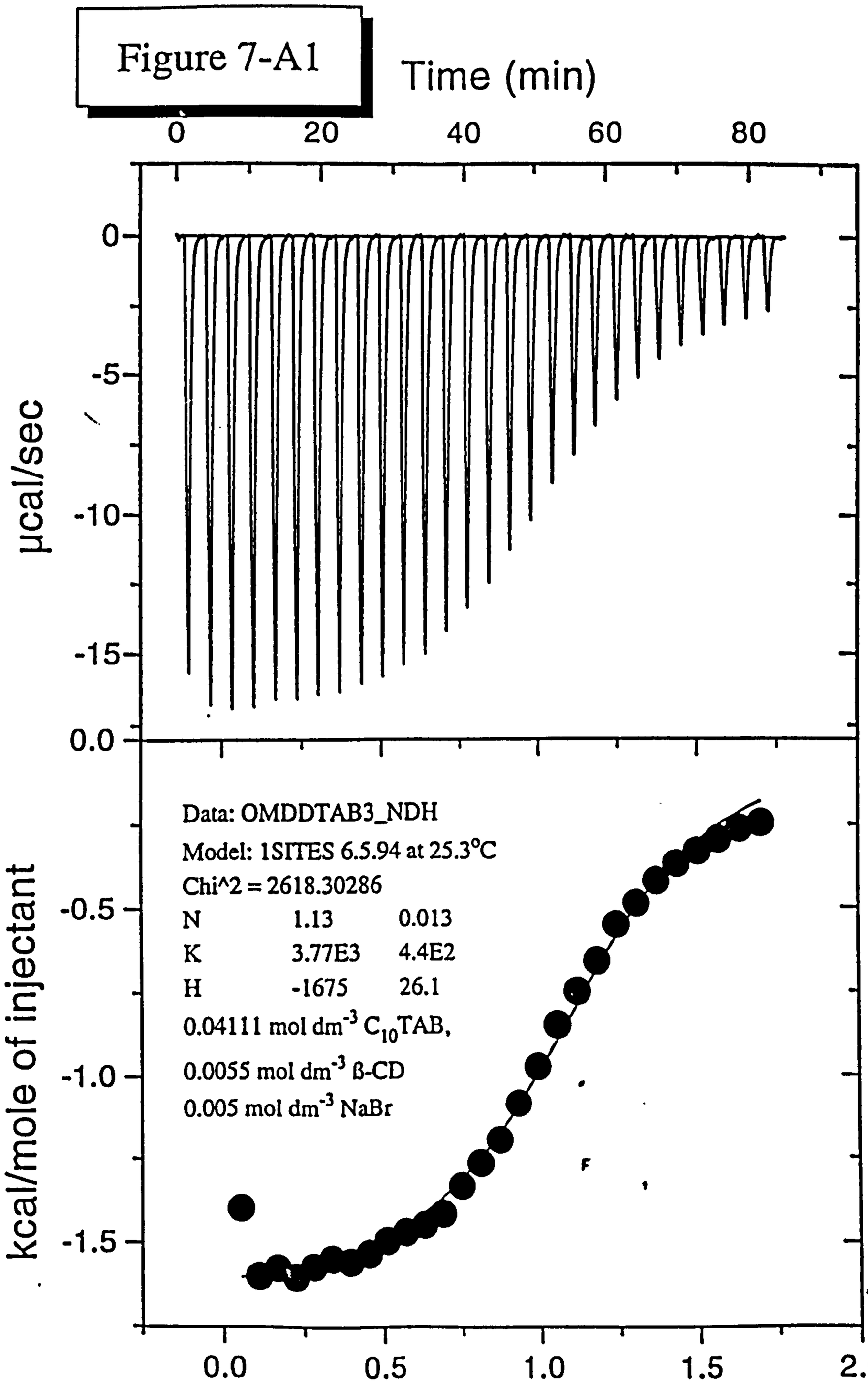
Time (min)
0
20
40
60
80
0
-5
-10
-15
0.0
µcal/sec
Data: OMDDTAB3_NDH
Model: 1SITES 6.5.94 at 25.3°C
Chi^2 = 2618.30286
N 1.13 0.013
K 3.77E3 4.4E2
H -1675 26.1
0.04111 mol dm-3 C10TAB,
0.0055 mol dm-3 ß-CD
0.005 mol dm-3 NaBr
-0.5
-1.0
-1.5
kcal/mole of injectant
0.0
0.5
1.0
1.5
2.0
Molar Ratio

Figure 7-A2

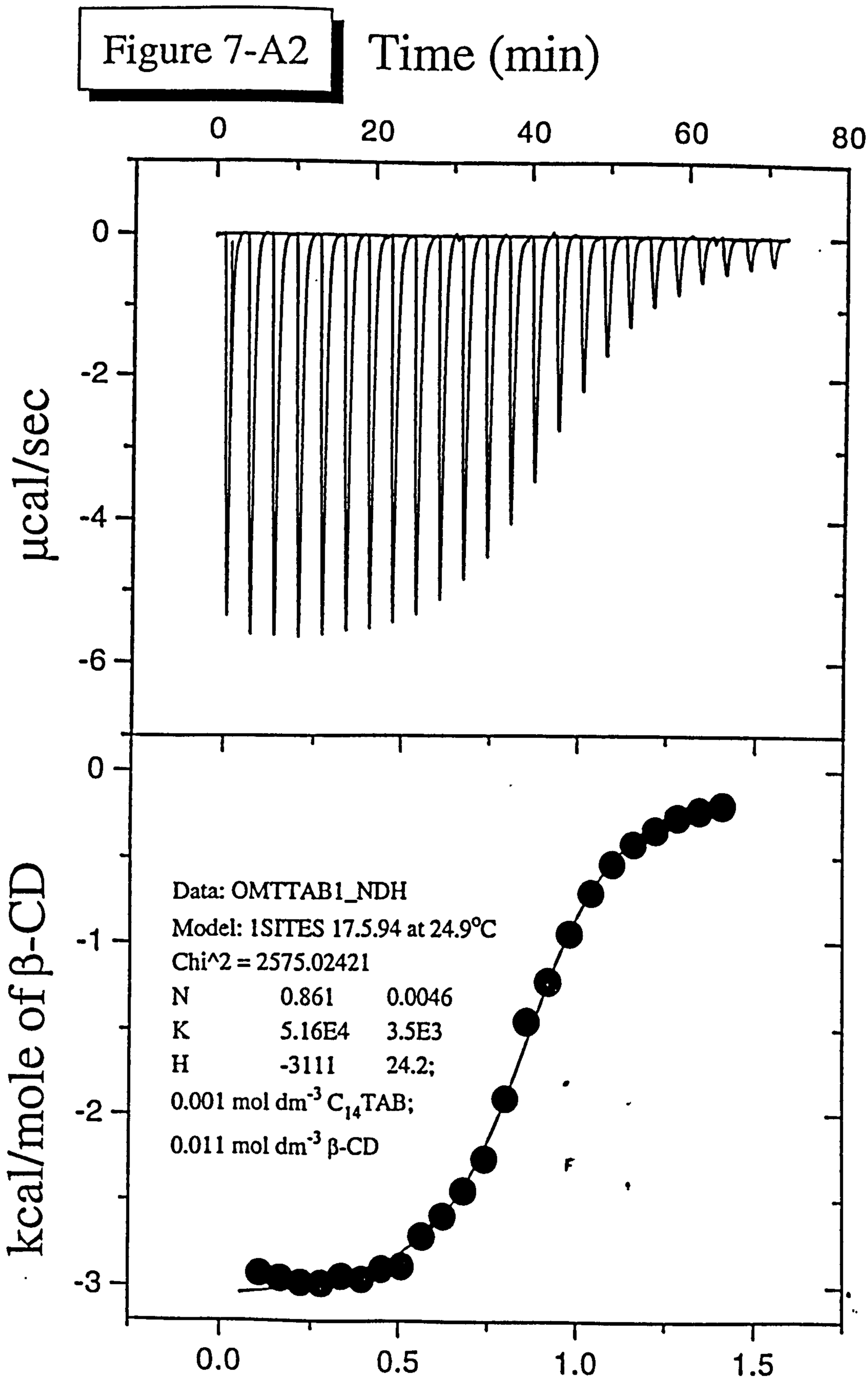
Time (min)
0
20
40
60
80
µcal/sec
0
-2
-4
-6
kcal/mole of β-CD
0
-1
-2
-3
Data: OMTTAB1_NDH
Model: 1SITES 17.5.94 at 24.9°C
Chi^2 = 2575.02421
N 0.861 0.0046
K 5.16E4 3.5E3
H -3111 24.2;
0.001 mol dm-3 C14TAB;
0.011 mol dm-3 β-CD
0.0
0.5
1.0
1.5
Molar Ratio

Figure 7-A3

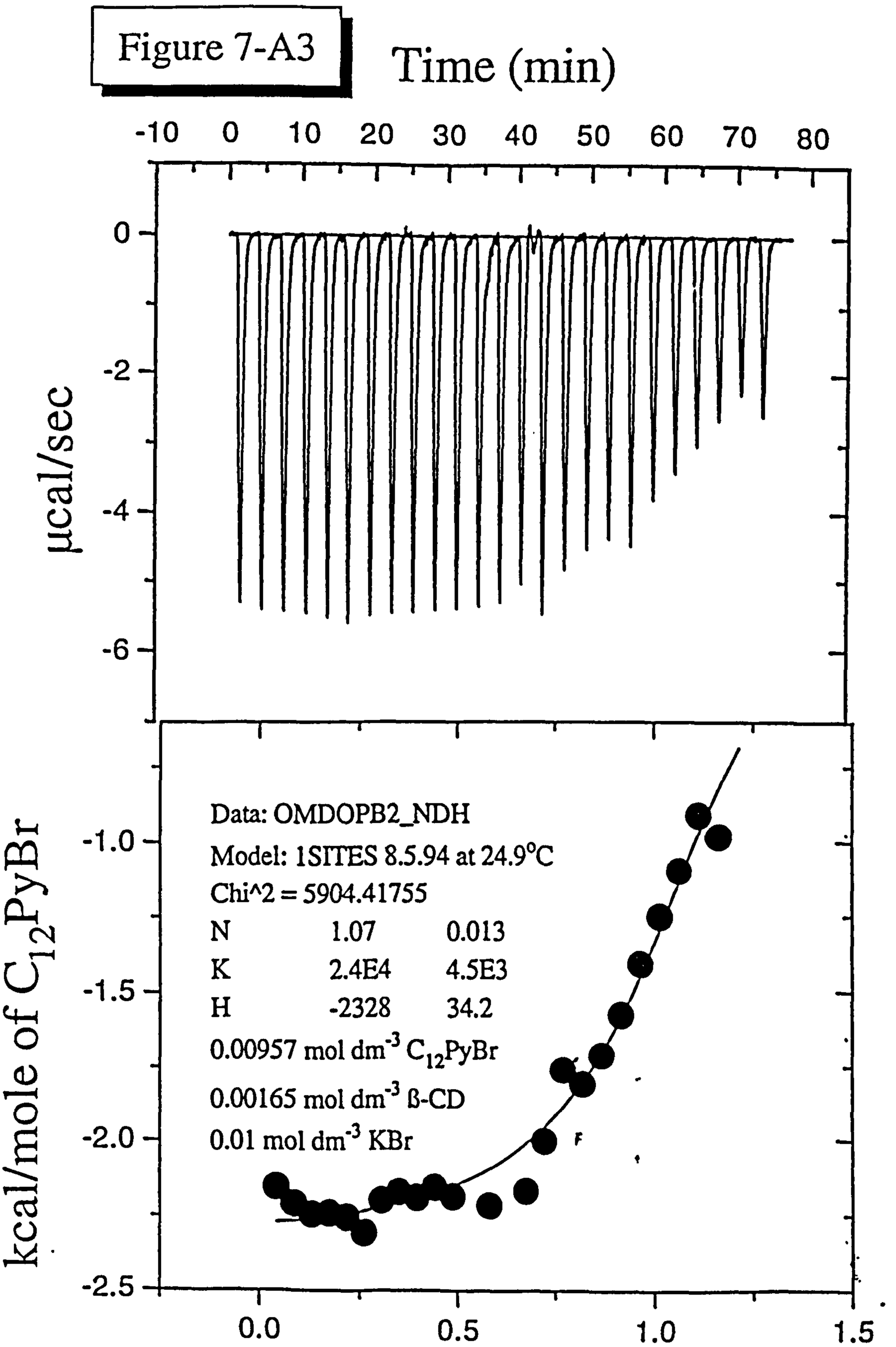
Time (min)
-10
0
10
20
30
40
50
60
70
80
0
-2
-4
-6
µcal/sec
-1.0
-1.5
-2.0
-2.5
kcal/mole of $C_{12}PyBr$
Data: OMDOPB2_NDH
Model: 1SITES 8.5.94 at 24.9°C
Chi^2 = 5904.41755
N 1.07 0.013
K 2.4E4 4.5E3
H -2328 34.2
0.00957 mol dm^{-3} $C_{12}PyBr$
0.00165 mol dm^{-3} ß-CD
0.01 mol dm^{-3} KBr
0.0
0.5
1.0
1.5
Molar Ratio

Figure 7-A4

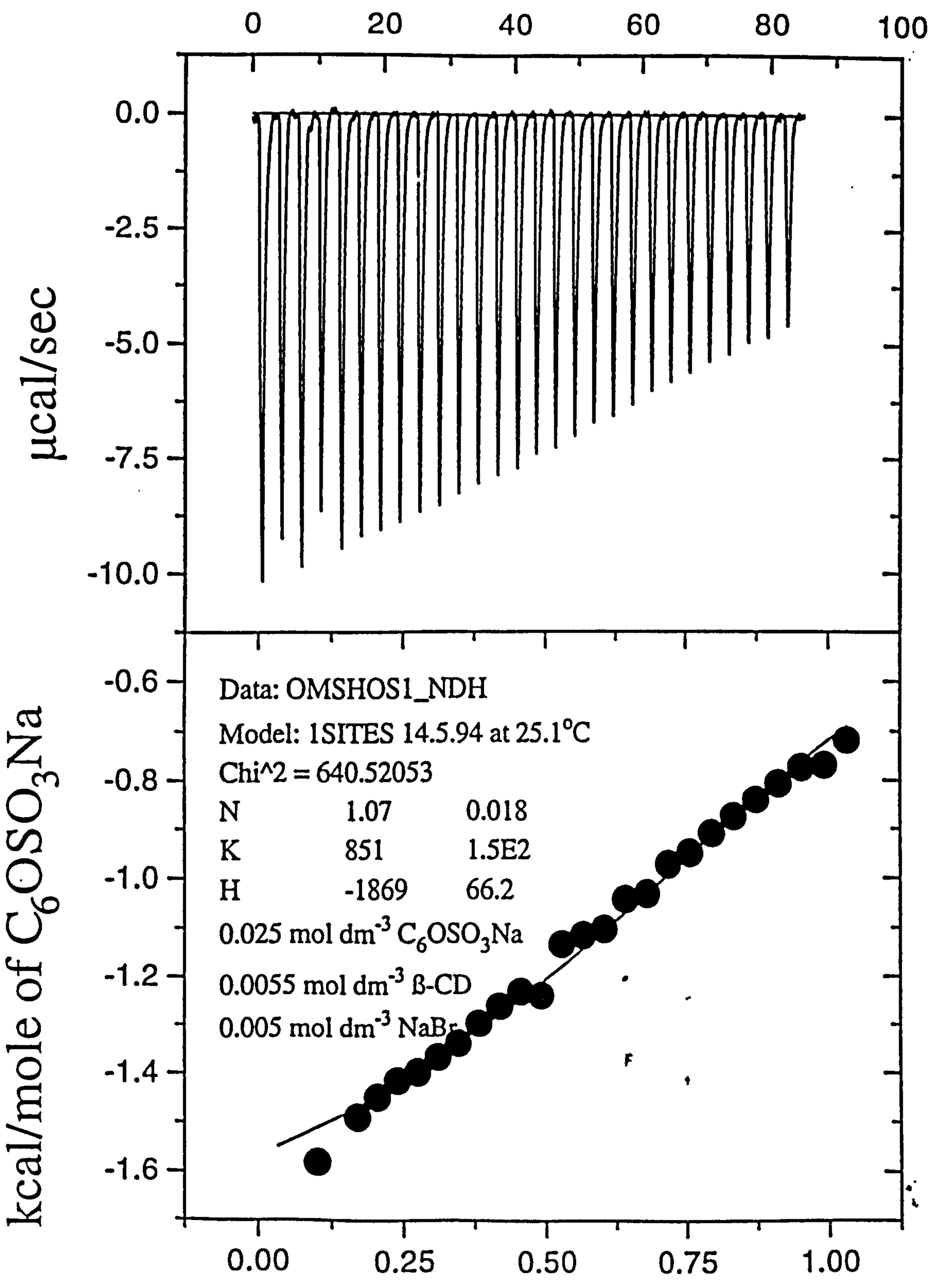
Time (min)
0
20
40
60
80
100
0.0
-2.5
-5.0
-7.5
-10.0
µcal/sec
-0.6
-0.8
-1.0
-1.2
-1.4
-1.6
kcal/mole of C_6OSO_3Na
Data: OMSHOS1_NDH
Model: 1SITES 14.5.94 at 25.1°C
Chi^2 = 640.52053
N 1.07 0.018
K 851 1.5E2
H -1869 66.2
0.025 mol dm^{-3} C_6OSO_3Na
0.0055 mol dm^{-3} ß-CD
0.005 mol dm^{-3} NaBr
0.00
0.25
0.50
0.75
1.00
Molar Ratio

Figure 7-A5

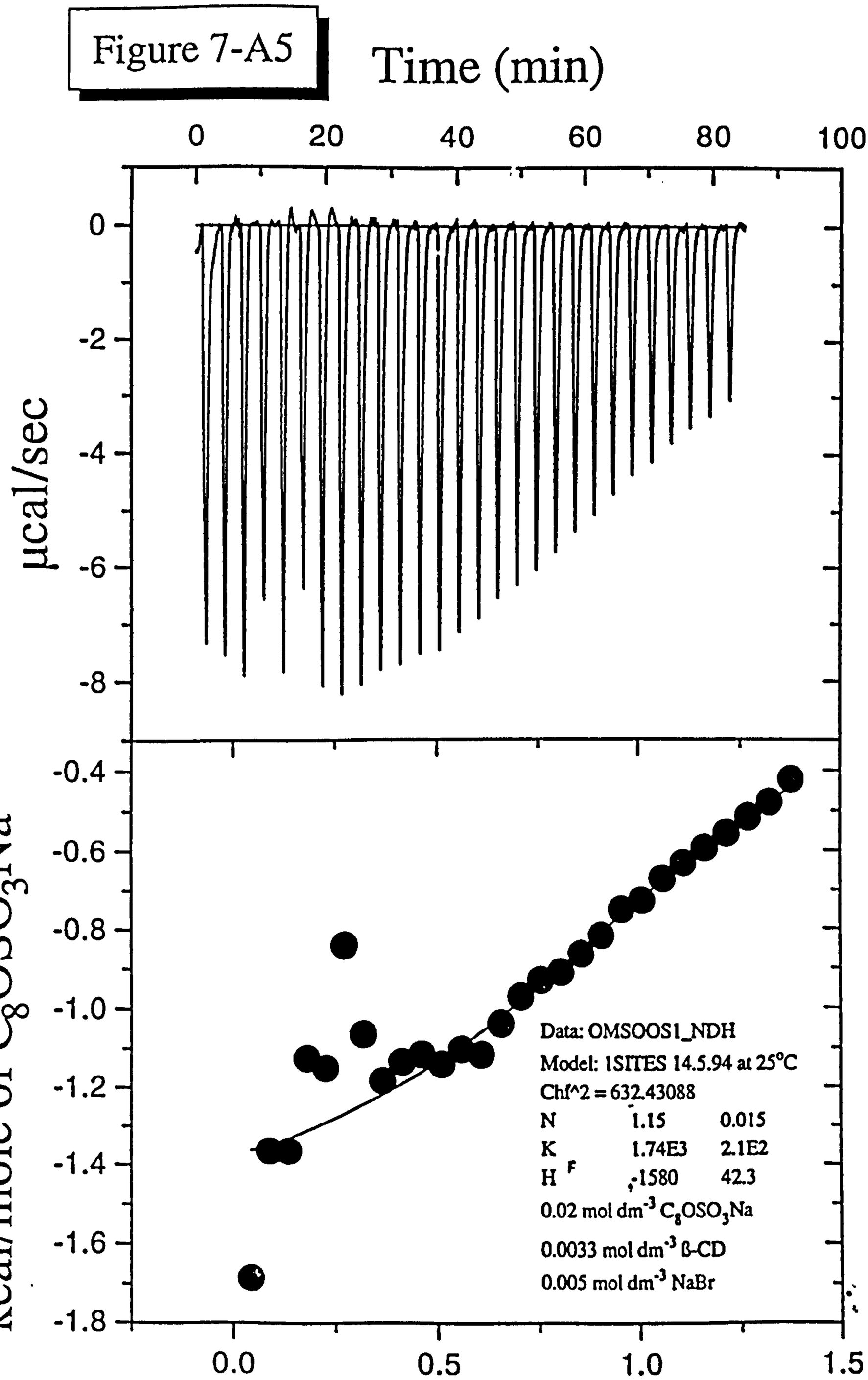
Time (min)
0
20
40
60
80
100
0
-2
-4
-6
-8
µcal/sec
-0.4
-0.6
-0.8
-1.0
-1.2
-1.4
-1.6
-1.8
kcal/mole of C_8OSO_3Na
Data: OMSOOS1_NDH
Model: 1SITES 14.5.94 at 25°C
Chi^2 = 632.43088
N 1.15 0.015
K 1.74E3 2.1E2
H -1580 42.3
0.02 mol dm^{-3} C_8OSO_3Na
0.0033 mol dm^{-3} ß-CD
0.005 mol dm^{-3} NaBr
0.0
0.5
1.0
1.5
Molar Ratio

Figure 7-A6

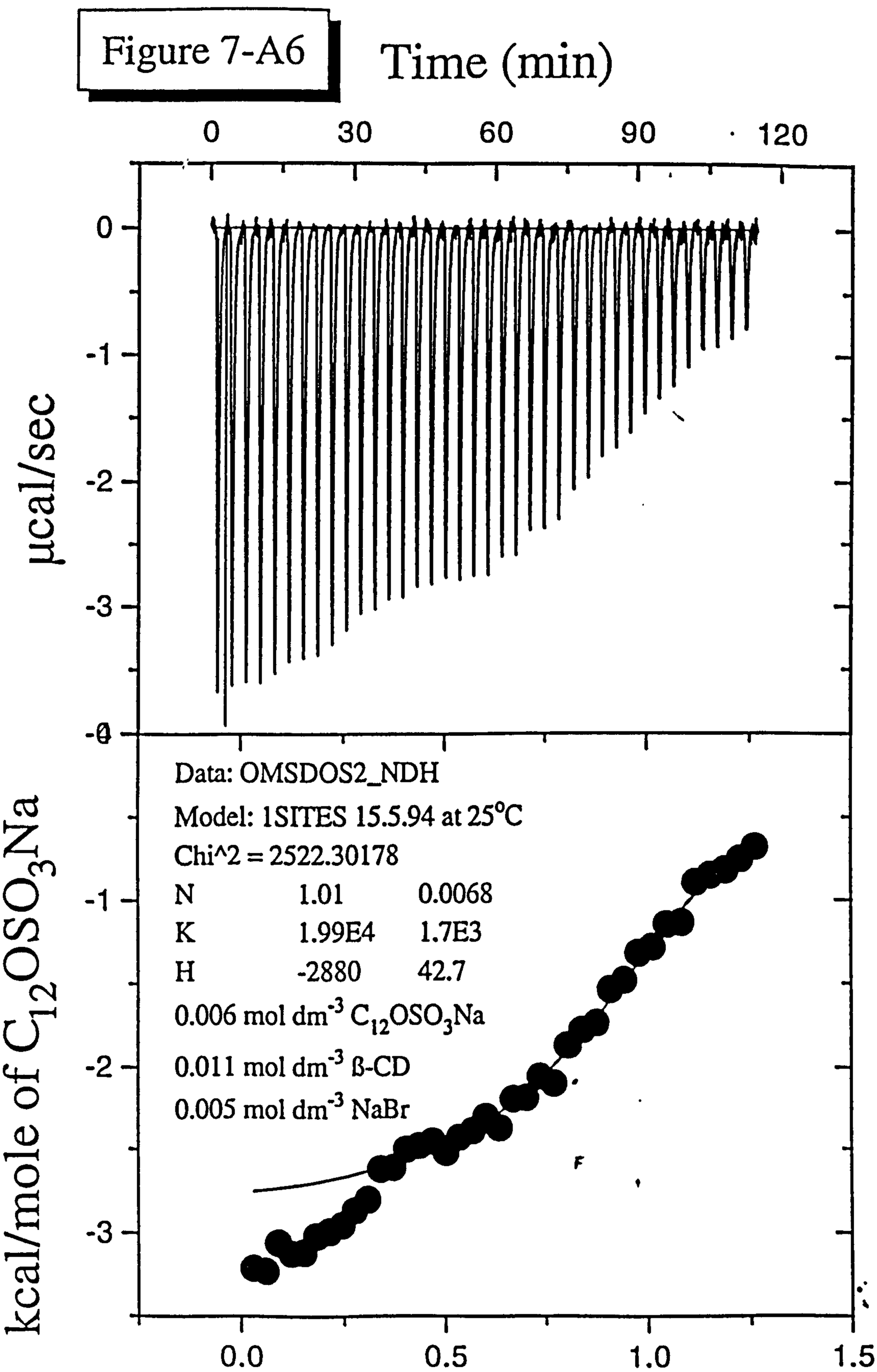
Time (min)
0
30
60
90
120
0
-1
-2
-3
-4
µcal/sec
Data: OMSDOS2_NDH
Model: 1SITES 15.5.94 at 25°C
Chi^2 = 2522.30178
N 1.01 0.0068
K 1.99E4 1.7E3
H -2880 42.7
0.006 mol dm-3 C12OSO3Na
0.011 mol dm-3 ß-CD
0.005 mol dm-3 NaBr
kcal/mole of C12OSO3Na
0.0
0.5
1.0
1.5
Molar Ratio

Figure 7-A7

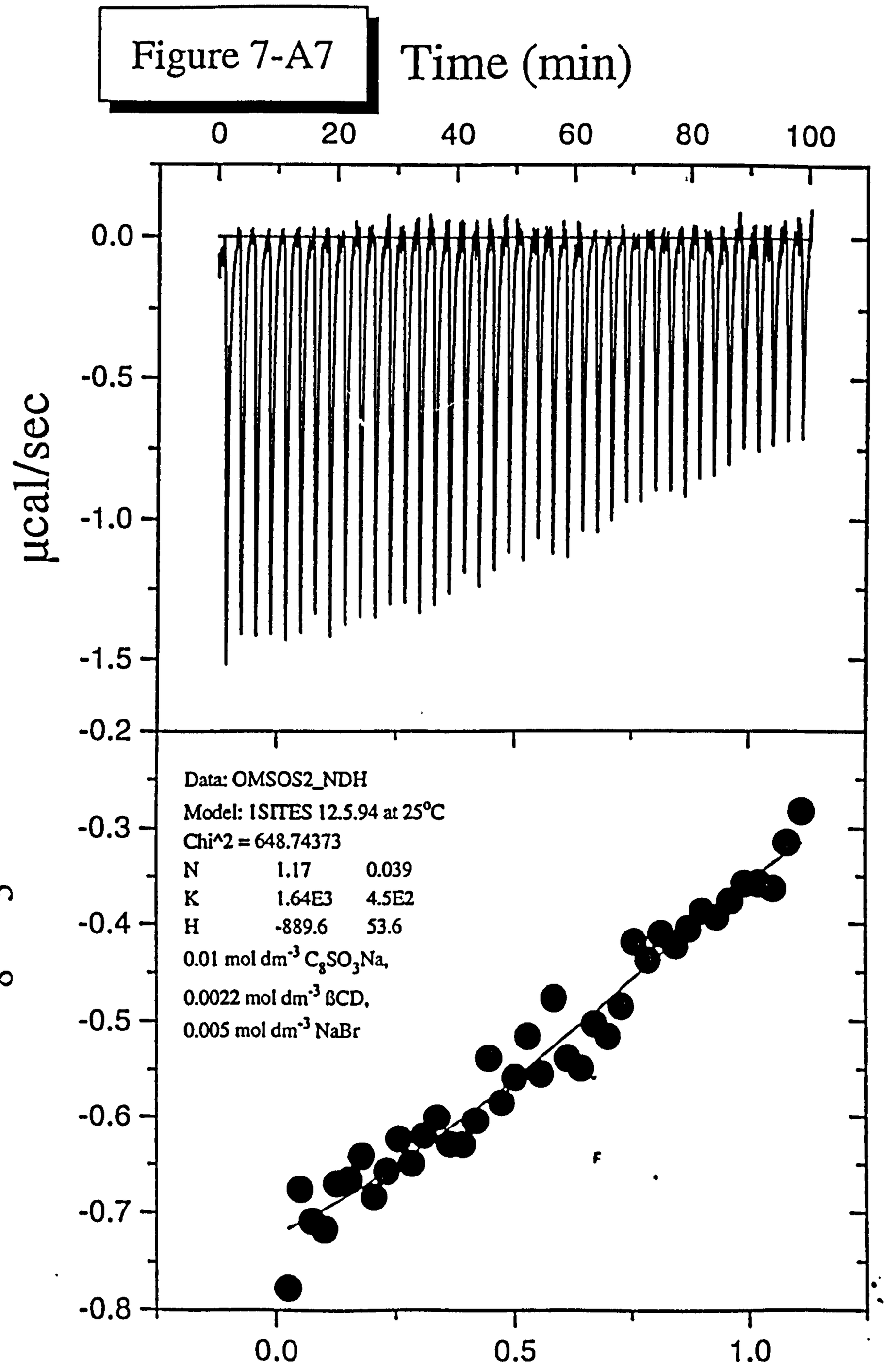
Time (min)
0
20
40
60
80
100
0.0
-0.5
-1.0
-1.5
-0.2
-0.3
-0.4
-0.5
-0.6
-0.7
-0.8
µcal/sec
kcal/mole of C_8SO_3Na
Data: OMSOS2_NDH
Model: 1SITES 12.5.94 at 25°C
Chi^2 = 648.74373
N 1.17 0.039
K 1.64E3 4.5E2
H -889.6 53.6
0.01 mol dm^{-3} C_8SO_3Na,
0.0022 mol dm^{-3} ßCD,
0.005 mol dm^{-3} NaBr
0.0
0.5
1.0
Molar Ratio

Figure 7-A8

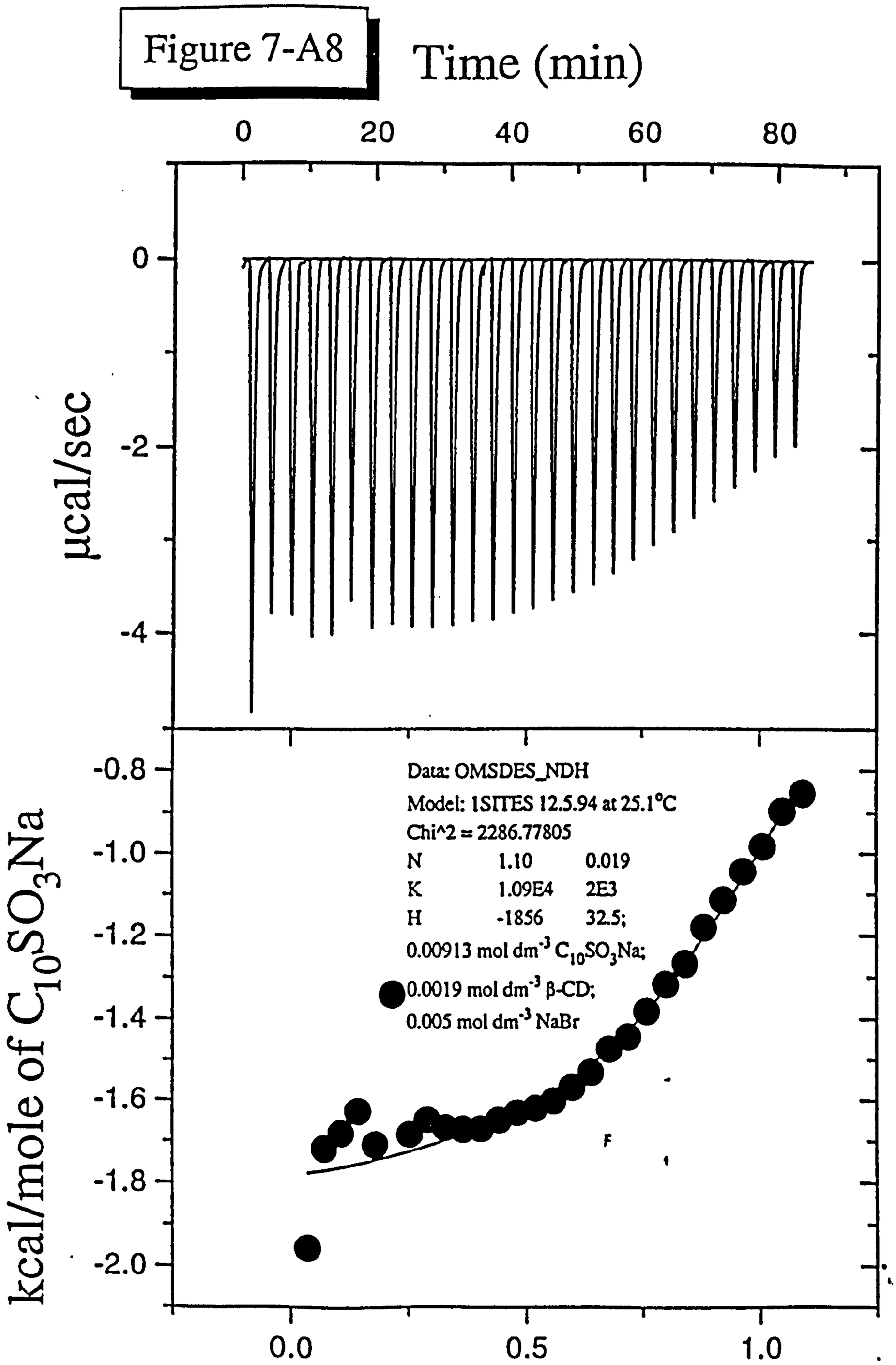
Time (min)
0
20
40
60
80
µcal/sec
0
-2
-4
Data: OMSDES_NDH
Model: ISITES 12.5.94 at 25.1°C
Chi^2 = 2286.77805
N 1.10 0.019
K 1.09E4 2E3
H -1856 32.5;
0.00913 mol dm-3 C10SO3Na;
0.0019 mol dm-3 β-CD;
0.005 mol dm-3 NaBr
kcal/mole of C10SO3Na
-0.8
-1.0
-1.2
-1.4
-1.6
-1.8
-2.0
0.0
0.5
1.0
Molar Ratio

Figure 7-A9

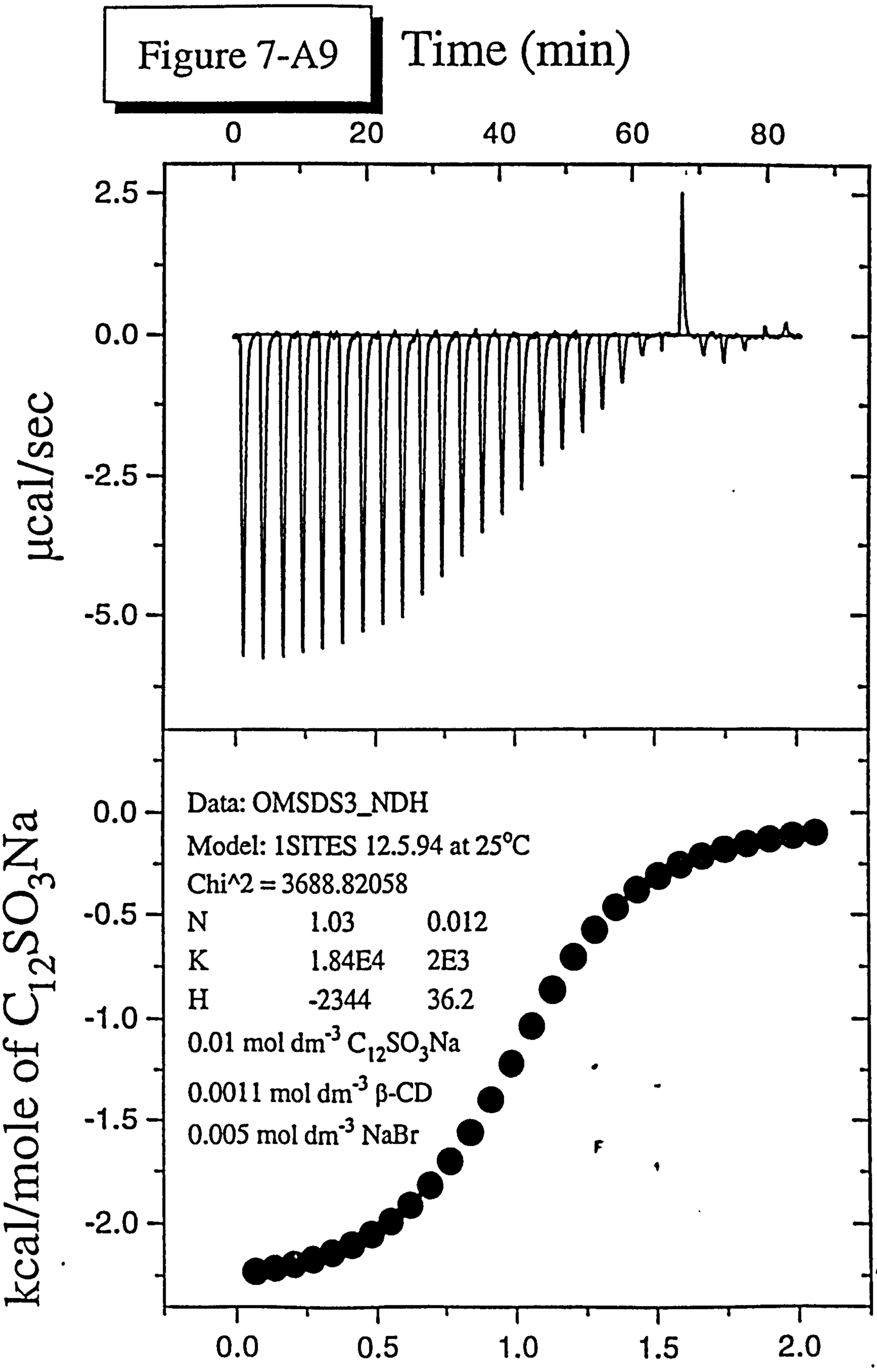
Time (min)
0
20
40
60
80
2.5
0.0
-2.5
-5.0
µcal/sec
0.0
-0.5
-1.0
-1.5
-2.0
kcal/mole of $C_{12}SO_3Na$
Data: OMSDS3_NDH
Model: 1SITES 12.5.94 at 25°C
Chi^2 = 3688.82058
N 1.03 0.012
K 1.84E4 2E3
H -2344 36.2
0.01 mol dm^{-3} $C_{12}SO_3Na$
0.0011 mol dm^{-3} β-CD
0.005 mol dm^{-3} NaBr
0.0
0.5
1.0
1.5
2.0
Molar Ratio

Figure 7-A10

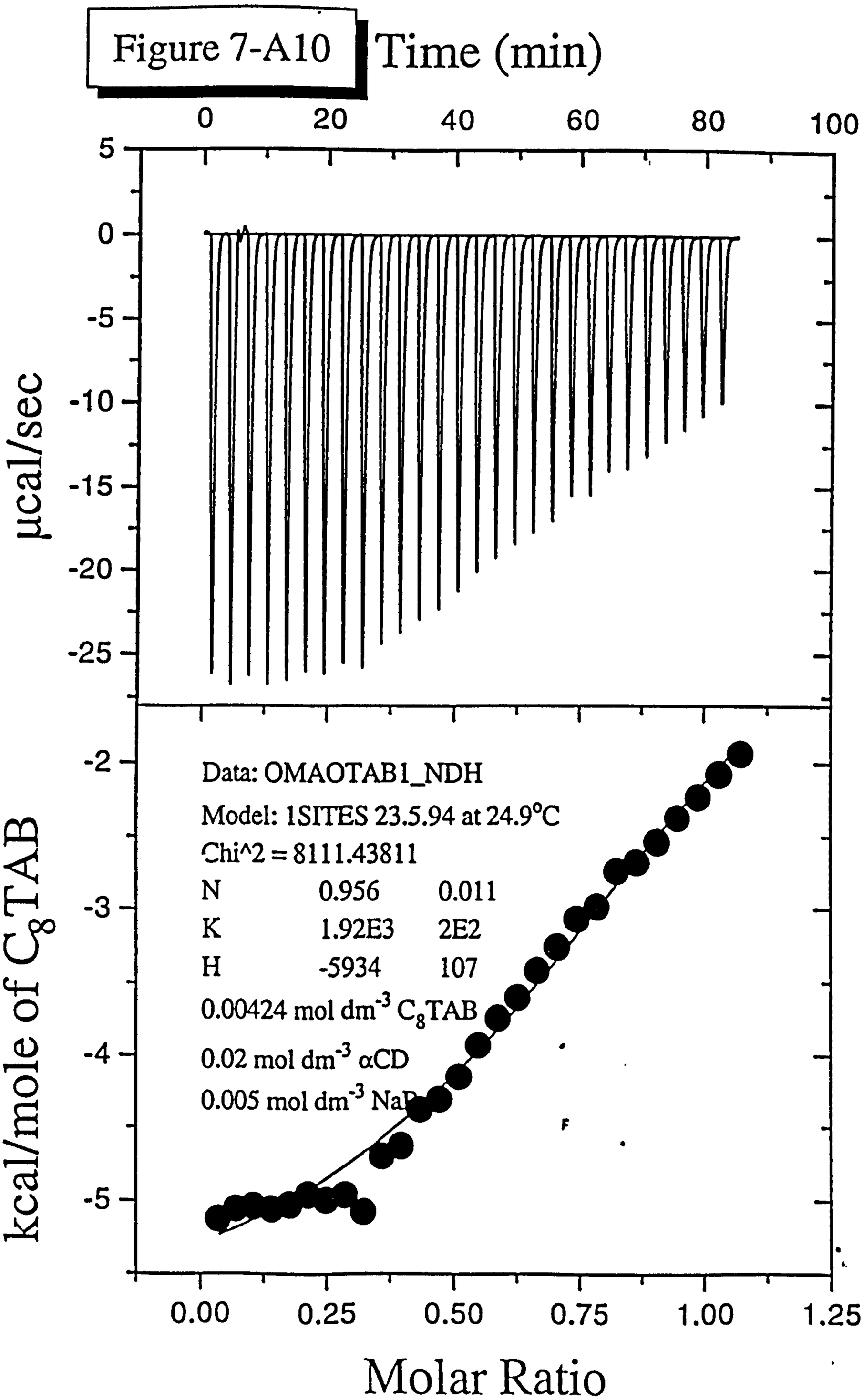
Time (min)
0
20
40
60
80
100
5
0
-5
-10
-15
-20
-25
µcal/sec
-2
-3
-4
-5
kcal/mole of C_8TAB
Data: OMAOTAB1_NDH
Model: 1SITES 23.5.94 at 24.9°C
Chi^2 = 8111.43811
N 0.956 0.011
K 1.92E3 2E2
H -5934 107
0.00424 mol dm^{-3} C_8TAB
0.02 mol dm^{-3} αCD
0.005 mol dm^{-3} NaP
0.00
0.25
0.50
0.75
1.00
1.25
Molar Ratio

Figure 7-A11

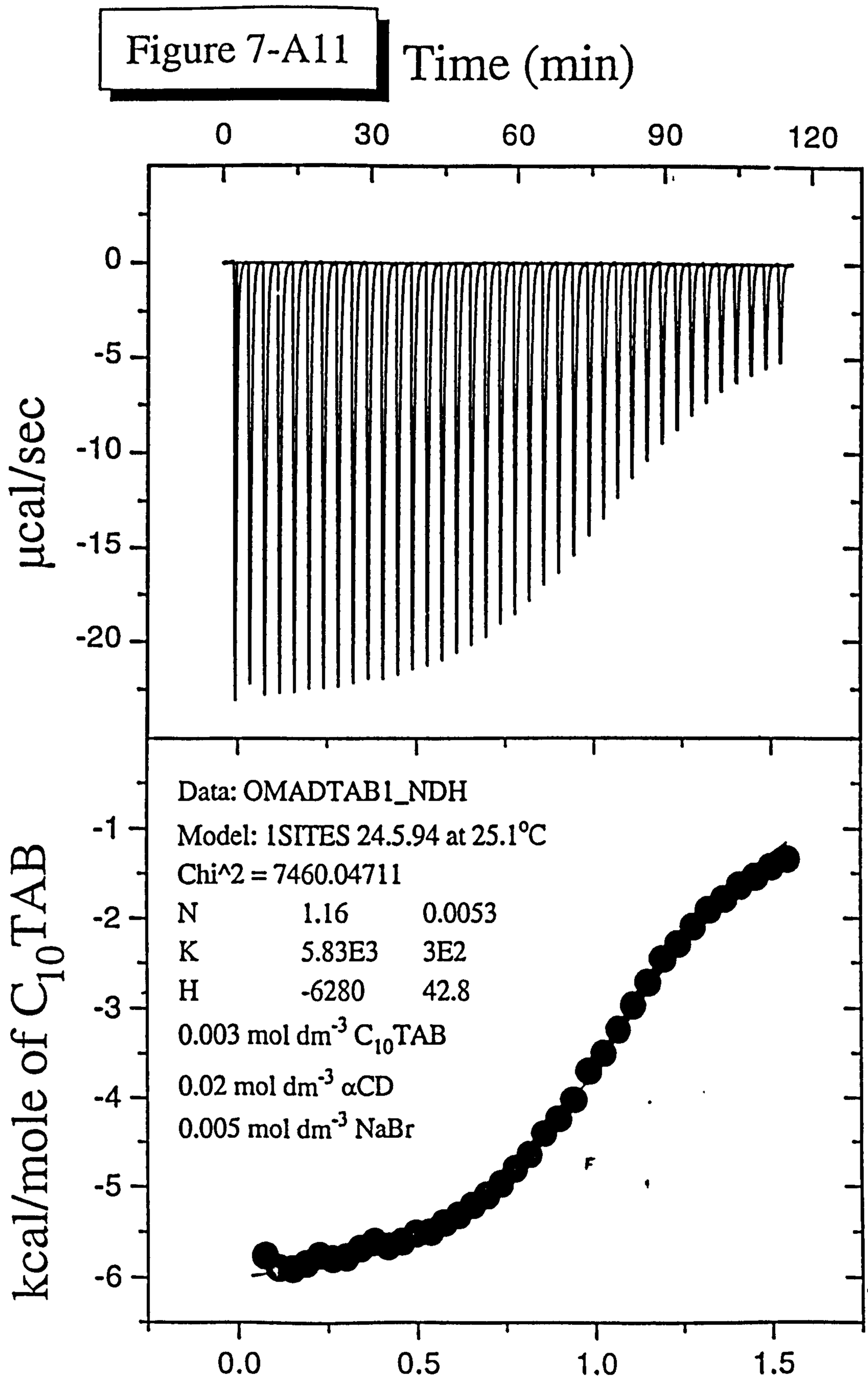
Time (min)
0
30
60
90
120
µcal/sec
0
-5
-10
-15
-20
kcal/mole of C_{10}TAB
-1
-2
-3
-4
-5
-6
Data: OMADTAB1_NDH
Model: 1SITES 24.5.94 at 25.1°C
Chi^2 = 7460.04711
N 1.16 0.0053
K 5.83E3 3E2
H -6280 42.8
0.003 mol dm^{-3} C_{10}TAB
0.02 mol dm^{-3} αCD
0.005 mol dm^{-3} NaBr
0.0
0.5
1.0
1.5
Molar Ratio

Figure 7-A12

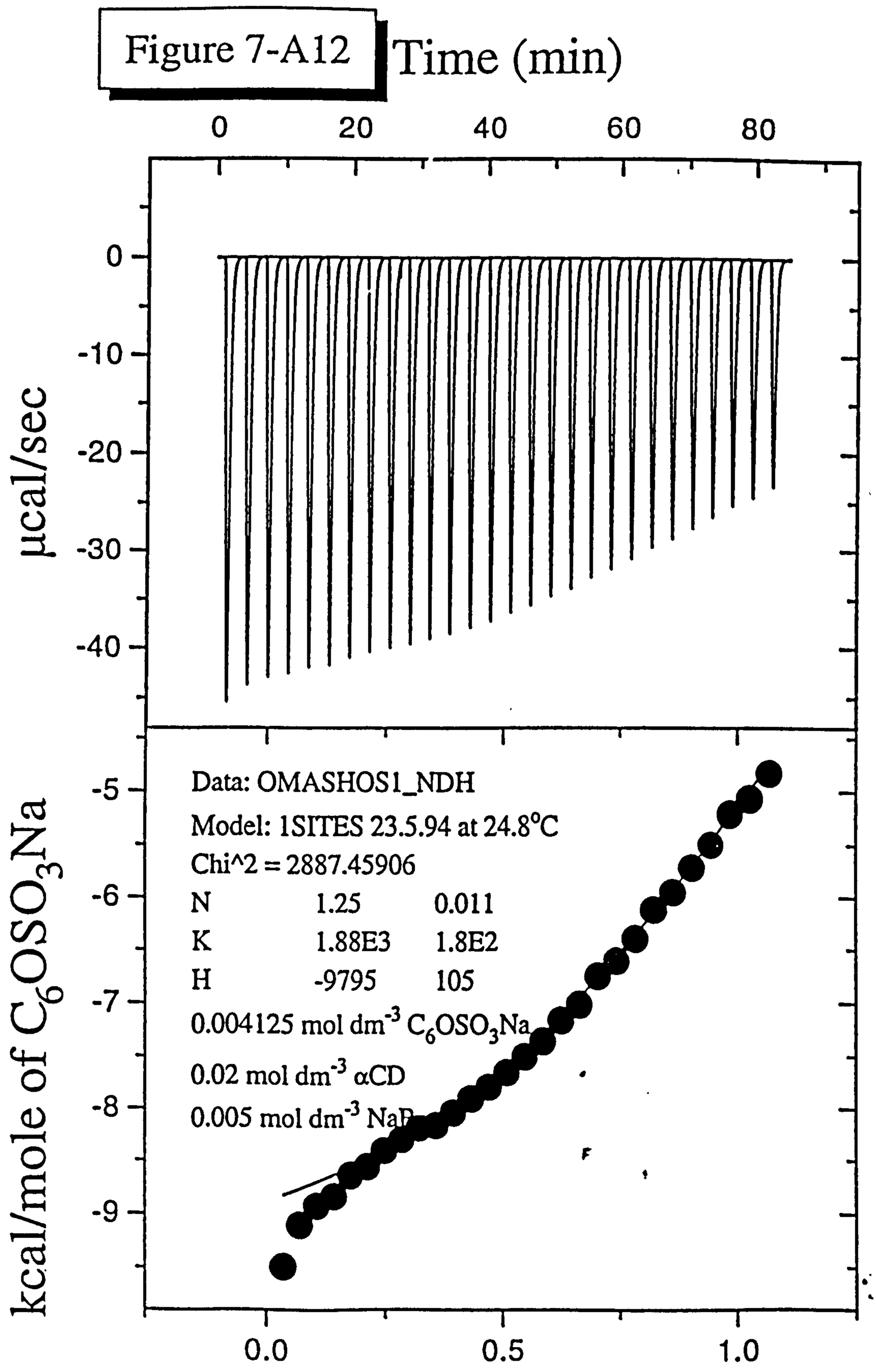
Time (min)
0
20
40
60
80
µcal/sec
0
-10
-20
-30
-40
kcal/mole of C_6OSO_3Na
-5
-6
-7
-8
-9
Data: OMASHOS1_NDH
Model: 1SITES 23.5.94 at 24.8°C
Chi^2 = 2887.45906
N 1.25 0.011
K 1.88E3 1.8E2
H -9795 105
0.004125 mol dm^{-3} C_6OSO_3Na
0.02 mol dm^{-3} αCD
0.005 mol dm^{-3} NaP
0.0
0.5
1.0
Molar Ratio

Figure 7-A13

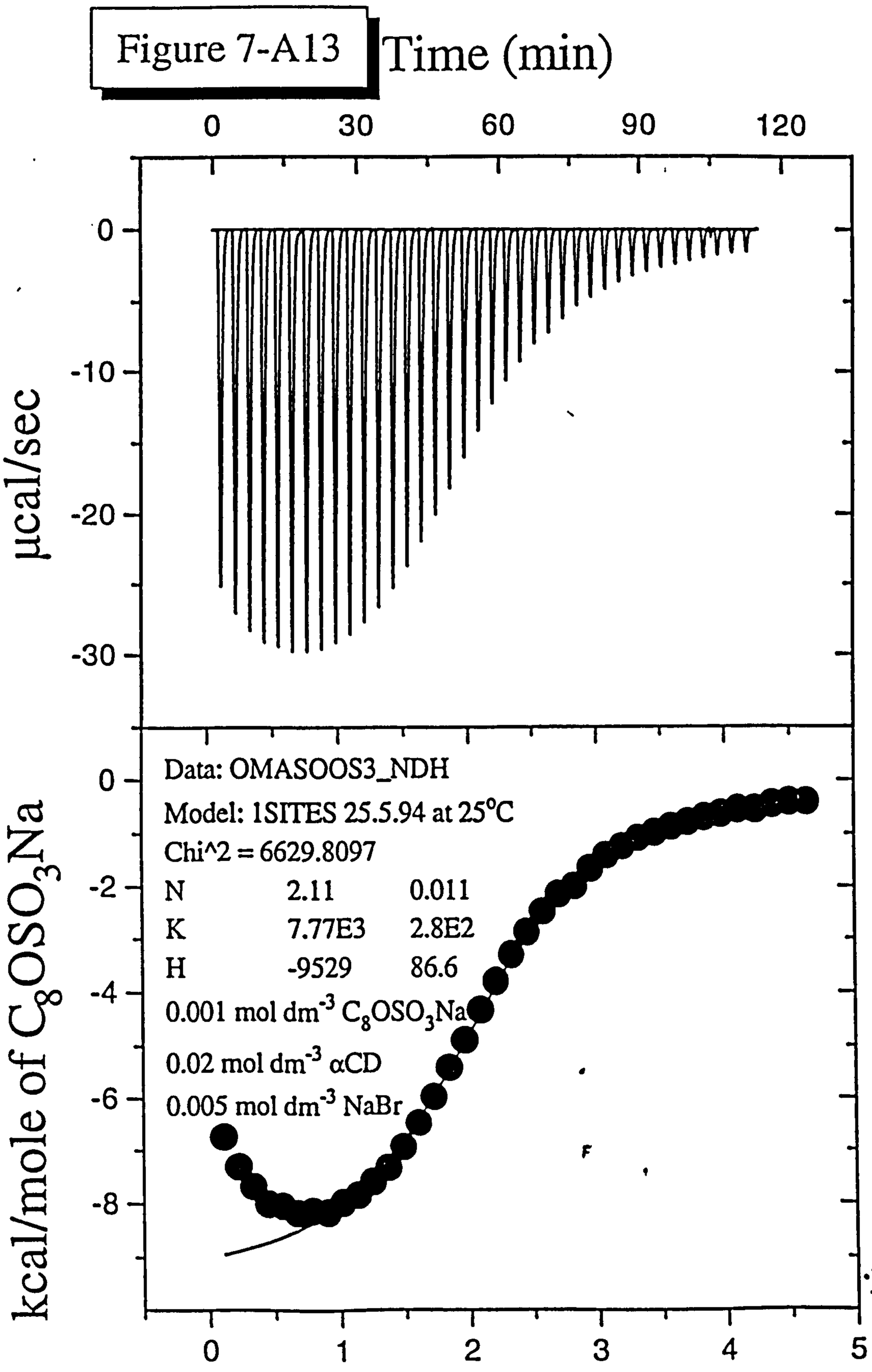
Time (min)
0
30
60
90
120
0
-10
-20
-30
µcal/sec
Data: OMASOOS3_NDH
Model: 1SITES 25.5.94 at 25°C
Chi^2 = 6629.8097
N 2.11 0.011
K 7.77E3 2.8E2
H -9529 86.6
0.001 mol dm-3 C8OSO3Na
0.02 mol dm-3 αCD
0.005 mol dm-3 NaBr
0
-2
-4
-6
-8
kcal/mole of C8OSO3Na
0
1
2
3
4
5
Molar Ratio

Figure 7-A14

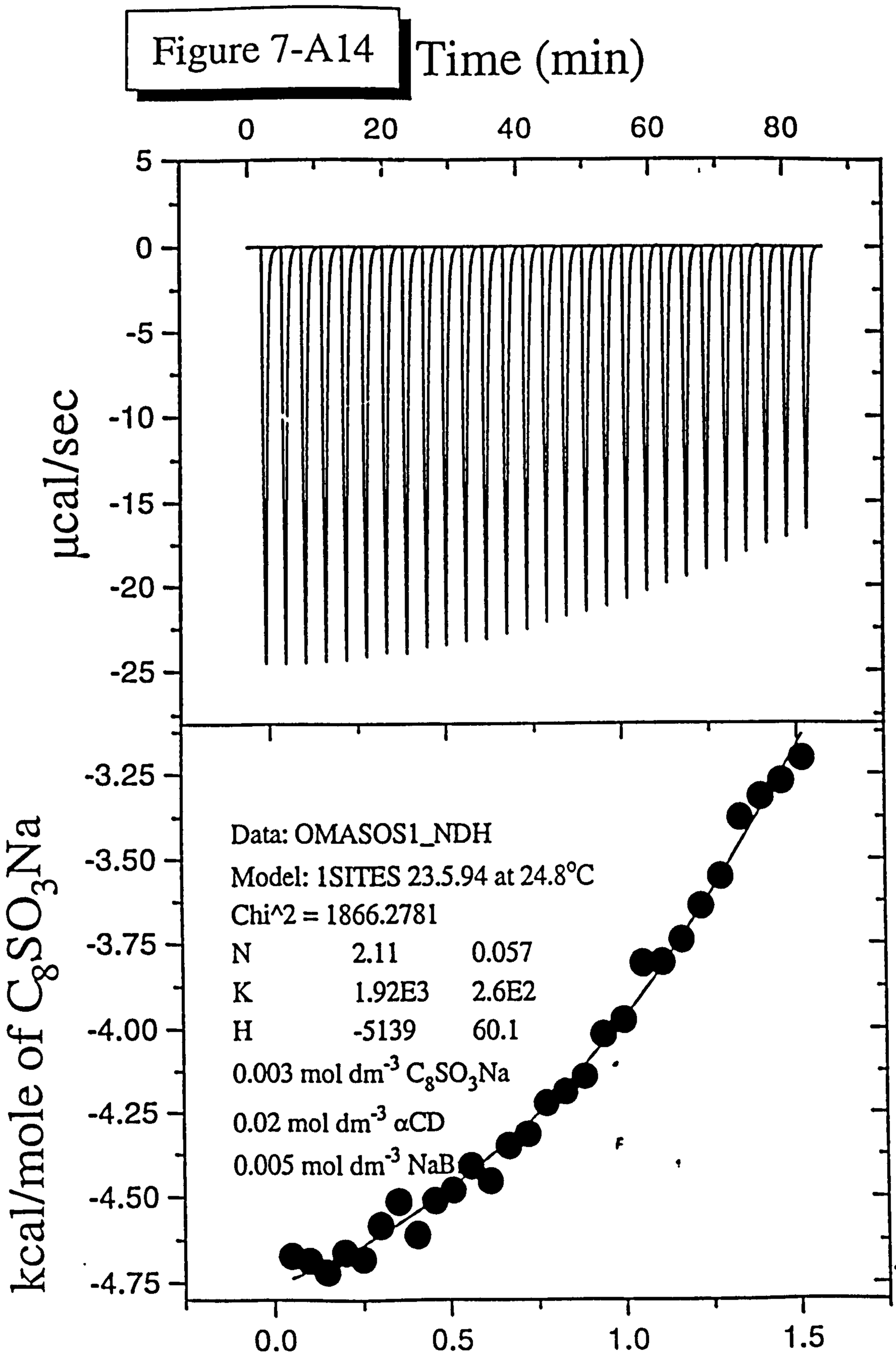
Time (min)
0
20
40
60
80
5
0
-5
-10
-15
-20
-25
µcal/sec
-3.25
-3.50
-3.75
-4.00
-4.25
-4.50
-4.75
kcal/mole of C_8SO_3Na
Data: OMASOS1_NDH
Model: 1SITES 23.5.94 at 24.8°C
Chi^2 = 1866.2781
N 2.11 0.057
K 1.92E3 2.6E2
H -5139 60.1
0.003 mol dm^{-3} C_8SO_3Na
0.02 mol dm^{-3} αCD
0.005 mol dm^{-3} NaB
0.0
0.5
1.0
1.5
Molar Ratio

Figure 7-A15

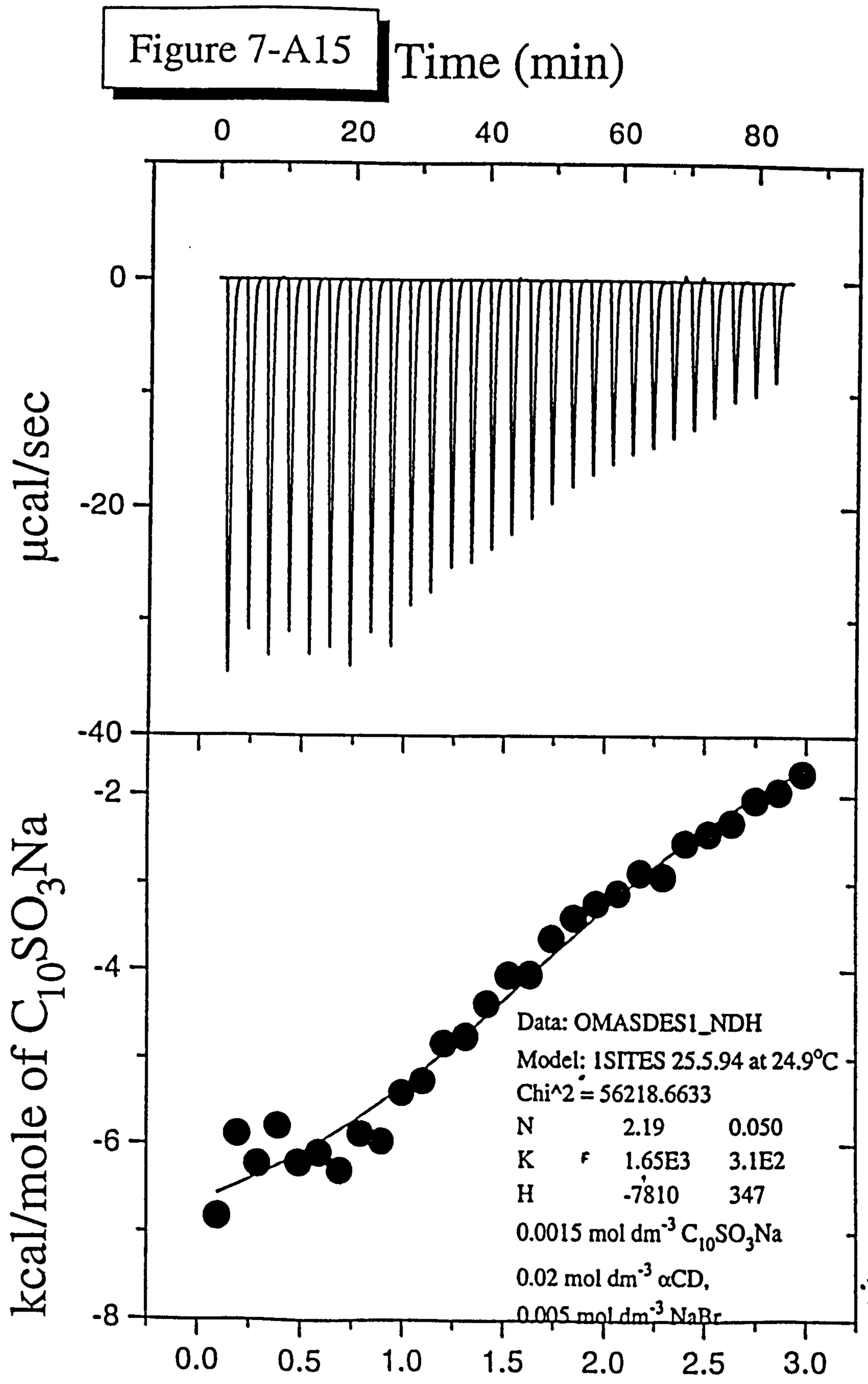
Time (min)
0
20
40
60
80
µcal/sec
0
-20
-40
kcal/mole of $C_{10}SO_3Na$
-2
-4
-6
-8
Data: OMASDES1_NDH
Model: 1SITES 25.5.94 at 24.9°C
Chi^2 = 56218.6633
N 2.19 0.050
K 1.65E3 3.1E2
H -7810 347
0.0015 mol dm^{-3} $C_{10}SO_3Na$
0.02 mol dm^{-3} αCD,
0.005 mol dm^{-3} NaBr
0.0
0.5
1.0
1.5
2.0
2.5
3.0
Molar Ratio

Figure 7-B1

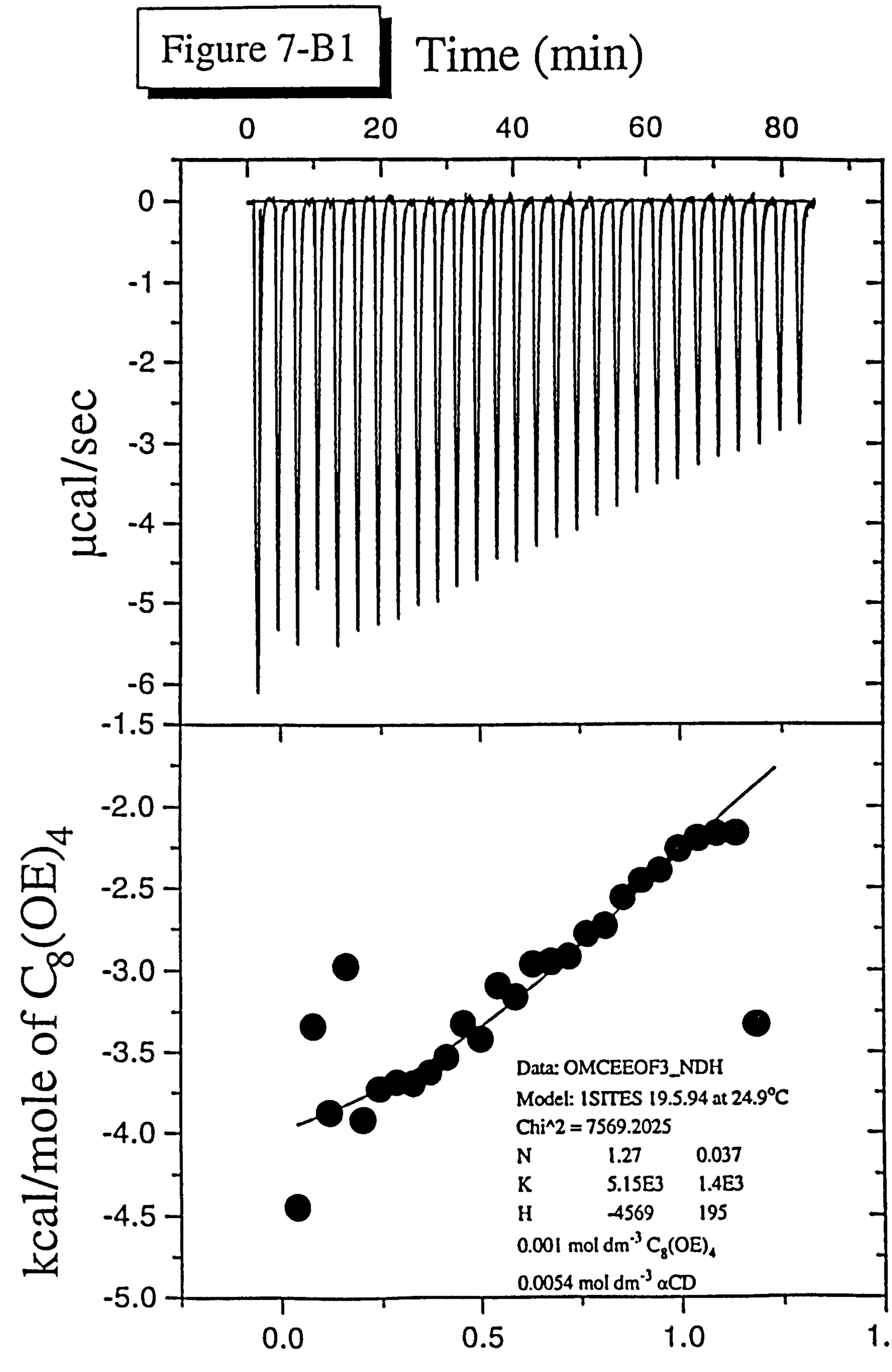
Time (min)
0
20
40
60
80
µcal/sec
0
-1
-2
-3
-4
-5
-6
kcal/mole of $C_8(OE)_4$
-1.5
-2.0
-2.5
-3.0
-3.5
-4.0
-4.5
-5.0
Data: OMCEEOF3_NDH
Model: ISITES 19.5.94 at 24.9°C
Chi^2 = 7569.2025
N 1.27 0.037
K 5.15E3 1.4E3
H -4569 195
0.001 mol dm^{-3} $C_8(OE)_4$
0.0054 mol dm^{-3} αCD
0.0
0.5
1.0
1.5
Molar Ratio

Figure 7-B2

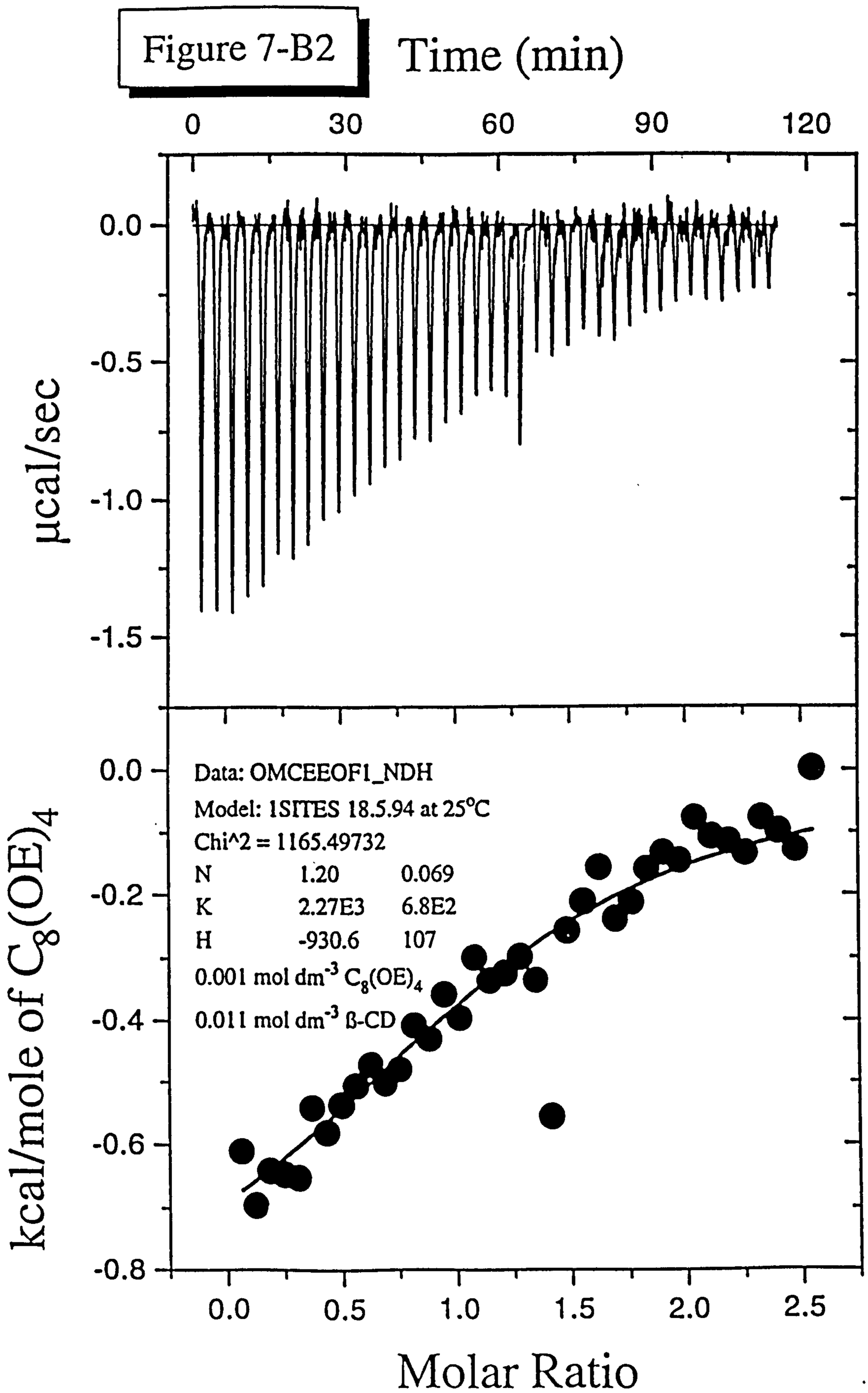
Time (min)
0
30
60
90
120
0.0
-0.5
-1.0
-1.5
µcal/sec
Data: OMCEEOF1_NDH
Model: 1SITES 18.5.94 at 25°C
Chi^2 = 1165.49732
N 1.20 0.069
K 2.27E3 6.8E2
H -930.6 107
0.001 mol dm-3 C8(OE)4
0.011 mol dm-3 ß-CD
0.0
-0.2
-0.4
-0.6
-0.8
kcal/mole of C8(OE)4
0.0
0.5
1.0
1.5
2.0
2.5
Molar Ratio

Figure 7-B3

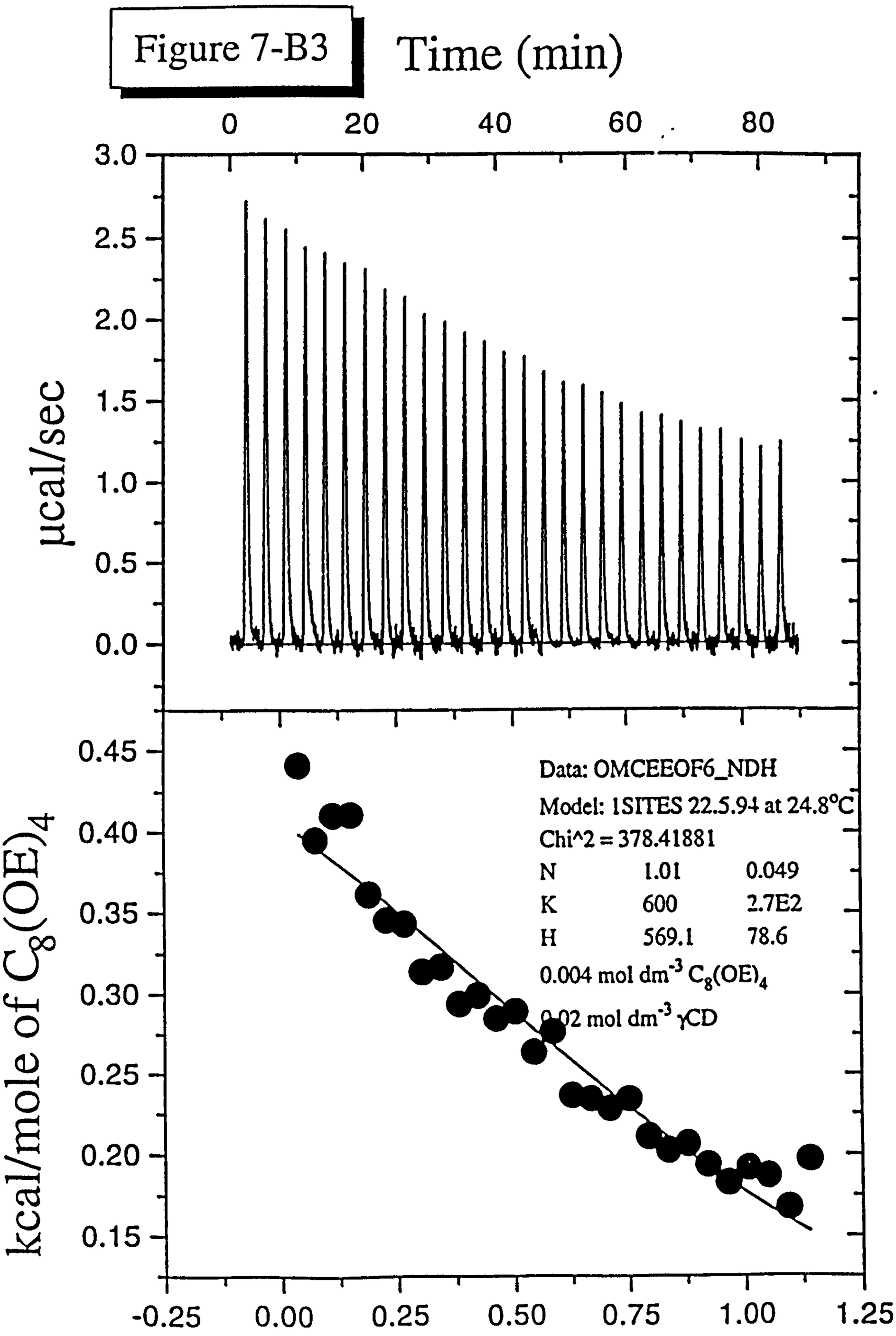
Time (min)
0
20
40
60
80
3.0
2.5
2.0
1.5
1.0
0.5
0.0
µcal/sec
0.45
0.40
0.35
0.30
0.25
0.20
0.15
kcal/mole of $C_8(OE)_4$
Data: OMCEEOF6_NDH
Model: ISITES 22.5.94 at 24.8°C
Chi^2 = 378.41881
N 1.01 0.049
K 600 2.7E2
H 569.1 78.6
0.004 mol dm^{-3} $C_8(OE)_4$
0.02 mol dm^{-3} γCD
-0.25
0.00
0.25
0.50
0.75
1.00
1.25
Molar Ratio

Figure 7-C1: A Two-Site Consecutive Fit for α-CD/C_{12}TAB system

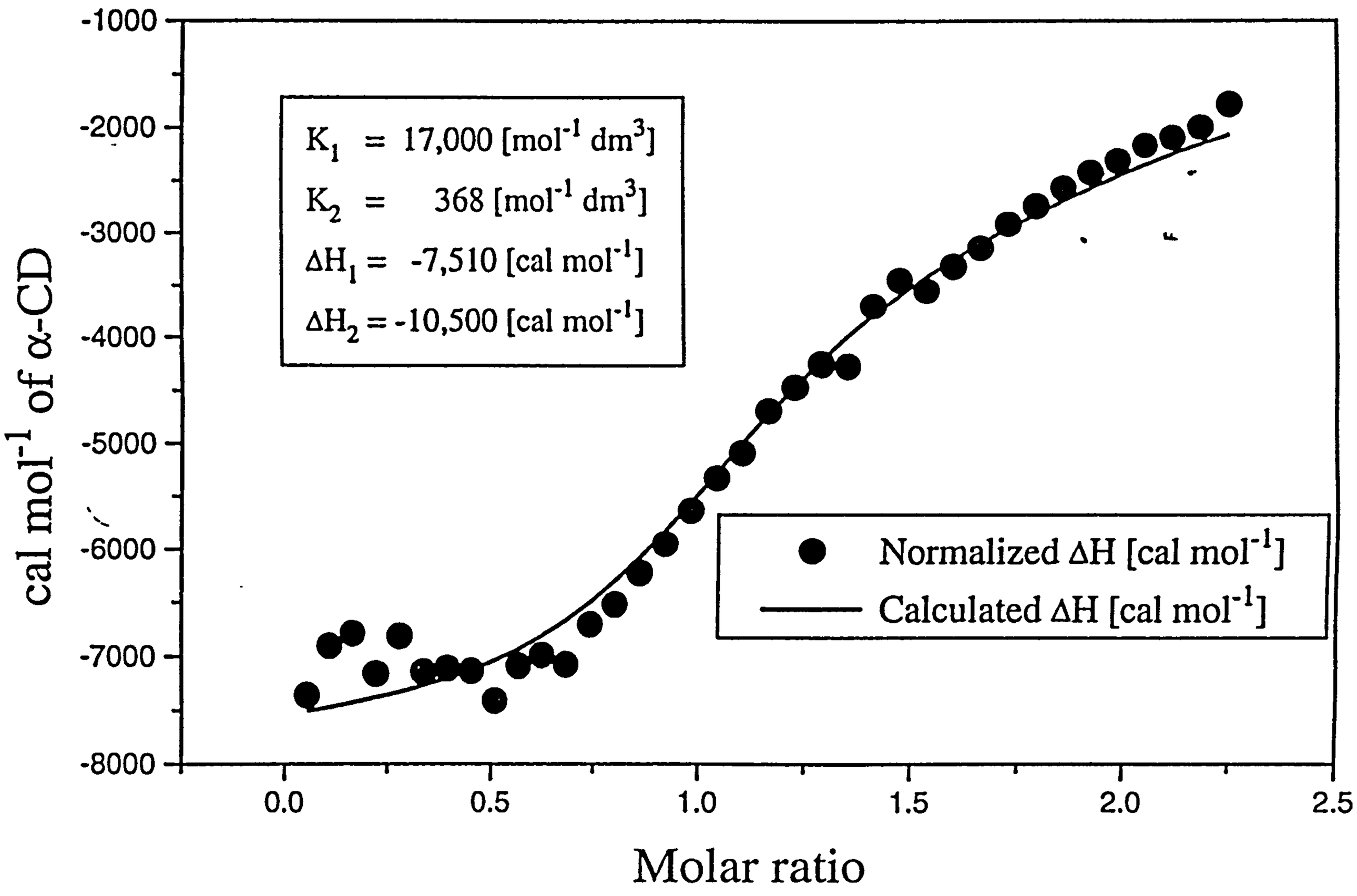

Figure 7-C2: A Two-Site Consecutive Fit for α-CD/C_{14}TAB system

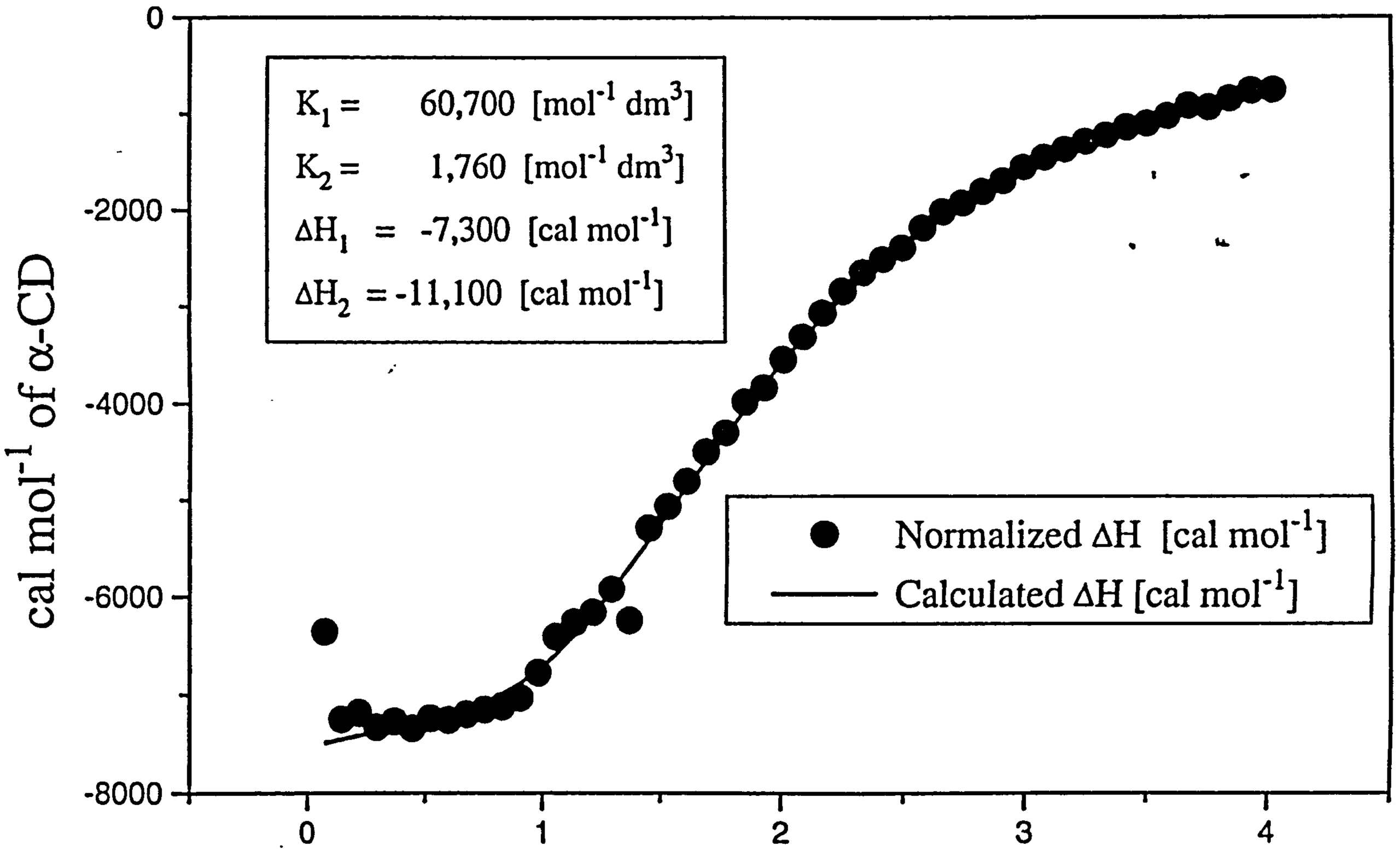

Figure 7-C3: A Two-Site Consecutive Fit for α-CD/C_{16}TAB system

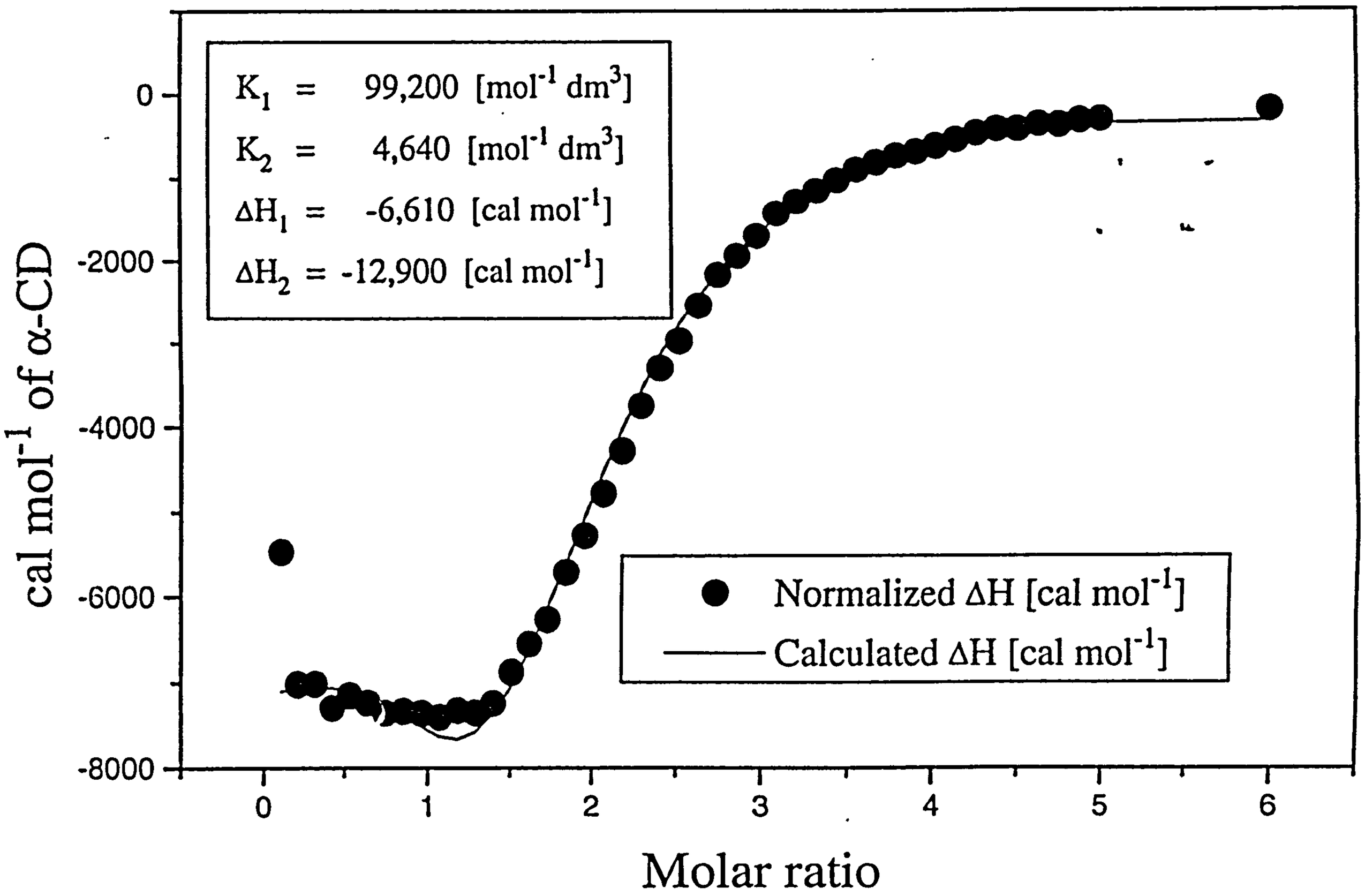

Figure 7-C4: A Two-Site Consecutive Fit for α-CD/C_{12}PyBr system

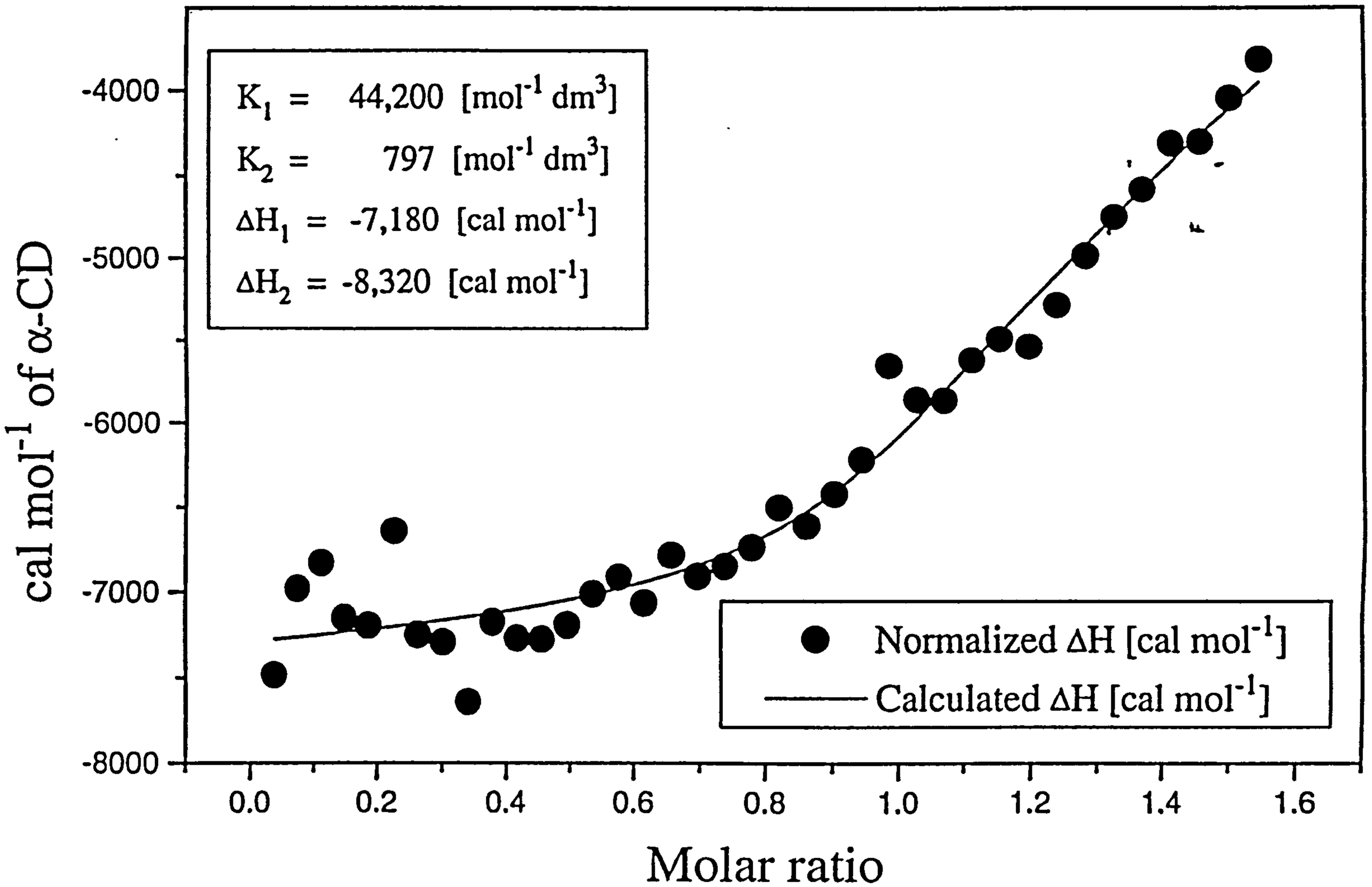

Figure 7-C5: A Two-Site Consecutive Fit for α-CD/C_{14}PyBr system

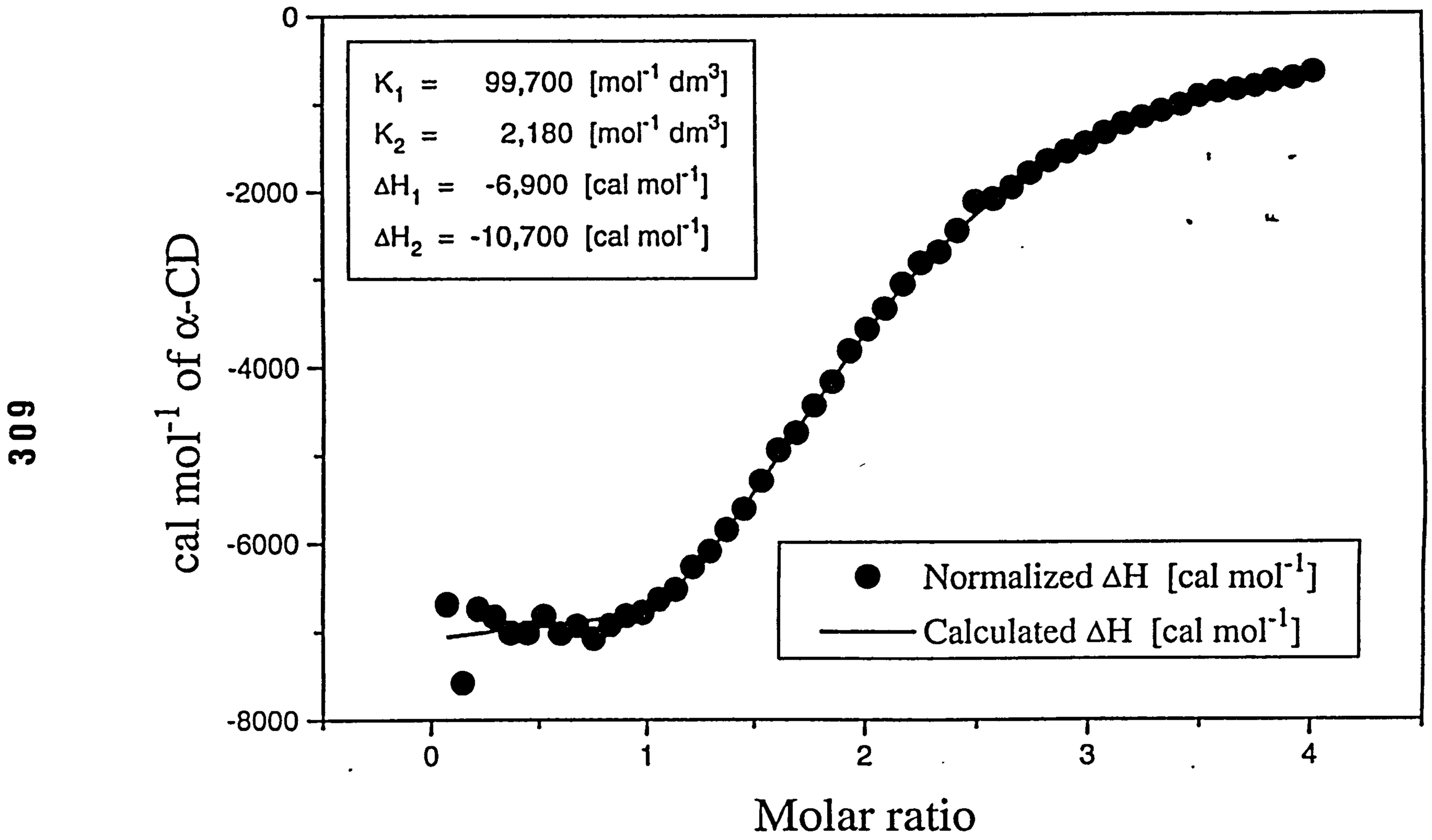

Figure 7-C6: A Two-Site Consecutive Fit for α-CD/C_{16}PyBr system

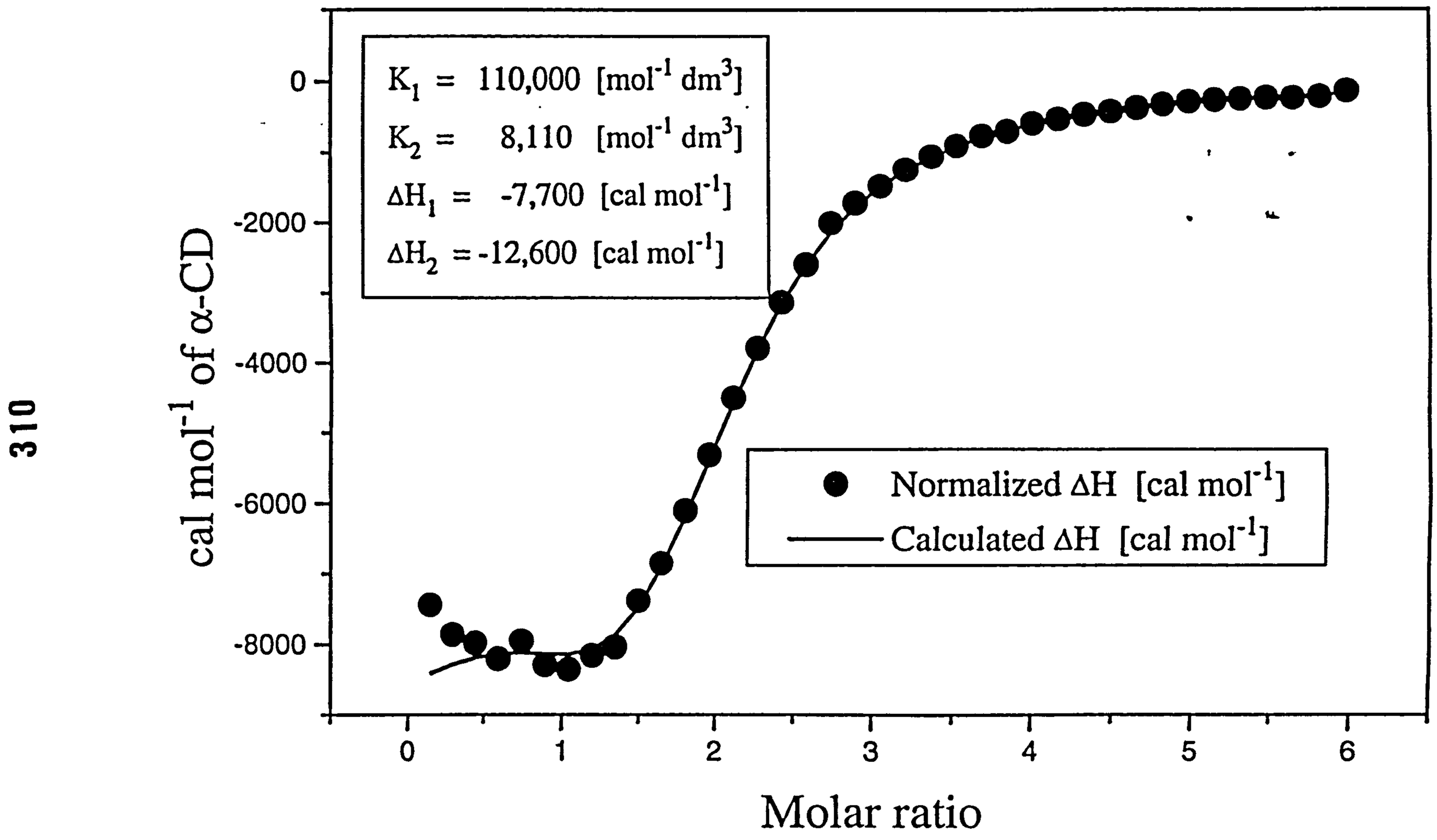

Figure 7-C7: A Two-Site Consecutive Fit for α-CD/$C_{10}OSO_3Na$ system

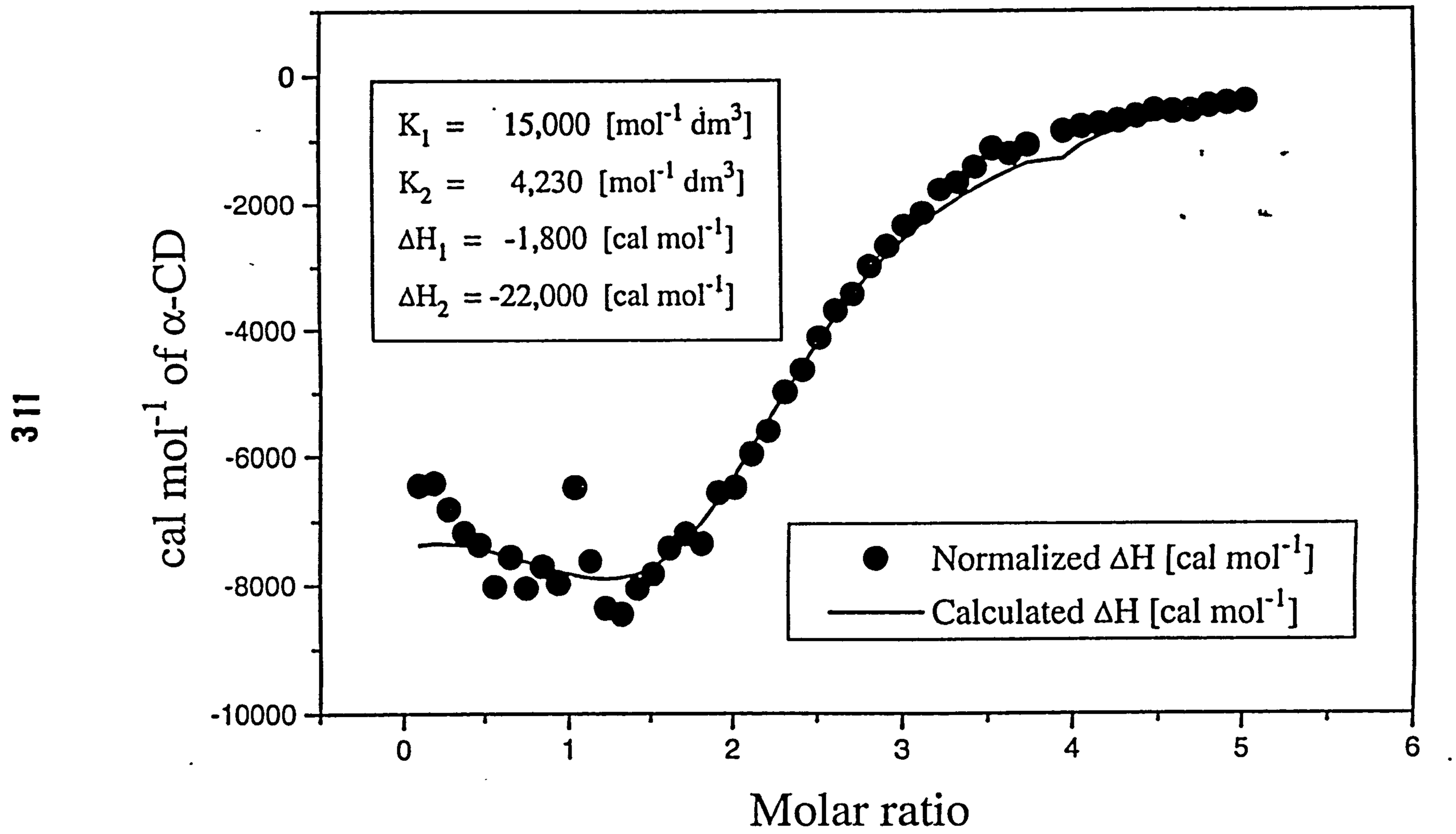

Figure 7-C8: A Two-Site Consecutive Fit for α-CD/$C_{14}OSO_3Na$ system

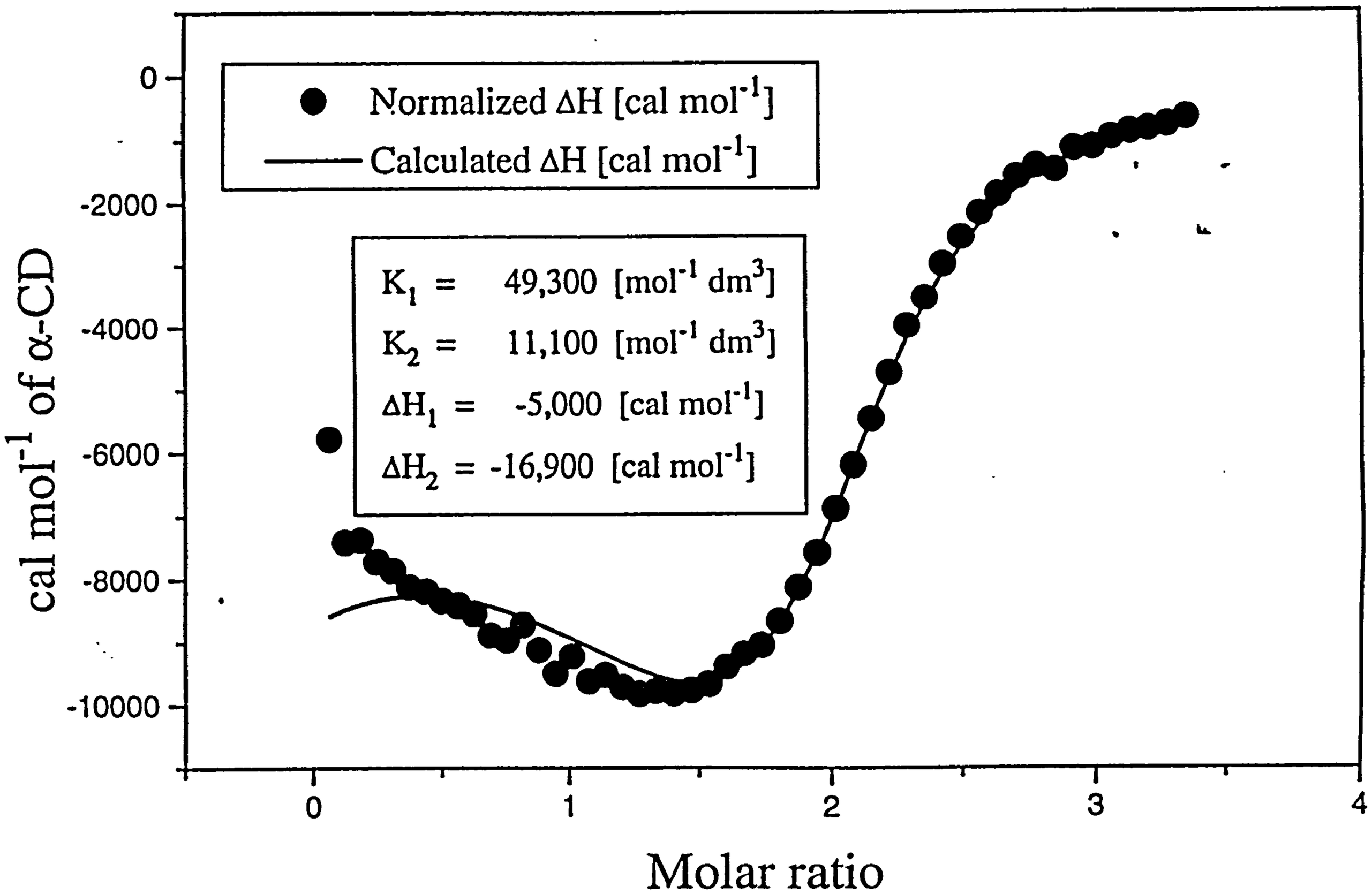

Figure 7-C9: A Two-Site Consecutive Fit for α-CD/$C_{12}SO_3Na$ system

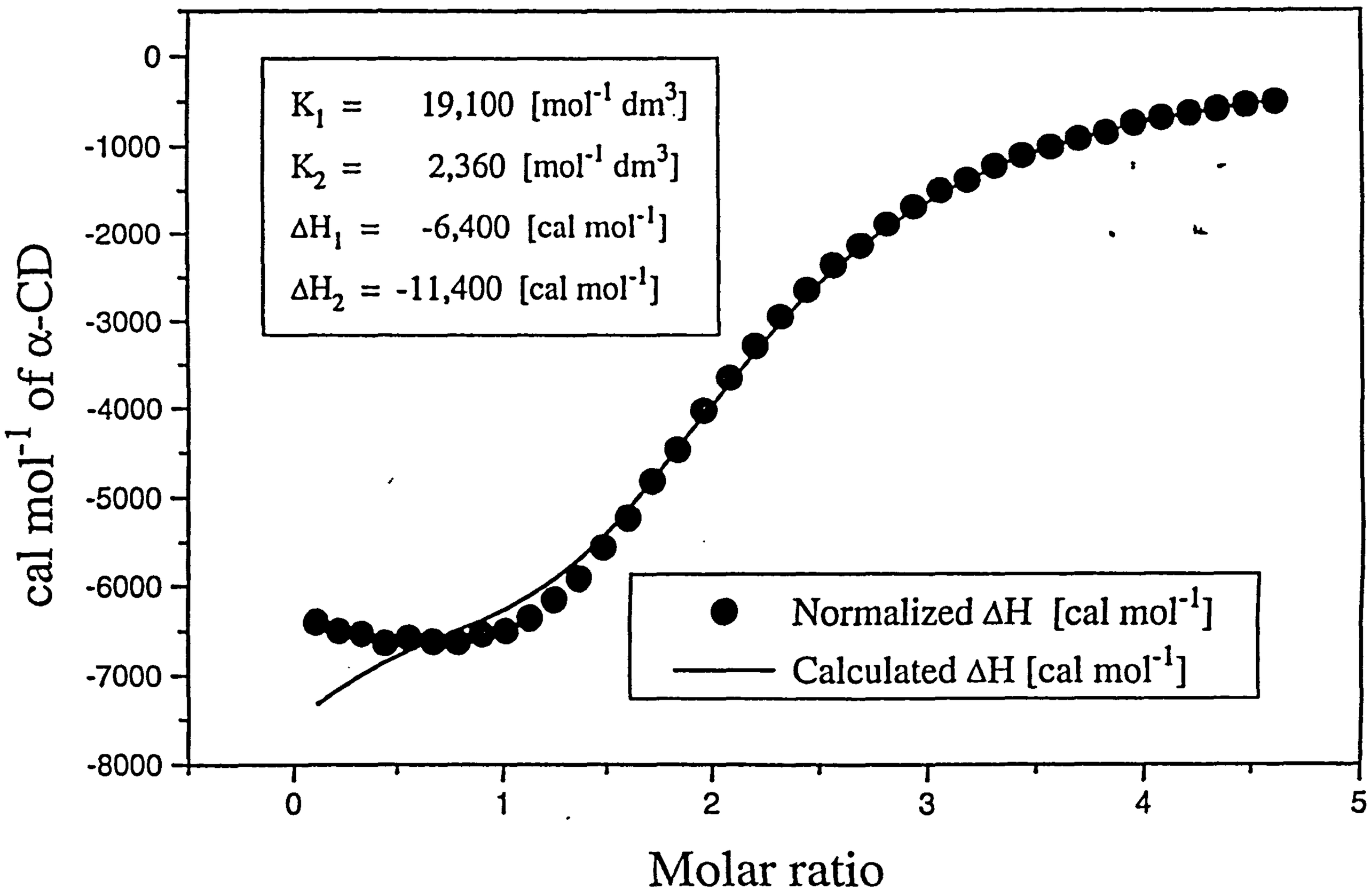

Figure 7-C10: A Two-Site Consecutive Fit for β-CD/C_{16}TAB system

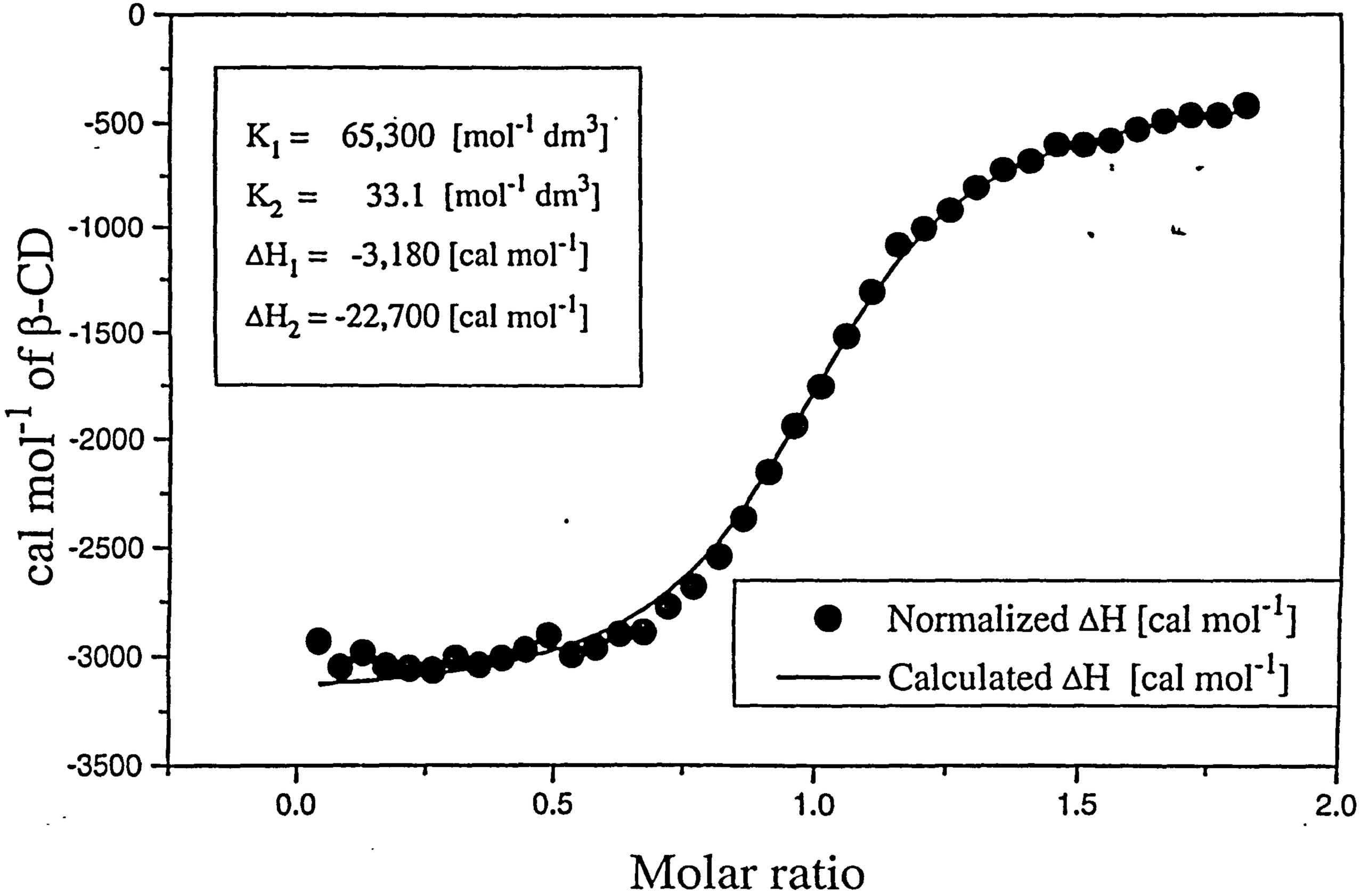

Figure 7-C11: A Two-Site Consecutive Fit for β-CD/$C_{14}OSO_3Na$ system

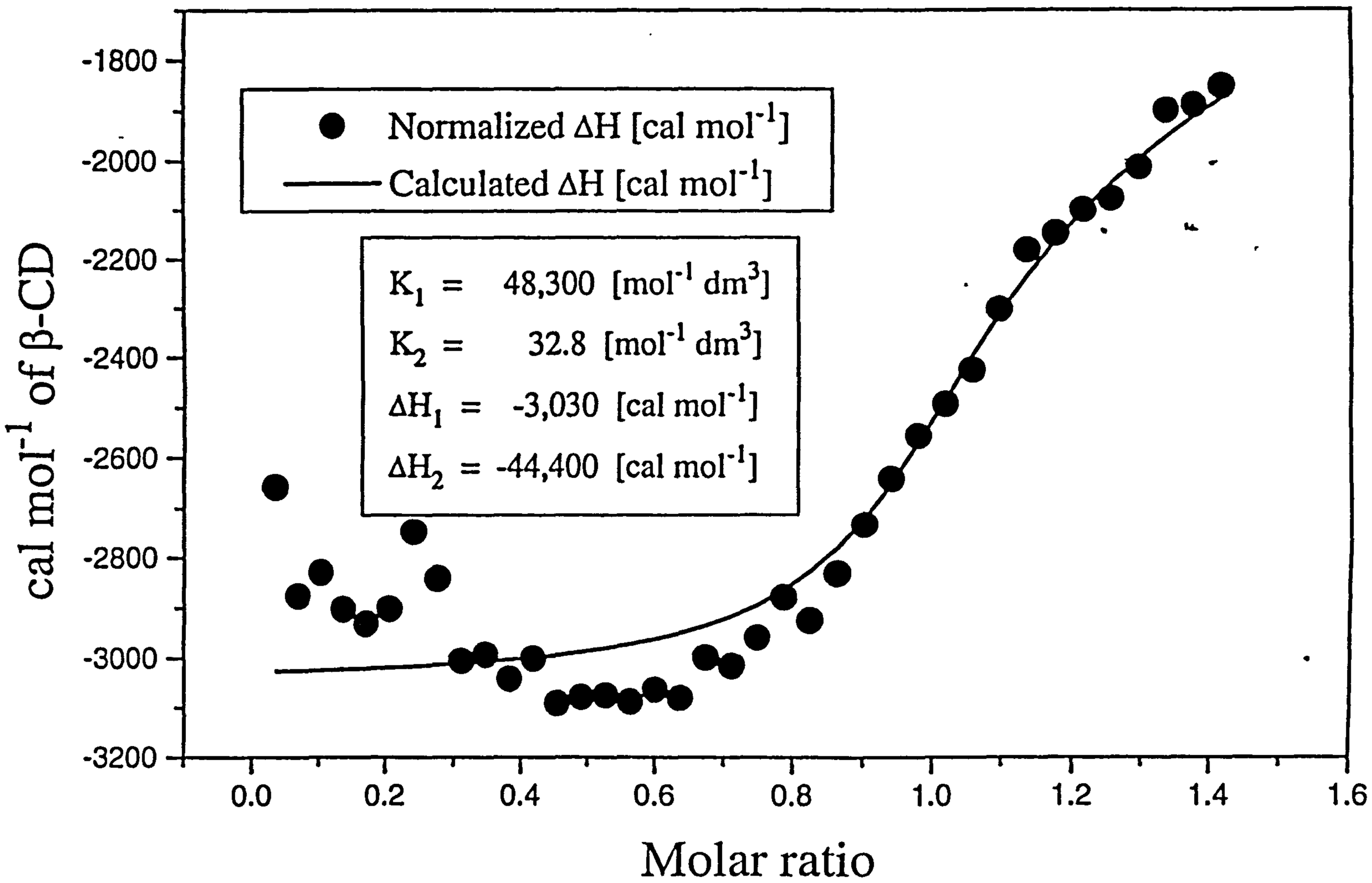

Figure 7-D1

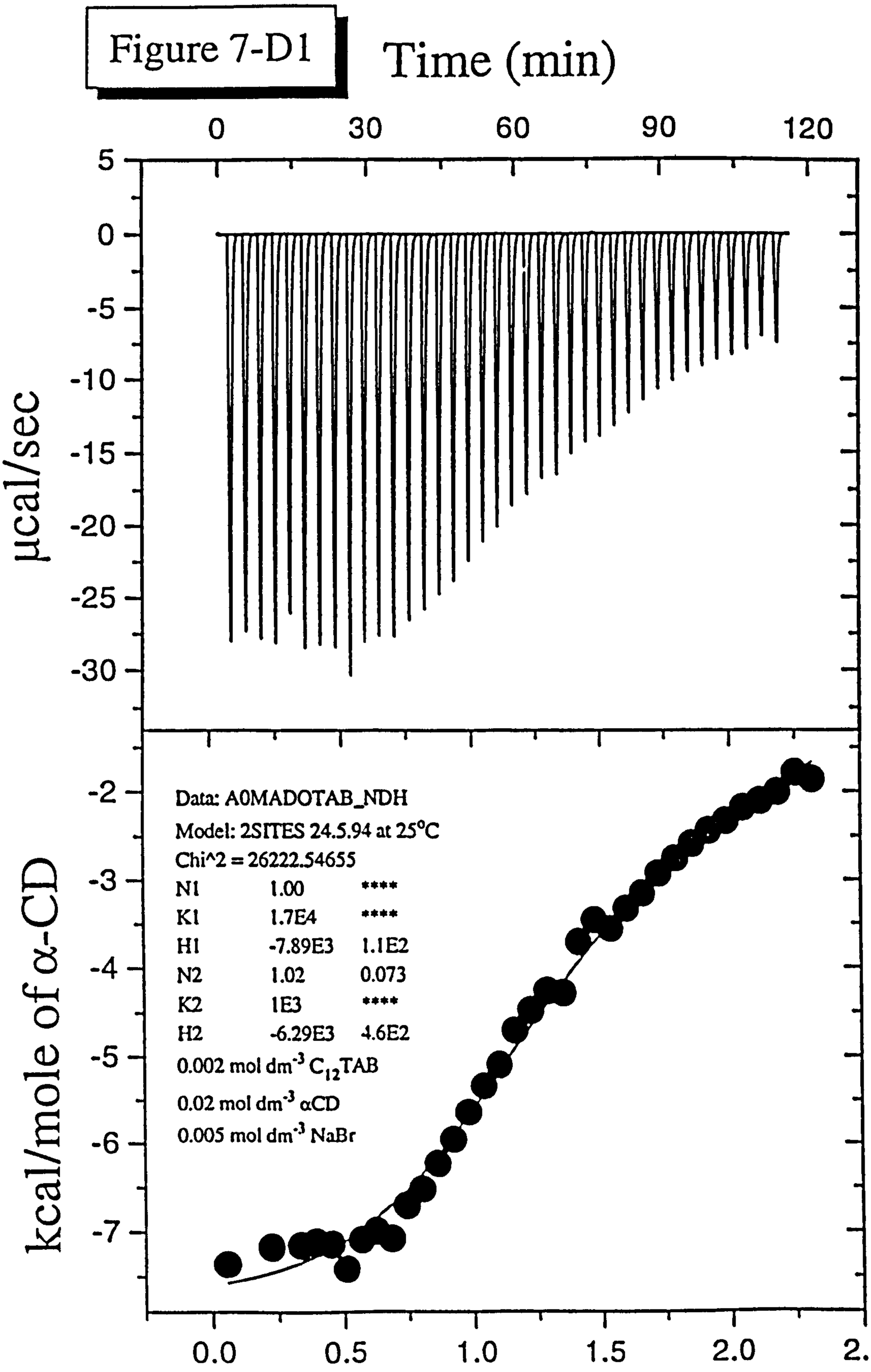
Time (min)
0
30
60
90
120
5
0
-5
-10
-15
-20
-25
-30
µcal/sec
-2
-3
-4
-5
-6
-7
kcal/mole of α-CD
Data: A0MADOTAB_NDH
Model: 2SITES 24.5.94 at 25°C
Chi^2 = 26222.54655
N1 1.00 ****
K1 1.7E4 ****
H1 -7.89E3 1.1E2
N2 1.02 0.073
K2 1E3 ****
H2 -6.29E3 4.6E2
0.002 mol dm-3 C12TAB
0.02 mol dm-3 αCD
0.005 mol dm-3 NaBr
0.0
0.5
1.0
1.5
2.0
2.5
Molar Ratio

Figure 7-D2

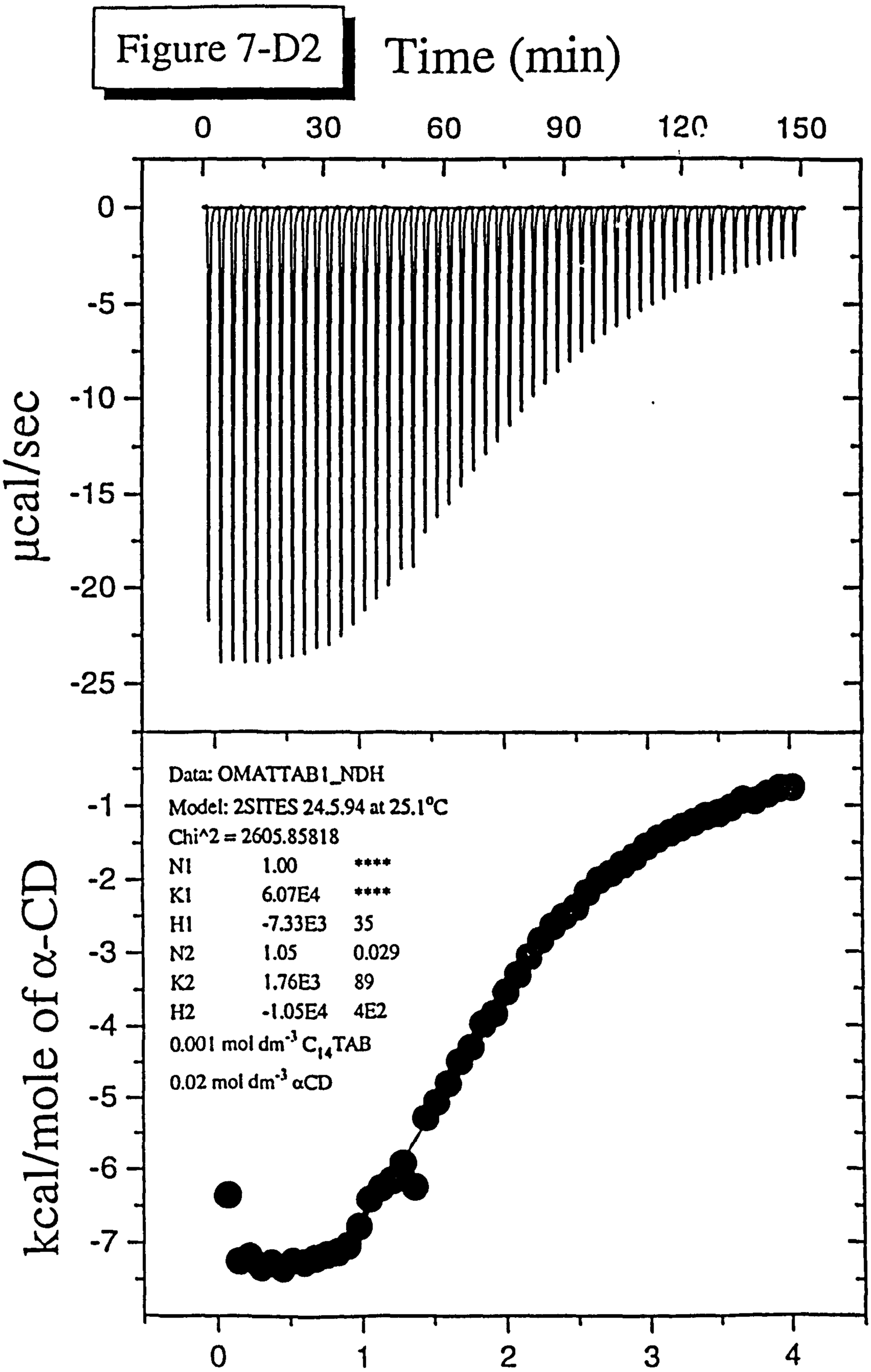
Time (min)
0
30
60
90
120
150
0
-5
-10
-15
-20
-25
µcal/sec
Data: OMATTAB1_NDH
Model: 2SITES 24.5.94 at 25.1°C
Chi^2 = 2605.85818
N1 1.00 ****
K1 6.07E4 ****
H1 -7.33E3 35
N2 1.05 0.029
K2 1.76E3 89
H2 -1.05E4 4E2
0.001 mol dm-3 C14TAB
0.02 mol dm-3 αCD
-1
-2
-3
-4
-5
-6
-7
kcal/mole of α-CD
0
1
2
3
4
Molar Ratio

Figure 7-D3

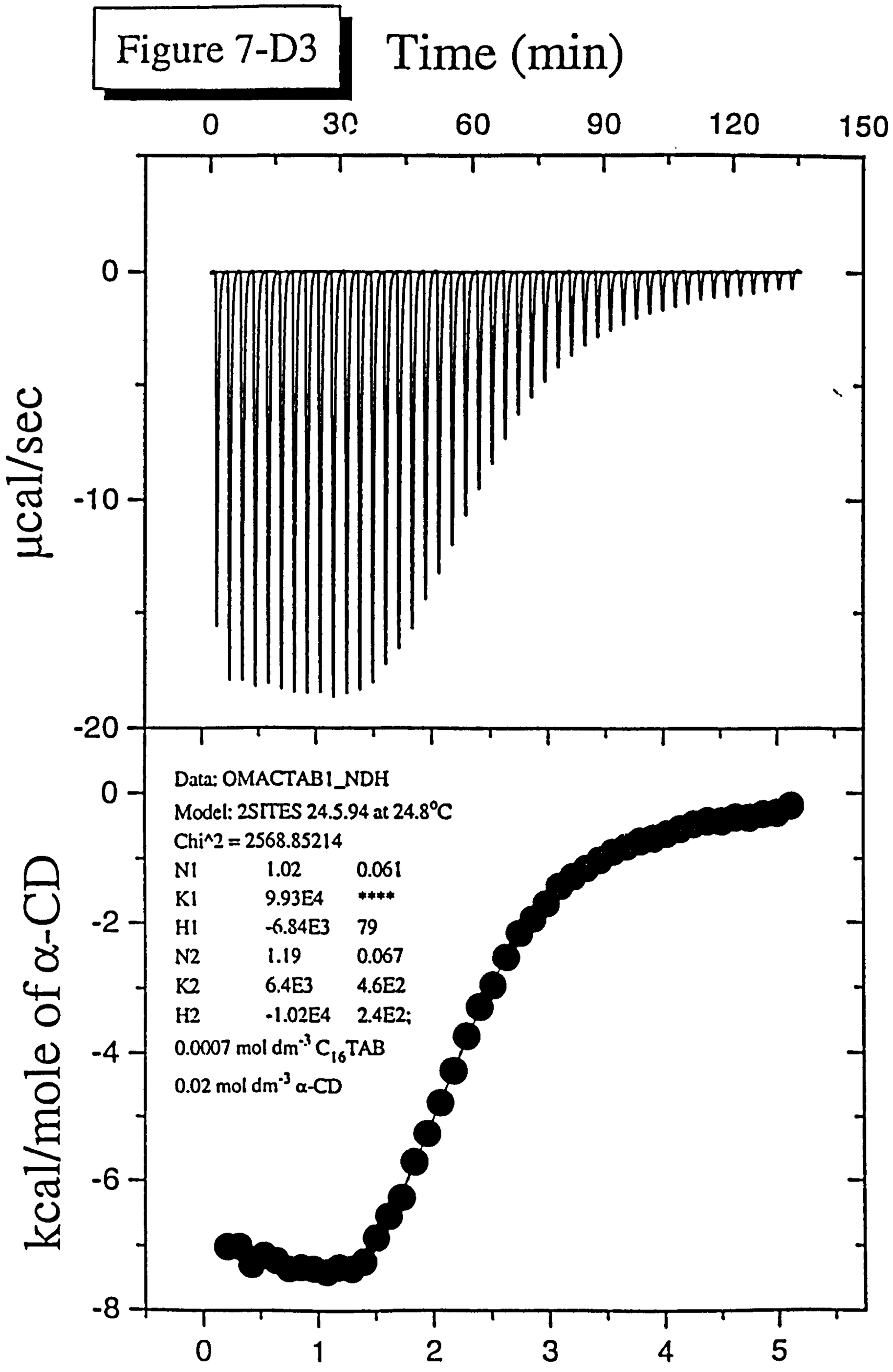
Time (min)
0
30
60
90
120
150
µcal/sec
0
-10
-20
Data: OMACTAB1_NDH
Model: 2SITES 24.5.94 at 24.8°C
Chi^2 = 2568.85214
N1 1.02 0.061
K1 9.93E4 ****
H1 -6.84E3 79
N2 1.19 0.067
K2 6.4E3 4.6E2
H2 -1.02E4 2.4E2;
0.0007 mol dm-3 C16TAB
0.02 mol dm-3 α-CD
kcal/mole of α-CD
0
-2
-4
-6
-8
0
1
2
3
4
5
Molar Ratio

Figure 7-D4

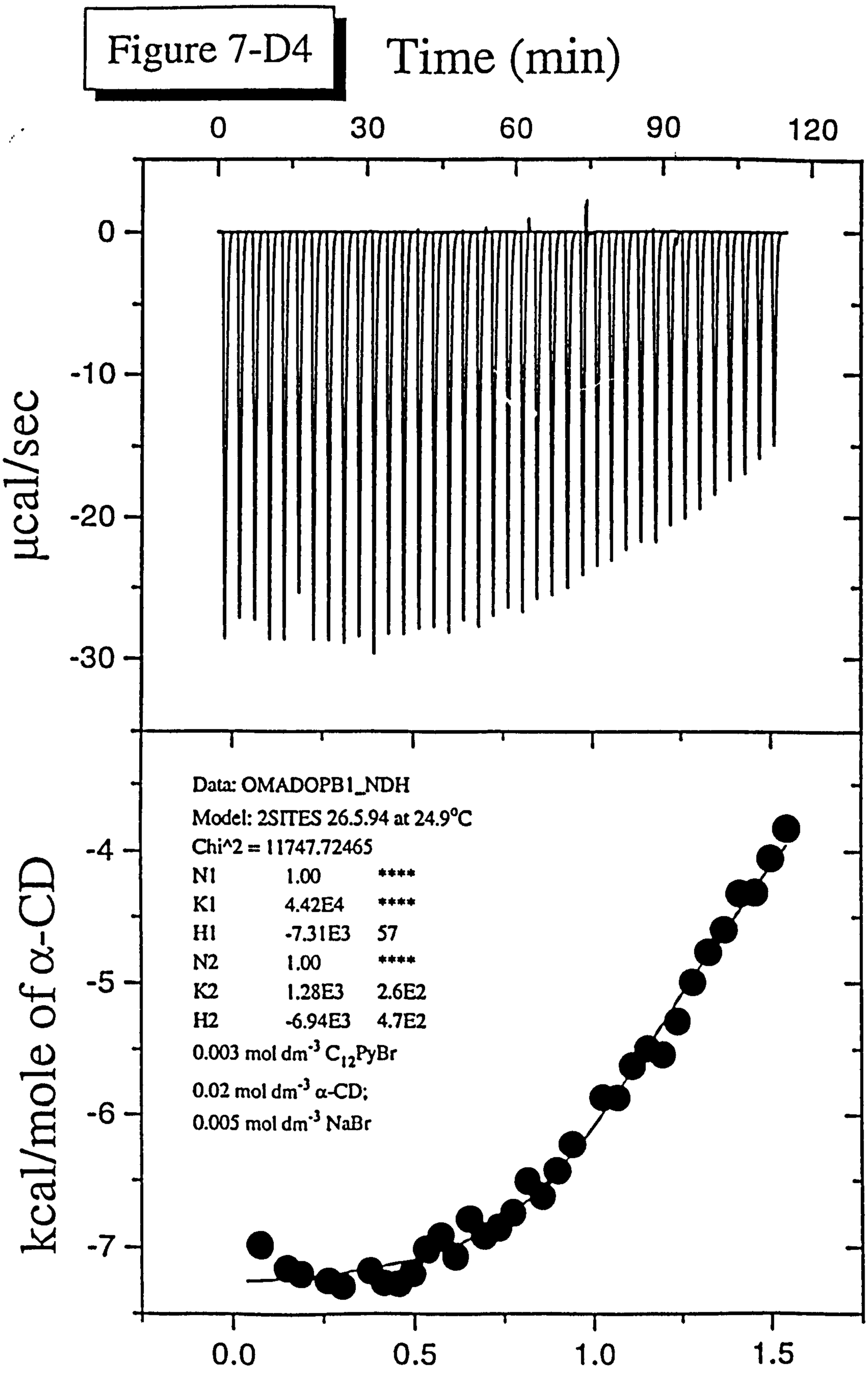
Time (min)
0
30
60
90
120
0
-10
-20
-30
µcal/sec
Data: OMADOPB1_NDH
Model: 2SITES 26.5.94 at 24.9°C
Chi^2 = 11747.72465
N1 1.00 ****
K1 4.42E4 ****
H1 -7.31E3 57
N2 1.00 ****
K2 1.28E3 2.6E2
H2 -6.94E3 4.7E2
0.003 mol dm-3 C12PyBr
0.02 mol dm-3 α-CD;
0.005 mol dm-3 NaBr
-4
-5
-6
-7
kcal/mole of α-CD
0.0
0.5
1.0
1.5
Molar Ratio

Figure 7-D5

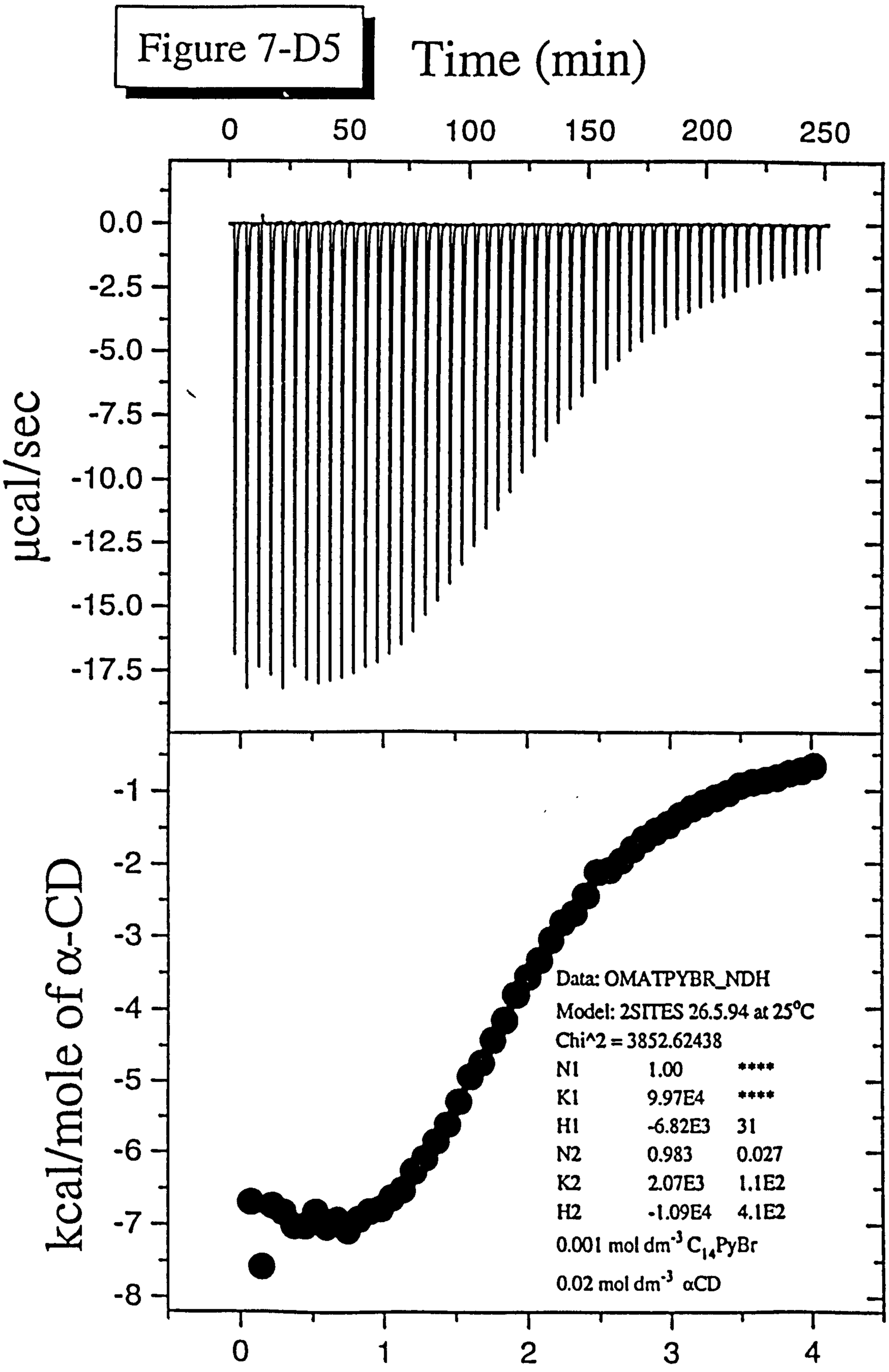
Time (min)
0
50
100
150
200
250
0.0
-2.5
-5.0
-7.5
-10.0
-12.5
-15.0
-17.5
µcal/sec
kcal/mole of α-CD
-1
-2
-3
-4
-5
-6
-7
-8
Data: OMATPYBR_NDH
Model: 2SITES 26.5.94 at 25°C
Chi^2 = 3852.62438
N1 1.00 ****
K1 9.97E4 ****
H1 -6.82E3 31
N2 0.983 0.027
K2 2.07E3 1.1E2
H2 -1.09E4 4.1E2
0.001 mol dm-3 C14PyBr
0.02 mol dm-3 αCD
0
1
2
3
4
Molar Ratio

Figure 7-D6

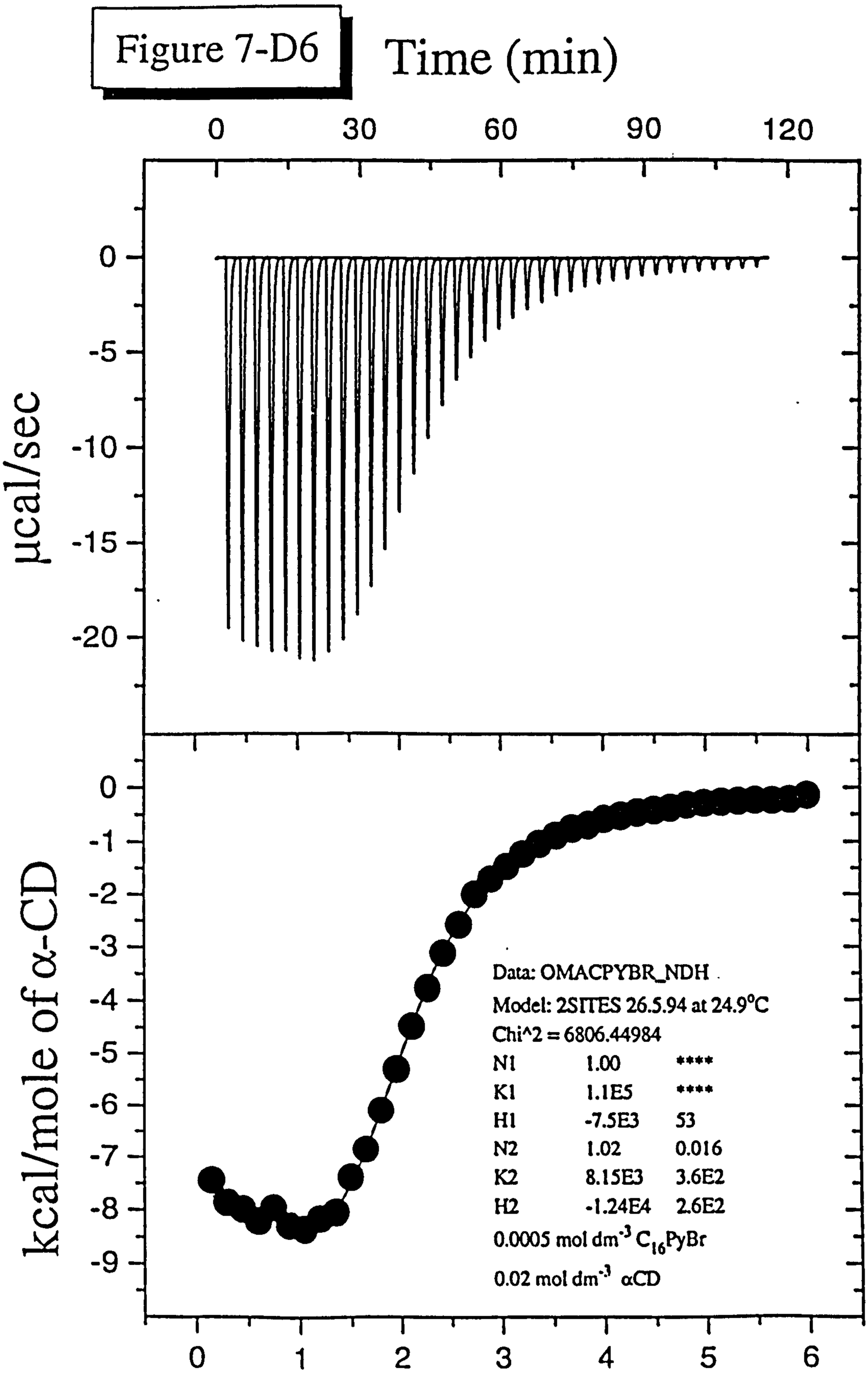
Time (min)
0
30
60
90
120
µcal/sec
0
-5
-10
-15
-20
kcal/mole of α-CD
0
-1
-2
-3
-4
-5
-6
-7
-8
-9
Data: OMACPYBR_NDH
Model: 2SITES 26.5.94 at 24.9°C
Chi^2 = 6806.44984
N1 1.00 ****
K1 1.1E5 ****
H1 -7.5E3 53
N2 1.02 0.016
K2 8.15E3 3.6E2
H2 -1.24E4 2.6E2
0.0005 mol dm-3 C16PyBr
0.02 mol dm-3 αCD
0
1
2
3
4
5
6
Molar Ratio

Figure 7-D7

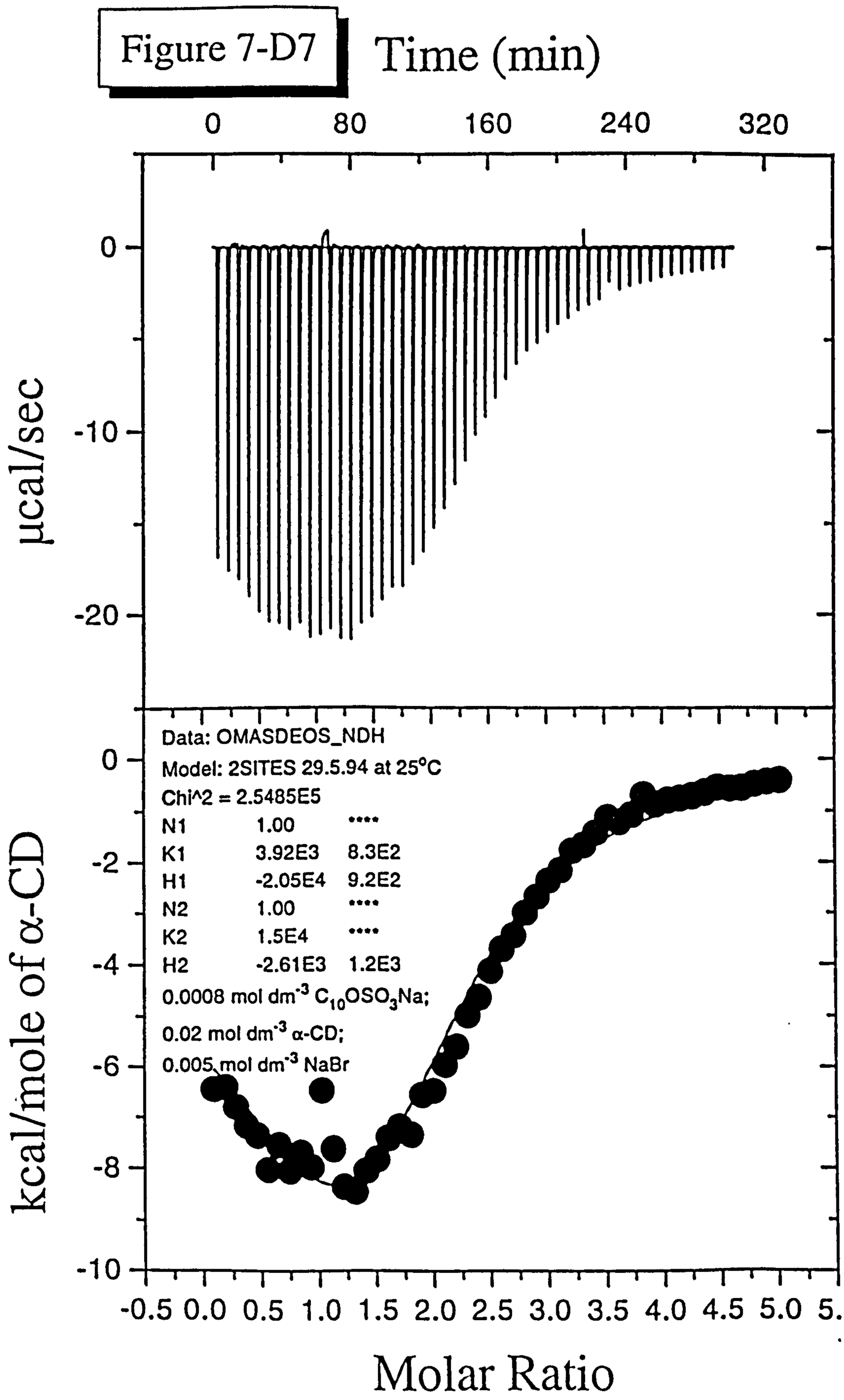
Time (min)
0
80
160
240
320
µcal/sec
0
-10
-20
Data: OMASDEOS_NDH
Model: 2SITES 29.5.94 at 25°C
Chi^2 = 2.5485E5
N1 1.00 ****
K1 3.92E3 8.3E2
H1 -2.05E4 9.2E2
N2 1.00 ****
K2 1.5E4 ****
H2 -2.61E3 1.2E3
0.0008 mol dm-3 C10OSO3Na;
0.02 mol dm-3 α-CD;
0.005 mol dm-3 NaBr
kcal/mole of α-CD
0
-2
-4
-6
-8
-10
-0.5 0.0 0.5 1.0 1.5 2.0 2.5 3.0 3.5 4.0 4.5 5.0 5.5
Molar Ratio

Figure 7-D8

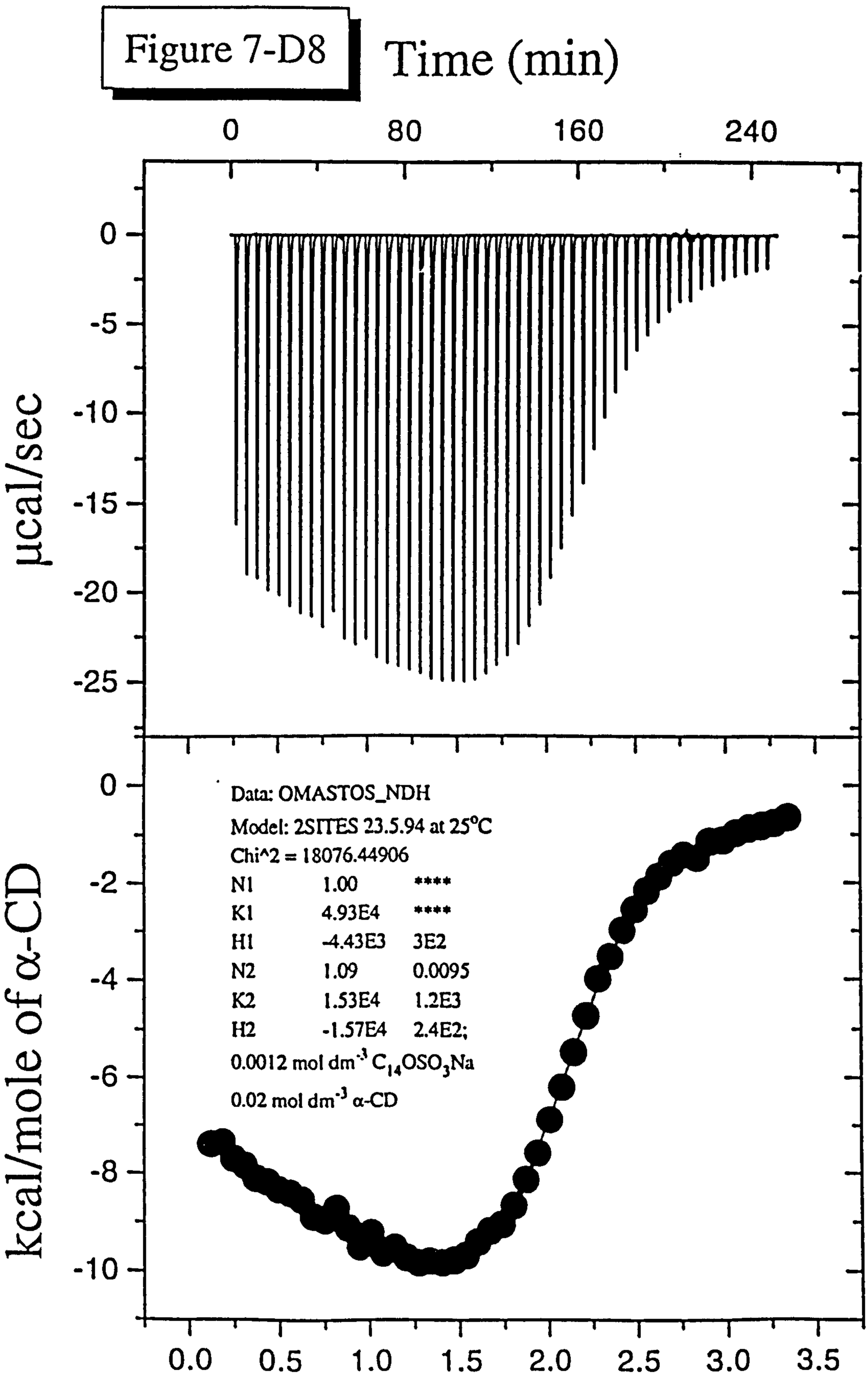
Time (min)
0
80
160
240
µcal/sec
0
-5
-10
-15
-20
-25
kcal/mole of α-CD
0
-2
-4
-6
-8
-10
Data: OMASTOS_NDH
Model: 2SITES 23.5.94 at 25°C
Chi^2 = 18076.44906
N1 1.00 ****
K1 4.93E4 ****
H1 -4.43E3 3E2
N2 1.09 0.0095
K2 1.53E4 1.2E3
H2 -1.57E4 2.4E2;
0.0012 mol dm-3 C14OSO3Na
0.02 mol dm-3 α-CD
0.0 0.5 1.0 1.5 2.0 2.5 3.0 3.5
Molar Ratio

Figure 7-D9

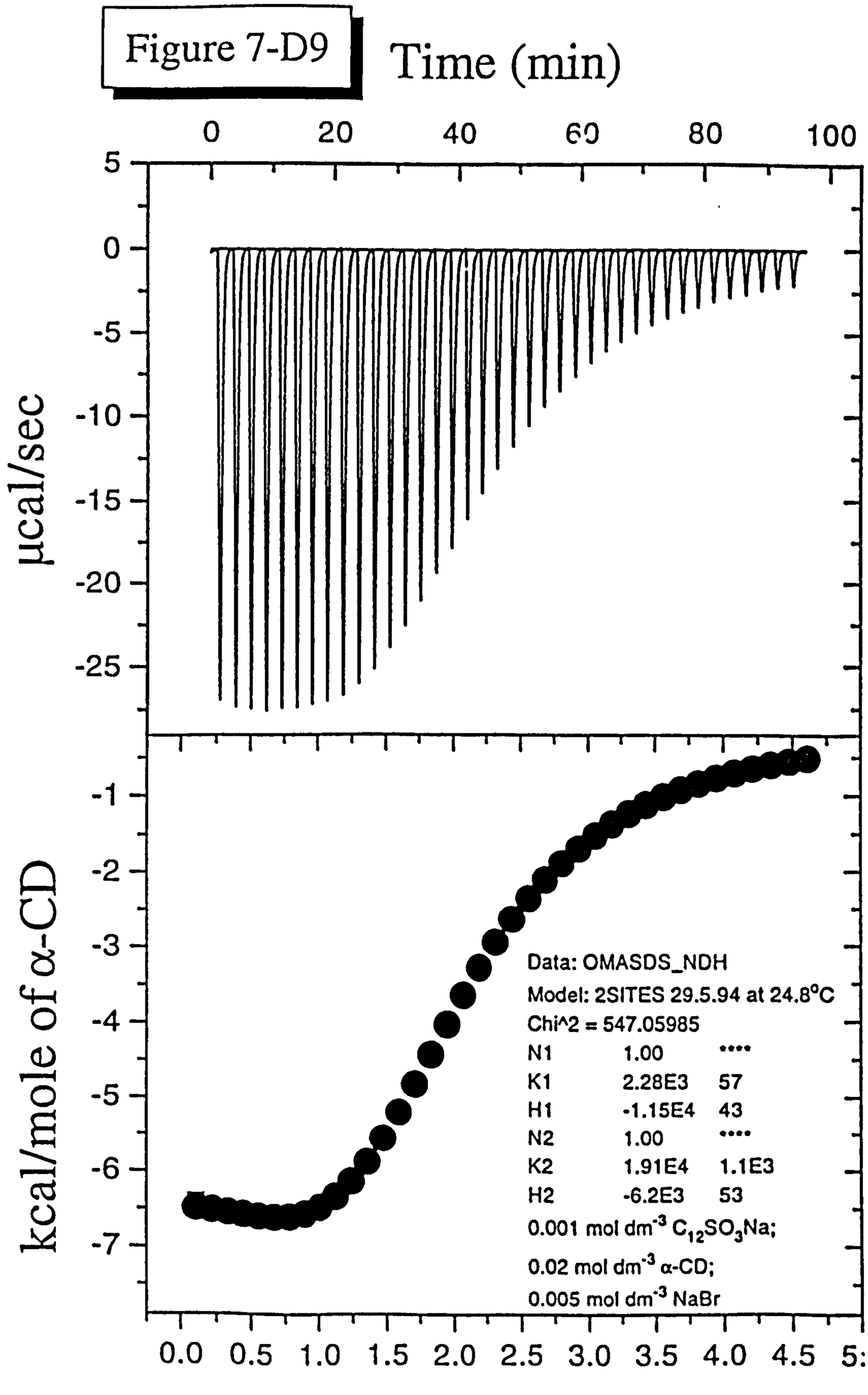
Time (min)
0
20
40
60
80
100
5
0
-5
-10
-15
-20
-25
µcal/sec
-1
-2
-3
-4
-5
-6
-7
kcal/mole of α-CD
Data: OMASDS_NDH
Model: 2SITES 29.5.94 at 24.8°C
Chi^2 = 547.05985
N1 1.00 ****
K1 2.28E3 57
H1 -1.15E4 43
N2 1.00 ****
K2 1.91E4 1.1E3
H2 -6.2E3 53
0.001 mol dm-3 C12SO3Na;
0.02 mol dm-3 α-CD;
0.005 mol dm-3 NaBr
0.0 0.5 1.0 1.5 2.0 2.5 3.0 3.5 4.0 4.5 5:0
Molar Ratio

Figure 7-D10

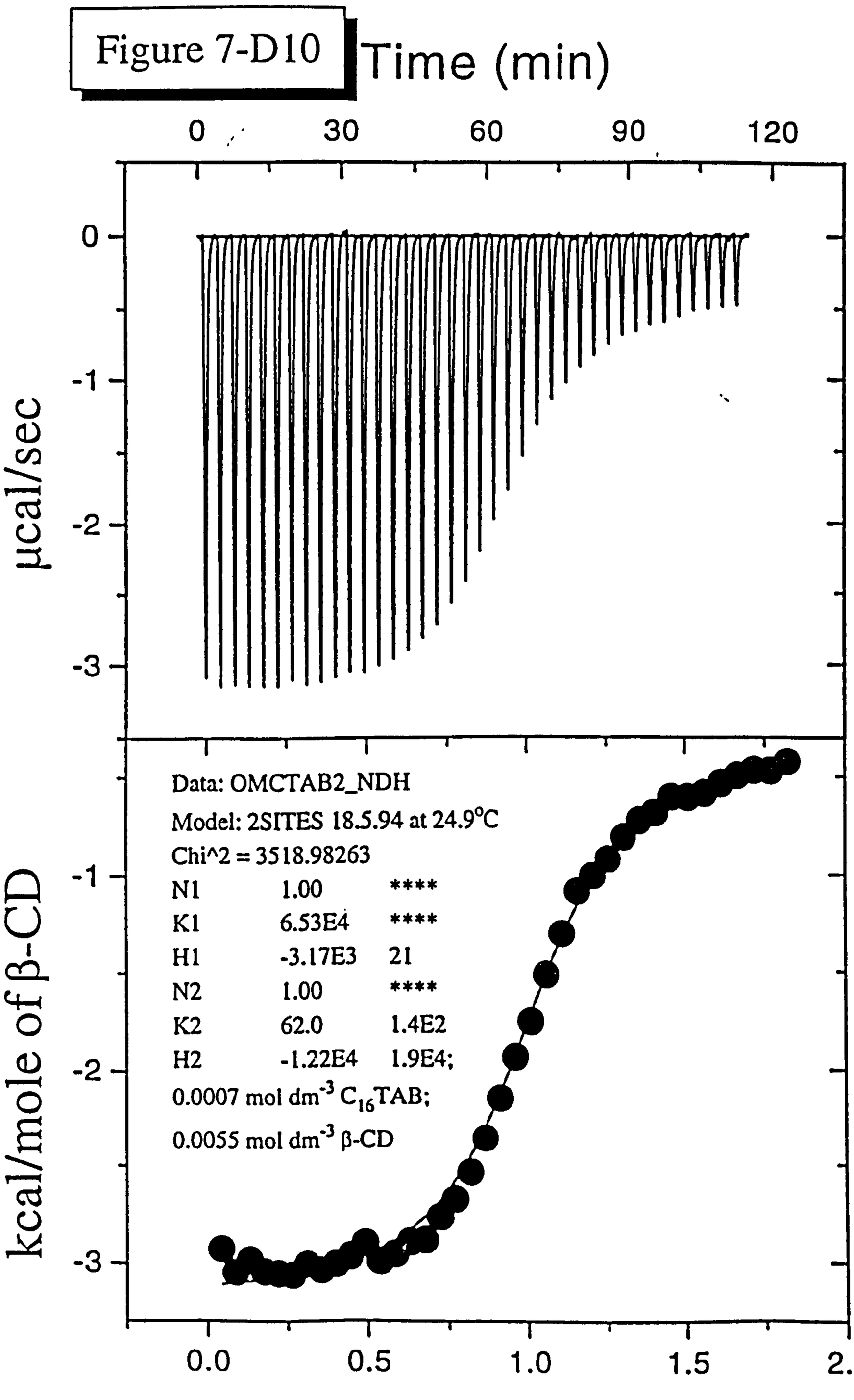
Time (min)
0
30
60
90
120
µcal/sec
0
-1
-2
-3
Data: OMCTAB2_NDH
Model: 2SITES 18.5.94 at 24.9°C
Chi^2 = 3518.98263
N1 1.00 ****
K1 6.53E4 ****
H1 -3.17E3 21
N2 1.00 ****
K2 62.0 1.4E2
H2 -1.22E4 1.9E4;
0.0007 mol dm-3 C16TAB;
0.0055 mol dm-3 β-CD
kcal/mole of β-CD
-1
-2
-3
0.0
0.5
1.0
1.5
2.0
Molar Ratio

Figure 7-D11

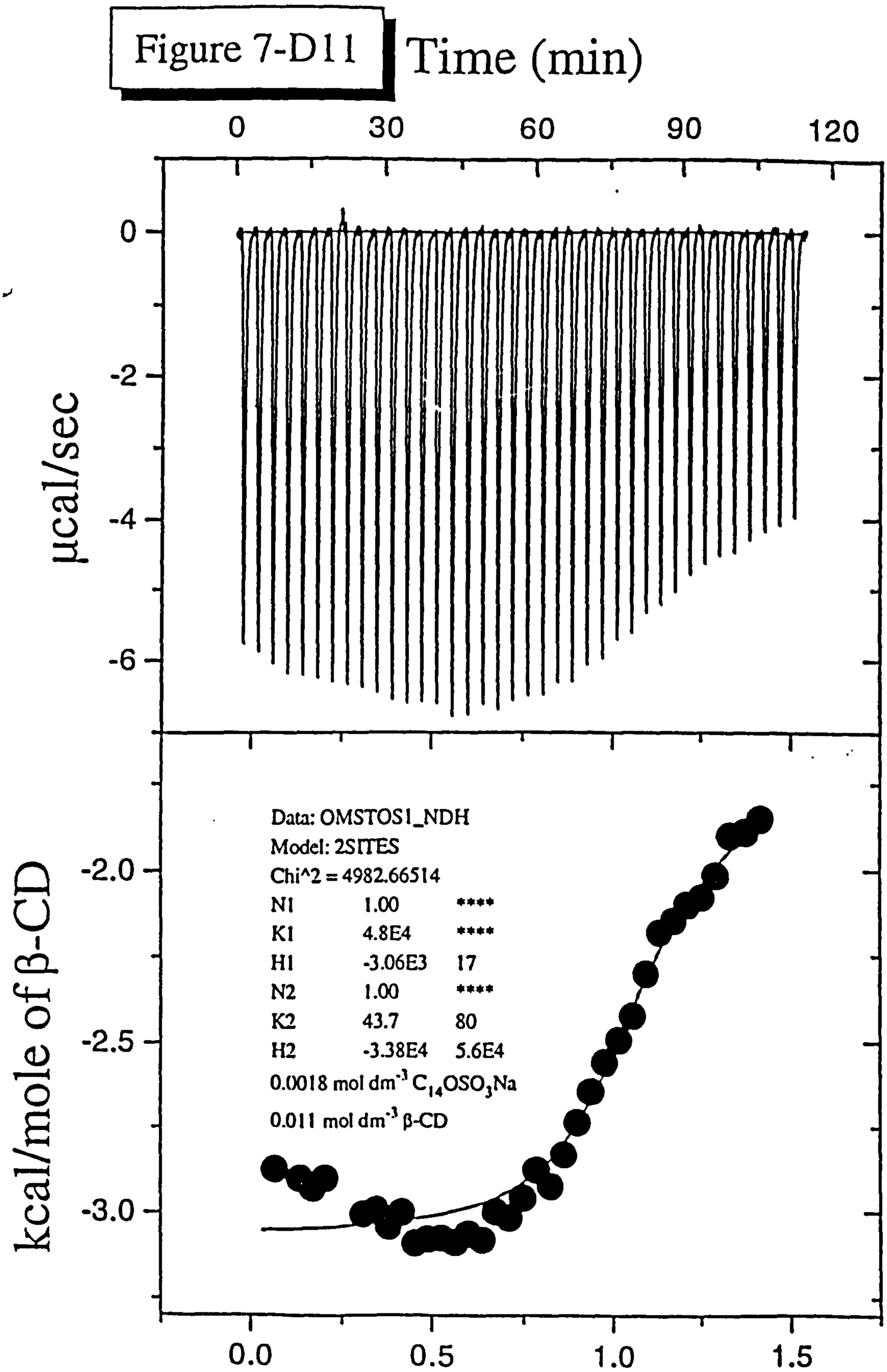
Time (min)
0
30
60
90
120
0
-2
-4
-6
µcal/sec
kcal/mole of β-CD
-2.0
-2.5
-3.0
Data: OMSTOS1_NDH
Model: 2SITES
Chi^2 = 4982.66514
N1 1.00 ****
K1 4.8E4 ****
H1 -3.06E3 17
N2 1.00 ****
K2 43.7 80
H2 -3.38E4 5.6E4
0.0018 mol dm-3 C14OSO3Na
0.011 mol dm-3 β-CD
0.0
0.5
1.0
1.5
Molar Ratio

Figure 7-D12

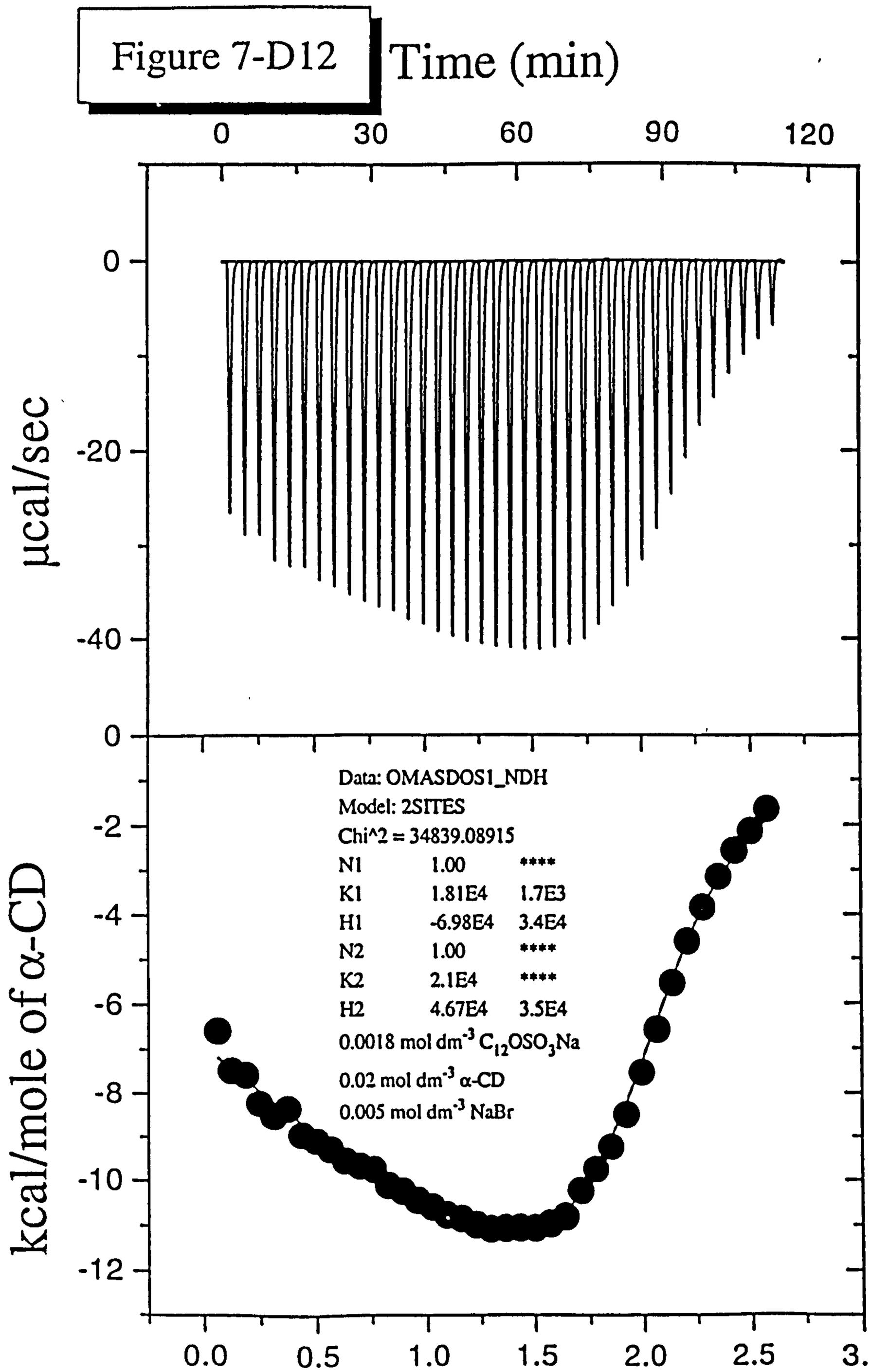
Time (min)
0
30
60
90
120
0
-20
-40
µcal/sec
0
-2
-4
-6
-8
-10
-12
kcal/mole of α-CD
Data: OMASDOS1_NDH
Model: 2SITES
Chi^2 = 34839.08915
N1 1.00 ****
K1 1.81E4 1.7E3
H1 -6.98E4 3.4E4
N2 1.00 ****
K2 2.1E4 ****
H2 4.67E4 3.5E4
0.0018 mol dm-3 C12OSO3Na
0.02 mol dm-3 α-CD
0.005 mol dm-3 NaBr
0.0
0.5
1.0
1.5
2.0
2.5
3.0
Molar Ratio